



HAL
open science

Implications of OEP16 protein in the photoprotection of *Arabidopsis thaliana* during light stress

Iga Samol

► **To cite this version:**

Iga Samol. Implications of OEP16 protein in the photoprotection of *Arabidopsis thaliana* during light stress. *Vegetal Biology*. Université Joseph-Fourier - Grenoble I, 2009. English. NNT : . tel-00764372

HAL Id: tel-00764372

<https://theses.hal.science/tel-00764372>

Submitted on 12 Dec 2012

HAL is a multi-disciplinary open access archive for the deposit and dissemination of scientific research documents, whether they are published or not. The documents may come from teaching and research institutions in France or abroad, or from public or private research centers.

L'archive ouverte pluridisciplinaire **HAL**, est destinée au dépôt et à la diffusion de documents scientifiques de niveau recherche, publiés ou non, émanant des établissements d'enseignement et de recherche français ou étrangers, des laboratoires publics ou privés.



Ecole Doctorale Chimie et Science du Vivant

THÈSE

Pour obtenir le grade de **DOCTEUR DE L'UNIVERSITÉ JOSEPH FOURIER**

Spécialité : *Biologie Végétale*

**Implications de la protéine OEP16 dans la
photoprotection d'*Arabidopsis thaliana* lors du stress
lumineux**

Présentée et soutenue par :

Iga SAMÓL

Le 18 septembre 2009

Composition du jury :

Felix Kessler	Professeur, Université de Neuchâtel, Suisse	Rapporteur
Graham Noctor	Professeur, Université de Paris sud XI, Orsay	Rapporteur
Michel Robert-Nicoud	Professeur, Université Joseph Fourier, Grenoble	Président du jury
Steffen Reinbothe	Professeur, Université Joseph Fourier, Grenoble	Directeur de thèse

Dla Kochanej Mamy

A Ma Chère Maman

REMERCIEMENTS

Je tiens tout d'abord à remercier Monsieur Felix Kessler et Monsieur Graham Noctor d'avoir accepté d'évaluer mon travail de thèse en tant que rapporteurs. Je tiens à remercier également Monsieur Michel Robert-Nicoud qui m'a fait l'honneur de présider ce jury ainsi que de son soutien dès le début de mon arrivée à l'Université Joseph Fourier.

Je remercie tout particulièrement et sincèrement mon directeur de thèse, Monsieur Steffen Reinbothe, pour son soutien moral et scientifique ainsi que l'indépendance et la confiance qu'il m'a accordé tout au long de ces années. Sa patience, sa disponibilité et son investissement m'ont beaucoup aidé, surtout pendant les dernières étapes de mon travail. Sans ses encouragements, ça aurait été beaucoup plus difficile.

Je tiens ensuite à remercier Monsieur Michel Herzog, directeur du Laboratoire Plastiques et Différenciation Cellulaire pour m'avoir accueilli et soutenu, notamment dans la continuation de ma carrière scientifique.

Un grand merci aux membres de l'équipe: Frank Bühr, pour ses conseils, sa bonne humeur et tous les desserts qui rendaient les journées très agréables; Claudia Roßig sur laquelle on peut toujours compter et Abder Lahroussi pour son aide régulière. J'ai une pensée très particulière pour Christiane Reinbothe, pour le partage de son expérience professionnelle sur la paillasse et surtout son amitié, sa joie de vivre qu'elle transmet quotidiennement aux autres. Je suis sûre que même en étant partie, tu veillais sur mon travail!

Je voudrais adresser mes remerciements particuliers à Marcel Kuntz, pour sa disponibilité et les discussions très intéressantes mais aussi pour son optimisme et sa grande aide en fin de parcours. Je remercie également l'ensemble des membres du laboratoire encore présents ou partis, pour leur sympathie et leur attitude amicale, je pense ici surtout à Livia (qui m'a fortement soutenue), Jean-Pierre (très enthousiaste et un improvisiste efficace), Madeleine («ma sœur cosmique» qui sait mieux que quiconque prendre soin des plantes), Éliane (un des rares exemples de féminité chaleureuse), Anne-Marie, Régis, Gilles, Daniel, Fred, Emeline et France. Je remercie tous les thésards et étudiants, Maryam, Abir, Wafa, Mohammed, Emilie, Laurence, Dhriti, Daniel, Christina et Séverine pour la bonne ambiance au travail.

Merci à Madame Lucile Sage pour sa gentillesse et sa disponibilité, Monsieur Stephan Pollmann, Armin Springer et Holger Schmidt pour leur collaboration.

Je souhaite également remercier tous les gens qui m'ont entouré de leur soutien à un moment ou à un autre, notamment Stéphane, Ghislaine, Tereza, Aurélie, Thomas. Un grand merci à mes amis fidèles: Hanane et Brice, pour leur soutien si important surtout les derniers temps. Vous étiez avec moi quand il le fallait, jour après jour, peu importe l'heure de la nuit. Et toi Brice, depuis toutes ces années (magnifiques!), merci pour tout !!!

Je termine par les remerciements adressés aux personnes les plus proches de mon cœur, ma famille en Pologne, qui m'a toujours fortement encouragée durant ces années en France et sans qui je n'aurais jamais pu en arriver là: à mon père et ma chère sœur Justynka, pour toute sa joie de vivre et en particulier à ma Maman, pour toutes les heures passées au téléphone, pour tous ces très bons conseils et pour son courage infailible. J'espère que, là où tu es, tu pourras voir maintenant les fruits de ce manuscrit, si délicat à écrire.

CONTENTS

LIST OF FIGURES	5
LIST OF TABLES	7
ABBREVIATIONS	8
CONVENTIONS	10
CHAPTER 1 INTRODUCTION	13
1.1 PLASTIDS	15
1.1.1 Origin and evolution of plastids	15
1.1.2 Different types of plastids	16
1.1.2.1 Etioplasts	17
1.1.2.2 Chloroplasts	18
1.1.2.3 Other plastid types	19
1.2 ROLE OF LIGHT SIGNALING IN GENE REGULATION DURING PLANT DEVELOPMENT	20
1.2.1 Plant developmental adaptations to light	20
1.2.2 Light perception and phytochrome action on photosynthetic genes	22
1.2.3 Chlorophyll biosynthesis	23
1.2.3.1 Steps, intermediates, enzymes	24
1.2.3.2 Regulation of the chlorophyll biosynthesis pathway by light	28
1.2.3.3 Feedback inhibition of 5-ALA synthesis in Angiosperms	29
1.2.3.4 Light-dependent Protochlorophyllide reduction	31
1.2.3.5 LHPP as a link between skotomorphogenesis and photosynthesis of higher plants	31
1.3 THE IMPORT OF THE pPORA AND pPORB INTO THE PLASTIDS	34
1.3.1 A brief overview of the general protein import pathway	34
1.3.2 Differential plastid import of the pPORA and pPORB	36
1.3.3 PTC52, a Pchl _a oxygenase located in the inner envelope of barley and Arabidopsis chloroplasts	37
1.3.4 TOC33 and TOC34, twin GTPases in the outer envelope with partially redundant roles	38
1.3.5 PTC16/OEP16, a solute and amino acid selective channel protein in the outer plastid envelope	39
CHAPTER 2 MATERIALS AND METHODS	43
2.1 PLANT MATERIAL AND CULTURE CONDITIONS	45
2.1.1 Choice of plant material	45
2.1.1.1 <i>Arabidopsis thaliana</i>	45
2.1.1.2 Barley	45
2.1.2 Ecotypes and mutant alleles	45
2.1.3 Cultivation of plants in soil	45
2.1.4 <i>In vitro</i> culture	46
2.1.5 Culture conditions	47

2.1.6	Photobleaching test conditions.....	47
2.2	CLONING OF CDNA CODING FOR AtOEP16-1 PROTEIN FROM <i>ARABIDOPSIS</i>	48
2.2.1	Bacterial genotypes, solutions and culture conditions.....	48
2.2.2	Vector constructions and cloning strategies.....	48
2.3	GENETIC MANIPULATIONS OF PLANTS	53
2.3.1	Stable transformation	53
2.3.1.1	Transformation by “floral dip”	53
2.3.1.2	Selecting transformants	53
2.3.2	Plant crossing.....	54
2.4	ANALYSIS OF NUCLEIC ACIDS	54
2.4.1	DNA.....	54
2.4.1.1	Synthesis of oligonucleotides	54
2.4.1.2	Amplification of DNA fragments by PCR.....	54
2.4.1.3	Analysis of nucleic acids on agarose gel	55
2.4.1.4	Extraction of DNA fragments from agarose gel	55
2.4.1.5	DNA sequencing.....	55
2.4.1.6	Plant genomic DNA extraction.....	56
2.4.1.7	Southern Blot.....	57
2.4.2	RNA.....	59
2.4.2.1	Extraction of total RNA.....	59
2.4.2.2	Determination of RNA concentration.....	59
2.4.2.3	Northern blot	59
2.4.2.4	<i>In vitro</i> translation	60
2.4.2.5	Polysomes isolation	61
2.5	PROTEIN ANALYSIS.....	62
2.5.1	Protein extraction	62
2.5.1.1	Rapid protein extraction	62
2.5.1.2	Long protein extraction.....	62
2.5.2	Determination of protein concentration.....	63
2.5.3	Analysis of proteins by polyacrylamide gel electrophoresis.....	63
2.5.3.1	One dimensional SDS-Polyacrylamide Gel Electrophoresis (SDS-PAGE).....	63
2.5.3.2	Two dimensional SDS-Polyacrylamide Gel Electrophoresis (SDS-PAGE)	64
2.5.3.3	Staining SDS-polyacrylamide gels with Coomassie brilliant blue.....	65
2.5.3.4	Silver Nitrate staining.....	66
2.5.3.5	Drying SDS-polyacrylamide gels	66
2.5.4	Transfer of proteins onto nitrocellulose membrane (Western Blot).....	66
2.5.5	Immunodetection.....	67
2.5.6	Production of an antibody against the AtOEP16-1 protein	67
2.5.6.1	Protein overexpression in <i>Escherichia coli</i>	67
2.5.6.2	Purification of AtOEP16-1 protein	68
2.5.6.3	Production of the antibody (INTERCHIM).....	69
2.5.7	Radioactive labeling of proteins <i>in vivo</i>	69
2.6	<i>IN VITRO</i> IMPORT INTO THE ORGANELLES	70

2.6.1	Construction of chimeric precursor proteins.....	70
2.6.2	Import assay.....	70
2.7	FLUORESCENCE OBSERVATIONS.....	71
2.7.1	Accumulation of protochlorophyllide and chlorophyll pigments.....	71
2.7.2	Detection of GFP and YFP fusion proteins.....	72
2.7.2.1	Epifluorescence microscopy.....	72
2.7.2.2	Confocal laser-scanning microscopy.....	72
2.8	ELECTRON MICROSCOPY IMAGING (EMI).....	72
2.8.1	Tissue fixation.....	72
2.8.2	Inclusion and observation.....	73
2.9	TETRAZOLIUM STAINING OF PLANT TISSUES.....	73
2.10	PIGMENT ANALYSIS BY HIGH PERFORMANCE LIQUID CHROMATOGRAPHY (HPLC).....	74
2.10.1	Sample preparation.....	74
2.10.2	Pigment extraction.....	74
2.10.3	Dosing and pigment analysis.....	75
CHAPTER 3	RESULTS.....	77
3.1	GENETIC COMPLEXITY OF THE <i>Atoep16-1</i> MUTANT BACKGROUND.....	79
3.1.1	Identification of the <i>Atoep16-1</i> mutant in Arabidopsis.....	79
3.1.2	Re-screening of original seed stock from the Salk Institute for additional <i>Atoep16-1</i> mutants....	83
3.1.2.1	Identification of two <i>Atoep16-1</i> mutant families with different phenotypes.....	83
3.1.2.2	<i>PORA</i> and <i>FLU</i> genes are unaffected in <i>Atoep16-1;5-8</i> .mutant lines.....	86
3.2	PHYSIOLOGICAL CHARACTERIZATION OF THE FOUR <i>Atoep16-1</i> MUTANT TYPES.....	91
3.2.1	Pigment analyses.....	91
3.2.1.1	Low-temperature fluorescence analysis of Pchl _{id} forms in etiolated <i>Atoep16-1;5-8</i> mutant seedlings ..	91
3.2.1.2	HPLC-analysis of pigments (carotenoids, chlorophylls).....	92
3.2.2	Viability of <i>Atoep16-1</i> mutant seedlings.....	99
3.2.2.1	Developmental control of seedling viability.....	99
3.2.2.2	Quantitative assessment of seedling viability.....	102
3.2.3	Singlet oxygen production in <i>Atoep16-1;5-8</i> mutant seedlings.....	104
3.2.4	Chloroplasts protein import.....	106
3.2.4.1	Chemical crosslinking and differential in vitro import of transA-DHFR and transB-DHFR into isolated <i>Atoep16-1</i> mutant plastids.....	106
3.2.4.2	Differential <i>in vivo</i> import of transA-GFP into plastids.....	108
3.2.5	Is the <i>Atoep16-1</i> mutation responsible for the photobleaching phenotype?.....	109
3.2.5.1	Complementation test.....	109
3.2.5.2	Localization of AtOEP16-1 in plastids.....	115
3.3	IDENTIFICATION OF TRANSLATION AS TARGET OF SINGLET OXYGEN ACTION IN <i>Atoep16-1;5-8</i> , <i>flu</i> AND <i>tig</i> ^{dl2} SEEDLINGS.....	117
3.3.1	Comparison of <i>Atoep16-1;5-8</i> with <i>flu</i>	119
3.3.1.1	<i>In vitro</i> -protein synthesis.....	119
3.3.1.2	<i>In vivo</i> -protein synthesis during greening and in response to photooxidative stress.....	120

3.4 PORPHYRIN-BASED CELL DEATH IN BARLEY: THE <i>tigrina</i> ^{d12} MUTANT	123
3.4.1 Effect of light and singlet oxygen on protein synthesis in etiolated <i>tig</i> ^{d12} seedlings	124
3.4.2 A detailed expression analysis of photosynthetic and stress proteins	126
3.4.3 Decrease of nucleus-encoded photosynthetic transcripts in <i>tig</i> ^{d12} upon light stress	128
3.4.4 Analysis of polysomal mRNAs in <i>tig</i> ^{d12} and wild type-seedlings in response to light stress.....	129
CHAPTER 4 DISCUSSION.....	133
4.1 ROLE OF AtOEP16-1 IN PLANTA	135
4.2 SALK T-DNA INSERTION IN THE GENE <i>ATOEP16-1</i> CONTAINS DIFFERENT MUTANTS	137
4.3 IS THE LACK OF AtOEP16-1 PROTEIN RESPONSIBLE FOR PHOTBLEACHING?.....	141
4.4 ARE THE CELL DEATH REGULATORY MECHANISMS IN MUTANTS <i>Atoep16-1;5</i> AND <i>1;6</i> THE SAME AS IN <i>flu</i> ?	144
4.5 REDUCED CAROTENOID CONTENT LEADS TO ENHANCED LIGHT SENSITIVITY IN IRRADIATED <i>Atoep16-1;5</i> AND <i>Atoep16-1;6</i> SEEDLINGS.....	146
CHAPTER 5 CONCLUSION.....	149
CHAPTER 6 VERSION ABREGEE EN FRANÇAIS	153
6.1 INTRODUCTION.....	155
6.2 LE FOND GENETIQUE COMPLEXE DU MUTANT <i>Atoep16-1</i> (CHAPITRE 3.1).....	156
6.2.1 Identification du mutant <i>Atoep16-1</i> chez <i>A.thaliana</i> (chapitre 3.1.1.)	156
6.2.2 Re-criblage du stock d'origine de mutant <i>Atoep16-1</i> de la collection SALK (chapitre 3.1.2)....	157
6.3 CARACTERISATION PHYSIOLOGIQUE DES QUATRE MUTANTS <i>Atoep16-1;5-8</i> (CHAPITRE 3.2)	158
6.3.1 Analyses de fluorescence de la Pchl _a à basse température chez les mutants <i>Atoep16-1;5-8</i> (chapitre 3.2.1).....	158
6.3.2 Viabilité des plantules <i>Atoep16-1;5-8</i> (chapitre 3.2.2).....	159
6.3.3 La production d'oxygène singulet chez les plantules <i>Atoep16-1;5-8</i> (chapitre 3.2.3)	160
6.3.4 L'import des protéines dans les chloroplastes des mutants <i>Atoep16-1;5-8</i> (chapitre 3.2.4)	160
6.3.5 La mutation <i>Atoep16-1</i> est-elle responsable du phénotype de photoblanchiment (chapitre 3.2.5) ?.....	161
6.4 ... IDENTIFICATION DE LA TRADUCTION EN TANT QUE CIBLE DE L'ACTION DE L'OXYGENE SINGULET CHEZ LES MUTANTS <i>Atoep16-1;5-8,flu</i> ET <i>tig</i> ^{d12} (CHAPITRE 3.3).	162
6.5 CONCLUSIONS GÉNÉRALES	164
REFERENCES.....	167
APPENDIX A	187
A. 1 PRIMER LIST	189
A. 2. OVEREXPRESSION AND PURIFICATION OF 6HIS-TAG-AtOEP16-1 PROTEIN	190
A. 3. PHENOTYPIC ANALYSIS OF DOUBLE MUTANT <i>Atoep16-1;7/flu</i>	192
A.4. IN VITRO IMPORT OF TRANSA-DHFR AND TRANSB-DHFR INTO ISOLATED <i>Atoep16-1</i> MUTANT PLASTIDS... 193	
APPENDIX B.....	195 - 277

List of Figures

Figure 1.1 The structure of the etioplast.	17
Figure 1.2 The structure of the chloroplast.	18
Figure 1.3 Photomorphogenesis and skotomorphogenesis in the model plant <i>Arabidopsis thaliana</i>	21
Figure 1.4 Chemical structure of chlorophyll.	24
Figure 1.5 The biosynthesis pathway leading to chlorophyll.	26
Figure 1.6 Interconversions between Chl a and b and their precursors.	28
Figure 1.7 Scheme of tetrapyrrole biosynthesis in angiosperms, highlighting the negative feedback loops exerted by heme and FLU on glutamyl-tRNA reductase.	30
Figure 1.8 Model of a Light-Harvesting POR-Protochlorophyllide (LHPP) complexes in etiolated angiosperm seedlings.	32
Figure 1.9 Schematic view of the differential import of pPORA and pPORB into the plastids.	34
Figure 1.10 Identification of barley OEP16-1 (HvOEP16-1).	40
Figure 2.1 Schematic representation of the photobleaching test for <i>Arabidopsis</i>	47
Figure 2.2 Schematic representation of Gateway TM system.	49
Figure 2.3 Expression vectors generated via Gateway technology.	51
Figure 3.1 Structure of the <i>Atoepl6-1</i> mutant gene (Salk_018024.50.90.X).	80
Figure 3.2 Conditional cell death phenotype of <i>Atoepl6-1</i>	81
Figure 3.3 Identification of four independent <i>Atoepl6-1</i> knock-out mutants in the original seed stock Salk_018024.50.90.X.	85
Figure 3.4 PCR verification of the T-DNA insertion in <i>AtOEP16-1;5-8</i>	86
Figure 3.5 Southern-blot analysis of <i>Atoepl6-1</i> mutant lines.	88
Figure 3.6 Absence of <i>AtOEP16-1</i> protein in mutants <i>Atoepl6-1;5-8</i>	89
Figure 3.7 Low temperature (77 K) fluorescence emission analysis of pigments in <i>Atoepl6-1; 5-8</i> mutant seedlings.	92
Figure 3.8 Biosynthesis of carotenoids in plants.	93
Figure 3.9 The effect of light on pigment accumulation in <i>Atoepl6-1;5-8</i> and wild-type seedlings.	96
Figure 3.10 Representative HPLC analysis of pigments found in the cotyledons of wild-type and <i>Atoepl6-1;5-8</i> mutant seedlings.	98
Figure 3.11 Seedling survival as a function of seedling age and hypocotyl length in <i>Atoepl6-1;6</i> and wild-type.	100
Figure 3.12 Photobleaching as a function of Pchlde overaccumulation in mutant <i>Atoepl6-1;6</i>	101

Figure 3.13 Tetrazolium staining of etiolated and light-exposed <i>Atoep16-1;5-8</i> versus wild-type seedlings, used to monitor cell death progression.....	103
Figure 3.14 Release of singlet oxygen in mutants <i>Atoep16-1;5-8,flu</i> and in the wild-type.	105
Figure 3.15 <i>In vitro</i> import and crosslinking of DTNB-activated 35S-transA-DHFR determined with plastids isolated from wild-type and mutants <i>Atoep16-1;5-8</i>	107
Figure 3.16 <i>In vivo</i> import of TransA-GFP into the plastids of mutants <i>Atoep16-1;5-8</i>	108
Figure 3.17 Experimental design underlying the complementation assay.	110
Figure 3.18 How to score successful complementation events.....	111
Figure 3.19 Detailed expression analysis of AtOEP16-1 in the 35S::OEP16-expressing line <i>Atoep16-1;6</i>	112
Figure 3.20 Complementation of <i>Atoep16-1;6</i> with 35S::GFP::OEP16.....	113
Figure 3.21 Lack of functional complementation in <i>Atoep16-1;6</i> transformed with 35S::OEP16::YFP.....	114
Figure 3.22 Cyto-localization of GFP and YFP in the generated transformants.....	116
Figure 3.23 Phenotype of <i>Atoep16-1;6</i> and <i>flu</i>	118
Figure 3.24 Pattern of proteins synthesized <i>in vitro</i> using RNA from mutants <i>Atoep16-1;5-8</i>	119
Figure 3.25 Pattern of proteins synthesized in mutants <i>Atoep16-1;5-8</i> and wild-type <i>in vivo</i>	121
Figure 3.26 Protein synthesis in wild-type, <i>flu</i> and <i>Atoep16-1;6</i> plants after a non-permissive 8 h dark-to-light shift.	122
Figure 3.27 Phenotype of <i>flu</i> in <i>Arabidopsis</i> and its ortholog, <i>tigrina</i> ^{d12} , in barley.....	123
Figure 3.28 Changes in the protein patterns of etiolated and irradiated <i>tigrina</i> ^{d12} and wild-type seedlings.....	125
Figure 3.29 Two-dimensional pattern of total leaf proteins in <i>tigrina</i> ^{d12} and wild-type seedlings.....	126
Figure 3.30 Expression of photosynthetic proteins in wild-type (WT) and <i>tigrina</i> ^{d12} (<i>tig</i> ^{d12}) seedlings after illumination.	127
Figure 3.31 RNA expression in etiolated wild-type and <i>tigrina</i> ^{d12} seedlings after 2 h of irradiation.....	129
Figure 3.32 Polysome binding of photosynthetic messengers in <i>tigrina</i> ^{d12} and wild-type plants.	130
Figure 3.33 Dissociation of 80S cytoplasmic ribosomes in long-term irradiated <i>tigrina</i> ^{d12} versus wild-type plants.	131

List of tables

Table 2.1 Culture conditions for plants cultivated in soil and <i>in vitro</i>	47
Table 2.2 Antibiotic concentrations used for the selection of clones in different bacterial hosts.	48
Table 3.1 Opposing results on <i>Atoep16-1</i> published in the literature.....	84
Table 3.2 Comparison of the different properties of <i>Atoep16-1</i> ; 5-8.....	90

Abbreviations

Ant	antheraxanthin
AOS	allene oxide synthase
APS	ammonium persulfate
At	<i>Arabidopsis thaliana</i>
ATP	adenosine 5' - triphosphate
BAP	<i>BONI-ASSOCIATED PROTEIN</i>
BON	<i>BONZAI</i>
bp	base pair
CAO	Chl a oxygenase
Chl	chlorophyll
cop	<i>constitutive photomorphogenic</i>
D	dark
d	days
det	<i>de-etiolated</i>
DHFR	dihydrofolate reductase
DNA	deoxyribonucleic acid
DTNB	5,5'-dithiobis(2-nitro)benzoic-acid
E.coli	<i>Escherichia coli</i>
EDS	<i>ENHANCED DISEASE SUSCEPTIBILITY</i>
EDTA	ethylenediamine tetra-acetic acid
EMI	Electron Microscopy Imaging
ER	endoplasmic reticulum
EXE	<i>EXECUTER</i>
FLU	fluorescent protein
GFP	green fluorescent protein
GluTR	glutamyl-tRNA reductase
GSA	glutamate 1-semialdehyde
h	hours
HIR	high-irradiance responses
HPLC	High-Performance Liquid Chromatography
hy	<i>hypocotyl</i>
IEF	Isoelectric focusing
JA	jasmonate

JIP	JA induced protein
kDa	kilo Dalton
L	light
LB	Luria Bertani Broth
LFR	low fluence responses
LHCI	Light Harvesting complex of PSI
LHCII	Light Harvesting complex of PSII
LHPP	Light Harvesting POR:Pchl _a complex
LSU	large subunit of Rubisco
MgProtoMe	Mg ²⁺ -Proto monomethyl ester
min	minutes
MS	Murashige and Skoog
NADPH	nicotinamide-adenosine dinucleotidephosphate
Neo	neoxanthin
nm	nano meter
OEP16	outer envelope protein of 16 kDa
OPDA	octadecaphytodienoic acid
PBG	porphobilinogen
Pchl_a	protochlorophyllide
PCR	Polymerase Chain Reaction
Pfr	phytochrome absorbing far red light
PHY	phytochrome
PORA	NADPH-protochlorophyllide oxydoreductase A
<i>ppi</i>	<i>plastid protein import</i>
Pr	phytochrome absorbing red light
Proto	protoporphyrin IX
PSI	photosystem I
PSII	photosystem II
PTC	Pchl _a -dependent translocon complex
RBSC	ribulose-1,5-bisphosphate carboxylase/oxygenase
RNA	ribonucleic acid
RNP	ribonucleoproteins
ROS	Reactive Oxygen Species
SCN	signalosome
SDS	sodium dodecylsulfate

SDS-PAGE	SDS polyacrylamide gel electrophoresis
SSU	small subunit of Rubisco
TCA	trichloroacetic acid
TEMED	N,N,N',N' tetramethylethylenediamine
TF	triphenylformazane
Thl	thermolysin
TIC	translocon complex in the inner envelope membrane of chloroplasts
<i>tig</i>^{d12}	<i>tigrina</i> ^{d12}
TOC	translocon complex in the outer envelope membrane of chloroplasts
transA	transit peptide of pPORA
Tris	tris (hydroxymethyl) aminomethane
TTC	triphenyltetrazolium chloride
Viola	violaxanthin
VLFR	very low fluence responses
w	weeks
YFP	yellow fluorescent protein
Zea	zeaxanthin
13-HPOT	13-hydroperoxy octadecatrienoic acid
¹O₂	singlet oxygen
5-ALA	5-aminolevulinic acid

Conventions

<i>GENE</i>	the name of genes is indicated in capital italic letters
<i>allele</i>	the name of mutated <i>alleles</i> is indicated in small italic letters
PROTEIN	the name of proteins is indicated in capital straight letters

Chapter 1 Introduction

1.1 Plastids

1.1.1 Origin and evolution of plastids

Chloroplasts are the most abundant organelles in a plant cell. Besides their familiar roles in photosynthesis, chloroplasts accomplish many other key metabolic processes. Phylogenetic, structural and biochemical analyses support a single primary origin of chloroplasts. Presumably as a result of a single symbiotic association between a cyanobacterium-like organisms and a mitochondriate eukaryote, a first plastid-containing species evolved. This event is estimated to have occurred between 1.6 and 0.6 Ga ago (Yoon *et al.*, 2004; Cavalier-Smith, 2006). Over time, the foreign cell was reduced to a plastid being surrounded by two membranes: the inner and outer membranes of the cyanobacterium (Reumann *et al.*, 2005). This endosymbiosis gave rise to a proto-alga, which diverged into three lineages: the green lineage (*Viridiplantae*, the green algae and land plants), the red lineage (*Rhodophyta*, the red algae) and the blue lineage (*Glaucophyta*, the glaucophytes) (Delwiche, 1999; Moreira *et al.*, 2000; Martin *et al.*, 2002; Palmer, 2003; Bhattacharya *et al.*, 2004; Dyall *et al.*, 2004; McFadden and van Dooren, 2004; Deschamps *et al.*, 2008).

It is estimated that an ancestral organelle, the "protoplastid", may have arisen after ca. 90% of the total gene transfer from the genome of the cyanobacterial endosymbiont to the host cell nucleus. Major constraints to keep the plastid functional were the followings: (i) to control the expression of genes encoding photosynthetic and other essential proteins and (ii) to evolve an envelope protein import machinery that allowed the gene products to be imported back into the semi-autonomous photosynthetic organelle (Martin and Herrmann, 1998; Martin & Müller, 1998; Martin *et al.*, 1998). As a result of all of these events, our today's plastids are semi-autonomous organelles that contain only limited coding information in their DNA. The plastid genome, the plastome, spans around 120 to 160 kbp whose size varies in different species. A comparison of today's plastid genome with that of an extant cyanobacteria reveal that only 2-5% of ancestral genes are maintained in the contemporary chloroplast genome. To synthesize the 50-150 of their own proteins, plastids retained the competence for DNA replication, transcription and translation. However, the vast majority of plastid proteins (2000-5000) are encoded in the nucleus.

Due to its symbiotic origin, plastids are surrounded by two membranes: the outer envelope membrane and the inner envelope membrane. It was proposed that the inner envelope was inherited from the endosymbiont while the outer membrane has a mixed origin. These two membranes present a barrier that cannot be crossed unassisted by proteins or metabolites (Stern *et al.*, 1997). Specific transport mechanisms thus were required. *Proteomics* approaches have identified a large number of potential transporters in the envelope membranes. Moreover, biochemical, cell biological and genetic studies have unveiled a pathway of protein import into chloroplasts and other plastid forms that relies on the operation of translocon complexes in the outer and inner envelope membranes designated as TOC and TIC (see below).

TOC and TIC facilitate and control the import of proteins into the organelle and thereby present one important regulatory point of nucleus-organelle interaction. The import machinery of modern plastids is presumed to be of dual origin and to comprise both host and symbiont components. However, the identity of the ancestral proteins contributing to the developing protein import apparatus and the evolutionary sequence of this process, remain thus far unresolved (Cavalier-Smith, 2000).

Plastids reproduce by division through binary fission which is morphologically similar to bacterial cell division and that does not depend on plant cell division (review in Aldridge *et al.*, 2005). In spite of similar genetic information, plastids vary in size, shape, content, internal structure and function. These different plastid types, influenced by cellular development and external conditions, are presented below.

1.1.2 Different types of plastids

The photosynthetically active chloroplast was the primal organelle that developed from the cyanobacterial endosymbiont. Within a time, evolution proceeded to create a family of various plastids that derived from the chloroplast. Very little is known about the evolutionary processes involved in the creation of different forms of plastids, however, it is assumed that their development was imposed onto plastid by the host cell, independently from endosymbiotic creation of the chloroplast, and thus cannot be ascribed to the cyanobacterial ancestor (Vothknecht and Westhoff, 2001).

In higher plants, plastids develop from small, round, colourless, nearly devoid of internal membranes, undifferentiated organelles called proplastids, which reside in dividing, meristematic cells. It is estimated that each meristematic cell contain 10 to 20 proplastids (Lyndon and Robertson, 1976). Proplastids differentiate into several plastid types, depending on the developmental stage and cell type during cell differentiation. Plastids have long been classified into different types by virtue of their storage components and internal structure. Currently, there is tendency to describe plastids rather as a continuous spectrum of types, because precise categorization is often difficult and not always biologically meaningful.

1.1.2.1 Etioplasts

Etioplasts are the organelles differentiated from proplastids in the absence of light. They lack chlorophyll, but produce a large amount of colourless chlorophyll precursor, protochlorophyllide (Pchl_{id}e). Etioplasts contain very few internal membranes and a characteristic, large paracrystalline structure called prolamellar body, consisting of lipids, carotenoids and essentially two isomeric proteins, the NADPH-protochlorophyllide oxidoreductase A (PORA) and B (PORB) (Figure 1.1).

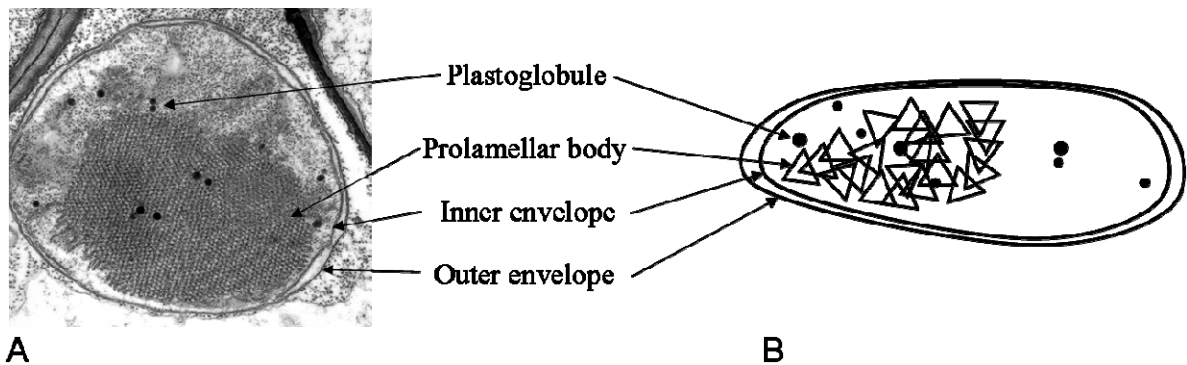


Figure 1.1 **The structure of the etioplast.**

Structure of a typical etioplast. Electron micrograph of an etioplast from barley (A) and schematic view (B). Courtesy of Armin Springer.

These types of plastids are generally found during development in darkness (skotomorphogenesis), in particular in seedlings germinating under the soil or covered by fallen leaves. Already after a short period of illumination etioplasts differentiate into chloroplasts, the prolamellar body is dispersed and thylakoids begin to form.

1.1.2.2 Chloroplasts

Chloroplasts are the most studied plastid types due to their photosynthetic activities. They contain a green pigment, chlorophyll and are found in green plant tissues such as leaves, stems and green fruits.

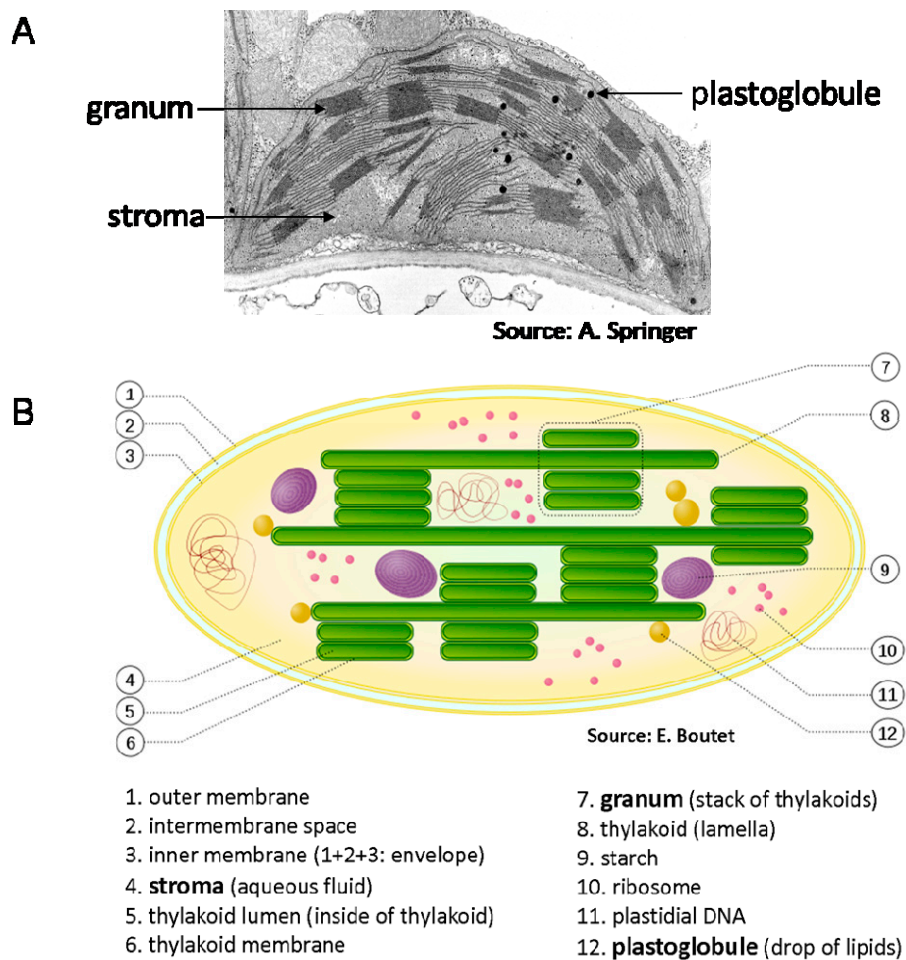


Figure 1.2 The structure of the chloroplast.

Structure of a typical leaf mesophyll chloroplast. Electron micrograph taken for barley (A) and schematic view (B). Courtesy of Armin Springer.

In higher plants, upon illumination, as meristematic cells begin to differentiate into mesophyll and palisade cells, proplastids differentiate into chloroplasts. During the progress of chloroplast maturation the internal membrane system develop thylakoid structure. First, long lamella are formed which are later accompanied by smaller, disc-shaped structures that associate into grana stacks (Figure 1.2). Simultaneously, the typical lens-shape form of the chloroplast develops. Finally, mature plant chloroplasts contain a complex and intertwined internal membrane system named from Greek “thylakoids” (sack-like) which are responsible for light energy capture and its transformation into chemical energy. In fully mature chloroplast, there is no continuation between the inner envelope and the thylakoids (Vothknecht and Westhoff, 2001). The conversion of proplastids into chloroplasts is accompanied by high transcription levels of plastid- and nuclear-encoded genes involved in the transcription/translation apparatus (Baumgarther *et al.*, 1989). The expression of these genes decreases once the mature chloroplast is established. In contrast, genes required for photosynthesis are highly expressed only later in development (Bisanz-Seyer *et al.*, 1989).

Chloroplasts are responsible for oxygenic photosynthesis as well as for the synthesis of amino acids, fatty acids, terpenoids and other key metabolites. Chloroplasts also play a role in reduction of nitrites and sulfates and their conversion into organic compounds, providing necessary products for cell function and metabolism. Last but not least, chloroplasts are also involved in the exchange of inorganic cations, anions and many other low molecular weight compounds and metabolic intermediates. Transport of all these compounds is facilitated by protein machineries residing in the chloroplast envelope membranes.

1.1.2.3 Other plastid types

The extended plastid family includes chromoplasts, amyloplasts and leucoplasts. These are specialized forms of plastids used for coloration or storage. Chromoplasts are carotenoid-containing plastids found in many flower petals, fruits and roots. Coloration of these organs is often ascribed to chromoplasts and this might even be their main function. Amyloplasts are non-green, starch-storing plastids, usually found in storage organs, such as root tubers. They resemble proplastids but contain starch granules. In root tips, amyloplasts serve also as statholits for the gravity-sensing apparatus (Morita and Tasaka, 2004). Leucoplasts are characterized by a lack of coloration and they are involved in the synthesis of monoterpene compounds (hydrocarbons and oxygenated compounds) which are volatile constituents of

essential oils. They are found in floral organs and in specialized secretory glands associated with leaf and stem trichomes.

It is believed that plastids are partially interconvertible. However, the conversion of different plastid types require dramatic changes in their ultrastructure, including the biogenesis, reorganization, or disassembly of internal membranes, which are not yet understood at a molecular level.

1.2 Role of light signaling in gene regulation during plant development

Light can act as a signal for activating a developmental program already during early plant growth. Its perception is mediated through the action of various photoreceptors, including phytochromes, cryptochromes and phototropins. They are implicated in coordination of specific signal transduction pathways, originating from chloroplast or nucleus, which in turn activate or repress expression of several thousand genes. Their expression is responsible for adaptation of plant development to changing environmental light conditions.

1.2.1 Plant developmental adaptations to light

Light plays very important roles in plant growth and development, besides its major and essential function in photosynthesis. Depending on the presence or absence of light, plants can follow two distinct developmental programs which are called skotomorphogenesis and photomorphogenesis. Plants which develop in the presence of light undergo a series of coordinated changes as a result of which they establish a photomorphogenetic phenotype (Kendrick and Kronenberg, 1994). Light-grown seedlings have short hypocotyls, unfolded and expanded, green leaves (Figure 1.3). Due to the differentiation of chloroplasts and the accumulation of chlorophyll (Chl), many metabolic processes associated with photosynthetic activities become operational. On the other hand, when plants are grown in the absence of light, they follow a distinct growth pattern, called skotomorphogenesis. Dark-grown, etiolated seedlings display long and thin hypocotyls topped by an apical hook, as well as closed and unexpanded cotyledons (Figure 1.3). Dark-grown angiosperm seedlings are devoid of Chl and thus incapable of photosynthetic function. If such plants are left to grow in the dark, they will finally die. However, under natural conditions, when the

seedlings break through the soil after germination, de-etiolation occurs. In the uppermost parts of the soil, light is harnessed and used to trigger Chl biosynthesis and chloroplast development. The cotyledons start to open, they continue to expand and begin to photosynthesize. In parallel, hypocotyl elongation is inhibited and cell differentiation in vegetative meristems is initiated. Proplastids present in leaf meristems and previously formed etioplasts in dark-grown tissues differentiate into photosynthetically active chloroplasts.

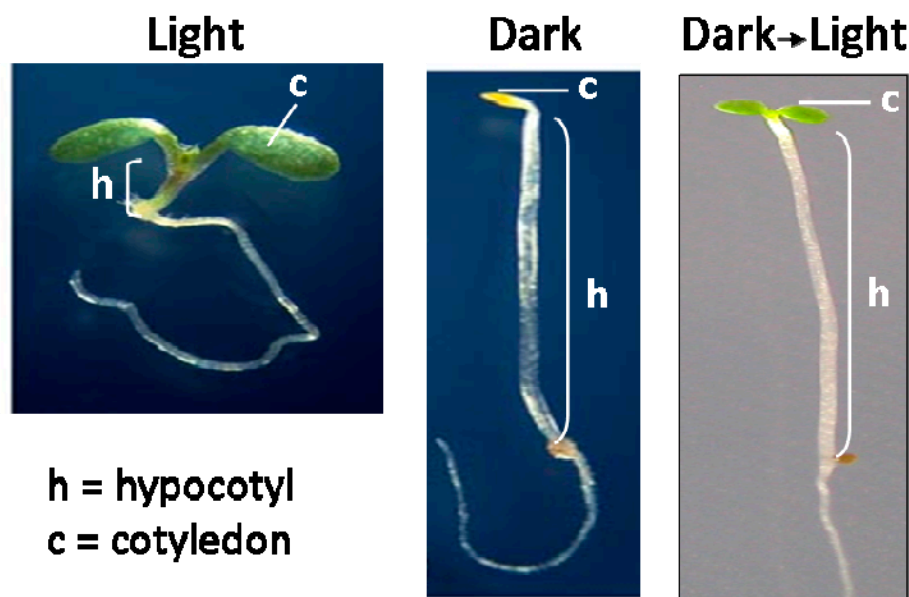


Figure 1.3 Photomorphogenesis and skotomorphogenesis in the model plant *Arabidopsis thaliana*.

When seedlings are grown in the light they undergo a developmental program known as photomorphogenesis. During this process, hypocotyl growth is inhibited and the cotyledons unfold and green. If, however, seedlings germinate in the dark, they follow a distinct growth pattern, designated skotomorphogenesis. During this process, all of the nutrient reserves in the seeds are invested into hypocotyls growth. Cotyledons remain tightly folded and closely apposed to the apical hook. There is no detectable greening in dark-grown seedlings. The images show 5 d-old seedlings of *Arabidopsis thaliana* (*A.th*) grown for 5 d in the light and dark, respectively, and seedlings that had been grown for 5 d in the dark and exposed to white light for 24 h.

1.2.2 Light perception and phytochrome action on photosynthetic genes

In plants, light-dependent responses are controlled by the action of three types of photoreceptors: phytochromes absorbing the red and far red light, cryptochromes absorbing blue, green and UV-A light and phototropins absorbing blue light.

Phytochrome is presumably the best characterized type of photoreceptor. It is a protein containing covalently attached chromophore, phytochromobilin. Phytochrome exists in two interconvertible conformations with different absorption spectra: biologically active Pfr absorbing far red light and Pr absorbing red light. In the dark, *de novo* synthesized phytochrome is present in the Pr form in the cytoplasm. Light contains more red than far red light and thus in daytime Pr is converted to Pfr form. Work of Nagy and Schaefer (2002) on *Arabidopsis* have shown that upon illumination there is a translocation of a fraction of Pfr to the nucleus, implicating signal transduction pathways coupling phytochrome action to nuclear gene activation. Ni et al. (1999) demonstrated phytochrome to physically interact with at least one transcription factor, PIF3, in a light dependent manner. Later, it was revealed that PIF3 binds to G-BOX elements of light regulated genes and is required for phytochrome-mediated regulation of several genes (Quail, 2000). Phytochrome mediates a variety of photomorphogenic phenomena including leaf expansion and inhibition of stem elongation. *Arabidopsis* contains five phytochrome genes, *PHYA-PHYE*, each with distinct but often overlapping functions. Different phytochromes control different plant processes in response to light. Depending on the amount of photons required to elicit a response, phytochrome responses fall into three categories: high-irradiance responses (HIR), low fluence responses (LFR) and very low fluence responses (VLFR). Phytochrome A and B appear to be the prominent forms controlling seed germination and post-germination development.

Much of our knowledge of light perception and signaling has come from genetic analyses of photomorphogenesis. Essentially two types of mutant screens, impaired in PHY signaling, have been performed: 1) screens for long *hypocotyl* (*hy*) mutants that look like dark-grown seedlings even in the presence of light due to their insensitivity to light, and 2) screens for *constitutive photomorphogenic* (*cop*)/*de-etiolated* (*det*) mutants that exhibit light-grown phenotype when grown in the dark. Studies on various *hy* mutants have enabled to verify the unique roles of PHYA and PHYB during seedling development and identify genes that

function as positive regulators of light signaling. For example, *hy3* and *hy8* were found to be deficient in the PHYB and PHYA apoproteins, respectively, while *hy1* is devoid of the phytochromobilin chromophore (Reed *et al.*, 1993; Whitelman *et al.*, 1993). The most severe phenotype was found in *hy5*, deficient in a bZIP transcription factor that operates both in PHYA and PHYB signalling (Oyama *et al.*, 1997).

The second major mutant class comprises the *cop/det* mutants that display constitutive photomorphogenesis in darkness and therefore are thought to function as negative regulators of light signaling (for a review, see Moller *et al.*, 2002). In other words, the normal function of *DET* and *COP* genes is to repress photomorphogenesis in the dark. Many of the *cop/det* mutants identified thus far, are defective in genes encoding proteins that form a large nuclear complex called the COP9 signalosome (SCN). The COP9 signalosome is a proteolytic complex that is presumed to degrade positive regulators of photomorphogenesis in the dark and negative regulators in the light after their ubiquitination (Hardtke and Deng, 2000). It is interesting to note that another COP protein COP1, may provide a direct link to the SCN complex. COP1 is similar to E3 ubiquitin ligases, which are involved in targeting proteins for 26S proteasome-mediated degradation. One of the targets of COP1 in the dark is HY5, which is ultimately directed for degradation by the SCN complex (Holm *et al.*, 2002).

1.2.3 Chlorophyll biosynthesis

Chlorophyll (Chl), a green pigment found in most plants, algae and cyanobacteria, was first isolated in 1817 by Joseph Bienaimé Caventou. Its name comes from Greek and means green leaf (*chloros phyllon*). It is involved in light absorption and energy transduction through photosynthesis. In plants, next to phycobilins (phytochromobilin) and Fe^{2+/3+}-porphyrins (hemes), Chl is the most abundant and probably most important tetrapyrrole. It belongs to Mg²⁺ porphyrins family and consists of four pyrrole rings (A, B, C, D) ligated into a tetrapyrrole ring with a magnesium atom inserted in the center and the phytol tail attached to ring D (Figure 1.4). We distinguish two types of Chl in higher plants: Chl *a* with a methyl group in position 3 and Chl *b* which has a formyl group instead of methyl group at this position.

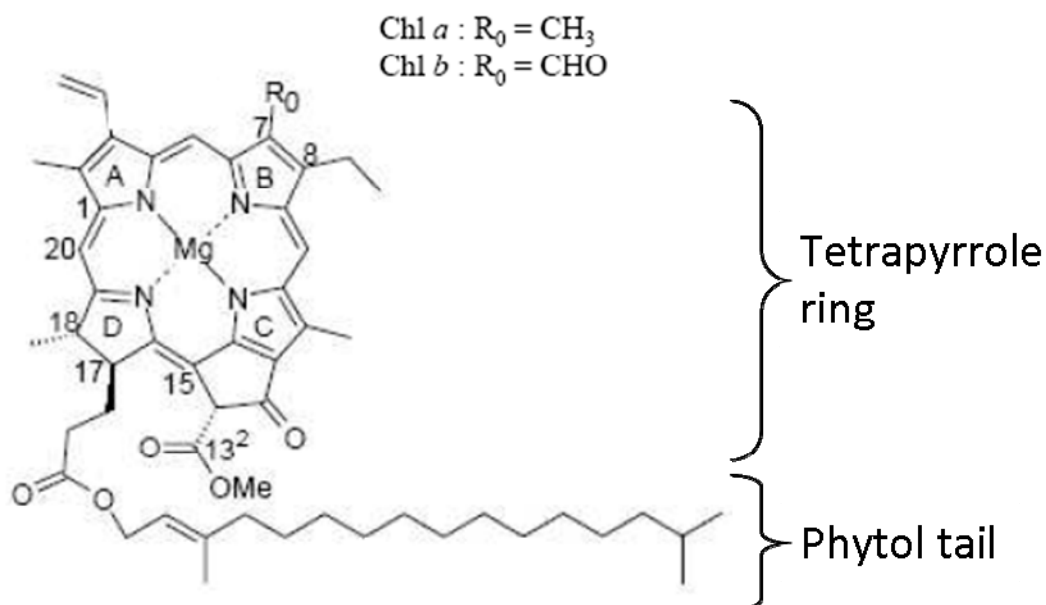


Figure 1.4 Chemical structure of chlorophyll.

The magnesium atom is enclosed in the centre of the tetrapyrrole ring, being composed of four pyrrole rings annotated A, B, C and D. A phytol tail is attached to the C17 position of the macrocycle. Chlorophylls *a* and *b* differ by the substituent at C7: a methyl group in Chl *a* and a formyl group in Chl *b*. Modified from Eckhardt *et al.* (2004).

1.2.3.1 Steps, intermediates, enzymes

Chl biosynthesis, as well as its accumulation and degradation, is tightly associated with chloroplast development, photomorphogenesis and chloroplast-nuclear signaling. Studies on mutants in *Arabidopsis* considerably helped in exploring the biochemistry and molecular biology of this pathway and its regulation. Recently, identification of almost all genes involved in Chl synthesis has been reported (Eckhardt *et al.*, 2004). The C5-pathway of chlorophyll synthesis comprises 15 enzymatic reactions which all take place in chloroplast. Chl synthesis is compartmentalized as follows: enzymes catalyzing the early steps in the Chl synthesis are highly soluble and thus mostly located in the chloroplast stroma, whereas enzymes of the late steps are associated with thylakoid or inner envelope membranes.

Indeed, Chl synthesis can be divided into three major parts: 1) formation of 5-aminolevulinic acid (5-ALA), the first committed precursor of all tetrapyrroles including Chl and heme; 2) formation of protoporphyrin IX (Proto) from eight molecules of 5-ALA; and 3) formation of Chl via the magnesium branch (Figure 1.5).

In the first stage of the C5-pathway, the amino acid glutamate is converted in a three-step reaction to 5-ALA. In plants, plastid 5-ALA synthesis requires the coordinated actions between three enzymes: glutamyl-tRNA synthetase, glutamyl-tRNA reductase (GluTR) and glutamate-semialdehyde amino transferase. Glutamyl-tRNA synthetase requires the cognate amino acid (glutamate) and tRNA as substrates, and the energy of ATP hydrolysis. This reaction is unusual in that it involves a covalent intermediate in which the amino acid is attached to a transfer RNA molecule. This reaction belongs to one of very few examples in biochemistry where a tRNA is used in a process other than protein synthesis. The resulted glutamyl-tRNA^{Glu} is then converted via GluTR in a NADPH and Mg²⁺ dependent manner into glutamate 1-semialdehyde (GSA) with the release of free tRNA that can be reused for aminoacylation by glutamyl-tRNA synthetase. Glutamate-semialdehyde amino transferase catalyzes the final step in 5-ALA synthesis, the transamination of GSA, to yield 5-ALA.

The second stage of the C5-pathway comprises the steps from 5-ALA to Proto. In a reaction catalyzed by 5-ALA dehydratase (also known as porphobilinogen synthase), two molecules of 5-ALA are condensed to form porphobilinogen (PBG), which ultimately form the pyrrole rings in Chl. The next stage is the assembly of a porphyrin structure from four molecules of PBG, catalyzed by PBG deaminase, to yield hydroxymethylbilane. It is followed by a ring closure and parallel isomerisation, leading to uroporphyrinogen III, the first macrocyclic tetrapyrrole. This reaction is catalyzed by uroporphyrinogen III synthase. Three subsequent reactions convert uroporphyrinogen III to Proto, leading to transformation of a hydrophilic, poor metal binding, photochemically unreactive species into one that is hydrophobic, binds metals tightly and is photochemically reactive. The establishment of all of these traits is necessary to allow light-harvesting and perform the photochemical functions by Chl. On the other hand, the porphobyrinogens are much less photoreactive than porphyrins. Thus, only at the last step, where the superior metal chelating properties of the porphyrin are needed, the conversion of porphyrinogen into a porphyrin takes place. In the first reaction, catalyzed by uroporphyrinogen III decarboxylase, the decarboxylation of the four acetate residues of uroporphyrinogen III occurs, yielding coproporphyrinogen III. Then, two successive oxidations catalyzed by coproporphyrinogen oxidase and protoporphyrinogen oxidase lead to the formation of protoporphyrinogen IX and Proto, respectively.

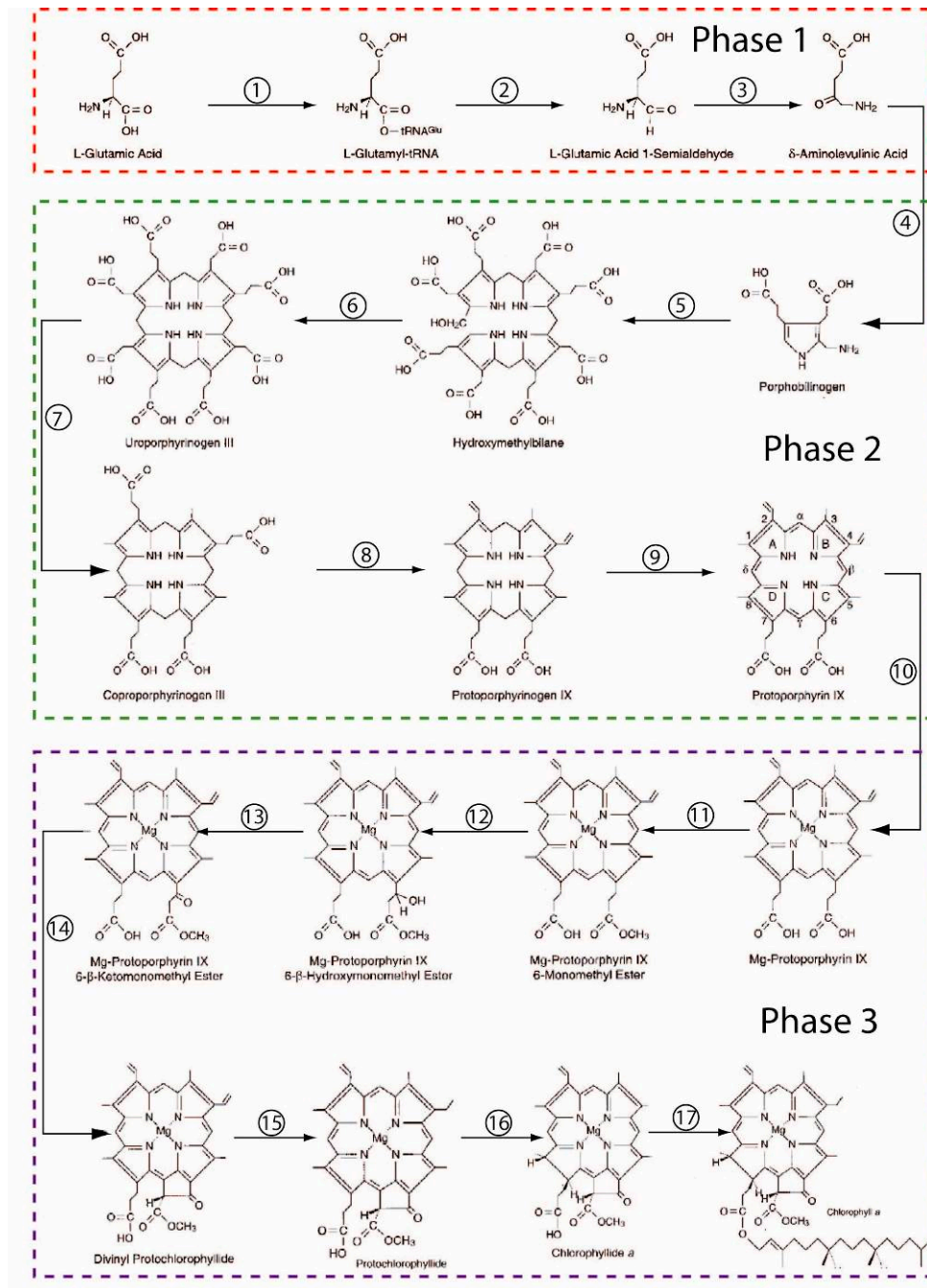


Figure 1.5 The biosynthesis pathway leading to chlorophyll.

The enzymes that catalyze the indicated steps of Chl biosynthesis are the followings: (1) glutamyl-tRNA synthetase; (2) glutamyl-tRNA reductase; (3) glutamate 1-semialdehyde aminotransferase; (4) porphobilinogen synthase; (5) hydroxymethylbilane synthase; (6) uroporphyrinogen III synthase; (7) uroporphyrinogen III decarboxylase; (8) coproporphyrinogen III oxidative decarboxylase; (9) protoporphyrinogen IX oxidase; (10) protoporphyrin IX Mg-chelatase; (11) *S*-adenosyl-L-methionine:Mg-protoporphyrin IX methyltransferase; (12–14) Mg-protoporphyrin IX monomethyl ester oxidative cyclase; (15) divinyl (proto)chlorophyllide 4-vinyl reductase; (16) light-dependent NADPH:protochlorophyllide oxidoreductase or light-independent protochlorophyllide reductase; (17) chlorophyll synthase. Modified from Beale (1999).

All the biosynthesis steps up to this point are the same for the synthesis of both Chl and heme. But then the pathway bifurcates, and the fate of the molecule depends on which metal is inserted into the center of the porphyrin ring system. Insertion of magnesium produces Mg-ProtoIX which needs to be modified further to produce Chl. Insertion of $\text{Fe}^{2+/3+}$ leads to heme. Steps which follow Mg-chelatase are the followings: first, Mg^{2+} -Proto is esterified to Mg^{2+} -Proto monomethyl ester (MgProtoMe) by a methyl transferase. Then, the isocyclic ring of the macrocycle is formed by the MgProtoMe cyclase. This reaction requires O_2 , NADPH, and some membrane-associated enzymes. The final product of Mg-branch is divinyl Protochlorophyllide *a* (Pchlido *a*). In angiosperms, in the dark, some or most of the divinyl Pchlido *a* is converted to monovinyl Pchlido *a* via 4-vinyl reductase. Subsequent reduction of the C17/C18 double bond in ring D requires light in angiosperms and is catalyzed by the NADPH-Pchlido oxidoreductase (POR), which is a key enzyme of Chl synthesis in angiosperms (see below). The final step in the Chl biosynthetic pathway involves the attachment of the phytol tail, which is catalyzed by an enzyme called Chl synthetase. Subsequent conversion of Chl *a* into Chl *b* is driven by Chl *a* oxygenase (CAO) (Oster *et al.*, 2000). Recently, it was shown that this enzyme can also catalyze a conversion of Chlido *a* into Chlido *b* (Reinbothe *et al.*, 2006 a). While previous dogmas in the field said that CAO would be the only enzyme involved in Chl *b* synthesis, alternative models suggest an early branching of the C5-pathway at the stage of Pchlido *a* (Figure 1.6). An enzyme was identified that can convert Pchlido *a* to Pchlido *b* *in vitro* (see below). *Vice versa*, enzymes that interconvert Chl *b* to Chl *a* and Pchlido *b* to Pchlido *a* have been identified in some plant species (Scheumann *et al.*, 1998; Reinbothe *et al.*, 2003 a) (summarized in Figure 1.6).

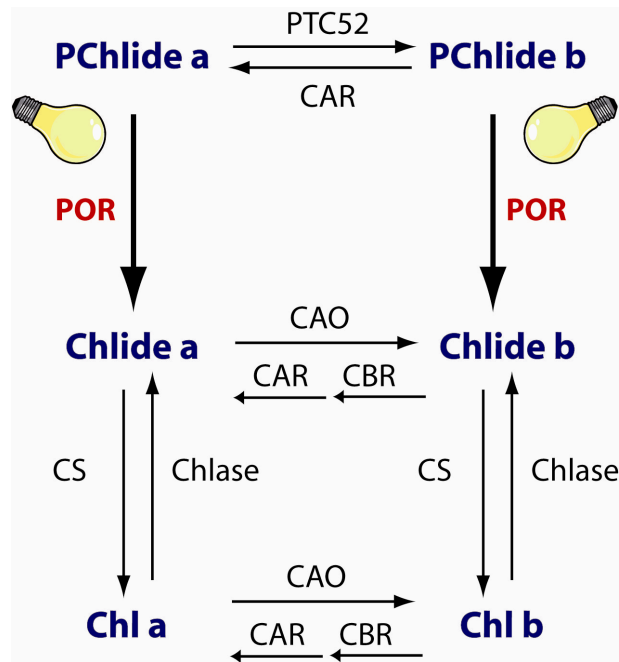


Figure 1.6 Interconversions between Chl a and b and their precursors.

PTC52: protochlorophyllide *a* oxygenase; POR: light-dependent protochlorophyllide oxidoreductase; CAR: 7-formyl reductase; CBR: chlorophyllide b reductase; CS: chlorophyll synthase; Chlase: chlorophyllase; CAO: chlorophyllide *a* oxygenase.

1.2.3.2 Regulation of the chlorophyll biosynthesis pathway by light

The biosynthetic pathway of Chl from 5-ALA to uroporphyrinogen III and beyond to Proto is essentially the same as that of heme. Thus, it is important to control tightly the synthesis of these components, accordingly to the needs of cell, tissue or organ. On the other hand, a chemical structure of tetrapyrrol intermediates (system of conjugated double bounds) is responsible for their extreme photoreactivity. In the presence of light and under aerobic conditions, free tetrapyrroles can be easily excited and then generate singlet oxygen as one form of reactive oxygen species (ROS). Singlet oxygen in turn can provoke pigment bleaching, lipid peroxidation and protein degradation. Both cytotoxic effects as well as specific signaling functions are currently discussed to account for the cell death phenotype triggered by singlet oxygen (op den Camp *et al.*, 2003). A subtle counterbalance between ROS production and quenching is normally maintained during photosynthesis where singlet oxygen is easily produced in the reaction center of photosystem 2 (PSII). However, perturbations of tetrapyrrole biosynthesis result in accumulation of excess amounts of free porphyrins operating as photosensitizers and thus are deleterious to the plant. This property

may explain why tetrapyrroles in plants need to be bound to proteins and why they are kept at very low levels as free pigments.

Plants have evolved several different strategies to cope with this problem. They in fact limit the accumulation of free tetrapyrroles among the cells by depressing expression of the entry enzymes of the C5-pathway in the dark. Moreover, an elaborate feedback control system prevents excess pigment accumulation in the dark. Another possibility is to rapidly “channel” the intermediates through larger complexes. This mechanism lowers the amount of solvent-accessible substrates and products and eliminates the risk of interaction with oxygen. For example, it was reported that Mg-chelatase interacts with Mg-Proto methyl transferase (Alawady *et al.*, 2005).

1.2.3.3 Feedback inhibition of 5-ALA synthesis in Angiosperms

The earliest control point of the C5-pathway is that of 5-ALA production, which is generally accepted to be the rate-limiting process of Chl biosynthesis (Beale and Weinstein, 1990). When angiosperms are grown in the dark, Chl synthesis leads to the formation of Pchlide, the only intermediate found to detectable levels. Once a critical level of Pchlide has been reached, 5-ALA synthesis is rapidly switched off (Granick, 1950). Only after illumination, when Pchlide is photoreduced to Chlide by POR, synthesis of 5-ALA resumes. In plants, the level of 5-ALA is controlled by a feedback loop exerted by heme and Pchlide at the level of GluTR (Beale, 1990; Huang *et al.*, 1989).

In *Arabidopsis*, GluTR is encoded by two genes, named *HEMA1* and *HEMA2*, which show different expression patterns (McCormac *et al.*, 2001). *HEMA1* is expressed in all photosynthetic tissues, whereas *HEMA2* is expressed only in roots. Despite the fact that *HEMA1* transcription is positively regulated by light, there are also two other mechanisms of control of GluTR, both exerted at the protein level. The first control is executed by an allosteric inhibitor of GluTR, heme. The first 31-34 amino acids at the N-terminus of the mature protein were accounted to be heme-responsive (Vothknecht, 1996). The second is executed by the FLUORESCENT (FLU) protein (Meskauskiene and Apel, 2002).

Meskauskiene *et al.* (2001) identified FLU in *Arabidopsis* using a genetic approach. In dark-grown angiosperms, Chl synthesis is blocked at the level of Pchlide and the authors found that this block is no longer operational in plants with a defective *FLU* gene. FLU interacts with GluTR and due to its absence, 5-ALA synthesis occurs in an uncontrolled

manner, leading to overproduction of free Pchlide molecules. Once illuminated, these free pigments trigger photooxidative damage (Meskauskiene *et al.*, 2001). Interestingly, FLU is unrelated to any of the enzymes known to be involved in tetrapyrrole synthesis. It is a nuclear-encoded plastid protein that, after import and processing, becomes tightly associated with plastid membranes. Orthologous of *FLU* occur in other plant species and have been named *TIGRINA*^{dl2} in barley (Lee *et al.*, 2003). Yeast two-hybrid screens allowed identification of its tetratricopeptide repeat motif, responsible for mediating the interaction with GluTR. Interestingly, the region of GluTR involved in protein-protein interaction with FLU, is located at the C-terminus and thus, far away from the heme regulatory site (Meskauskiene and Apel, 2002). This work explains how heme and FLU can independently regulate the C5-pathway (Figure 1.7). Nevertheless, the details on the mechanisms explaining how FLU can sense the actual Pchlide level are unknown.

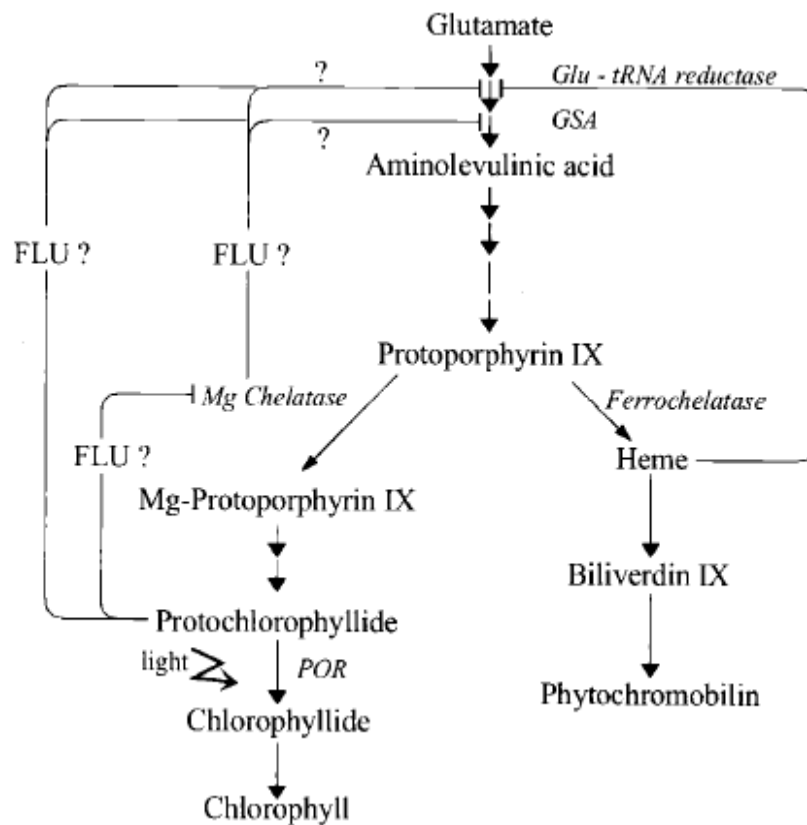


Figure 1.7 Scheme of tetrapyrrole biosynthesis in angiosperms, highlighting the negative feedback loops exerted by heme and FLU on glutamyl-tRNA reductase.

Names of controlling enzymes are indicated and question marks show several possibilities of how FLU may regulate 5-ALA synthesis. Taken from Meskauskiene *et al.* (2001).

In contrast to enzymes required for 5-ALA synthesis, all of the other enzymes catalyzing further steps of Chl biosynthesis seem to be present at levels that are not rate limiting. Their abundance and activity, however, may be under the control of other factors such as cell type and age of the plant (Spano and Timko, 1991; Witty *et al.*, 1993).

1.2.3.4 Light-dependent Protochlorophyllide reduction

The second major point of control of the C5-pathway occurs at the step of Pchl_{id}e reduction, the only light-requiring step in Chl synthesis. In higher plants, this reaction is catalyzed by light-dependent POR (Apel *et al.*, 1980). This enzyme is essential for plant greening, because unlike most other photosynthetic organisms, angiosperms have no other alternative to reduce Pchl_{id}e in the dark (see review by Armstrong, 1998). Eukaryotic light-dependent POR is a peripheral membrane-associated, monomeric enzyme of 35-38 kDa (Holtorf *et al.*, 1995). It is nucleus-encoded protein which is synthesized as a larger precursor: preprotein, containing a transit peptide at its N-terminus in the cytosol (Apel, 1981). During or after its post-translational import into the plastids, the transit peptide is cleaved off and POR operates as a mature protein once located inside the plastids.

In *Arabidopsis*, three structurally related but differentially expressed POR proteins and genes were identified, designated PORA, PORB and PORC (Reinbothe *et al.*, 1995; Armstrong *et al.*, 1995; Oosawa *et al.*, 2000). While PORA is active only during very early stages of the light-induced greening of etiolated seedlings, PORB persists during the transition from etiolated to light growth and is also abundant in green plants. The third POR enzyme, PORC, is expressed in older seedlings and adult plants. It was shown that both PORB and PORC play redundant roles in maintaining light-dependent Chl biosynthesis in green plants, and its expression is essential for their growth and development (Frick *et al.*, 2003).

1.2.3.5 LHPP as a link between skotomorphogenesis and photosynthesis of higher plants

At first glance, one might expect the PORA and PORB to accomplish redundant roles *in vivo*. In barley, PORA and PORB share approximately 85% of identity in amino acid sequences, both are light-dependent and NADPH-dependent enzymes that reduce Pchl_{id}e to Chl_{id}e *in vitro*. Although their reaction specificities are identical, they are strikingly different in their substrate requirements. There are several forms of Pchl_{id}e present in the

plastidic Pchlde pool which can be distinguished by spectroscopic techniques (Ryberg and Sundqvist, 1991). Structurally different forms of Pchlde, such as Pchlde *a* and Pchlde *b*, as well as their esterified and nonesterified forms, have been detected within different plastid compartments. The functions of most of these different Pchlde forms remain largely unknown. However, *in vitro* reconstitution experiments with the zinc analogs of Pchlde *a* and Pchlde *b*, permitted to propose a role for the PORA and PORB in etiolated barley plants.

During a couple of experiments it was first shown that the PORA and PORB display different substrate specificities. PORA was found to be specific for Pchlde *b* and PORB for Pchlde *a*. Moreover, *in vivo* studies detected Pchlde *b* and Pchlde *a* in etiolated barley plants and even allowed demonstrating that only Pchlde *a* bound with NADPH to PORB was reduced to Chlide *a*. In the reconstituted and isolated native complexes, a 5:1 stoichiometry of PORA-Pchlde *b*-NADPH to PORB-Pchlde *a*-NADPH was observed (Reinbothe *et al.*, 1999 and 2003). The major roles of the complex dubbed Light-Harvesting POR: Pchlde complexes (LHPP) were (i) light trapping and (ii) conferring photoprotection onto newborn seedlings after their germination in darkness (Figure 1.8).

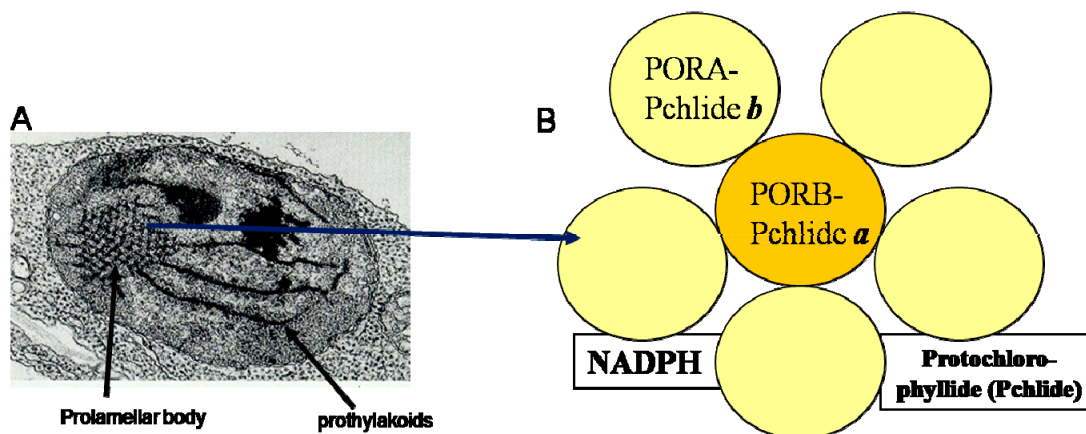


Figure 1.8 Model of a Light-Harvesting POR-Protochlorophyllide (LHPP) complexes in etiolated angiosperm seedlings.

LHPP is supposed to consist of 5 PORA-Pchlde *b*-NADPH ternary complexes and 1 PORB-Pchlde *a*-NADPH complexes, that are held together in ring-like structures in conjunction with membrane lipids of the prolamellar body of etioplasts. LHPP's two major functions are (i) light-harvesting and (ii) excess light energy dissipation.

The way of how LHPP may function is reminiscent to that of the major Light-Harvesting Complex of photosystem II, LHCII (Kühlbrandt *et al.*, 1994). By analogy to LHCII, which is composed of Chl *a* and Chl *b*, LHPP also contains two different types of pigments: Pchl *a* and Pchl *b*. However, in contrast to LHCII, these two pigments are bound to two different proteins: PORB and PORA, respectively. In the case of LHCII, a single protein is sufficient to function with both attached Chls. Furthermore, monomeric LHCII assembles to operate as trimer (Dreyfuss and Thornbeer, 1994), whereas LHPP contains even larger assemblies of the two POR proteins that additionally are developmentally regulated and may vary in size (Reinbothe *et al.*, 2004, Plant Sci.). As LHPP is located in prolamellar body of etioplasts, the native LHPP complex additionally contains galacto- and sulfolipids which drastically affect the spectral properties of the complex and help establish an overlap with the action spectrum of phytochrome operating in seedling de-etiolation. All of LHPP's constituents may be held together in ring-like structures in the prolamellar body of etioplast. In LHCII, energy absorbed by Chl *b* is rapidly (within less than 1ps) transferred to Chl *a*, where it remains for 1-3 ns. This energy transfer between different Chls is possible because of the different energy contents and life times of their excited states (Palsson *et al.*, 1994). Presumably, for the same reasons, a similar mechanism of energy transfer between Pchl *b* and Pchl *a*, operates in LHPP. Hereby, Pchl *b* bound to PORA in the periphery of the complex is not photoconvertible in the first instance but operates as antenna. When a conversion of Pchl *a* to Chl *a* by virtue of PORB has occurred, LHPP dissociates, as deduced from the *in vitro*-reconstitution experiments and PORA gains active as Pchl *b* reducing enzyme. This reaction, however, operates only for short period after de-etiolation, after which PORA is degraded by proteases. By contrast, PORB remains active in illuminated plants and may cooperate with PORC in mature plants.

1.3 The import of the pPORA and pPORB into the plastids

1.3.1 A brief overview of the general protein import pathway

Chloroplasts contain approximately 2000-3000 different proteins of which the overwhelming part is encoded in nuclear DNA. It was for a long time believed that most of the proteins destined to the primordial chloroplast acquired cleavable NH₂-terminal transit sequences for import (Keegstra *et al.*, 1989). However, recent proteomic studies have shown that this view is too simple.

Kleffmann *et al.* (2004) identified 604 chloroplast proteins of which only 376 were predicted to contain NH₂-terminal transit sequences. Of the remainder, 37 were predicted to have a mitochondrial targeting signal, 40 to have a signal peptide for translocation into the endoplasmic reticulum (ER), and 142 to possess no cleavable presequences. Evidence is emerging for the dual targeting of cytosolic proteins to mitochondria and chloroplasts (Peeters and Small, 2001), for the plastid import of transit peptide-less precursors (Miras *et al.*, 2002, 2007), and for the involvement of the ER in the import of certain precursors into chloroplasts (Villarejo *et al.*, 2005).

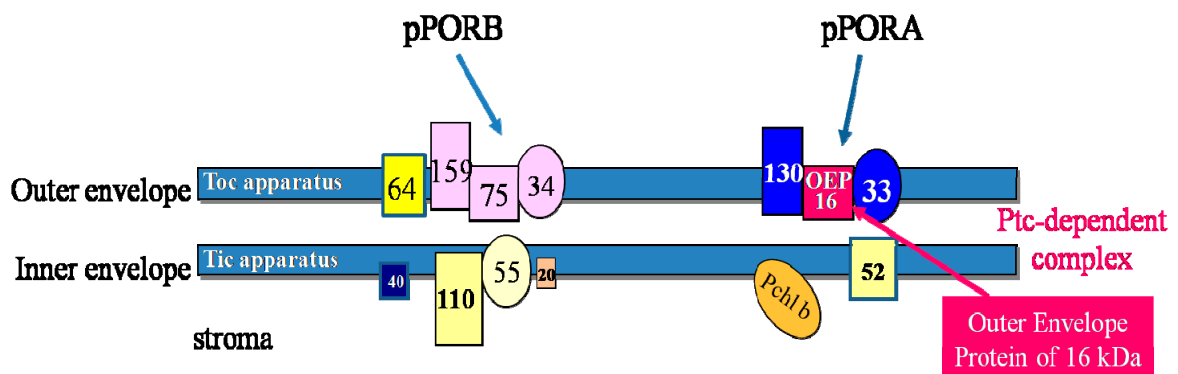


Figure 1.9 Schematic view of the differential import of pPORA and pPORB into the plastids.

While pPORA embarks the protochlorophyllide-dependent translocon, PTC, during its substrate-dependent import, pPORB enters the plastids via the TOC and TIC machineries. Numbers give molecular masses of the components operating in either pathway.

Chloroplast precursor proteins containing cleavable NH₂-terminal transit sequences interact with translocon complexes of the outer and inner plastid envelope membranes, called the TOC and TIC machineries (Schnell *et al.*, 1997). Pioneering work performed for pea chloroplasts identified the TOC complex to consist of three core components: TOC159, TOC75, and TOC34 (Perry and Keegstra, 1994; Hirsch *et al.*, 1994; Kessler *et al.*, 1994; Schnell *et al.*, 1994; Tranel *et al.*, 1995; Bölter *et al.*, 1998a; Chen *et al.*, 2000; Jelic *et al.*, 2002), (Figure 1.9). Likely in concert, these three proteins mediate the recognition, binding and translocation of the cytosolic precursors across the outer plastid envelope membrane (see Keegstra and Cline, 1999; Jackson-Constan and Keegstra, 2001; Bedard and Jarvis, 2005; Hofmann and Theg, 2005; Kessler and Schnell, 2006, for reviews).

Biochemical and molecular genetic studies using the model plant *Arabidopsis thaliana* have challenged the view that all of the different transit peptide-containing cytosolic precursors would enter the organelle through the same, trimeric, TOC159/TOC75/TOC34 import machinery. Bauer *et al.* (2000) identified two TOC proteins that complement the previously discovered main preprotein receptor protein TOC159. All three proteins share conserved GTP binding domains and membrane anchors but differ in the length of their cytosolically exposed NH₂-terminal presequence receptor domains (Bauer *et al.*, 2000; Ivanova *et al.*, 2004). Pull-down and genetic assays confirmed that while TOC159 is involved in import of photosynthetic precursors, TOC120 and TOC130 are responsible for the import of other, non-photosynthetic proteins (Smith *et al.*, 2004). Furthermore, it was shown that a TOC regulatory GTP-binding protein consists of twin components, termed TOC33 and TOC34, which exhibit different precursor specificities and expression patterns during plant development (Jarvis *et al.*, 1998; Gutensohn *et al.*, 2000; Jelic *et al.*, 2003; Kubis *et al.*, 2004), (see below). Last but not least, the β -barrel protein TOC75, which establishes a hydrophilic translocation channel through which the majority of the cytosolic precursors are transported across the outer envelope (Hinnah *et al.*, 1997, 2002), is encoded by three genes in *Arabidopsis* of which two have different expression patterns and presumed functions (Baldwin *et al.*, 2005). Evidence is accumulating for the existence of multiple, regulated TOC complexes in the outer envelope of chloroplasts.

The TIC complex is less well characterized than the TOC complex. It consists of at least three core components: TIC110 (Kessler and Blobel, 1996), TIC40 (Wu *et al.*, 1994; Stahl *et al.*, 1999) and a caseinolytic protein (Clp) C-class Hsp93 chaperone (Akita *et al.*, 1997; Nielsen *et al.*, 1997; Constan *et al.*, 2004). Other, presumably auxilliary components

comprise TIC55 (Caliebe *et al.*, 1997), TIC22 and TIC20 (Kouranov *et al.*, 1998; Kouranov *et al.*, 1999; Chen *et al.*, 2002), as well as TIC62 (Küchler *et al.*, 2002). The different TIC proteins were isolated by their co-purification with certain model precursors in transit across the inner envelope and chemical crosslinking.

1.3.2 Differential plastid import of the pPORA and pPORB

All angiosperm POR proteins are nucleus-encoded plastid proteins that must be imported post-translationally from the cytosol. *In vitro* and *in vivo* experiments have shown that the precursors of PORA (pPORA) and PORB (pPORB) enter the plastids through different pathways (Figure 1.9). Import of pPORA depends on the presence of its substrate, Pchl_{ide} (Reinbothe *et al.*, 2000; Kim and Apel, 2004), which is localized in the envelope membranes (presumably at the stromal side of the inner envelope, S. Reinbothe, unpublished results). By contrast, import of pPORB does not depend on the presence of Pchl_{ide}.

Several approaches were used to answer the question of whether the pPORA and pPORB would enter the plastids through the same or distinct protein import complexes. These include: (i) competition experiments using excesses of the small subunit of ribulose-1,5-bisphosphate carboxylase/oxygenase, ferredoxin and other photosynthetic proteins, (ii) antibodies against known components of the TOC machinery and (iii) crosslinking carried out with different derivative pPORA and pPORB precursors. These studies revealed that pPORB enters the plastids via the standard protein import machinery, whereas pPORA enters the plastids via a non-canonical import machinery. Using crosslinking approaches, plastid envelope proteins could be identified that interact with the pPORA during its Pchl_{ide}-dependent import, called protochlorophyllide-dependent translocon proteins, PTCs. Using a ¹²⁵I-APDP-derivatized precursor, Reinbothe *et al.* (2004a) could show that 8-10 different proteins co-purify with the precursor in junction complexes between the outer and inner envelope membrane that were established at 0.1 mM Mg-GTP and 0.1 mM Mg-ATP. Four of these proteins could be identified by protein sequencing. The structure and role of three of these proteins that are of immediate interest to the present work will be briefly discussed here.

1.3.3 PTC52, a Pchlide *a*-oxygenase located in the inner envelope of barley and *Arabidopsis* chloroplasts

PTC52 belongs to a small, 5-member family of ubiquitous non-heme oxygenases that is defined by the presence of Rieske and mononuclear iron binding domains. Besides PTC42, members of this family comprise the inner plastid envelope translocon protein TIC55, the lethal leaf spot protein LLS1, chlorophyllide *a* oxygenase (CAO), cholin monooxygenase (CMO). A comprehensive bioinformatics study suggests that PTC52, PAO (Pheophorbide *a* oxygenase), CAO, and TIC55 evolved from a cyanobacterial ancestral gene (*SLR1747*) whose function may have evolved during the transition to oxygenic photosynthesis (Gray *et al.*, 2004). In contrast, the *CMO* gene appears to have a separate origin and is more closely related to enzymes in soil bacteria that catabolize aromatic compounds (Gray *et al.*, 2004). In addition to the highly conserved Rieske (CxHx₁₆₋₁₇Cx₂H) and mononuclear iron binding (Nx₂Dx₃₋₄Hx₄H) motifs, PTC52, PAO and TIC55 proteins from different plant species share the presence of a conserved, CxxC motif reminiscent of thiolreductases at approximately 73 amino acids from the carboxy terminus which is also found in homologs from *Synechocystis* and *Anabena*. Via this CxxC motif, TIC55, PTC52 and PAO are prone to regulation by the thioredoxin system and also respond to oxidative stress (Bartsch *et al.*, 2008). No CxxC motif is present in CAO, which exhibits a larger amino terminus not contained in PTC52, PAO or TIC55, and CAO does not respond to either the thioredoxin system or oxidative stress (Bartsch *et al.*, 2008).

All of these Rieske Fe-S proteins are predicted to be chloroplast-localized. CAO and LLS1 act in chlorophyll biosynthesis and degradation, respectively. By contrast, PTC52 has an anabolic function. It associates with the pPOR at late stages of import when the precursor is accessing the inner envelope. *In vitro* import, fractionation and other biochemical experiments showed that PTC52 is an inner plastid envelope Pchlide *a* oxygenase which drives synthesis of Pchlide *b*, the cognate substrate of PORA. Loss-of-function mutation in the *Arabidopsis* *PTC52* gene gave rise to an embryo-lethal phenotype, suggesting an essential role of PTC52 *in planta*.

1.3.4 TOC33 and TOC34, twin GTPases in the outer envelope with partially redundant roles

The second component that was isolated by its co-purification with pPORA is a 33kDa protein related to TOC33 and TOC34. TOC33 and TOC34 are GTP binding proteins first identified in pea and later in *Arabidopsis* chloroplasts. They share the same basic architecture and consist of a GTP-binding domain (G-domain) and a membrane anchor domain (M-domain), (Bauer *et al.*, 2000; Chen *et al.*, 2000). Nevertheless, they exhibit major differences in their expression patterns (Jarvis *et al.*, 1998; Gutensohn *et al.*, 2000).

Functional tests have made use of pull-down assays employing AtTOC33 and AtTOC34 mutant proteins lacking their M-domains, called AtTOC33 Δ M and AtTOC34 Δ M, respectively. Gutensohn *et al.*, (2000) reported that AtTOC33 Δ M bound higher levels of pSSU than AtTOC34 Δ M when both proteins were preincubated in the presence of 1 mM GTP. However, AtTOC33 Δ M and AtTOC34 Δ M preincubated without GTP showed no difference in the binding capacity for pSSU. The employed experiments used some sort of competition assay in which the amount of non-bound precursor was determined by its sequestration by isolated spinach chloroplasts. The use of high GTP concentrations (1 mM instead of 0.1 mM or nothing) to analyze the initial steps of protein translocation into isolated plastids makes difficult to compare these results with data obtained by others. Using biochemical procedures it could be demonstrated, for example, that cross-linking of pea TOC34 to preproteins occurs only in the absence of added GTP or ATP (Kouranov and Schnell, 1997). Interestingly, the observed phenotype (especially the chlorophyll deficiency) of the *ppi1* mutant could be complemented by overexpression of either TOC33 or TOC34 (Jarvis *et al.*, 1998) implying that both proteins are able to bind the same set of precursors, at least when the plants were grown in continuous white light. In addition, in two recently isolated knock-out lines that are deficient in AtTOC33 and AtTOC34 called *ppi3-1* and *ppi3-3*, respectively, no changes were observed with respect to chlorophyll content, chloroplast ultrastructure, endogenous levels of chloroplast proteins, and chloroplast protein import (Constan *et al.*, 2004). These results implicate redundant functions of AtTOC33 and AtTOC34 *in planta*.

Mutants that are defective in the AtTOC33 and AtTOC34 genes have been isolated (Jarvis *et al.*, 1998; Reinbothe *et al.*, 2005). Despite the fact that import of certain precursor proteins was slightly diminished (15-25% of wild-type levels) under *in vitro* conditions, the

plastid protein import (ppi) 1 mutant that lacks AtTOC33 showed especially reduced amounts of POR in darkness and formed abnormal prolamellar bodies (Jarvis *et al.*, 1998) where POR is the major protein constituent (Dehesh and Ryberg, 1985). Strikingly, *ppi1* etioplasts accumulated massive amounts of a POR-related higher molecular mass protein of 40 kDa (Jarvis *et al.*, 1998), indicative of the PORA precursor (Reinbothe *et al.*, 1996). Findings that etiolated seedlings displayed a delay in greening upon light exposure seemed further suggestive of a lack of import of pPORA. It was further demonstrated that import of pPORA is drastically reduced in *ppi1* plastids *in vitro*. *In vivo* studies using the same AtTOC33-deficient *ppi1* as well as AtTOC34-deficient *ppi3* mutant suggested, however, that AtTOC34 rather than AtTOC33 would be operative in the substrate-dependent import of pPORA (Kim *et al.*, 2005). Work is needed to explore this point.

1.3.5 PTC16/OEP16, a solute and amino acid selective channel protein in the outer plastid envelope

Among the PTC proteins identified for barley and *Arabidopsis* there is a 16 kDa outer plastid envelope protein (Figure 1.9) related to a previously characterized envelope protein of pea chloroplasts called OEP16 (Pohlmeyer *et al.*, 1997; Baldi *et al.*, 1999). OEP16 in barley and pea chloroplasts is a nuclear gene product (Pohlmeyer *et al.*, 1997; Baldi *et al.*, 1999). In contrast to other nucleus-encoded chloroplast proteins, PTC16 (OEP16) is synthesized without cleavable chloroplast transit peptide for import. Work of Pohlmeyer *et al.* (1997) suggested that pea OEP16 inserts into the lipid bilayers spontaneously and does not interact with other proteins. By contrast, work performed by Reinbothe *et al.* (2005) revealed an association of pPORA with OEP16 and plastid envelope proteins of 130 kDa (PTC130), 52 kDa (PTC52) and 33 kDa (PTC33) forming the PTC complex (Reinbothe *et al.*, 2004 b).

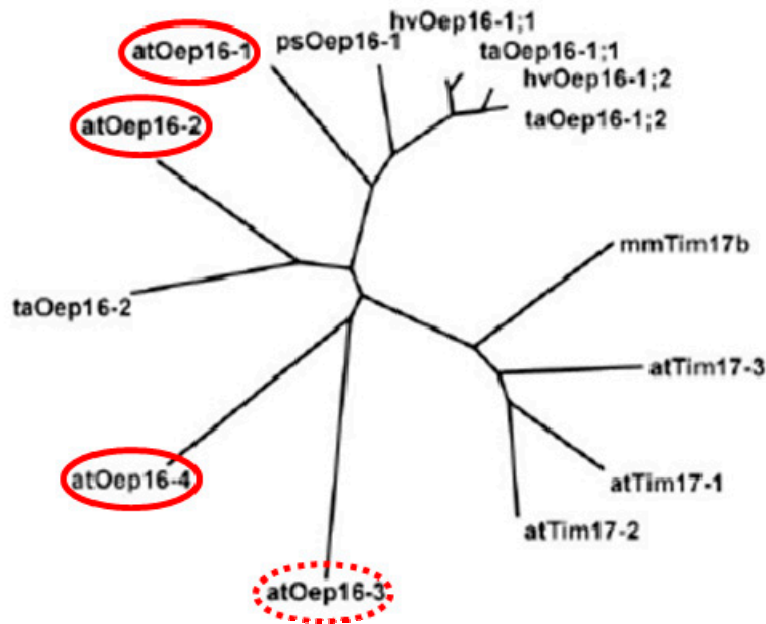


Figure 1.10 Identification of barley OEP16-1 (HvOEP16-1).

Barley OEP16-1, identified as a crosslink partner of pPORA, is a member of the protein and amino acid transporters (PRAT) family that comprises OEP16 proteins as well as TIM proteins operating in the translocation of nucleus-encoded proteins across the inner mitochondrial membrane. Red circles indicate *AtOep16-1*, *AtOep16-2*, *AtOep16-3* and *AtOep16-4*. While *AtOep16-1*, *AtOep16-2*, *AtOep16-4* are plastid proteins, *AtOep16-3* is found in mitochondria. Modified from Reinbothe *et al.* (2004).

OEP16 establishes a small gene family comprising three members, designated *AtOEP16-1* (At2g28900), *AtOEP16-2* (At4g16160) and *AtOEP16-4* (At3g62880), (Figure 1.10), (Drea *et al.*, 2006). A fourth relative exists (*AtOEP16-3*; encoded by At2g42210) that appears not to belong to this group and is, unlike the other members predicted to be plastid proteins, localized in mitochondria (Philippar *et al.*, 2007). *AtOEP16-1* shows the highest protein sequence identity (62%) to OEP16 from pea (Pohlmeyer *et al.*, 1997; Murcha *et al.*, 2007) and to HvOEP16-1;1 from barley (52%), which was identified as partner of the cytosolic precursor of NADPH:protochlorophyllide (Pchl_{ide}) oxidoreductase A (pPORA) during its Pchl_{ide}-dependent plastid import (Reinbothe *et al.*, 2004 a+b). Two non-exclusive functions currently being considered for the OEP16-1 protein in the outer envelope of chloroplasts are (i) a voltage-gated, amino acid-selective channel (Philippar *et al.*, 2007) and (ii) an import channel for pPORA (Reinbothe *et al.*, 2004 a +b). Knock-out mutants in *A. thaliana* for *AtOEP16-1* (designated *Atoep16-1* corresponding to At2g28900) have provided different results (Pollmann *et al.*, 2007; Philippar *et al.*, 2007). We found that the absence of *AtOEP16-1* correlates with the lack of import of pPORA, aberrant etioplast

ultrastructures and the accumulation of free, photoexcitable Pchl_a molecules that triggered cell death upon irradiation of dark-grown plants (Pollmann *et al.*, 2007). By contrast, Philippar *et al.* (2007) observed no import defects of pPORA, normal etioplast ultrastructures and unimpaired greening.

In the present work, two major questions were addressed. What is the reason for completely different phenotypes described for two *Atoep16-1* knock-out mutants derived from the same T-DNA insertion SALK_018024.50.90.X (Pollmann *et al.*, 2007; Philippar *et al.*, 2007)? Is the cell death regulation in the *Atoep16-1* mutant that we identified (Pollmann *et al.*, 2007), comparable to the singlet oxygen-dependent pathway reported for the *flu* mutant (Meskauskiene *et al.*, 2001; op den Camp *et al.*, 2004; Wagner *et al.*, 2004; Danon *et al.*, 2005)? To this end, four independent *Atoep16-1* mutants were isolated from the original seed stock provided by the Salk Institute that displayed different cell death properties. Two of these mutants have phenotypes suggestive of the presence of additional, exogenic mutations that, besides the main mutation in the *AtOE16-1* gene, affected singlet oxygen production and/or signalling. The other two mutants correspond to the lines described by Pollmann *et al.* (2007) and Philippar *et al.* (2007), thus solving the controversy in the literature with regard to the phenotype of *Atoep16-1*. In the second part of this work, evidence is presented that cell death execution in mutant *Atoep16-1* occurs in a *flu*-independent manner. This result underscores the complexity of cell death regulation in *Arabidopsis* in response to singlet oxygen.

Chapter 2 Materials and Methods

2.1 Plant material and culture conditions

2.1.1 Choice of plant material

2.1.1.1 *Arabidopsis thaliana*

Arabidopsis thaliana is a model organism for a wide range of research in plant biology. Its small genome is entirely sequenced (the AGI, 2000) and many mutants of that plant are available. In order to complete the biochemical data about AtOEP16-1 protein function, the *in vivo* studies were done using a reverse genetic approach.

2.1.1.2 Barley

Barley (*Hordeum vulgare* L.) is a plant which represents more advantages in biochemical studies than *Arabidopsis*, due to the greater quantities of available fresh material.

2.1.2 Ecotypes and mutant alleles

Arabidopsis thaliana wild type and mutants used in these studies: *Atoep16-1* (At2g28900) and *flu-g* (At3g14110) belong to Columbia ecotype and were purchased from SALK Institute (<http://signal.salk.edu/>) through TAIR (<http://www.arabidopsis.org/>).

As wild type barley, the German spring barley variety Scarlett was used. Homozygous *tigrina-d¹²* mutant (*Hordeum vulgare* L.cv. Svalöf's Bonus) grains were kindly donated by Diter von Wettstein.

2.1.3 Cultivation of plants in soil

Both plants, *Arabidopsis* and barley, were grown in soil mixture provided by Motte-Domaine. To eliminate pests, the soil was presoaked with distilled water and then sterilized in an autoclave for at least 20 min at 120°C. Finally, the soil was treated with Trigard, a chemical pesticide for insect abatement, accordingly to manufactured instructions. The grains, without being sterilized, were sowed directly on the soil and kept for 48 h at 4°C (vernalization) before exposure to light. Drug-resistant plants at a stage of transplant small

seedlings were transferred from agar plates to soil. In order to keep a well-moistened soil, the pots were covered with a plastic dome for several days. Proper drainage of the soil was achieved by using pots with bottom perforations. Plants were watered by subirrigation twice a week.

2.1.4 *In vitro* culture

In vitro culture was applied only to *Arabidopsis thaliana*. To keep the sterile conditions, all necessary manipulations with seeds and plants were done under the laminar flow bench.

Seeds sterilization:

Surface sterilization of seeds was done by first washing seeds for 5 min in the chlorine solution 5 times diluted in 95% ethanol. Chlorine solution is prepared by dissolving one pill of bleach (Eau Ecarlate) in 40 ml of distilled water. Afterwards, the chlorine solution was removed and seeds were washed twice in 95% ethanol for 5 min. Finally, seeds were air-dried under the laminar flow overnight.

Use of solid medium:

Sterilized seeds were sowed on sterile MS medium. 1L of growth medium contains: 4,33 g of Murashige and Skoog (MS) mineral salts (Sigma), 10 g of sucrose, 0,5 g of MES and 8-12 g of agar. After adjusting pH to 5,7 with KOH, a medium was sterilized by autoclaving and finally poured into the Petri dishes. Drug-resistant plants were selected on MS media containing a suitable selective agent. In the presence of the drug, sensitive plants died, lost chlorophyll or arrested their development. Working concentrations of drugs used in this thesis were:

- Kanamycin sulfate (Sigma), [50 µg/ml]
- Glufosinate ammonium (Riedel-de Haën), [5 µg/ml]

Before exposing Petri dishes with seeds to light, they were placed in the dark at 4°C for 48 h to overcome dormancy.

2.1.5 Culture conditions

	Light conditions	Light intensity	Temperature	Lamps
Cultivation in soil	Long day (16h\8h)	80 $\mu\text{mol}/\text{m}^2\text{s}$	Day: 23°C Night: 21°C	White = Mazda Fluor 36W Fluorescent = Osram Fluora 36W
	Continuous day	60 $\mu\text{mol}/\text{m}^2\text{s}$	23°C	White = Mazda Fluor 58W
<i>In vitro</i> culture	Long day (16h\8h)	90 $\mu\text{mol}/\text{m}^2\text{s}$	Day: 23°C Night: 21°C	White = Mazda Fluor 58W Fluorescent = Osram Fluora 58W
	Continuous day	120 $\mu\text{mol}/\text{m}^2\text{s}$	23°C	White = Philips 40W

Table 2.1 Culture conditions for plants cultivated in soil and *in vitro*

2.1.6 Photobleaching test conditions

Seeds of *Arabidopsis* were plated next to each other in a parallel line, on plates with MS - medium containing 12 g of agar /L (see a Figure 2.1). They were placed for 2 d in the cold room and then transferred for one hour to light ($120 \mu\text{mol}/\text{m}^2\text{s}$) to induce germination (Figure 2.1, T_0). Afterwards plates were kept for 5 d in the dark in a vertical orientation (to visualize the length of hypocotyls), (Figure 2.1, T_5). Etiolated plants were then exposed to strong continuous light ($210 \mu\text{mol}/\text{m}^2\text{s}$ provided by Philips Master lamps or $125 \mu\text{mol}/\text{m}^2\text{s}$ provided by Mazda Fluor). Photos were taken 24 h, 48 h, 5 d or 3 w after exposure to light.

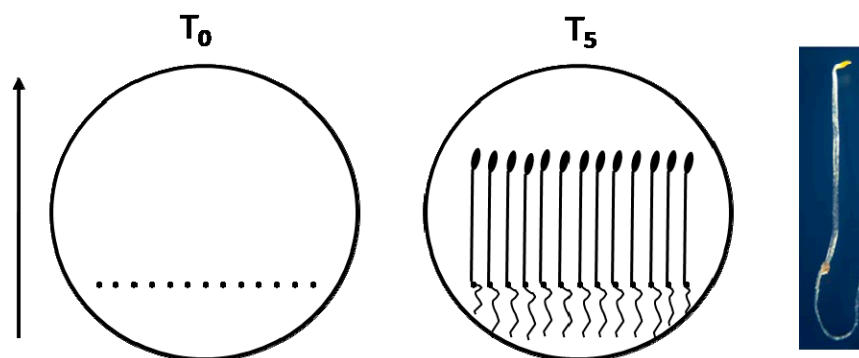


Figure 2.1 Schematic representation of the photobleaching test for *Arabidopsis*

T_0 : time before etiolation ; T_5 : 5 d of etiolation. A vertical arrow represents a vertical growth. A photo shows a representative *Arabidopsis thaliana* seedling grown in dark for 5 d.

2.2 Cloning of cDNA coding for AtOEP16-1 protein from *Arabidopsis*

2.2.1 Bacterial genotypes, solutions and culture conditions

Two bacterial hosts were used: *Escherichia coli* with strains DH5 α for cloning and *Agrobacterium tumefaciens* strain GV3121 for stable *Arabidopsis* transformation.

Bacterial transformation was done by electroporation (Gene Pulser TM of Biorad – Resistance: 200 Ohms – Voltage: 2,5 kV – Capacitance: 25 μ F – Pulse length: 5 msec) according to the provided instructions.

Transformed bacteria were incubated in LB (Luria Bertani Broth, Sigma) liquid media with gentle agitation (~200 rpm) or on LB agar plates (LB + 1,5% agar) for 12 h at 37°C for *Escherichia coli* and for 48 h at 28°C for *Agrobacterium tumefaciens*. Selection of transformed bacteria was done by incubating them in growing medium containing appropriate antibiotic (depending on the resistance marker in chosen vectors) at standard concentrations:

Host	Antibiotic	Final concentration
E.coli DH5 α	Spectinomycin	100 μ g/ml
A.tumefaciens GV3121	Rifampycin	50 μ g/ml
	Gentamycin	25 μ g/ml
	Spectinomycin	100 μ g/ml

Table 2.2 Antibiotic concentrations used for the selection of clones in different bacterial hosts.

2.2.2 Vector constructions and cloning strategies

In order to complement *Atoep16-1* mutant, three constructions were performed:

- 35S::OEP16
- 35S::GFP::OEP16
- 35S::OEP16::YFP.

Additionally, fusions of fluorescent proteins: GFP (Green Fluorescent Protein) and YFP (Yellow Fluorescent Protein) to AtOEP16-1 protein at their N- and C-terminus respectively, under the control of the CaMV 35S promoter, enabled to visualize *in vivo* a subcellular localization of AtOEP16-1 protein.

DNA cloning was performed following Gateway Technology (Invitrogen). It is a cloning method (Figure 2.2) based on the bacteriophage lambda site-specific recombination system which facilitates the integration of viral genes into the *E.coli* chromosome and switch between the lytic and lysogenic pathways. Lambda-based recombination involves two major components: 1) the DNA recombination sequences (*att* sites) and 2) the proteins that mediate the recombination reaction (Clonase enzyme mix). The advantage of using such technology for cloning is the ease of manipulation and the big gain of time. Indeed, within the few hours (the same day) we can prepare the insert, clone it in the appropriate vector and transform the bacterias. Such cloning results in recombinant vectors (Entry vectors) that can be easily used to transfer and to clone the insert in a set of vectors for multiple purposes (*eg.* overexpression, RNA silencing, reporter gene fusions etc.).

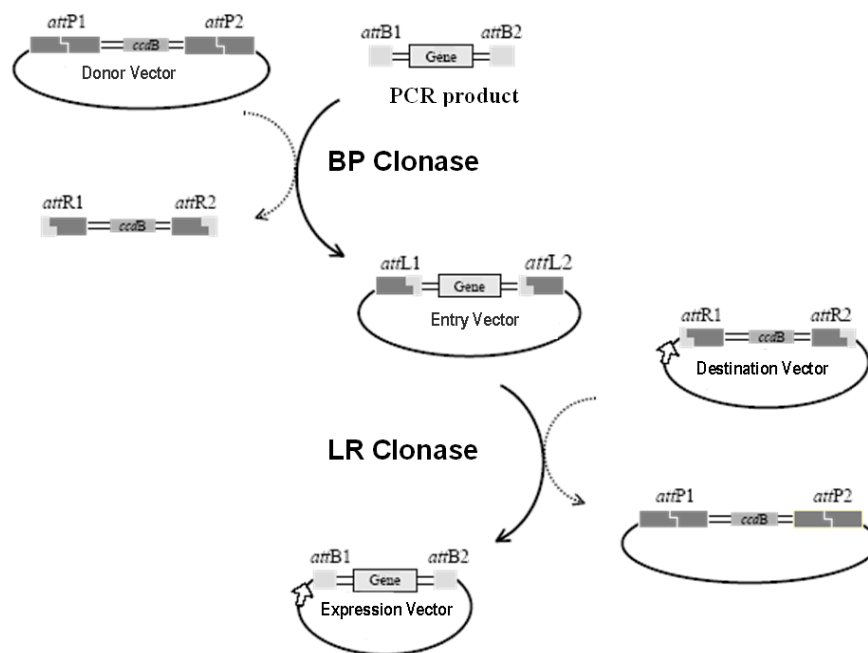
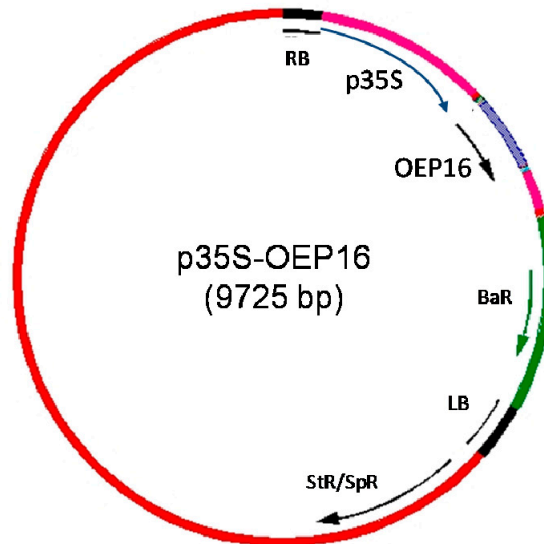


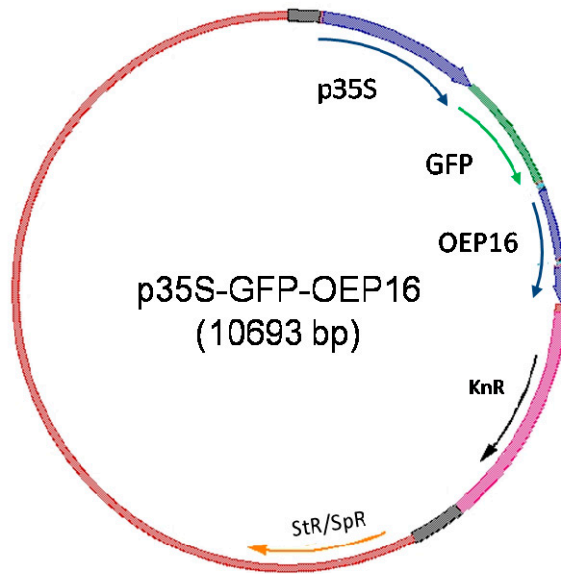
Figure 2.2 Schematic representation of Gateway TM system

attP, *attB*, *attR* and *attL*: recombinaison sites. *ccdB*: encoding a toxic protein for most bacterias.

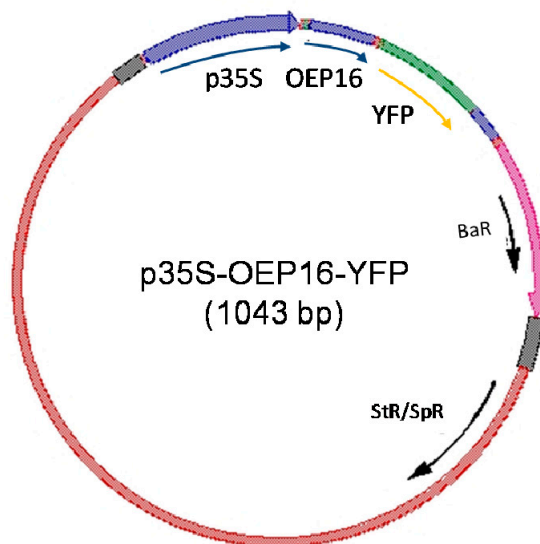
PCR reactions with primers containing *attB* sites to amplify cDNA coding for AtOEP16-1 protein of *A.thaliana* were generated by Jean-Marc Bonneville. For 35S::OEP16::YFP construction, cDNA of AtOEP16-1 without codon STOP was amplified. The *attB*-flanked PCR products were put via BP reaction (according to the manufacturer's instructions, performed by Gabrielle Tichtinsky) into the donor vector pDONR221 to yield the entry clones: pEOEP16 and pEOEP16_no_STOP. The final fusion products were generated via LR reaction in the Gateway compatible binary T-DNA destination vectors: pB7WG2, pK7WGF2 and pB7YWG2 (<http://www.psb.ugent.be/gateway>). The resulting expression vectors are referred to as: p35S-OEP16, p35S-GFP-OEP16 and p35S-OEP16-YFP, respectively (Figure 2.3).



a) p35S-OEP16



b) p35S-GFP-OEP16



c) p35S-OEP16-YFP

Figure 2.3 Expression vectors generated via Gateway technology.

a) p35S-OEP16; b) p35S-GFP-OEP16; c) p35S-OEP16-YFP. They consist of binary vectors carrying the resistance for the antibiotic spectinomycin (*StR/SpR*). Their T-DNA contains AtOEP16-1 coding sequence (without codon STOP in c) under the control of promoter and terminator 35S and the genes *BaR* (for a and c) and *KnR* (for b) conferring resistance to the herbicide glufosinate ammonium and for the antibiotic kanamycin, respectively.

Afterwards, 2 μ l of each of LR reactions were used for the transformation by electroporation of *E.coli* bacteria. Subsequently, transformants were selected on LB agar plates containing spectinomycin (resistance marker for all of three used gateway binary vectors: pB7WG2, pK7WGF2 and pB7YWG2). Additionally, PCR of several colonies using appropriate primers for the insert helped in selecting clones which carry the correct insert. Expression vectors (p35S-OEP16, p35S-GFP-OEP16 and p35S-OEP16-YFP) were then purified from colonies harboring the correct insert, using a DNA miniprep method based on the alkaline lysis procedure (developed by Birnboim and Doly; Nucleic Acids Research 7:1513, 1979) and characterized, using subsequent restriction analysis. The sequence of the correct construct in T-DNA was also verified by sequencing, using a primer in the CaMV 35S promoter. Sequencing was restricted to the following vector parts:

- 1) For p35S-OEP16, the fusion site between the CaMV 35S promoter and the *AtOEP16-1* gene
- 2) For p35S-GFP-OEP16, the fusion site between the CaMV 35S promoter and GFP protein as well as between GFP and *AtOEP16-1* gene
- 3) For p35S-OEP16-YFP, the fusion site of the CaMV 35S promoter to the *AtOEP16-1* gene (without STOP codon) on the one hand and its fusion site to YFP on the other hand.

Subsequently, the vectors were transformed into the *A.tumefaciens* bacteria, strain GV3121, via electroporation. The presence of the correct T-DNA was verified by PCR in selected colonies, before proceeding with plant transformation experiments. One colony of *Agrobacterium* for each construct was chosen to transform *Atoep16-1* mutant plants destined for the complementation.

2.3 Genetic manipulations of plants

2.3.1 Stable transformation

2.3.1.1 Transformation by “floral dip”

A.thaliana plants of *Atoep16-1* mutants (4 w old), ecotype Columbia, were transformed by the “floral dip” method (adapted from Clough and Bent; 1998) based on dipping the inflorescence shoots into the 400 mL of *Agrobacterium* (OD₆₀₀=0,8) suspension. Each construction was used for 6 pots (one pot contained around 50 plants).

2.3.1.2 Selecting transformants

After each transformation experiment, selection of the first, the second and the third generation of transgenic plants (T1, T2 and T3) was performed as follows:

1) Sawing 100 mg of sterile dry seeds of transformed plants on 150 mm Petri dishes with MS (8g of agar/L) medium containing:

→ antibiotic kanamycin sulfate (Sigma) [50µg/mL] for *Atoep16-1* mutants transformed with 35S::GFP::OEP16 construct

→ herbicide glufosinate ammonium (Riedel-de Haën) [5µg/mL] for *Atoep16-1* mutants transformed with 35S::OEP16 and 35S::OEP16::YFP constructs.

The choice of the selection medium was based on the presence of resistance markers in the gateway binary vectors used in this study. Successful transformed plants grew as green seedlings with long roots whereas untransformed seedlings were yellowish with short roots. Green transformants were then transferred to soil.

2) Subsequently, once the plants start to flower, PCR of transformants using appropriate primers for the insert was used to select those plants which contained the correct construct of interest.

3) Finally, transformants containing the fluorescent proteins GFP and YFP (35S::GFP::OEP16 and 35S::OEP16::YFP) were observed first, under epifluorescence microscope and later under confocal microscope (see § 2.7.2.).

2.3.2 Plant crossing

Arabidopsis naturally self-pollinates, therefore the generation of cross-progeny requires some intervention by the investigator. It is crucial to select suitable flowers in the cross. To reduce the possibility of self-fertilization, only closed flowers from the female parents in which the tips of the petals were just visible, were chosen. Other flowers were removed. For the male parents, opened flowers with visibly shedding pollen were selected. Crossing procedure was performed under a dissecting microscope using the forceps. All anthers (6) were removed, but the intact carpels were left on the female parent. After 48 h, an opened flower from the male parent was removed and squeezed near the base with the forceps. This spread out the flower parts, separating the anthers from the other organs. The convex surface of the anthers was brushed against the stigmatic surface of the exposed carpels on the female parent. Finally, the crosses were labeled by tying a piece of sewing thread around the stem of the female parent. The F1 seeds were collected 2 w afterwards.

2.4 Analysis of nucleic acids

2.4.1 DNA

2.4.1.1 Synthesis of oligonucleotides

Synthesis of oligonucleotides was performed by Sigma-Aldrich, Genosys company. They were used as primers for PCR methods. A list of used oligonucleotides is enclosed in the appendix A.

2.4.1.2 Amplification of DNA fragments by PCR

Amplification by PCR of *AtOEP16-1* cDNA for cloning purposes was performed using high-fidelity *Taq* DNA Polymerase *Pfx* (Fermentas), accordingly to recommended standard reaction conditions. Cycling conditions consisted of an initial denaturation step of 94°C for 5 min, followed by 10 cycles of 94°C for 15 seconds, 52°C for 10 seconds and 68°C for 45 seconds, followed by 20 cycles of 94°C for 15 seconds and 68°C for 1 minute, with final elongation step of 68°C for 10 min. A list of used primers is enclosed in the appendix A.

For genotyping and bacterial colony screening purposes, Biotaq™ DNA polymerase (Bioline) was used. Final reaction volume of 20 µL consisted of 10-20 ng of DNA (1 µL), 0,2 mM of each dNTP, 1,5 mM MgCl₂, 0,4 mM of each primer, 1U of DNA polymerase and 2 µL of 10X buffer (supplied by Bioline). After denaturation at 94°C for 5 min, n number of amplification cycles were performed (5 min at 94°C followed by 1-1,5 min at 55°C -62°C ; depending on size of amplified fragment and T_m of primers; and a cycle of 72°C for 1 min), then final elongation step of 5 min at 72°C. A list of used primers is enclosed in the appendix A.

2.4.1.3 Analysis of nucleic acids on agarose gel

Nucleic acids mixed with 3% glycerol (v/v) and 0,025% bromophenol blue (w/v), were separated by electrophoresis on agarose gel (1% of agar (w/v), 50 mM Tris acetate, 50 mM boric acid, 1,25 mM EDTA, 2% of ethidium bromide (w/v)). Finally, nucleic acids were visible after exposing agarose gel to UV light (320 nm).

2.4.1.4 Extraction of DNA fragments from agarose gel

After amplification of DNA fragments and subsequent separation of nucleic acids on agarose gels, a gel band corresponding to size of a fragment of interest was cut under UV light. Then, DNA was purified from agarose gel using NucleoSpin® Extract II kit (Machery-Nagel), accordingly to manufacturer's protocol.

2.4.1.5 DNA sequencing

The dideoxynucleotidic incorporation method originally developed by Sanger *et al.* (1977) was used for sequencing of DNA fragments (amplified or cloned into the plasmids). DNA sequencing was performed in Pôle Biologie Campus (Grenoble) using a BigDye Terminator Sequencing Ready Reaction kit, V1.1 (Perkin-Elmer) according to the manufacturer's instructions. 500 ng of template were used for reaction. After removal of non-incorporated fluorescent nucleotides (by ethanol precipitation) automated sequencing cycles were generated on the GeneAmp 9700 (Applied Biosystems). Nucleotide sequences were analysed using different programs and data banks accessible on internet (Chromas Lite, NCBI-BLAST, TAIR).

2.4.1.6 Plant genomic DNA extraction

Depending on the purpose two procedures of plant genomic DNA extractions were performed:

→ Rapid extraction (using Edwards buffer). This kind of extraction was used for genotyping by PCR.

→ Long extraction (using Nucleon Phytopure Genomic DNA Extraction kit; GE Healthcare). This method enabled to isolate greater quantities of pure DNA, therefore it was suited for Southern-blot analysis.

Rapid extraction

One leaf of a young plant was grinded in an Eppendorf tube using a piston (Polylabo). Immediately after that, 500 μ L of Edwards buffer (Tris-HCl 200mM pH7,5 ; NaCl 250mM ; EDTA 25mM ; SDS 0,5 %) were added to grinded tissues and the mixture was vortexed gently and quickly before centrifugation at 13000 rpm for 1 minute. Then, 350 μ L of supernatant were retrieved and DNA was precipitated with isopropanol. Furthermore, DNA was harvested by another centrifugation of 5 min at 13000 rpm speed and pellets were dried at room temperature for 2 h under the laminar flow hood. Finally, DNA was resuspended in 20 μ L of sterile water and 1 μ L was used for PCR during genotyping.

Long extraction

Long plant DNA extraction was performed using the Nucleon Phytopure Genomic DNA Extraction kit (GE Healthcare). The so prepared DNA was suited for Southern-blot analysis. First, plant tissues were grinded in mortar with the liquid nitrogen and 500 μ L of resulting plant powder were used for subsequent steps of cell lysis, DNA extraction and DNA precipitation, according to manufactured instructions. Resulting DNA pellets were air-dried for around 12 min and resuspended in 30 μ L of autoclaved TE buffer each. DNA was stored for 2 d at 4°C to achieve complete solution before any digestion.

2.4.1.7 Southern Blot

→ Digestion and transfer of genomic DNA

10 µg of genomic DNA was used for each digestion reaction with the final volume of 20 µL. Reactions were performed overnight (for ~16 h) at the optimal temperature of chosen enzymes. Next day in the morning, digestion was stopped by incubating the tubes containing reaction mix for 10 min at 65°C. Subsequently, the tubes were put on ice. After addition of 3% glycerol (v/v) and 0,025% bromophenol blue (w/v), nucleic acids were separated by electrophoresis running at 40 V on 1% agarose gel containing 0,1 µg of ethidium bromide. When migration of nucleic acids was finished, DNA was visualized under UV light (320 nm) and a photo was taken. Subsequently, the restriction fragments present in the gel were denatured by washing it twice in denaturation buffer (0,4 M NaOH; 1 M NaCl) for 20 min and then transferred onto nylon membrane (SensiBlot™ Plus Nylon membrane, Fermentas) by blotting. Transfer was realized overnight in the presence of denaturation buffer, accordingly to Sambrook and Russell (2001). Next day, the membrane was rinsed with neutralization buffer (1 M NaCl; 0,5 M Tris pH 7,2) for 15 min before being dried at 80°C for 2 h (fixing genomic DNA).

→ Probe labeling

Labeling method was based on the optimized conditions for chemiluminescent detection of digoxigenin-labeled DNA probes. Digoxigenin-labeled probe of *ATOEP16-1* gene was obtained by amplification of this gene from wild-type *Arabidopsis* genomic DNA by PCR method using 0,8 mM DIG-11-dUTP (Roche) in addition to the other deoxynucleotides to give a final volume of 25 µL. The PCR conditions were 95°C for 5 min, followed by 40 cycles of 95° for 1 min, 55°C for 1 min, and 72°C for 1 min and 30 seconds, then final elongation step of 5 min at 72°C. Total volume of PCR reaction was used in agarose gel electrophoresis and a band of interest was excised and purified from agarose. 700 ng of the labeled PCR product was used in the hybridization.

→ Hybridization and signal detection

The membrane was incubated in a glass tube with hybridization buffer (25 mL 20X SSC: 3M NaCl, 0,3M Na-citrate; 1 mL 10% [w/v] lauroylsarcosine, 200 µL 10% [w/v] SDS, 1% [w/v] blocking reagent - Roche) under agitation for 4 h at 64°C to permanently crosslink the DNA to the membrane. Just before the begin of hybridization, a probe was denatured for 5 min at 97°C and immediately after, put on ice. Hybridization buffer was replaced by a fresh one containing a probe (700 ng of DNA). Hybridization was realized under agitation at 64°C overnight. Next day, the membrane was washed twice for 10 min at room temperature with a buffer “1” (2X SSC; 0,1% [w/v] SDS), followed by washing twice for 30 min at 70°C with a buffer “2” (0,1X SSC; 0,1% [w/v] SDS). Then, the membrane was equilibrated in washing buffer (0,1M maleic acid; 0,15M NaCl; pH 7,5) for 5 min and then incubated under agitation in a blocking buffer (1% [w/v] blocking reagent; 0,1M maleic acid; 0,15M NaCl; pH 7,5) for 1 hour. From now on, the membrane was washed at room temperature. In the next step, a previously used blocking buffer was discarded and a fresh one containing 5 µL of labeled antibody Anti-DIG-Fab- Fragments (Roche) was added and the incubation under agitation was done for 45 min. Subsequently, the membrane was washed twice for 20 min in washing buffer and finally incubated in detection buffer (Tris; NaCl pH 9,5) for 5 min. Next, the membrane was incubated with the dye reagent CSPD ready-to-use (Roche) in the dark and then covered with a plastic dome to be stored in the dark at 4°C overnight. The following day, the membrane was exposed on autoradiography film Kodak Biomax MS-1 in a cassette containing two intensifying screens (Biomax MS intensifying screen) for 15 min at room temperature. In the end, the film was developed in a dark room by washings in a developer (developer KODAK diluted at 1/5) until the appearance of signals, followed by rinsing a film with water and subsequent washing in fixing solution (fixator KODAK diluted at 1/5). After rinsing with water for several times, the films were air-dried.

2.4.2 RNA.

2.4.2.1 Extraction of total RNA

The gloves were worn while manipulating with RNA. All solutions were pre-treated with diethyl pyrocarbonate (DEPC), then autoclaved and the glass material was sterilized at 180°C for 3 h.

Plant material was grinded in mortar in the liquid nitrogen and 500 µL of resulting powder was used for RNA extraction with extraction buffer as indicated in Martinez-Zapater and Salinas (1998). This treatment led to the denaturation of cellular proteins, including RNase. RNA was then separated from the remaining cellular debris by differential phenol-chloroforme extraction and precipitated with ethanol 100%. RNA pellet was resolved in 30 µL of sterile water.

2.4.2.2 Determination of RNA concentration

RNA concentration and purity were estimated by absorbance (A) measurement of diluted RNA (1/100) at 260 nm (for nucleic acids) and at 280 nm (for proteins) using a spectrophotometer (Biophotometer, Eppendorf). The ratio A 260/280 provided an indication of purity with respect to interfering proteins; for pure RNA: A 260/280 = 2,0. The use of third point wavelength detection of 310 nm permitted correction for diffusion and allowed it to be subtracted from the readings. RNA concentration (µg/mL) was calculated as follows:

$$C = (A_{260 \text{ nm}} - A_{310 \text{ nm}}) \times 40 \times 100 \text{ µg/mL}$$

where 40 is for coefficient of RNA and 100 µg/mL stands for sample dilution.

2.4.2.3 Northern blot

→ Sample preparation, electrophoresis and transfer of RNA

10 µg of each total RNA sample were mixed with 49% formamide (v/v), 17% formaldehyde (v/v) and 10 % 5X 3-(N-morpholino) propanesulfonic acid (MOPS), (0,1 M MOPS pH 7,0; 40mM Na-Acetate; 5 mM EDTA pH 8,0) (v/v). Samples were incubated at 65°C for 5 min and subsequently put on ice. After addition of 3% glycerol (v/v) and 0,025% bromophenol blue (w/v), ribonucleic acids were separated by electrophoresis running at 32

V on 1% denaturing agarose gels containing 0,1 µg of ethidium bromide, 3% formaldehyde (v/v) and 20% 5X MOPS (v/v). When migration of ribonucleic acids was finished, RNA was visualized under UV light and a photo was taken. Subsequently, the gel was incubated twice in 5X SSC buffer for 20 min. Transfer was realized overnight as for southern-blot but in the presence of 5X SSC buffer. Next day, the membrane was dried at room temperature for 1 hour and then at 80°C for 2 h.

→ Probe labeling

³²P-labelled probes for the *RBCS* and *CAB* (*Hordeum vulgare*) genes were synthesized with the RadPrime DNA Labeling System (InVitrogen GmbH) in the presence of [³²P] dATP and [³²P] dCTP (Hartmann GmbH, specific activity 3000Ci/mmol) according to the instructions of the supplier.

→ Hybridization and signal detection

The membrane was incubated in a glass tube with hybridization buffer (HYB-9 Hybridization solution, Genra Systems) under agitation for 2 to 4 h to saturate the membrane (pre-hybridization). Before the begin of hybridization, probes were denatured for 5 min at 95°C, quickly placed on ice and transferred into the hybridization solution. Hybridization was performed under agitation at 62°C overnight. Next day, the membrane was washed twice for 20 min at 50°C with a buffer “1” (2X SSC; 0,1% [w/v] SDS), followed by washing twice for 20 min at 50°C with a buffer “2” (0,1X SSC; 0,1% [w/v] SDS). From now on, the membrane was treated as for southern-blot analysis (as described in §2.4.1.7).

2.4.2.4 *In vitro* translation

5 µg of each total RNA sample was used for *in vitro* translation using the Wheat Germ Extract System (Promega), according to the protocol adapted from manufacturer's instructions. To increase the efficiency of translation, template RNAs were denatured at 67°C for 10 min and immediately cooled on ice prior to translation. Reaction mixture at final volume of 25 µL (containing 5 µg of RNA, 12,5 µL of wheat germ extract, 2 µL of

amino acid mixture, 1 μL of TNT buffer, 0,5 μL of RNasin[®] Ribonuclease Inhibitor and isotopically labeled amino acid: [³⁵S] methionine; Amersham) was incubated at 25°C for 2 h. For protein analysis, 5 μL aliquot of translation reaction was removed and added to 20 μL of SDS sample buffer with 0,1% of bromophenol blue, while the remainder of the reaction was stored at -20°C. The proteins were denatured at 95°C for 10 min before loading on 10-20% gradient SDS polyacrylamide gel and. Once, the migration was finished, the gel was washed in fixating solution for 30 min, followed by soaking in amplify fluorographic reagent (Amersham) with agitation for 30 min. Then, the gel was dried at 80°C for 2 h and finally exposed with autoradiographic film Kodak Biomax MS-1 in cassette containing two intensifying screens (Biomax MS intensifying screen) for at least one week at -80°C. In the end, a film was developed in a dark room, as described in § 2.4.1.7) and scanned.

2.4.2.5 Polysomes isolation

Polysomes were isolated as described by Reinbothe *et al.*, 1990. For preparative assays, 500 g of leaf material was used. For further analytical assays, 25 g of leaf material was used. Leaf material was ground under liquid nitrogen until a fine powder was obtained. After resuspension in buffer A (50 mM Tris/HCl (pH 8,0); 250 mM KCl; 10 mM β -mercaptoethanol; 10 $\mu\text{g}/\text{mL}$ cycloheximide (CHX); 200 $\mu\text{g}/\text{mL}$ heparin), the thawed cell homogenate was filtered through two layers of filter gaze (120 μm and 70 μm mesh width). The crude cell extract was differentially centrifuged at 2000, 4000 and 12000 rpm speed for 5 min each in a Sorvall RC-5B centrifuge using a HB6 rotor in order to remove cell debris and organelles. Triton X-100 was added to the final supernatant (1% (v/v) final concentration). The solution was either loaded onto a discontinuous sucrose step gradient consisting of 2 mL 2M; 2 mL 1,75 M; 2 mL 1,5 M; 4 mL 1,25 M; 6 mL 1,0 M; 6 mL 0,75 M and 6 mL 0,5 M sucrose in buffer B (50 mM Hepes/KOH (pH 8,5); 25 mM KCl; 10 mM MgCl_2 ; 10 mM β -mercaptoethanol; 10 $\mu\text{g}/\text{mL}$ CHX; 500 $\mu\text{g}/\text{mL}$ heparin) or was supplemented with magnesium chloride (0,1 M final concentration) to precipitate ribonucleoprotein material (as described by Reinbothe *et al.*, 1993). After centrifugation at 60 000 rpm speed in a Beckman Spinco L75 centrifuge, rotor Ti 60, for 1 hour at 4°C, the gradient was harvested from bottom to top in a modified Beckman harvesting device with continuous monitoring of the absorbance at 254 nm (2138 Uvicord S, LKB). After integration of the areas below the curves, the P/T ratio was calculated as follows: (area of polysomes) / (area of polysomes + ribosomal subunits + monosomes). From the arbitrarily

defined gradient fractions, each corresponding to 10 drops (ca. 0,35 mL; Redirac Fraction Collector, LKB), the RNAs were recovered by ethanol precipitation and subsequently used for Northern blot hybridization or *in vitro* translation (see above § 2.4.2.3 and 2.4.2.4, respectively). In parallel assays, proteins were extracted from the polysomal fractions with trichloroacetic acid (TCA) and washed extensively with ethanol and diethylether.

2.5 Protein analysis

2.5.1 Protein extraction

2.5.1.1 Rapid protein extraction

Plant material was grinded in mortar in liquid nitrogen and 500 µL of resulting powder was used for protein extraction with 1X SDS-PAGE sample buffer (2,9% SDS; 68 mM Tris/HCl pH 6,8; 10% glycerol; 0,1 M β-mercaptoethanol). The resulting mixture was homogenized by vortexing and then denatured at 95°C for 5 min followed by centrifugation at maximum speed for 5 min to pellet cellular debris. Then, resulting supernatant (protein extract) was retrieved and used for 1D SDS polyacrylamide gel electrophoresis analysis.

2.5.1.2 Long protein extraction

For 2D SDS polyacrylamide gel electrophoresis analysis, protein extracts must be devoid of pigments and lipids which may disturb the migration. For that purpose, protein extracts obtained after rapid protein extraction were subjected to an overnight protein precipitation at 4°C with 5% TCA. Next day, centrifugation at maximum speed at 4°C was performed to pellet proteins. Subsequently, proteins were washed twice with cooled 100% acetone and then twice with cooled 100% ethanol. A resulting protein pellet was air-dried (the tubes were still kept on ice) for 2 h under the laminar flow bench and finally resuspended in 50-200 µL of 1X protein extraction buffer.

2.5.2 Determination of protein concentration

Protein concentration was determined by ESEN assay (Esen, 1978). 5 μ L of each protein sample were put on equally sized pieces of Whatman paper. BSA (Bovine Serum Albumine) diluted in 1X protein extraction buffer at concentration of 2 mg/mL was used as a reference. Proteins were washed under agitation in fixing buffer (25% isopropanol; 10% acetic acid) for 5 min, followed by washing in staining buffer (fixing buffer + 0,1% coomassie brilliant blue G 250) for 15 min. Whatman paper was subsequently rinsed twice with cold water for 5 min followed by two washings with boiling water for 5 min. Protein spots were cut and destained with 0,5% SDS at 55°C for 20 min. The absorbance was read at 578 nm using a spectrophotometer (Biophotometer, Eppendorf) and protein concentration was calculated by comparing the absorbance values with BSA.

2.5.3 Analysis of proteins by polyacrylamide gel electrophoresis

2.5.3.1 One dimensional SDS-Polyacrylamide Gel Electrophoresis (SDS-PAGE)

In order to separate effectively the proteins sharing weak differences in molecular mass, for example PORA and PORB proteins (37, 36 kDa for Arabidopsis and 36, 38 kDa for barley, respectively), a gradient 10-20% of polyacrylamide (acrylamide/N,N'-methylenebisacrylamide 30/0,8) gel was used. In addition, to optimize the effect of protein separation, the Protean II xi (Biorad) system, with large glass plates (14 cm length), was used.

The gel consisted of three parts, starting from the bottom: the bottom gel, the separation gel and the stacking gel at a top.

→ The bottom gel consisted of light (LL) solution (10% [v/v] acrylamide/bisacrylamide [30/0,8] ; 0,4 M Tris-HCl pH8,8 ; 0,1% [w/v] SDS). For polymerization, 5 mL of LL solution mixed with 75 μ L of 10% [w/v] ammonium persulfate (APS) and 25 μ L of N,N,N',N'-tetramethylethylenediamine (TEMED) was poured into the gap between the glass plates.

→ Special casting equipment was used for a preparation of gradient gel, such as a gradient mixer (Biorad) and a pump (Minipuls3, Gilson). The separation 10-20% gradient gel was made by progressive mixing 10 mL of the sucrose-containing heavy solution (SL solution: (

20% [v/v] acrylamide/bisacrylamide [30/0,8] ; 0,4 M Tris-HCl pH8,8 ; 0,1% [w/v] SDS ; 10% [w/v] sucrose)) with 30 mL of LL solution. In addition, each solution was mixed with 10% APS [w/v] (25 μ L and 50 μ L for SL and LL solutions, respectively) and TEMED (4 μ L and 12 μ L) to polymerize the acrylamide gel.

→ 10 mL of the stacking gel containing 7,2% [v/v] acrylamide/bisacrylamide [30/0,8], 120 mM Tris-HCl pH 6,8 and 0,1% [w/v] SDS, mixed with 50 μ L 10% APS [w/v] and 10 μ L TEMED was poured directly onto the surface of the polymerized separation gel. Immediately a Protean II xi comb (Biorad) was inserted into the stacking solution. When polymerization was complete, the comb was removed and using the Hamilton syringe, the wells were washed with the migration buffer (0,25 M Tris-HCl pH 8,3 ; 1,92 M glycine ; 0,1% [w/v] SDS).

Proteins in 1X SDS-PAGE sample buffer containing 0,1% [w/v] bromophenol blue were denatured at 95°C for 5 min. Immediately after, the samples were put on ice and together with 10 μ L of marker proteins (Page Ruler Prestained Protein Ladder Plus, Fermentas) loaded in a predetermined order into the bottom of the wells using the Hamilton syringe. Electrophoresis was carried in migration buffer at 4°C overnight at constant current of 10 mA per gel, in the electrophoresis apparatus Protean II xi (Biorad), until the bromophenol blue reached the level of the bottom gel.

2.5.3.2 Two dimensional SDS-Polyacrylamide Gel Electrophoresis (SDS-PAGE)

Isoelectric focusing (IEF)

First, the radioactively labeled barley proteins were separated accordingly to their isoelectric points by isoelectric focusing. The gradient gels (pH 3-10) were prepared in glass tubes (2x4x160; Biorad) such that each sample was separated per glass tube. Before pouring the gel solution (9,2 M urea ; 4% [v/v] Ac/Bis [28,38/1,62] ; 2% [v/v] NP40 (Fluka) ; 4% [v/v] Ampholine pH 5-8 (Amersham) ; 1% [v/v] Ampholine pH 3-10 (Amersham)) into the glass tubes, it was filtered through the 0,45 μ m filter to eliminate any unresolved urea particles and the glass tubes were pretreated with 0,01% [v/v] TritonX-100 for 2-3 h and air-dried. Then, the tubes were filled with gel solution containing 10 μ L TEMED and 12,5 μ L 10% APS [w/v] corresponding to 13,5 cm height. Each gel was overlaid with 25 μ L 8M urea and after polymerization, the top of the gel was equilibrated

with 20 µL of U1 solution (8,66 M urea ; 3,3% [v/v] Ampholine pH 3-10 ; 4% NP40) for 2 h. Afterwards, 90 µL of each protein sample (containing 170 µg of total proteins in the volume of 65 µL 1X SDS buffer ; 12,8M urea ; 11,5% [v/v] NP40 and 5,4% [v/v] Ampholine pH 3-10) was loaded directly on a gel in a glass tube, subsequently the proteins were covered with 20 µL of U2 solution (7,5 M urea ; 1,63% [v/v] Ampholine pH 3-10) and then with 20 µL 1N NaOH. The migration was carried at room temperature in 0,02M NaOH and 0,01M H₃PO₄ buffers at 300V for 30 min followed by constant voltage of 500V for 12-14 h and terminated at 600V for 1 hour. Once the migration was finished, the gels were carefully removed from the glass tubes, using a syringe with the extrusion needle (Biorad) along the bottom edge of the glass tubes and by flushing with 0,5% [w/v] SDS solution. Subsequently, each gel was equilibrated in 5 mL of buffer D (0,06M Tris-HCl pH 6,8 ; 1,2% [w/v] SDS; 10% [v/v] glycerol ; 5% [v/v] β-mercaptoethanol ; 0,1% [w/v] bromophenol blue) and stored at – 20°C until the second dimension electrophoresis.

2nd dimension electrophoresis

Next, the proteins were separated according to their size on 10-20% gradient gels, described above. The equilibrated gels after isoelectric focusing were fixed at the top of a stacking gel with preheated solution C (0,05M Tris-HCl pH 6,8 ; 2% [w/v] SDS ; 5% [v/v] β-mercaptoethanol ; 0,5% [w/v] agarose). The migration was carried out in migration buffer at 4°C overnight at constant current of 10 mA per gel, in the electrophoresis apparatus Protean II xi (Biorad), until the bromophenol blue reached the level of the bottom gel. Finally, the gels were fixed, stained, soaked in amplify fluorographic reagent (Amersham) and dried as described in further paragraphs. The exposition of the gels was carried out in a cassette containing two intensifying screens (Biomax MS intensifying screen) and autoradiographic film Kodak Biomax MS-1, for at least one week at -80°C. Autoradiography films were developed as described in § 2.4.1.7).

2.5.3.3 Staining SDS-polyacrylamide gels with Coomassie brilliant blue

Staining of proteins was performed by incubating the gels under agitation for 30 min in fixing solution (25% [v/v] ethanol; 10% [v/v] acetic acid), then for 30 min in staining solution (fixing solution + 0,1% [w/v] Coomassie brilliant blue G 250 - Serva). Destaining of the gels was done by several washings under agitation in fixing buffer until optimal coloration was achieved.

2.5.3.4 Silver Nitrate staining

To achieve a better detection of minor quantities of proteins, the silver nitrate staining method was used. First, the gel was incubated under agitation for 20 min in fixing solution I (50% [v/v] methanol; 5% [v/v] acetic acid) and afterwards washed twice for 10 min in solution II (50% methanol) and once in distilled water. Subsequently, it was briefly shaken in fresh sodium thiosulfate solution (0,02% [w/v]) and immediately after rinsed with distilled water. Then, incubation of the gel for 20 min in solution IV (0,1% [w/v] silver nitrate) was performed, followed by rinsing with distilled water. The gel was developed in solution V (2% [w/v] sodium carbonate; 0,04% [v/v] formaldehyde [37%, v/v]) for 1-5 min, depending on the intensity of the coloration. Once optimal staining was achieved, the gel was agitated for 5 min in solution II (5% [v/v] acetic acid) to stop further coloration process. In the end, the gel was dried as described below.

2.5.3.5 Drying SDS-polyacrylamide gels

Once staining was finished, the gels were put on a piece of Saran Wrap and attached to a piece of Whatman 3MM paper. Such a sandwich of 3MM paper/gels/Saran Wrap was placed in a drying apparatus (BioRad) where it was dried for 2 h at 80°C.

2.5.4 Transfer of proteins onto nitrocellulose membrane (Western Blot)

Proteins separated by electrophoresis were electrically transferred onto nitrocellulose membrane (Schleicher & Schuell) using transfer apparatus (trans-blot cell, BioRad). The gel and its attached nitrocellulose membrane were put between four pieces of Whatman 3MM paper and two sponges that have been soaked in transfer buffer. The sandwich was then placed between graphite plate electrodes of transfer apparatus, with the nitrocellulose membrane on the anodic side. Transfer was realized with constant current of 240 mA for 5 h at 4°C in the presence of transfer buffer (26 mM Tris; 0,19 M Glycine ; 0,04 % (p/v) SDS; 20 % (v/v) Ethanol). A quality of transfer was checked by staining the proteins: a membrane was incubated in Ponceau S solution (0,5 % [p/v] Ponceau S (Sigma) in 1 % [v/v] acetic acid), next rinsed with distilled water for several times until optimal appearance of protein bands. A membrane was scanned before complete destaining of proteins with TBS buffer (20 mM Tris; 0,14 M NaCl pH 7,4 ; 0,1 % Tween).

2.5.5 Immunodetection

Nitrocellulose membranes were blocked by incubation for at least 1 hour at room temperature in TBS buffer containing 5% [w/v] nonfat dried milk. Next, an unlabeled primary antibody (diluted: 1/1000-1/3000) specific for the target protein was first incubated with the nitrocellulose membrane in the presence of blocking solution for 1 hour at room temperature. The membrane was then washed 3 times for 10 min with TBS buffer and incubated with a secondary antibody coupled to alkaline phosphatase enzyme (Roche). To visualize the antigen-antibody-antibody complex, the membrane was incubated quickly in alkaline phosphatase buffer (0,1M NaCl; 5mM MgCl₂; 0,1M Tris/HCl pH 9,5) and subsequently in color solution (alkaline phosphatase buffer containing the enzyme substrates: NBT and BCIP). A purple precipitate (formazan) is produced by the alkaline phosphatase. When the bands had the desired color intensity, 2-3 drops of HCl were added to stop staining process. The membrane was subsequently washed in distilled water for 5 min to remove HCl.

2.5.6 Production of an antibody against the AtOEP16-1 protein

2.5.6.1 Protein overexpression in *Escherichia coli*

The *E.coli* Expression System with Gateway[®] Technology (Invitrogen) was used for the expression of recombinant AtOEP16-1 protein. This system takes advantage of Gateway[®]-adapted destination vectors designed to facilitate high-level, inducible expression of recombinant proteins in *E.coli* using the pET system.

After cloning (via BP reaction) the cDNA coding for AtOEP16-1 protein into the Gateway[®] donor vector pDONR221, the entry clone pEOEP16 was obtained. Next, to create the expression clone, the LR recombination reaction was performed between pEOEP16 and pDEST[™]17 destination vector. In this vector, expression of *AtOEP16-1* gene was controlled by a strong bacteriophage T7 promoter, specifically recognized by T7 RNA polymerase. In addition, this vector contains the polyhistidine (6xHis) tag which is located at the N-terminus of the fusion protein enabling further detection and purification of recombinant fusion protein 6His-tag-AtOEP16-1. To propagate and maintain the resulting expression clones, 2 µl of LR reaction were used for the transformation by electroporation of *E.coli* bacteria, strain DH5α. Subsequently, transformants were selected on LB agar plates

containing ampicillin [100µg/mL]. Expression vectors (pDEST17-OEP16-6His-tag) were then purified from ampicillin-resistant colonies, using a DNA miniprep method based on the alkaline lysis procedure (developed by Birnboim and Doly; Nucleic Acids Research 7:1513, 1979).

For the expression of T7 RNA polymerase regulated *AtOEP16-1* gene, the BL21-AI™ *E.coli* (Invitrogen) strain was used. This strain contains a chromosomal insertion of the gene encoding T7 RNA polymerase into the *araB* locus of the *araBAD* operon. It allows the induction of the expression of T7 RNA polymerase by L-arabinose. The BL21-AI™ *E.coli* bacteria were transformed by electroporation with purified DNA of pDEST™17-OEP16 clone. Subsequently, transformants were selected on LB agar plates containing ampicillin [100µg/mL]. Ampicillin-resistant BL21-AI™ bacteria were cultured in LB medium containing 100µg/mL ampicillin at 37°C with shaking until the OD₆₀₀ reached 0,6. 500 µL of the culture were removed and pelleted at maximum speed for 2 min. Induction of synthesis of recombinant fusion protein 6His-tag-AtOEP16-1 was initiated by addition of L-arabinose to the culture to a final concentration of 0,2%. 4 h after the induction, 500 µL of the culture were removed, pelleted and resuspended in 80 µL of 1X SDS-PAGE sample buffer. After boiling the samples (one induced and another uninduced used as a negative control) at 95°C for 5 min, 10 µL of each sample was loaded on SDS-PAGE gel and analysed by electrophoresis. First, the polyacrylamide gel was stained with coomassie brilliant blue to identify recombinant protein 6His-tag-OEP16-1 as a band of increased intensity of the expected size (expression of AtOEP16-1 protein with N-terminal tag increased the size of recombinant protein to 18,6 kDa). Afterwards, a western-blot was performed with anti-His primary antibody (QIAexpress) to confirm that the overexpressed band was a true 6His-tag-AtOEP16-1 protein.

2.5.6.2 Purification of AtOEP16-1 protein

The presence of the N-terminal 6xHis tag in pDEST™17 allowed affinity purification of recombinant fusion protein using a nickel-chelating resin Ni-NTA. The procedure of batch purification under denaturing conditions was adapted from the protocol of the QIAexpressionist (Qiagen). Bacterial pellets of cultures grown with L-arabinose for 4 h were lysed in lysis buffer B (8 M urea; 0,1 M NaH₂PO₄; 0,01 M Tris/HCl pH 8,0). The lysis was performed using a French press. Then, the cellular debris were pelleted by centrifugation at 10000 g for 30 min and a cleared lysate was mixed with 1 mL of the 50%

Ni-NTA slurry on a rotary shaker at 200 rpm during night. Next day, a mixture lysate-resin was loaded into an empty column (Biorad). Then, a column was washed twice with 2 x 4 mL buffer C (8 M urea; 0,1 M NaH₂PO₄; 0,01 M Tris/HCl pH 6,3). Finally, the recombinant protein 6His-tag-OEP16 was eluted with 4 x 0,5 mL buffer D (8 M urea ; 0,1 M NaH₂PO₄ ; 0,01 M Tris/HCl pH 5,9), followed by 4 x 0,5 mL buffer E (8 M urea ; 0,1 M NaH₂PO₄ ; 0,01 M Tris/HCl pH 4,5). The fractions eluted with buffer D and E were analysed by SDS-PAGE. Then, the polyacrylamide gel was stained with coomasie brilliant blue to identify recombinant protein 6His-tag-AtOEP16-1 as a single band of increased intensity, which was finally cut.

2.5.6.3 Production of the antibody (INTERCHIM)

2 mg of recombinant protein 6His-tag-AtOEP16-1, in SDS-polyacrylamide gel stained with coomasie brilliant blue, was used for the primary immunization and booster injections of rabbits performed by Interchim enterprise. Two booster injections of the antigen were given to two rabbits at regular intervals and their sera containing the antibodies raised against 6His-tag-AtOEP16-1 protein were taken. Rabbit sera with Anti-OEP16-1 antibodies were directly used in western-blot analysis in [1:3000] dilution without any further purification steps.

2.5.7 Radioactive labeling of proteins *in vivo*

5-d old seedlings (450 mg per condition) of *A.thaliana* ecotype Columbia (wild type, *Atoep16-1*) and barley (wild type Scarlett, *tigrina-d^{l2}*) were harvested and cut with a knife in little pieces. Immediately after, 1 mL of 0,1% [v/v] Tween solution containing 50 µCi of ³⁵S-Methionine (Amersham) was added. The labeling was carried out for 2 h under gentle shaking. Then, after aspiration of radioactive solution and the harvest of seedlings, protein extraction was done (as described in § 2.5.1). Subsequently, protein concentrations were determined by ESEN assay (see § 2.5.2) and 30 µg of proteins were separated on 1D 10-20% polyacrylamide SDS gradient gels or 170 µg of proteins by 2D SDS-PAGE. After staining the gels (as described in § 2.5.3.3), they were soaked in amplify fluorographic reagent (Amersham) with agitation for 30 min. Afterwards, the gels were dried for 2 h at 80°C and finally exposed with autoradiographic film Kodak Biomax MS-1 in a cassette

containing two intensifying screens (Biomax MS intensifying screen) for at least one week at -80°C. In the end, a film was developed in a dark room, as described in § 2.4.1.7.

2.6 *In vitro* import into the organelles

2.6.1 Construction of chimeric precursor proteins

Chimeric precursor proteins consisting of the transit peptide of the pPORA (transA) fused to dihydrofolate reductase (DHFR) reporter protein of mouse and the transit peptide of the pPORB (transB) fused to DHFR, were constructed by a PCR-based approach as previously described by Reinbothe *et al.*, 1997. The DNA sequence encoding transA was generated with primers TransA-F and TransA-R, that for transB with primers TransB-For and TransB-Rev, using the cDNA clones A7 (Schulz, 1989) and L2 (Holtorf *et al.*, 1995), encoding the pPORA and pPORB, respectively as templates. The amplified DNAs encoding transA and transB were inserted into the *Bam*HI site of the pSP64 vectors (Promega). For the construction of transA- DHFR and transB-DHFR clones, *Bam*HI-digested DNAs encoding transA and transB were subcloned in exchange for the DNA of transPC into plasmid pSPPC1-67DHFR, which encodes a chimeric transPC-DHFR protein consisting of the transit peptide of plastocyanin (transPC) of *Silene pratensis* fused to a cytosolic DHFR of mouse. A list of used oligonucleotides is enclosed in the appendix A.

2.6.2 Import assay

In vitro-import reactions were carried out using cDNA-encoded, wheat germ-translated, urea-denatured, ³⁵S-Methionine-labeled transA-DHFR and transB-DHFR precursors produced by coupled transcription/translation (as described in §2.4.2.4) of respective clones and Percoll/sucrose-purified chloroplasts from *A. thaliana* (Schemenewitz *et al.*, 2007). ³⁵S-Methionine-labeled transA-DHFR and transB-DHFR were activated with 5,5'-dithiobis(2-nitro) benzoic acid (DTNB)(Reinbothe *et al.*, 2004). DTNB, also known as Ellman reagent, is a symmetrical aryl disulfide that undergoes a thiol-disulfide interchange reaction in the presence of a free thiol, to yield a mixed disulfide and thionitrobenzoate

(TNB). TransA-DHFR and transB-DHFR likewise contain a unique cysteine residue at position 80 of the DHFR that was activated with DTNB. Then the precursors were added to isolated chloroplasts that had been isolated from 14 d-old, light-grown *Atoepl6-1* and wild type *Arabidopsis* seedlings and energy-depleted on ice for 1 h. Incubation of DTNB-derivativized ³⁵S-Methionine-labeled precursors with isolated plastids was carried out in the presence of 0,1 mM Mg-ATP and 0,1 mM Mg-GTP (Reinbothe *et al* 2004a, b). At these nucleotide triphosphate concentrations, transA-DHFR and transB-DHFR bind to and integrate into the outer plastid envelope membrane and also form junction complexes with components of the inner envelope membrane (Reinbothe *et al.*, 2004). For achieving full import of transA-DHFR and transB-DHFR across the outer and inner envelope membranes, the assays were supplemented with 2,5 mM Mg-ATP and 0,1 mM Mg-GTP (Reinbothe *et al.*, 2004a, b). To trigger the Pchlide-dependent import of transA-DHFR, isolated chloroplasts were pretreated with 5-aminolevulinic acid for 15 min in the dark to cause in organelle pigment biosynthesis. Post-import analysis of bound and translocated precursors included precipitation of protein with TCA [5% (wt/vol) final concentration], several washing steps with acetone, ethanol and diethylether, and electrophoresis in denaturing but non-reducing 10-20% (w/v) polyacrylamide gradient gels, followed by detection via autoradiography (see §2.4.1.7).

2.7 Fluorescence observations

2.7.1 Accumulation of protochlorophyllide and chlorophyll pigments

Protochlorophyllide accumulation was observed in seedlings grown in the dark for 5 d (*Arabidopsis* and barley) while chlorophyll accumulation was observed in light-grown plants. Observation of both types of pigments was carried under blue light (400-450 nm) using the epifluorescence microscope (Olympus).

2.7.2 Detection of GFP and YFP fusion proteins

Subcellular localization of AtOEP16-1 protein was carried out with transgenic *Atoep16-1* and wild type (ecotype Columbia) *Arabidopsis* plants transformed with GFP (Green Fluorescent Protein) and its derivative YFP (Yellow Fluorescent Protein) fused to AtOEP16-1 protein at her N- and C-terminus respectively, under the control of the CaMV 35S promoter. For the controls, we used transgenic *Arabidopsis* plants (kindly donated by Norbert Rolland) carrying 35S::GFP and 35S::transit SSU::GFP constructs targeted to the cytoplasm and the stroma of plastids, respectively. Both, GFP and YFP imaging were performed on an inverted epifluorescence microscope and confocal laser-scanning microscope.

2.7.2.1 Epifluorescence microscopy

Plants grown under continuous light for 7 and 14 d were analyzed with an epifluorescence microscope (Olympus) using 470-490 nm Zeiss excitation filter, dichroic mirror and a 505-530 nm Zeiss emission filter.

2.7.2.2 Confocal laser-scanning microscopy

Young seedlings grown under continuous light for 3-5 d were harvested and analyzed under the Leica confocal microscope, using 63x water immersion objective and Argon/Krypton laser. For imaging GFP, a 488 nm excitation filter in combination with a 493-573 nm emission filter were used. For the YFP variant, a 514 nm excitation filter and 520-550 nm emission filter were used.

2.8 Electron Microscopy Imaging (EMI)

2.8.1 Tissue fixation

The procedure of tissue preparation was carried out in the dark. Cotyledons of *Arabidopsis* plants grown in continuous dark for 5 d were fixed by harvesting and placing them directly into fixative solution (2% [v/v] glutaraldehyde in 0,1M Sodium Cacodylate buffer at pH 7,2) in Eppendorf tubes. The tissues were subjected to 8 vacuum infiltrations until all

cotyledons were placed at the bottom of Eppendorf tubes. Afterwards, the fixation buffer was removed and a fresh one was added. The samples in the Eppendorf tubes were wrapped in aluminum foil and stored at 4°C before sending them to Dr. Armin Springer (Technische Universität of Dresden, Germany) for further analysis.

2.8.2 Inclusion and observation

Each post-fixation procedure was done by Dr. Armin Springer. The samples were embedded in a resin Epon (Fluka) and observed under transmission electron microscope CM10 (FEI). The images were photographed using the XR60 AMT (Advanced Microscopy Techniques, Danvers, MA, USA) camera.

2.9 Tetrazolium staining of plant tissues

Cotyledons with hypocotyls of 100 *Atoep16-1* and wild type *Arabidopsis* seedlings grown under:

- continuous dark for 5 d
- continuous dark for 5 d and exposed to high light for:
 - 30 min
 - 2 h
 - 4 h

were cut from the roots and immersed in 1,5 mL of 1% (w/v) solution of 2,3,5-triphenyltetrazolium chloride (TTC; Sigma). Samples were incubated at room temperature in darkness for at least 2 d to obtain optimal staining before being photographed.

2.10 Pigment analysis by High Performance Liquid Chromatography (HPLC)

2.10.1 Sample preparation

450 mg of cotyledons of *Atoep16-1* and wild type *Arabidopsis* plants grown under:

- continuous light for 5 d,
- continuous dark for 5 d,
- continuous dark for 5 d and illumination for 2 h,
- continuous dark for 5 d and illumination for 12 h

were harvested and grinded in liquid nitrogen. 400 mg of a resulting free flowing powder were lyophilized for 48 h in the dark. 2 mg of dried tissues were used for further pigment extraction.

2.10.2 Pigment extraction

Pigment extraction was carried out in the dark. 100 μ L of methanol (Carlo Erba, HPLC quality), previously neutralized with 5 mM Tris pH 7,5, were added to 2 mg of dried tissues and the resulting mixture was vortexed for several times until the pigments were completely extracted and the powder became white. Between each vortex, the samples were kept on ice in the dark. Afterwards, the mixture was centrifuged at 13000 rpm for 10 min at 4°C and the resulting supernatant was collected. This extraction procedure was repeated twice with the same plant tissue and collected supernatants were combined and then evaporated with nitrogen. Pigments were then stored at -20°C overnight in the dark. Next day, pigments were dissolved in 100 μ L dimethylformamid (DMF; Carlo Erba, HPLC quality) and centrifuged twice at 13000 rpm for 10 min at 4°C to eliminate any cellular debris. 50 μ L of resulting supernatant was used for HPLC analysis.

2.10.3 Dosing and pigment analysis

HPLC analyses were performed by Dr Marcel Kuntz using a Varian ProStar 410 machine and Varian ProStar 240 pump. Pigment composition of the samples used in this study was done on an YMC C30 column (Schermbek, Germany). The mobile phases used were: methanol (A), methanol 80% in water (v/v) containing 0,2% ammonium acetate (B) and tert-methyl-butyl ether (C). Isocratic elution was carried out with a mixture of 95%A - 5%B solvents for 12 min followed by a mixture of 80%A - 5%B -15%C in linear gradient until 30%A - 5%B - 65%C was reached, disposed for 25 min. Then, the column was equilibrated with a mixture of 5%A - 95%B solvents for 25 min. The flow rate was set to 1 mL/min and the temperature of the column was kept at 30°C during the entire time of chromatography procedure.

The pigments were identified according to their retention times and spectral properties when compared to standard substances (PolyView 2000 software, Varian). Values presented in histograms correspond to the peak areas of pigments. HPLC experiments were carried out in triplicate to ensure the reproducibility of the technique.

Chapter 3 Results

3.1 Genetic complexity of the *Atoep16-1* mutant background

3.1.1 Identification of the *Atoep16-1* mutant in *Arabidopsis*

OEP16 is a protein of 16 kDa in the outer envelope of chloroplasts. It belongs to the preprotein and amino acids transporter (PRAT) family of proteins and shares homology with TIM proteins of the inner mitochondrial membrane (Rassow *et al.*, 1999). It was shown that OEP16 of pea chloroplasts forms an amino acid-selective channel (Pohlmeyer *et al.*, 1997). Later, a 16 kDa plastid envelope protein was identified by chemical crosslinking as a protein interacting with pPORA during its posttranslational import into isolated chloroplasts of barley, *Arabidopsis*, pea and other plant species (Reinbothe *et al.*, 2004 a+b). Protein sequencing confirmed that the protein identified in barley is an orthologue of pea OEP16 (Reinbothe *et al.*, 2004 a+b).

In *Arabidopsis* there are 4 *OEP16* genes named *AtOEP16-1* - *AtOEP16-4* (Reinbothe *et al.*, 2004; Philippar *et al.*, 2007). *AtOEP16-1* (At2g28900) is most closely related to the barley OEP16 protein (HvOep16-1) identified by crosslinking. The relationships of *AtOEP16-1* to HvOep16-1 is 52% and that to pea OEP16 (PsOEP16) is (62%). *AtOEP16-1* contains 6 exons and 5 introns (Figure 3.1). A reverse genetics approach was taken to isolate *Atoep16-1* (At2g28900) mutant plants lacking OEP16-1 protein in the Columbia ecotype of *Arabidopsis*. A respective T-DNA insertion line was identified in the mutant collection of the Salk Institute (Salk_018024.50.90.X). Sequencing showed that this mutant contains a single, head-to-tail T-DNA insertion that disrupts the second exon of the *AtOEP16-1* gene. To eliminate possible parasite mutations, the mutant was backcrossed twice with wild-type plants. After self-pollination and subsequent segregation analyses on medium containing Kanamycin, resistant plants were propagated on soil and used to establish seed stocks. Only mutants at homozygous state were self-pollinated until the third generation (F3). Such homozygous *Atoep16-1* plants were used for further biochemical and cell biological studies of which the most important shall be summarized here.

***AtOEP16-1* gene (At2g28900): 6 exons, 5 introns**

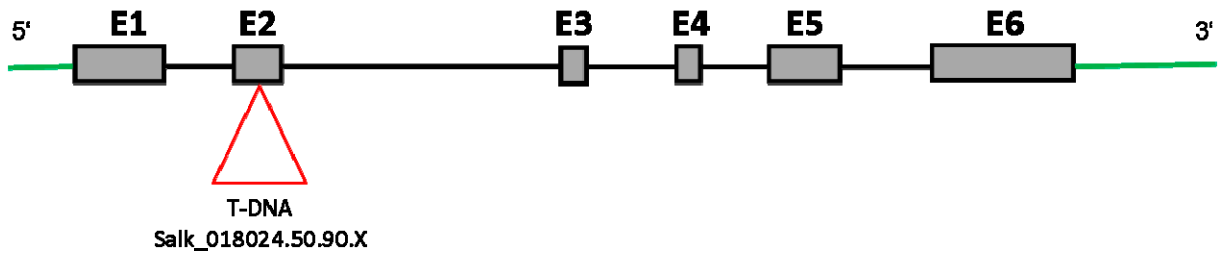


Figure 3.1 Structure of the *AtOEP16-1* mutant gene (Salk_018024.50.90.X).

AtOEP16-1 (At2g28900) consists of 6 exons (represented by grey rectangles) and 5 introns (represented by black lines separating each exon). 5'- and 3'- untranslated regions (UTRs) are shown in green. The T-DNA insertion, which disrupts the second exon of *AtOEP16-1*, is indicated as a red triangle (not drawn to scale).

Southern blotting was used to determine the number of T-DNA insertions. Genomic DNA was isolated from homozygous *Atoep16-1* plants, digested with different restriction enzymes, separated on agarose gels, and blotted onto nitrocellulose membranes. Then, the filter-bound DNA was hybridized with a T-DNA-specific probe (Pollmann *et al.*, 2007). These analyses revealed that the isolated mutant contained only one single T-DNA insertion detectable on Southern-blots. Further Western blot analyses using a heterologous antiserum from barley demonstrated a lack of *AtOEP16-1* protein in *Atoep16-1* plants. This result showed that the mutant is null with respect to the *AtOEP16-1* gene (Pollmann *et al.*, 2007).

Atoep16-1 seedlings exhibit a conditional cell death phenotype (Figure 3.2, taken from Pollmann *et al.*, 2007). If seedlings were grown for 5 d in darkness, they showed a strong red fluorescence under blue light indicative of the presence of free pigment molecules. High performance liquid chromatography (HPLC) analyses revealed that etiolated *Atoep16-1* seedlings overproduce free Pchl*a* molecules and that the pigment elutes at a retention time specific for Pchl*a*. Upon illumination, etiolated *Atoep16-1* seedlings rapidly died, most likely as a result of singlet oxygen accumulation triggered by free Pchl*a* molecules operating as photosensitizer.

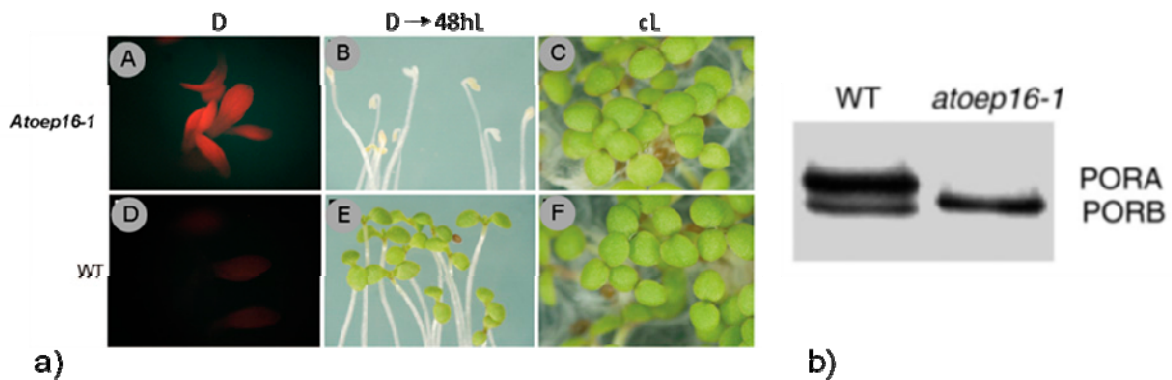


Figure 3.2 Conditional cell death phenotype of *Atoep16-1*.

(a) *Atoep16-1* (A-C) and wild-type (D-F) seedlings were germinated and grown for 5 d in the dark, before being inspected under blue light (400nm-450nm)(A and D). The emitted red fluorescence is indicative of the presence of free Pchl_a molecules. Upon illumination, these pigment molecules operate as photosensitizer and trigger singlet oxygen production and cell death (B and E). The phenotype of *Atoep16-1* is related to plant etiolation (skotomorphogenesis). In seedlings that are grown in continuous white light right from the beginning of germination, no cell death occurs and the plants are fully viable (C and F). (b) Immunoblot analysis of total proteins extracted from 5 d-old etiolated *Atoep16-1* and wild-type plants showing the absence of PORA protein in mutant versus wild-type seedlings. A heterologous antibody against total POR proteins from barley and an ECL system were used to develop the blots (taken from Pollmann *et al.*, 2007).

Both the high pigment fluorescence and cell death properties of *Atoep16-1* were reminiscent of those described for the *flu* mutant of *Arabidopsis* (Meskauskiene *et al.*, 2001; see also *Introduction*). Therefore photobleaching tests were carried out to define more precisely the conditions that lead to the establishment of the cell death phenotype. *flu* seedlings are fully viable and look like the wild-type when grown under continuous white light. By contrast, *flu* seedlings die when grown in the dark and exposed to white light (Meskauskiene *et al.*, 2001). Seeds of *Atoep16-1* and wild-type were sowed on MS agar medium, vernalized for 2 d in a cold room, transferred for 1 h to light to induce germination, and subsequently kept for 5 d in the dark, before being exposed to white light of approximately 125 $\mu\text{mol}/\text{m}^2\text{s}$. While *Atoep16-1* seedlings bleached out and died presumably as a result of Pchl_a-sensitized singlet oxygen formation, wild-type seedlings greened normally. When *Atoep16-1* seeds were germinated in the presence of white light right from the beginning of germination, they did not show any phenotype and closely resembled the wild-type. These results demonstrated that *Atoep16-1*, like *flu*, exhibits a conditional cell death phenotype associated with the process of seedling de-etiolation. Nevertheless, pigment analyses by HPLC uncovered differences in the amount and composition of tetrapyrrole pigments in *Atoep16-1* and *flu* plants. Pigment quantification showed that *flu* seedlings accumulate 8.5

higher levels of total Pchl a than wild-type, while *Atoep16-1* plants contained only 4.5 fold higher pigment levels. Moreover, *Atoep16-1* accumulated Pchl a , whereas *flu* plants accumulated elevated levels of Pchl b , as compared with wild-type (Pollmann *et al.*, 2007). It is attractive to hypothesize that these subtle differences may explain the different time courses of bleaching in these initial experiments where we found that *flu* seedlings were bleaching more rapidly than *Atoep16-1*.

Since previous biochemical experiments had shown that AtOEP16-1 interacts with pPORA during its Pchl a -dependent import, additional experiments were carried out. Plastids were isolated from dark-grown and light-grown plants and incubated with a chimeric protein consisting of the transit peptide of pPORA (transA) that had been fused to the dihydrofolate reductase (DHFR) reporter protein of mouse. As summarized in Pollmann *et al.* (2007) these experiments showed that *Atoep16-1* is specifically impaired in import of pPORA *in vitro*. This conclusion was supported by transient *in planta* expression studies using cDNAs encoding fusions of transA with the green jellyfish fluorescent protein (GFP). After ballistic bombardment, expression of transA-GFP was followed by confocal microscopy. It was found that only wild-type chloroplasts could import transA-GFP, whereas chloroplasts of mutant *Atoep16-1* were not able to do so. However, import of a similar chimeric protein consisting of the transit peptide of pPORB (transB) and GFP was detectable for both wild-type and *Atoep16-1* plants.

The import defect of pPORA, as deduced from the *in vitro* and *in planta* import experiments, along with the conditional cell death phenotype, suggested strong perturbations in etioplast ultrastructure in *Atoep16-1* plants. To address this point, electron microscopy was carried out by Armin Springer (from University of Bayreuth, Germany). These studies unveiled that etiolated *Atoep16-1* seedlings almost completely lacked prolamellar bodies. Instead of these paracrystalline structures, ghost-like areas were seen on the electron micrographs. Moreover, a drastic increase of plastoglobules was observed. Plastoglobules are thought to operate as metabolite carriers. For example, plastoglobules isolated from chloroplasts contain prenylquinones, such as plastoquinone and phylloquinone, as well as α -tocopherol (see Bréhélin *et al.*, 2007; Kessler and Vidi, 2007; for reviews). In

chromoplasts of fruits, also triacylglycerols, β -carotene and carotenoid esters accumulated. These different constituents are held together via specific plastoglobulins. In addition, plastoglobules contain metabolic enzymes putatively involved in abscisic acid metabolism and vitamin E synthesis. Several other proteins with unknown functions were found. Results, that some of the plastoglobulins are induced more strongly than others under adverse conditions, provoke the view of structural and functional heterogeneity of plastoglobules in adaptive responses to stress. Presumably because of technical difficulties to separate them from the envelope membranes, plastoglobules from senescent plants have less well been characterized. It seems likely that they may be involved in sequestering carotenoids released from the thylakoids upon the disassembly of the LHC proteins. It is also important to note that α -tocopherol synthesis requires phytol which could easily be released from Chl by virtue of chlorophyllase. However, such mechanism would require the transport of chlorophyll from the thylakoids to the envelope by either membrane flow or Chl carrier proteins and subsequent phytol loading to plastoglobulins. The role of plastoglobules during greening is unresolved but may now be studied by using the *Atoep16-1* mutant.

3.1.2 Re-screening of original seed stock from the Salk Institute for additional *Atoep16-1* mutants

3.1.2.1 Identification of two *Atoep16-1* mutant families with different phenotypes

In marked contrast to our results (Pollmann *et al.*, 2007), Philippar *et al.* (2007) reported that *Atoep16-1* did not exhibit a photobleaching phenotype. *In vitro* protein import studies revealed no differences between the import of either pPORA or pPORB into *Atoep16-1* and wild-type chloroplasts. In addition, etioplasts of homozygous *Atoep16-1* mutants looked similar to those of wild-type seedlings, and no differences in the size and ultrastructure of the prolamellar bodies were observed. Because protein mass spectrometry identified both PORA and PORB in etiolated *Atoep16-1* seedlings (summarized in Table 3.1), it was concluded that AtOEP16-1 is not involved in the import of pPORA (Philippar *et al.*, 2007).

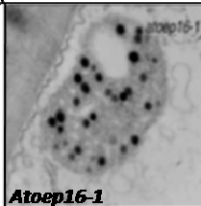
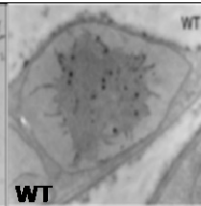
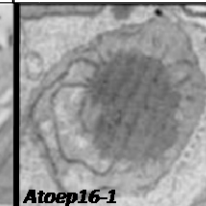
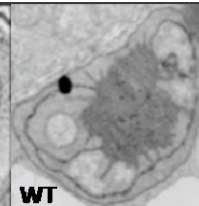
Mutant	<i>Atoep16-1</i>	
Articles	Pollmann et al., 2007	Philippa et al., 2007
Phenotypes under stress conditions (D → L)	Photobleaching	Not examined
Presence of PORA	- (<i>in vivo</i> , <i>in vitro</i> import)	+ (MS, <i>in vitro</i> import)
Etioplasts (electronic microscopy)	Absence of prolamellar bodies	WT (presence of prolamellar bodies)
		
		

Table 3.1 Opposing results on *Atoep16-1* published in the literature.

In two independent publications, Pollmann *et al.* (2007) and Philippa *et al.* (2007), compared the properties of *Atoep16-1* with regard to the phenotype after de-etiolation, PORA abundance and etioplast ultrastructure. Both mutants are obviously different. Electron micrographs were taken from Pollmann *et al.* (2007) and Philippa *et al.* (2007), respectively.

To solve this controversy in the literature, the original seed stock of the Salk Institute was rescreened for *Atoep16-1* mutants that may have a different phenotype than the one reported by Pollmann *et al.* (2007). Several independent *Atoep16-1* mutant plants, identified by genotyping, were backcrossed once with the wild-type. The offspring of these backcrosses was used to select homozygous plants and establish seed stocks. Aliquots of these seed stocks were grown in the dark for 5 d and analyzed with regard to their photobleaching properties and the presence/absence of PORA protein on Western blots. Analysis of the progeny of these stocks resulted in identifying 4 mutant types, belonging to two families: mutants that bleached out during de-etiolation and mutants that did not bleach out after this dark-to-light shift. Each family segregated into two groups: one group lacking PORA protein on Western blots and one group containing PORA protein. We designated the resulting mutants *Atoep16-1;5-8*. From the data summarized in Table 3.2 it is likely that mutant *Atoep16-1;5* may correspond to the mutant described by Pollmann *et al.* (2007),

which was obtained after two backcrosses, whereas line *Atoep16-1;8* may correspond to the mutant described by Philippar *et al.* (2007). Mutants *Atoep16-1;5-6* and *Atoep16-1;5-7* represent intermediate phenotypes with new phenotypic properties (Figure 3.3 a and b).

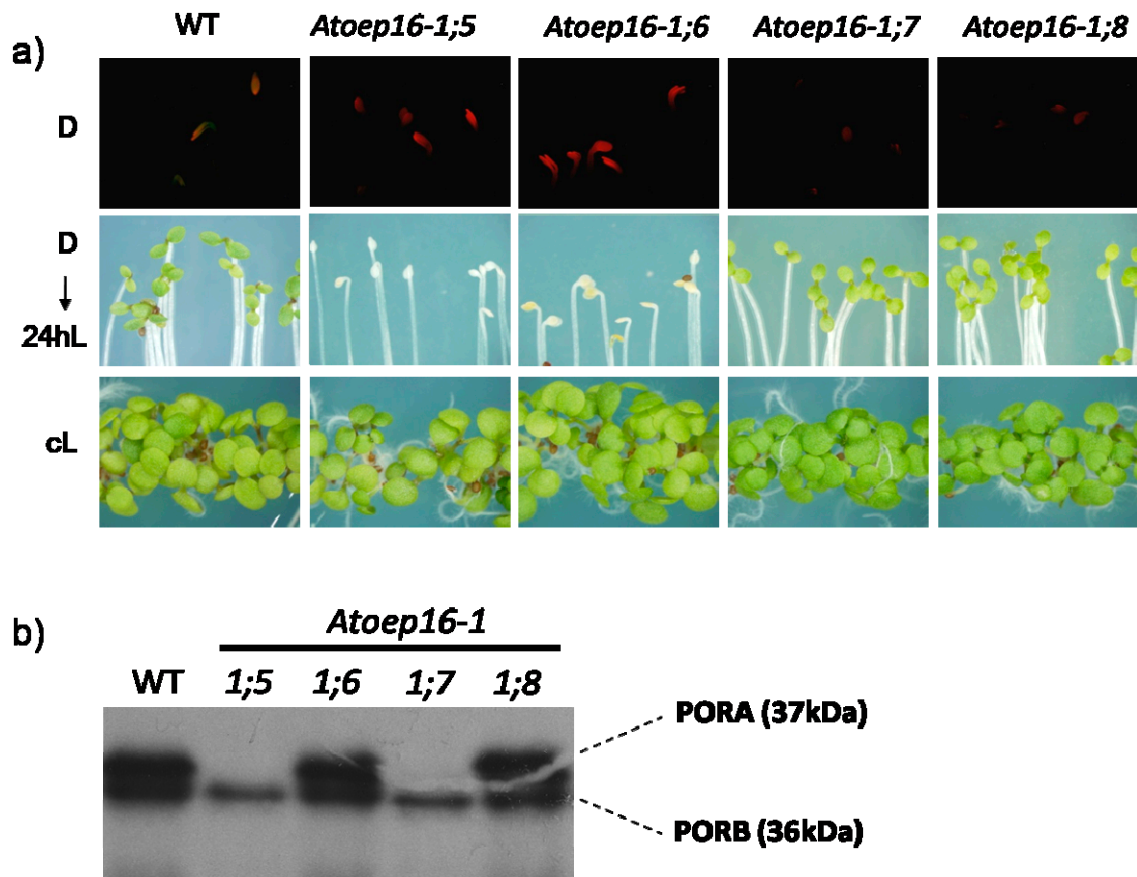


Figure 3.3 Identification of four independent *Atoep16-1* knock-out mutants in the original seed stock Salk_018024.50.90.X.

After having rescreened the original seed stock provided by the Salk Institute (Salk_018024.50.90.X), four independent *Atoep16-1* knock-out mutant types were found that differ in their phenotype after growth in the dark and after illumination. These mutant types were designated *Atoep16-1;5-8*. (a) Phenotypic analysis performed for 5 d-old *Atoep16-1;5-8* and wild-type (WT) seedlings after growth in darkness for 5 d (D), after a non-permissive dark-to-light shift for 24 h (D→24hL) and after growth in continuous white light (cL). Note the red Pchl_a fluorescence under blue light (400 nm–450 nm) in seedlings of mutants *Atoep16-1;5* and *Atoep16-1;6* and the lack of a corresponding fluorescence in seedlings of mutants *Atoep16-1;7* and *Atoep16-1;8*. Upon illumination, free Pchl_a molecules trigger singlet oxygen production and cell death in mutants *Atoep16-1;5* and *Atoep16-1;6*. In all four types of *Atoep16-1;5-8* mutant seedlings that were grown in continuous white light right from the beginning of illumination, no phenotype is detectable. (b) Western blot analysis on plastid proteins extracted from 5 d-old etiolated *Atoep16-1;5-8* and wild-type seedlings, using heterologous barley POR antiserum.

3.1.2.2 *PORA* and *FLU* genes are unaffected in *Atoep16-1;5-8* mutant lines

Pilot experiments were carried out to reconfirm the homozygous nature of the isolated *Atoep16-1;5-8* mutants. Using a PCR-based approach, the presence of the T-DNA and interrupted *AtOEP16-1* gene was assessed with genomic DNA isolated from the third generation (F3) of *Atoep16-1;5-8* and wild-type plants. As shown in Figure 3.4 (panel a), all four *Atoep16-1;5-8* mutants were homozygous with regard to the *AtOEP16-1* mutation.

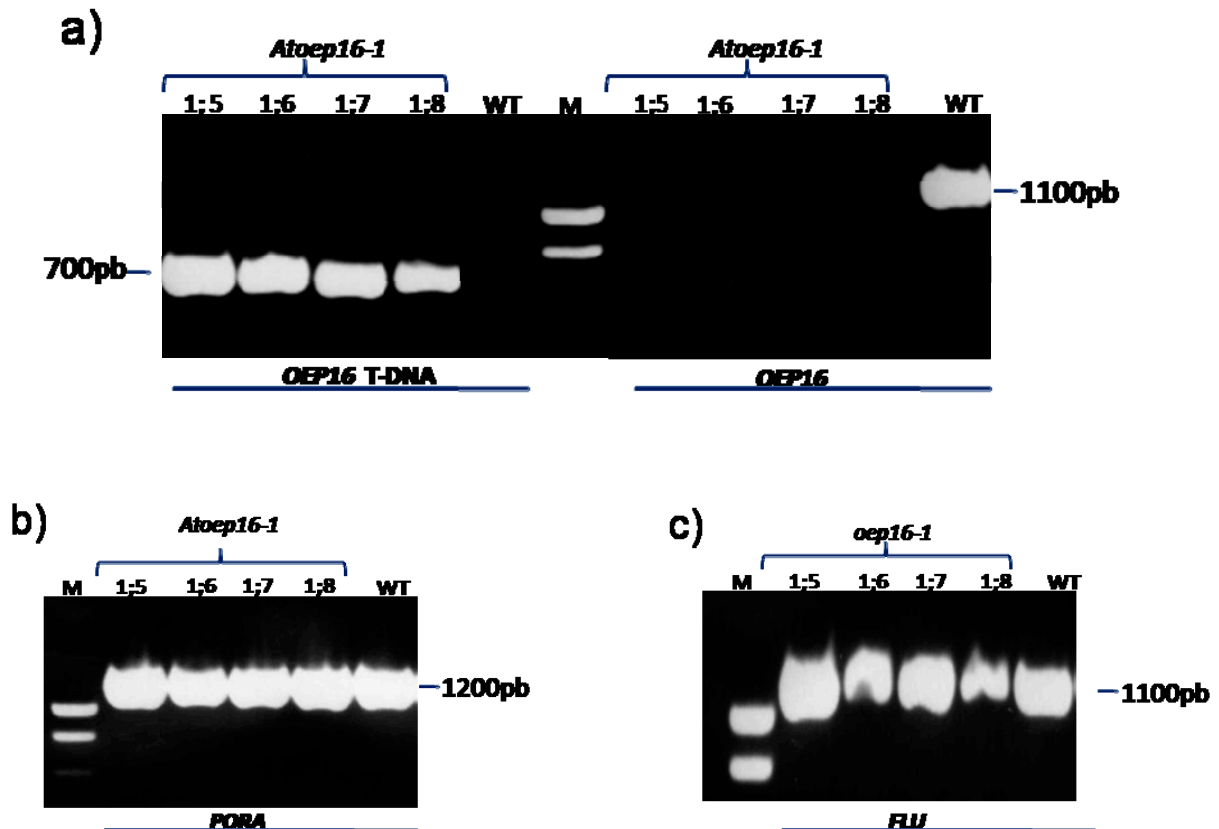
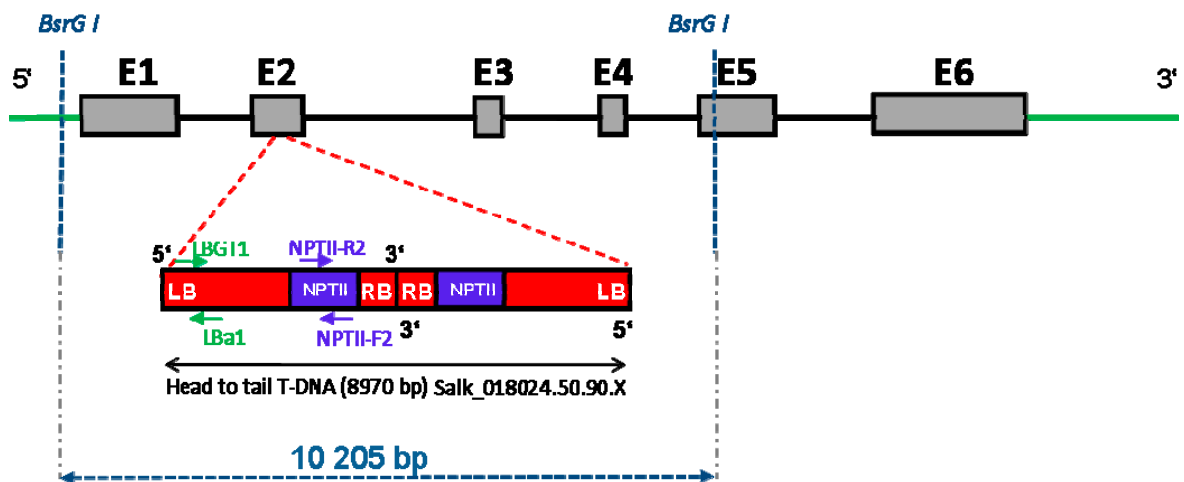


Figure 3.4 PCR verification of the T-DNA insertion in *AtOEP16-1;5-8*.

a) PCR-based verification of the absence of *AtOEP16-1* in the four *Atoep16-1;5-8* mutant types. PCR was carried out using genomic DNA and a pair of specific primers for the wild-type *AtOEP16-1* gene and a pair of primers corresponding to the T-DNA plus *AtOEP16-1* gene. b) and c) PCR analyses to verify the absence of T-DNA insertions in the *PORA* (b) and *FLU* (c) genes. Amplification products corresponding to the wild-type *PORA* and *FLU* genes, respectively, were detected both for *Atoep16-1;5-8* as well as wild-type plants. Thus, neither gene contains a detectable T-DNA insertion. M stands for Smart Ladder DNA marker (Eurogentec).

A reason for the appearance of different phenotypes in mutants *Atoep16-1;5-8* could be the presence of additional T-DNA insertions that were not crossed out after the first backcross. To test this hypothesis, genomic DNA was isolated from mutants *Atoep16-1;5-8* and digested with the restriction endonucleases *BsrG I* and *Cla I*. Southern blots were further hybridized with different probes corresponding to either the Kan resistance gene and the left border regions of the T-DNA. The results in Figure 3.5 showed that there was only one T-DNA insertion detectable in all four *Atoep16-1;5-8* mutants.

a) *AtOEP16-1* gene (At2g28900): 6 exons, 5 introns



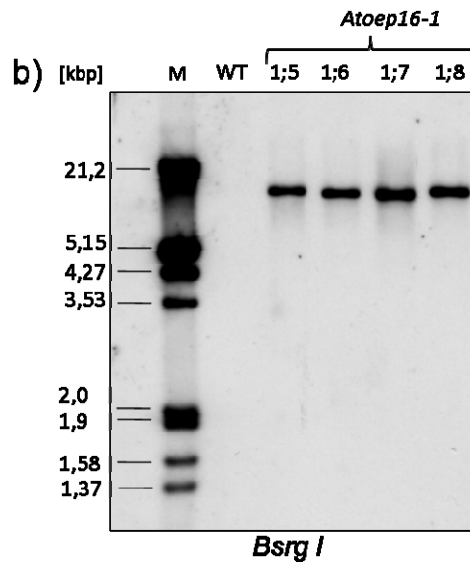


Figure 3.5 Southern-blot analysis of *Atoep16-1* mutant lines.

Upon genotyping and sequencing of the *AtOEP16-1* gene in mutants *Atoep16-1;5-8*, all were found to contain head-to-tail insertions of two T-DNA copies. To confirm this conclusion, Southern blotting was used. Genomic DNA was digested with *BsrGI* which cuts 471 bp before first exon and in the position of 516 bp of the fifth exon. Probes were generated by a) PCR, using the following primer combinations: LBGT1 plus Lba1, for the left border T-DNA probe (326 bp) or neomycin phosphotransferase (NPT)II-R2 plus NPTII-F2, for the right border (NPT II, 551 bp) probe. b) Autoradiogram showing the result of the Southern blot analysis for DNA of mutants *Atoep16-1;5-8* hybridized with a digoxigenin-labeled right border T-DNA probe. The expected size of the detectable T-DNA fragment is 10205 bp, whereas the detected fragment is approximately two-fold larger because of the head-to-tail insertion of the two T-DNA copies. M stands for λ DNA marker that had been labeled with digoxigenin.

An alternative reason for the obviously different phenotypes of mutants *Atoep16-1;5-8* could be the presence of small DNA fragments that might have occurred by the loss of previously inserted T-DNA copies. Such mutations would not be detectable by Southern blotting and could concern genes for key players of the seedling de-etiolation response such as *PORA* and *FLU*. We therefore tested the possible presence of such mutations by sequencing the *PORA* and *FLU* genes using genomic DNA isolated from all of the different *Atoep16-1;5-8* mutants. PCR analyses showed that amplified DNA fragments corresponding to the expected sizes of the *PORA* and *FLU* genes were identical to those in the wild-type (Figure 3.4 b and c). Subsequent sequencing of the different PCR fragments revealed that no changes in the nucleotide sequences of the *PORA* and *FLU* genes occurred. Our results vindicated that no detectable DNA rearrangements occurred in the *PORA* and *FLU* genes in mutants *Atoep16-1;5-8*.

To verify the absence of AtOEP16-1 protein in mutants *Atoep16-1;5-8*, Western blotting was carried out. An antibody was raised against the bacterially expressed and purified AtOEP16-1 protein (see Appendix A.2). A hexa-His-tagged version of AtOEP16-1 was expressed in strain BL21-AI™ of *E.coli* using Gateway® technology (Invitrogen). Recombinant protein was purified by Ni-NTA agarose chromatography and sent to Interchim enterprise for immunizing rabbits. Different boosts of the antiserum containing anti-OEP16 antibodies were obtained and tested on Western blots using total proteins extracted from 2 w-old *Atoep16-1;5-8* mutant plants that had been grown under standard long day (16h/8h) light conditions at 80 $\mu\text{mol}/\text{m}^2\text{s}$. Figure 3.6 demonstrates that no OEP16 signal was detectable on the Western blots, confirming that all four *Atoep16-1;5-8* mutants were truly null for the *AtOEP16-1* gene.

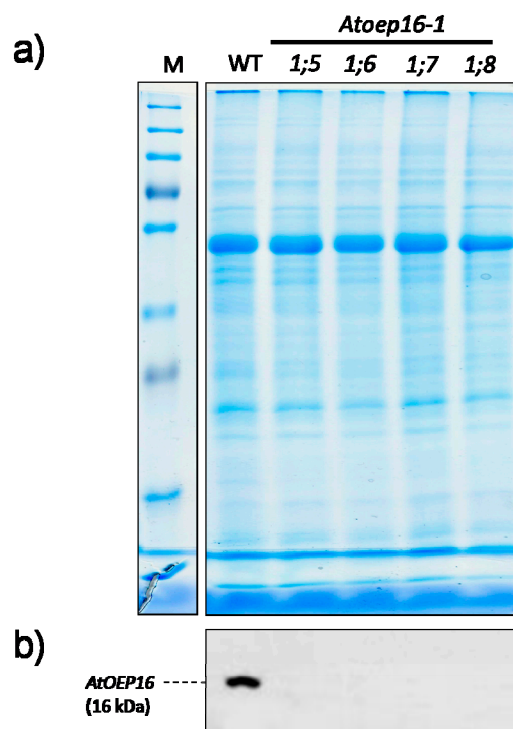
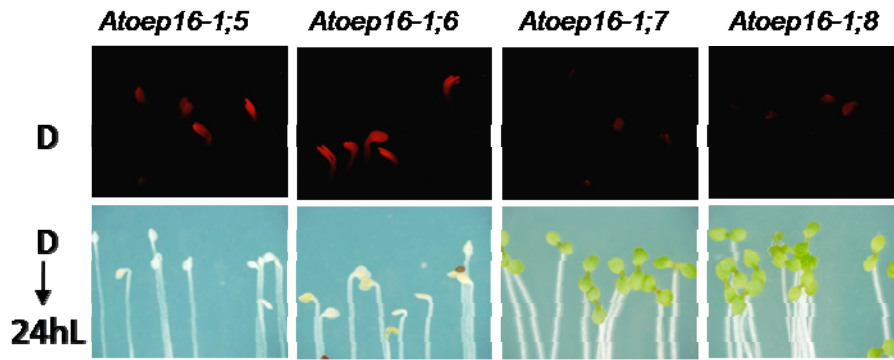


Figure 3.6 Absence of *AtOEP16-1* protein in mutants *Atoep16-1;5-8*.

Total protein extracts were prepared from 10 d-old, light-grown *Atoep16-1;5-8* plants and separated by SDS-PAGE on a 15% polyacrylamide gel. **a)** Coomassie blue stained PAGE (40 μg protein per lane) shows equal loading of the samples. **b)** Western blot corresponding to (a) AtOEP16-1-related proteins. The absence of AtOEP16-1 protein was confirmed using protein extracts from isolated etioplasts of mutants *Atoep16-1;5-8* (see Appendix B).



T-DNA	1	1	1	1
AtOEP16-1	-	-	-	-
PORA	-	+	-	+
Cell death	+	+	-	-

Table 3.2 Comparison of the different properties of *Atoep16-1; 5-8*.

Despite the presence of only one T-DNA fragment on Southern blots that leads to the absence of AtOEP16-1, all four *Atoep16-1;5-8* mutants exhibit different phenotypes. They either overproduce Pchlide in the dark or not and contain or lack PORA protein as indicated.

Taken together, different properties of all four *Atoep16-1; 5-8* lines are summarized in a Table 3.2.

3.2 Physiological characterization of the four *Atoep16-1* mutant types

3.2.1 Pigment analyses

3.2.1.1 Low-temperature fluorescence analysis of Pchlde forms in etiolated *Atoep16-1;5-8* mutant seedlings

A comparison of the red pigment fluorescence in the cotyledons of 5 d-old dark-grown *Atoep16-1;5-8* and wild-type seedlings revealed higher Pchlde levels in mutants *Atoep16-1;5* and *1;6*, suggestive of the presence of free, non-photoconvertible Pchlde molecules not bound to POR. Low-temperature fluorescence spectroscopy was used to assess the functional state of pigments *in planta*. During low-temperature fluorescence spectroscopy Pchlde normally gives rise to two spectral pigment species: Pchlde-F631 and Pchlde-F655 (Lebedev and Timko, 1998). Pchlde-F655 is also called photoactive Pchlde because it can be converted to Chlide under a 1-msec flash of white light. The presence of Pchlde-F655 indicates the establishment of functional PORA:PORB-pigment complexes in the prolamellar bodies of etioplasts (Reinbothe *et al.*, 1999 and 2003). These complexes are involved in light trapping and excess light energy dissipation during seedling de-etiolation. By contrast, Pchlde-F631, also called photoinactive Pchlde, cannot immediately be converted to Chlide (Lebedev and Timko, 1998). It was shown that Pchlde-F631 comprises PORA-Pchlde *b* complexes and free, non-protein bound Pchlde molecules (Reinbothe *et al.*, 1999 and 2003).

In order to determine the *in vivo* states of Pchlde in the four different *Atoep16-1* mutant types, low-temperature (77 K) fluorescence spectroscopy was performed for 5 d-old etiolated mutant seedlings and compared with that of wild-type seedlings. The low-temperature fluorescence spectra of etiolated wild-type seedlings confirmed the presence of two main emission bands, with maxima at 631 and 655 nm, which represent photoinactive and photoactive Pchlde, respectively (Figure 3.7). In contrast to the wild-type, the *Atoep16-1;5* mutant contained large amounts of Pchlde-F631, whilst the major, photoactive Pchlde-F655 form was missing. Etiolated seedlings of mutant *Atoep16-1;6* contained higher levels of photoinactive Pchlde-F631 and reduced levels of photoactive Pchlde-F655 when

compared with wild-type. In line *Atoep16-1;7*, traces of Pchl_a were present that were exclusively established by photoinactive Pchl_a-F631. Unlike the low temperature spectrum of *Atoep16-1;5-7*, the spectrum of mutant *Atoep16-1;8* closely resembled that of wild-type seedlings and both photoactive and photoinactive Pchl_a were seen (Figure 3.7).

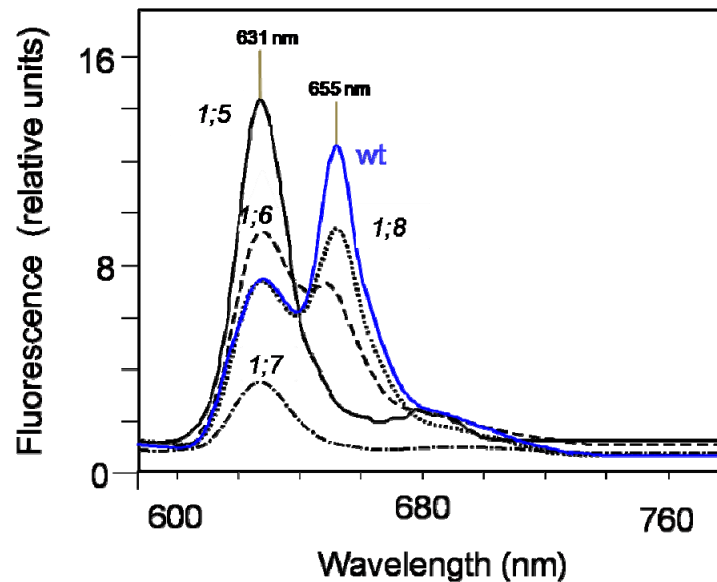


Figure 3.7 Low temperature (77 K) fluorescence emission analysis of pigments in *Atoep16-1; 5-8* mutant seedlings.

Low temperature spectroscopy was carried out at an excitation wavelength of 440 nm. The different peaks correspond to photoinactive Pchl_a, emitting at 631nm, and photoactive Pchl_a, emitting at 655nm. Life Sciences spectrometer, model LS50, Perkin Elmer Corp., Norwalk, CT, was used for spectroscopy.

Together these findings corroborated the view that mutant *Atoep16-1;5* may correspond to the line originally described by Pollmann *et al.* (2007), while mutant *Atoep16-1;8* may be identical to the line identified by Philippar *et al.* (2007).

3.2.1.2 HPLC-analysis of pigments (carotenoids, chlorophylls)

Previous photobleaching tests (Figure 3.3 a) had revealed that mutants *Atoep16-1;5* and *1;6* were more prone to photooxidative stress than mutants *Atoep16-1;7* and *1;8*. While the former bleached when grown in darkness and exposed to high white light, the latter turned green normally and developed like wild-type seedlings. We asked whether, besides Chl, also differences in other pigments, in particular in the composition and concentration of different carotenoids (Figure 3.8), would be present in the four *Atoep16-1* mutant lines.

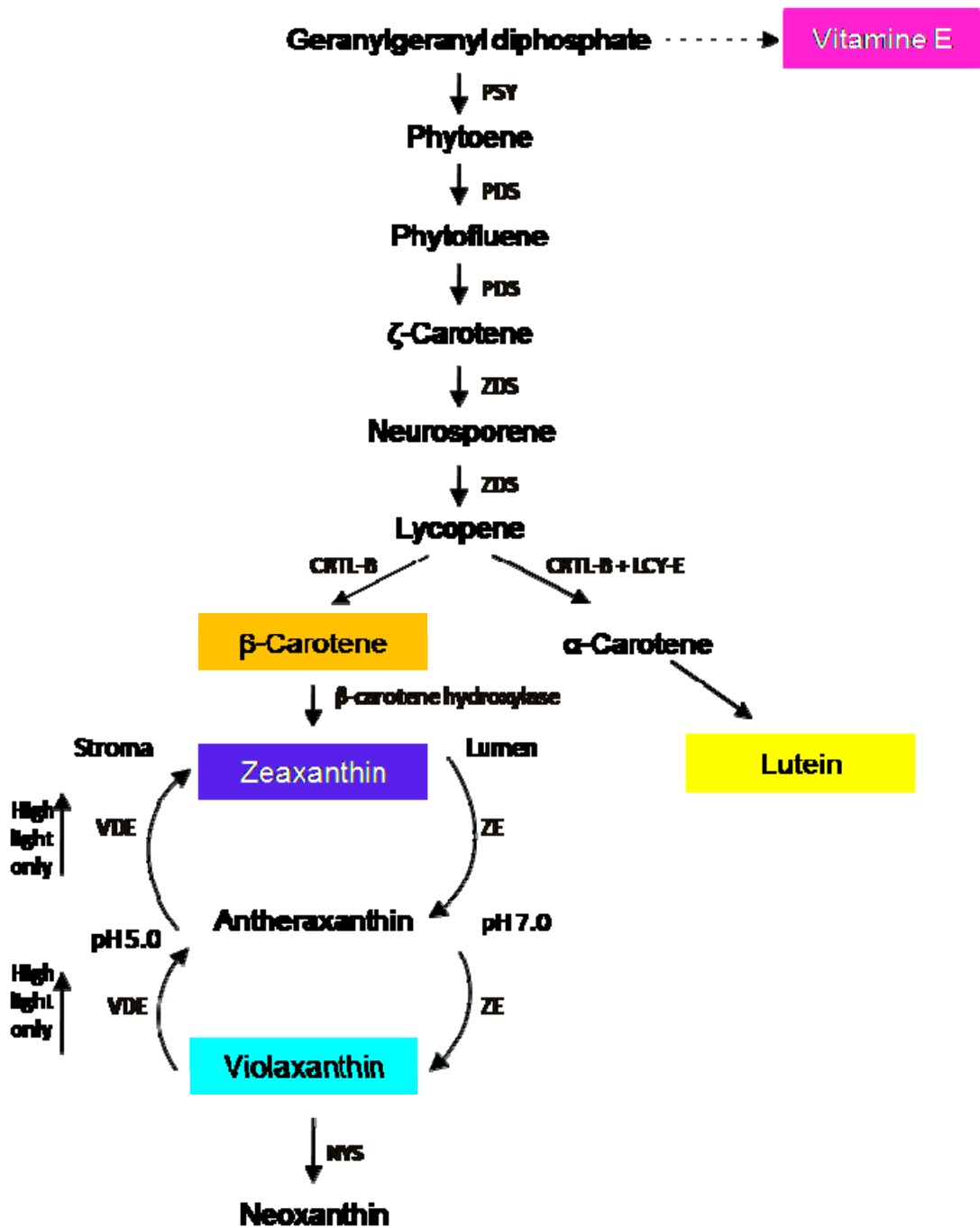
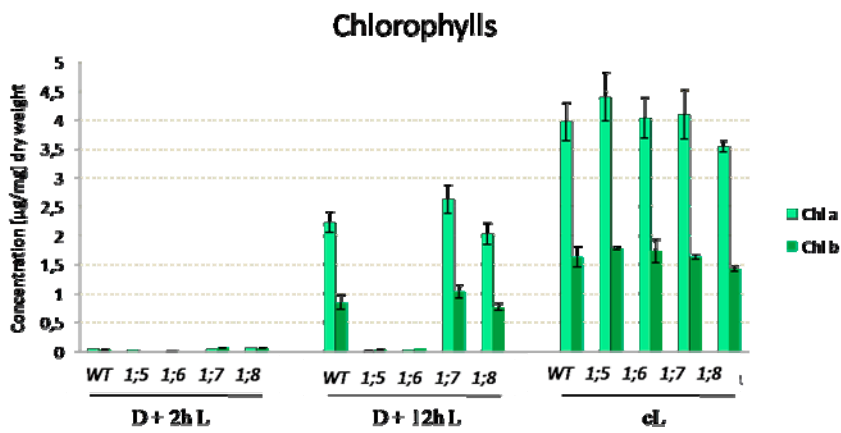


Figure 3.8 Biosynthesis of carotenoids in plants.

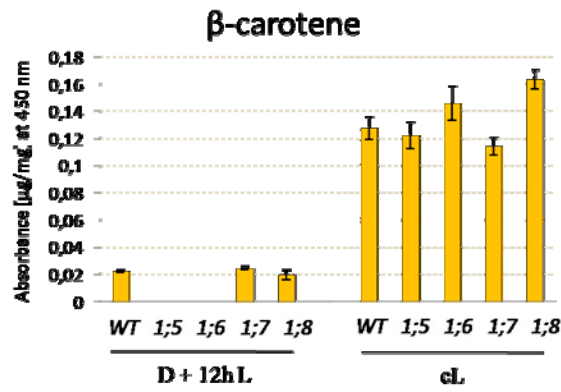
Carotenoids and vitamine E investigated in our studies are shown in colours. Light blue circle represents the xanthophylls cycle. PSY: phytoene synthase, PDS: phytoene desaturase, ZDS: ζ carotene desaturase, CRTL-B: lycopene β-cyclase, LCY-E: lycopene epsilon cyclase, ZE: zeaxanthin epoxidase, VDE: violaxanthin de-epoxidase, NYS: neoxanthin synthase (adapted from Simkin, 2002 and Szabo *et al.*, 2005).

Pigment analyses were carried out by high-performance liquid chromatography (HPLC) using methanol extracts from wild-type and *Atoep16-1;5-8* mutants that had been grown in darkness for 5 d and transferred to high light intensity of 210 $\mu\text{mol}/\text{m}^2$ for 2 h and 12 h, respectively. For comparison, plants were grown for 5 d under continuous white light.

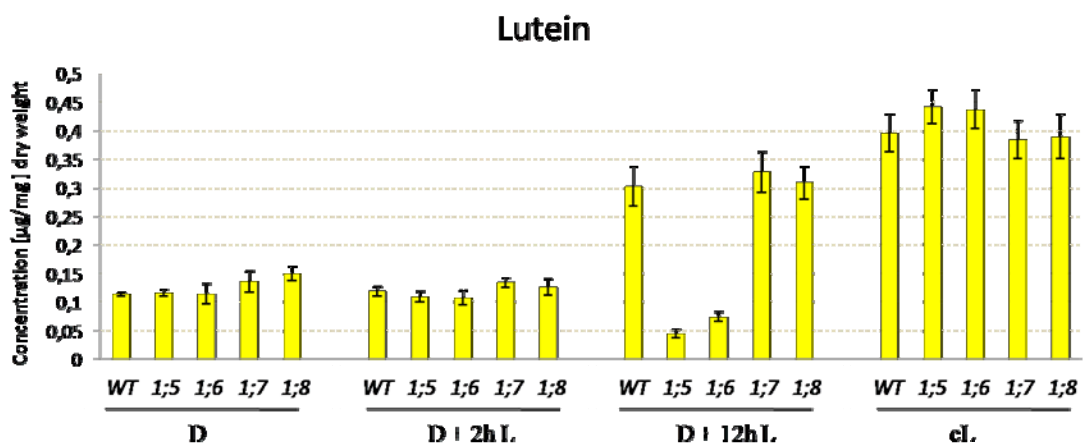
From the HPLC tracings it turned out that all four *Atoep16-1;5-8* mutants showed the same pigment content as the wild-type both after growth in darkness or continuous white light. Cotyledons of plants grown in the dark for 5 d accumulated similar amounts of violaxanthin (viola), neoxanthin (neo; data not shown) and lutein, while Chl *a* and Chl *b*, as well as β -carotene were not detectable (Figure 3.9). Already after 2 h of high white light exposure, some differences in pigment accumulation occurred. Chl *a* and Chl *b*, as well as xanthophylls started to accumulate in all lines. Viola levels increased by around 10-20% in *Atoep16-1;7* and *1;8*, similarly to wild-type, whereas the viola content was slightly reduced (by about 5%) in mutant *Atoep16-1;5* and *1;6* (Figure 3.9 d). Simultaneously, zeaxanthin (zea) appeared in all of the four *Atoep16-1;5-8* mutants. Detection of such pigments was not surprising since oxygenated carotenoids (xanthophylls) are widely recognized to play an important role in the light-harvesting complexes of the photosystems. We suppose that when dark-grown plants are exposed for 2 h to strong saturating white light to support upcoming photosynthesis, the luminal pH of the thylakoids may diminish because of difficulties to dissipate the proton gradient across the membrane by the ATP synthase. In turn, an activation of the viola deepoxidase enzyme could occur that is responsible for viola deepoxidation to zea via antheraxanthin (ant) (Verhoeven *et al.*, 1996). It is well known that deepoxidase together with epoxidase (catalyzing the reverse epoxidation reaction: conversion of zea to viola) operate within the “xanthophyll cycle” (Figure 3.8). This reversible, light-induced synthesis of zea is involved in the protection mechanism of the photosynthetic apparatus against excess light energy. Thus, newly synthesized zea could directly quench the singlet excited state of photosystem II (PSII) Chls, protecting the sensitive reaction centre from overexcitation. Such mechanism of deepoxidation is commonly observed in plants stressed with high light. The level of another xanthophyll, lutein, remained unchanged in all of the examined genotypes (*Atoep16-1;5-8*, wild-type) when compared to dark conditions (Figure 3.9 c).



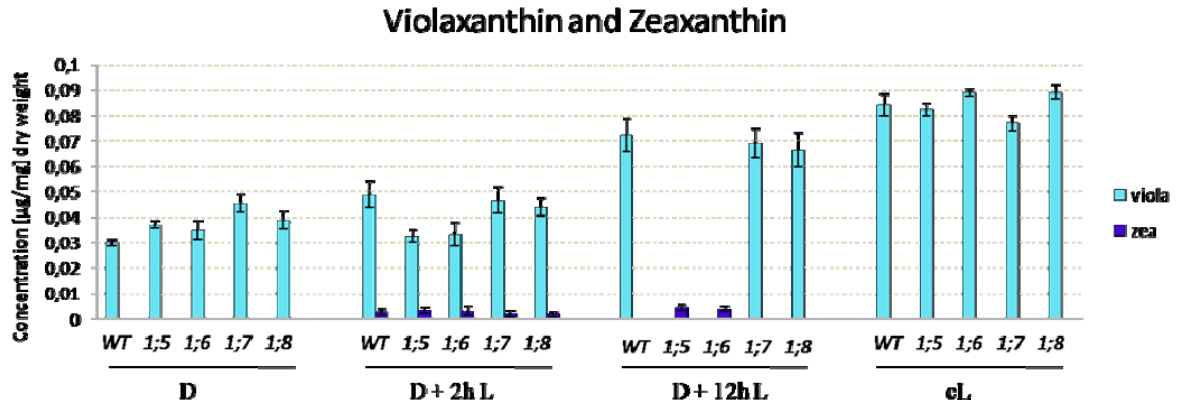
a) Concentration of chlorophylls. Chl a: chlorophyll a; Chl b: chlorophyll b.



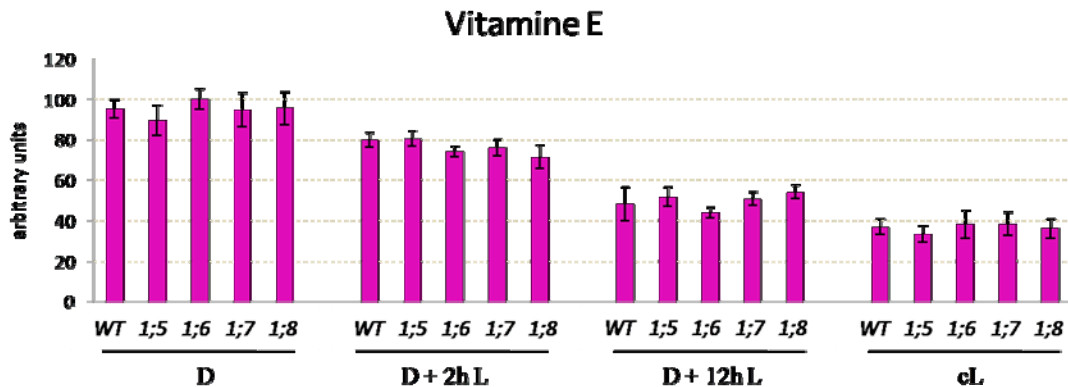
b) Concentration of β-carotene.



c) Concentration of lutein.



d) Concentration of violaxanthin and zeaxanthin. Viola: violaxanthin; Zea: zeaxanthin.



e) Accumulation of vitamine E.

Figure 3.9 The effect of light on pigment accumulation in *Atoep16-1;5-8* and wild-type seedlings.

HPLC analyses were performed on etiolated seedlings that had been grown in darkness for 5 d (D) and extracted with methanol. Similarly, etiolated seedlings that had been exposed to white light for 2 h (D + 2h L) and 12 h (D + 12h L), respectively, were extracted with methanol. As control, seedlings of the same age were used that had been grown under continuous white light (cL). Error bars indicate standard deviations of mean values (+/- SD) derived from three independent measurements. Levels of vitamine E are expressed in arbitrary units and not as absolute values.

The most pronounced changes in pigment accumulation were observed in dark-grown plants transferred to high light for 12 h. The HPLC analyses (Figure 3.10) showed a decrease of carotenoids and Chls in mutants *Atoep16-1;5* and *1;6*, whereas in wild-type and

mutants *Atoep16-1;7* and *1;8* these pigments did not decline. Mutants *Atoep16;1-5* and *Atoep16;1-6* were not able to accumulate Chl. This result is in marked contrast to mutants *Atoep16-1;7* and *1;8*, which behaved like wild-type. They accumulated similar levels of Chl, although at different Chl *a*:Chl *b* ratios (Figure 3.9 a). Interestingly, lutein and viola levels were reduced in mutants *Atoep16-1;5* and *1;6*, while they increased by about 50% in *Atoep16-1;7* and *1;8*. β -carotene was not detected in *Atoep16;1-5* and *Atoep16;1-6*, in contrast to wild-type and mutants *Atoep16-1;7* and *1;8* (Figure 3.9 b, c and d). Higher levels of zeaxanthin accumulated in mutants *Atoep16-1;5* and *1;6*, whereas zeaxanthin was no longer detected in wild-type, neither in *Atoep16-1;7* nor in *1;8* (see Figure 3.9 d). The absence of β -carotene and increase in zeaxanthin content in mutants *Atoep16-1;5* and *1;6* may be the consequence of the hydroxylation of β -carotene, which - if not integrated in photosynthetic complexes - is available for the conversion to zeaxanthin. In addition, a reduction in viola content in mutants *Atoep16;1-5* and *Atoep16;1-6* may be due to the fact that a long (12 h) light stress can maintain viola deepoxidation, leading to zeaxanthin accumulation. Since mutants *Atoep16-1;7* and *1;8* turned green after 12 h of illumination, it seems unlikely that the light conditions (light quality and quantity) were generally unfavourable for the establishment of the photosynthetic apparatus. Thus, the measured higher levels of viola may be the consequences of: (i) an inactivation of the deepoxidase, (ii) efficient conversion of zeaxanthin to viola by the epoxidase, and (iii) an integration of viola in newly built antenna complexes.

Zeaxanthin provides effective photoprotection through two mechanisms: by the modulation of the thermal energy dissipation and by acting as an efficient scavenger for ROS. Havaux *et al*, (2003) demonstrated that the photoprotective function mediated by zeaxanthin overlaps with the other antioxidant mechanisms of chloroplasts involving, for example, α -tocopherol (vitamin E). To gain deeper insights into the regulatory mechanisms of photoprotection in *Arabidopsis*, we analyzed the accumulation of vitamin E in wild-type and mutants *Atoep16-1;5-8* (Figure 3.9 e). The results indicated a continuous decrease in the α -tocopherol content during illumination of dark-grown seedlings. However, there were no significant differences between all of the four *Atoep16-1* mutants and wild-type. Despite the fact that mutants *Atoep16-1; 5* and *1;6* had a significant reduction in their total Chl content and accumulated zeaxanthin, they did not show an increase in the α -tocopherol content with respect to wild-type seedlings.

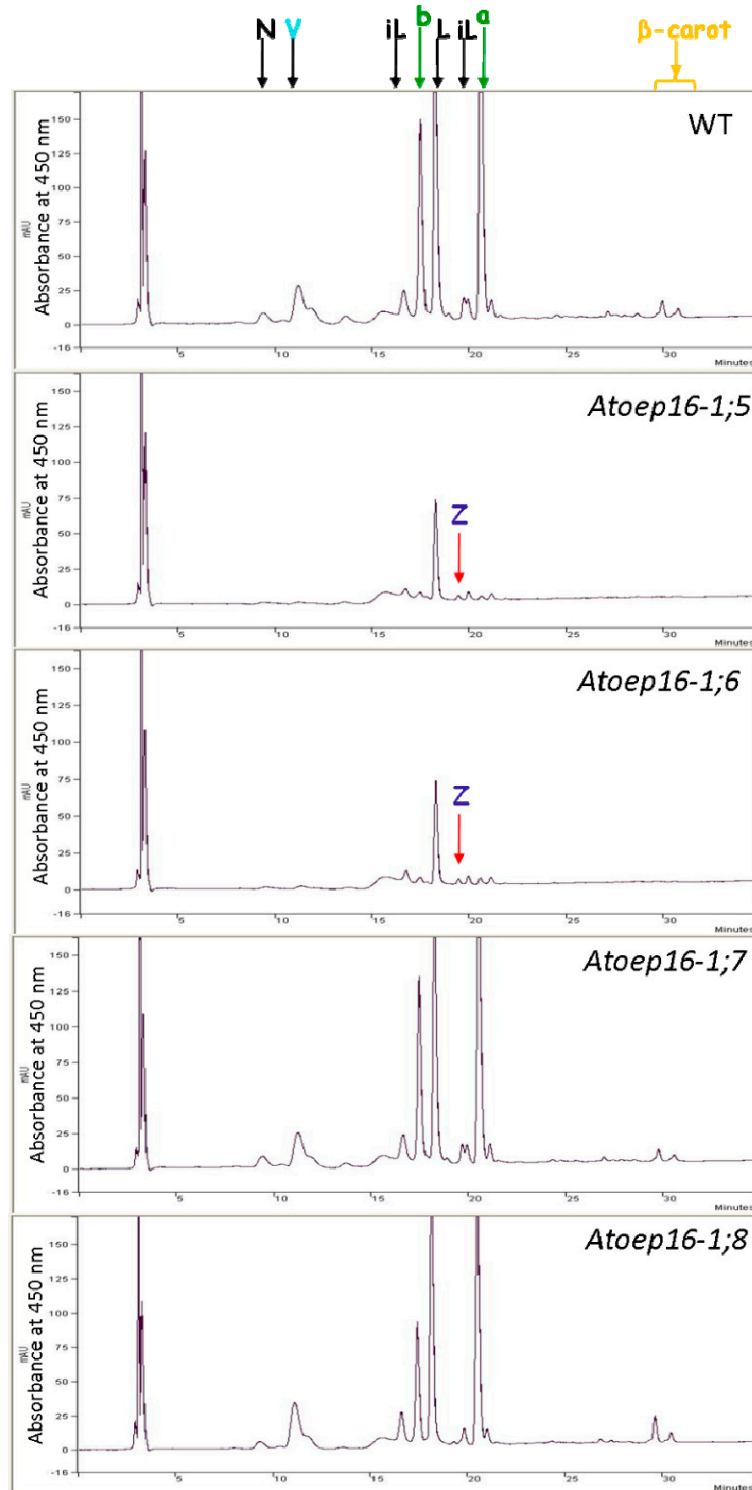


Figure 3.10 Representative HPLC analysis of pigments found in the cotyledons of wild-type and *Atoep16-1;5-8* mutant seedlings.

Each chromatogram represents absorbance (Abs) readings at 450 nm of pigments found in the cotyledons of 5 d-old dark-grown seedlings after their exposure to high light ($210 \mu\text{E}/\text{m}^2$) for 12h. N: neoxanthin; V: violaxanthin; L: lutein; iL: isomers of lutein; b: chlorophyll *b*; a: chlorophyll *a*; Z: zeaxanthin; β -carot: β -carotene. Retention time is indicated in min.

Taken together, the results of the HPLC analyses showed that high white light stress in *Atoep16-1;5* and *1;6* plants (which are more sensitive to photooxidative stress than *oep16-1;7* and *1;8*), leads not only to reductions in the Chl content but also to viola and β -carotene depletion and a reduction in the amount of lutein. Moreover, both mutants *Atoep16-1;5* and *1;6* accumulated higher levels of zeaxanthin when compared to mutants *Atoep16-1;7* and *1;8* and wild-type. We assume that the decrease of viola, lutein and β -carotene was not enough compensated for by an accumulation of zeaxanthin and vitamin E to prevent a bleaching phenomenon and a further cell death in irradiated *Atoep16-1;5* and *1;6* seedlings .

3.2.2 Viability of *Atoep16-1* mutant seedlings

3.2.2.1 Developmental control of seedling viability

The establishment of the cell death phenotype in mutants *Atoep16-1;5* and *Atoep16-1;6* depends on seedling age, hypocotyls length and the time period and intensity of illumination. In time-course experiments we observed that the increase of time of seedling growth in darkness (and thus seedling age) provoked an increase in hypocotyl length and greater light sensitivity. This effect is illustrated for *Atoep16-1;6* and wild-type in Figure 3.11.

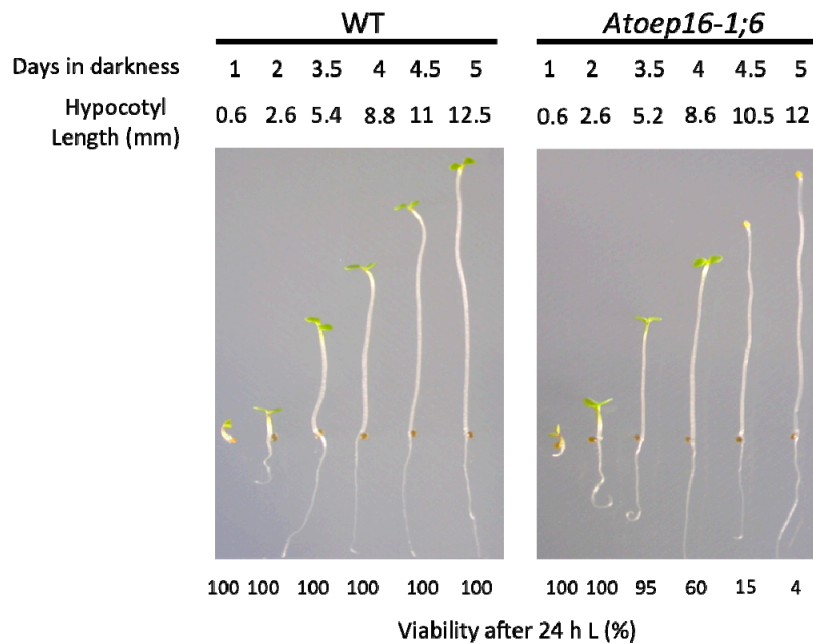


Figure 3.11 Seedling survival as a function of seedling age and hypocotyl length in *Atoep16-1;6* and wild-type.

Atoep16-1;6 and wild-type seedlings were grown in the dark for 1 d to 5 d and then transferred to white light ($125 \mu\text{mol}/\text{m}^2$) for 24 h. Seedling viability was assessed as described in Figure 3.2 using the greening defect. Note that the phenotype is dependent on seedling age and is reflected in the increasing hypocotyl length.

The increased sensitivity to light of dark-grown *Atoep16-1;6* seedlings can be attributed to the higher Pchl_a levels accumulated in older versus younger seedlings (Figure 3.12 a). We observed similar Pchl_a fluorescence levels in the cotyledons of *Atoep16-1;6* and wild-type when the seedlings were grown in the dark for only 1 or 2 d. Thereafter, in most experiments beginning after 3,5 d of growth in the dark, we detected increasing Pchl_a fluorescence levels in *Atoep16-1;6* mutant seedlings, whereas in wild-type seedlings the fluorescence level of Pchl_a remained low (Figure 3.12 a and b). When such etiolated plants were subsequently exposed to strong white light ($210 \mu\text{mol}/\text{m}^2\text{s}$) for 24 h, most of the *Atoep16-1;6* mutant seedlings had turned yellow, indicating that they kept their carotenoids for this period. When illumination periods were extended to 48 h or longer time spans, almost all of the previously yellow seedlings became white, suggesting a pigment degradation to occur during cell death (Figure 3.12 d). In contrast to mutant *Atoep16-1;6*, wild-type seedlings greened normally under all tested conditions.

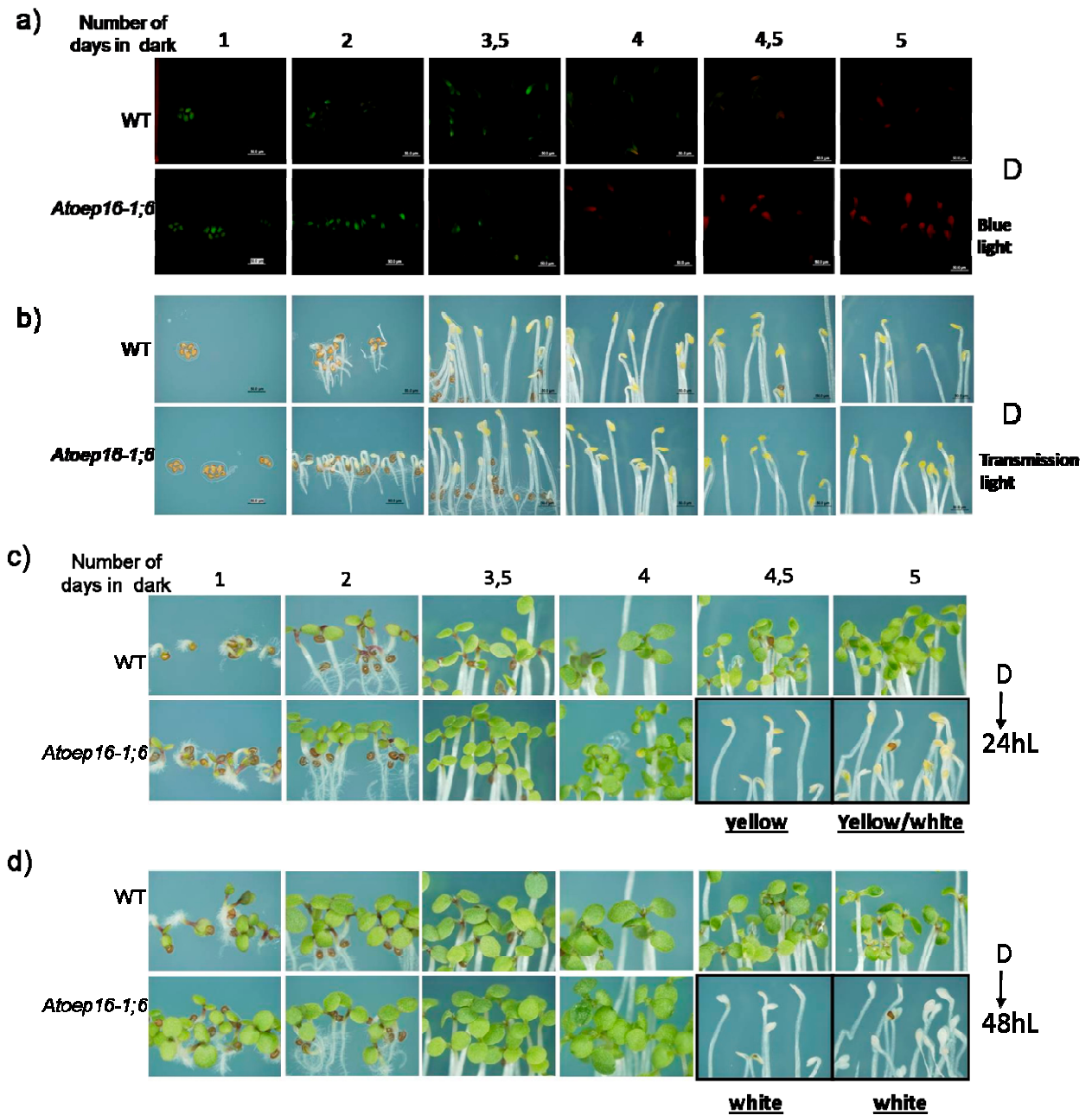


Figure 3.12 Photobleaching as a function of Pchl a overaccumulation in mutant *Atoep16-1;6*.

Atoep16-1;6 and wild-type seeds were germinated for different periods in darkness (a and b) and subsequently exposed to strong white light ($210 \mu\text{mol}/\text{m}^2$) for 24 h c) or 48 h d). a) Red Pchl a autofluorescence was monitored under blue light (400 nm-450 nm). b) The same as in a), but showing the seedlings under normal daylight. c) and d) Phenotypes after irradiating etiolated seedlings with white light for 24 h and 48 h, respectively.

3.2.2.2 Quantitative assessment of seedling viability

From the previous experiments we concluded that the establishment of the bleaching phenotype is controlled developmentally and depends on seedling age. Time-course experiments were carried out to gain insight into the progression of cell death. Seeds were germinated for 5 d in the dark and exposed to strong white light ($125 \mu\text{mol}/\text{m}^2\text{s}$) for different time periods: 30 min, 2 h and 4 h. Then the seedlings were incubated with a solution of triphenyltetrazolium chloride (TTC). The employed test is based on the activity of the dehydrogenase enzyme systems linked to the mitochondrial respiratory chain. As the tissues of viable seedlings respire, through oxidation and reduction, they liberate hydrogen ions. The hydrogen then combines with TTC, which is normally colorless, producing, through reduction, a triphenylformazane (TF), which is an insoluble, non-diffusive, red-colored pigment that stains infiltrated tissues (Baskin and Baskin 1998a). Thus, only viable seedlings, that is, seedlings with biochemically active mitochondria in their cotyledons, reduce TTC to TF and become red, while dead seedlings remain uncolored.

While seedlings of all four mutant types (*Atoep16-1;5-8*) were similarly viable in the dark, they responded differentially to illumination. The microscopic images (Figure 3.13 a) and determined seedling survival curves (Figure 3.13 b) demonstrate that cell death occurred most rapidly in seedlings of mutant *Atoep16-1;5*. The time course was delayed for seedlings of mutant *Atoep16-1;6*. After 4 h of illumination of 5 d-old dark-grown seedlings, we found approximately 35% of viable seedlings in mutant *Atoep16-1;5* and 60% in mutant *Atoep16-1;6*. By contrast, the large majority of seedlings of mutants *Atoep16-1;7* and *Atoep16-1;8* remained viable (95% and 86%, respectively) and thus were similar to the wild-type.

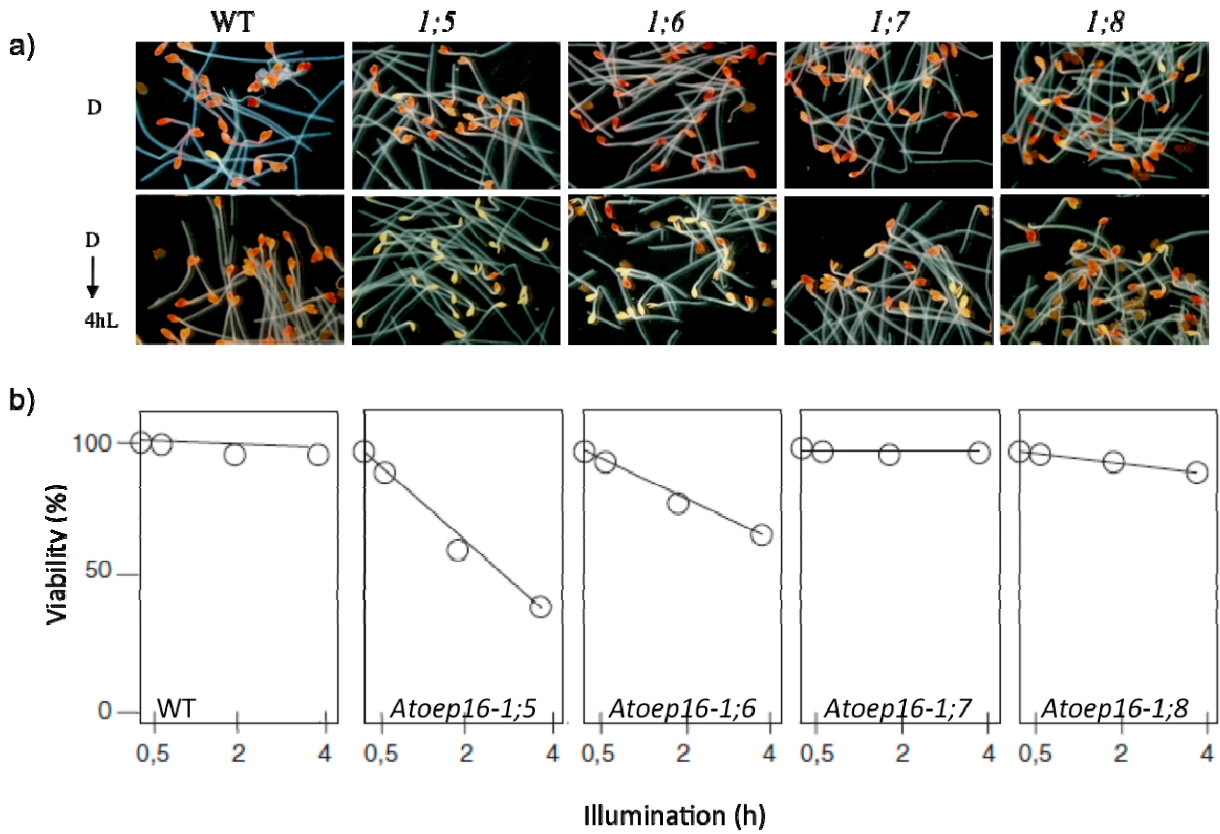


Figure 3.13 Tetrazolium staining of etiolated and light-exposed *Atoep16-1;5-8* versus wild-type seedlings, used to monitor cell death progression.

a) *Atoep16-1;5-8* seedlings were grown in the dark for 5 d and exposed to white light ($125 \mu\text{mol}/\text{m}^2$) for 30 min, 2 h and 4 h, respectively. Then tetrazolium staining was used to score seedling viability. Whereas vital seedlings show a strong red staining in their cotyledons, dead seedlings are unable to retain the dye and look whitish. b) Percentages of viable seedlings, as determined from three independent experiments using each 250 seedlings per time point.

3.2.3 Singlet oxygen production in *Atoep16-1;5-8* mutant seedlings

The strong red Pchl_a fluorescence in 5 d-old etiolated seedlings of mutants *Atoep16-1;5* and *Atoep16-1;6* and their subsequent photobleaching suggested the presence of free Pchl_a molecules not bound to POR. Upon excitation, these free Pchl_a molecules could operate as photosensitizer and, by triplet-triplet interchange with ground state molecular oxygen, they could trigger singlet oxygen formation. In order to explore the possible release of singlet oxygen, we performed DanePy fluorescence measurements, accordingly to Hideg *et al.* (1998). DanePy is a dansyl-based singlet oxygen quencher. After excitation at 345 nm it emits fluorescence with a maximum at 532 nm. Upon reacting with singlet oxygen, however, there is a partial quenching of fluorescence induced by energy transfer from the fluorophore moiety (dansyl) to the nitroxide.

5 d-old, dark-grown mutant and wild-type seedlings were infiltrated with DanePy under a green safety light, before being exposed to strong white light (125 $\mu\text{mol}/\text{m}^2$) for 30 min. Figure 3.14 shows that mutants *Atoep16-1;5* and *Atoep16-1;6* produced significant amounts of singlet oxygen, as evidenced by the quenching of DanePy fluorescence collected between 425 and 625 nm. Reduction of DanePy fluorescence in mutant *Atoep16-1;5* was closely similar to that detected in *flu* seedlings used as control, whereas DanePy fluorescence quenching was less pronounced in mutant *Atoep16-1;6*. In seedlings of wild-type and mutant *Atoep16:1-7*, no DanePy fluorescence quenching indicative of the generation of singlet oxygen occurred. In *Atoep16:1-8* seedlings, some minor decrease in DanePy fluorescence was observed in two out of three independent experiments, suggesting that some low amounts of singlet oxygen accumulated.

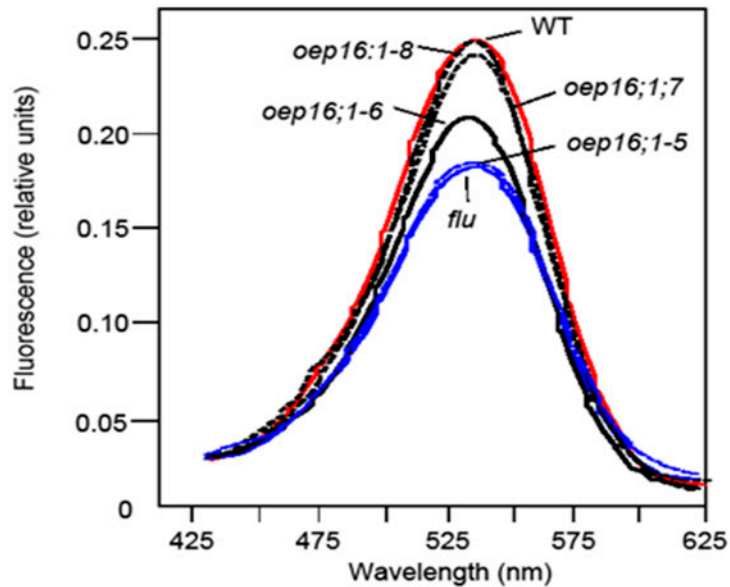


Figure 3.14 Release of singlet oxygen in mutants *Atoep16-1;5-8*, *flu* and in the wild-type.

Mutants *Atoep16-1;5-8* were grown in the dark for 5 d and infiltrated with DanePy under green, safe light, before being illuminated with white light ($125 \mu\text{mol}/\text{m}^2$) for 30 min. Singlet oxygen evolution was measured by following DanePy fluorescence quenching (Hideg *et al.*, 1998). The curves show DanePy fluorescence emission spectra between 425 nm and 625 nm at an excitation wavelength of 330 nm for *Atoep16-1;5* (blue dotted line), *Atoep16-1;6* (black solid line), *Atoep16-1;7* (black dashed line), and *Atoep16-1;8* (black hatched line) versus *flu* (blue solid line) and wild-type seedlings (red solid line). Life Sciences spectrometer, model LS50, Perkin Elmer Corp., Norwalk, CT, was used for spectroscopy.

3.2.4 Chloroplasts protein import

3.2.4.1 Chemical crosslinking and differential *in vitro* import of transA-DHFR and transB-DHFR into isolated *Atoep16-1* mutant plastids

Because low temperature spectroscopy had showed that *Atoep16-1;6* does not accumulate wild-type levels of photoactive Pchlde-F655, in spite of the presence of PORA, we assumed that import of pPORA into the plastids in this mutant may not proceed via the PTC complex, described previously (Reinbothe *et al.*, 2004), but may proceed via another import pathway. To test this hypothesis, *in vitro* import and crosslinking experiments were performed. Crosslinking of the ³⁵S-methionine labeled transA-DHFR precursor molecules (consisting of the first 67 NH₂-terminal amino acids of pPORA, referred to as transA, and the cytosolic dihydrofolate reductase (DHFR) reporter protein of mouse) and transB-DHFR (consisting of the first 82 NH₂-terminal amino acids of pPORB and DHFR) was followed in chloroplasts isolated from 14 d-old light-grown wild-type and *Atoep16-1;5-8* mutant plants. TransA- and transB- coupled DHFR precursor molecules were activated with 5,5'-dithiobis(2-nitro)benzoic acid (DTNB), (Reinbothe *et al.*, 2004) and then added to energy-depleted chloroplasts. After a 15 min dark incubation of precursor molecules with isolated chloroplasts, in the presence of 0,1 mM Mg-GTP and 2,5 mM Mg-ATP, proteins were recovered by precipitation with trichloroacetic acid, separated by SDS-PAGE and detected by autoradiography.

Figure 3.15 shows that chloroplasts of mutants *Atoep16-1;5* and *Atoep16-1;7* differed markedly from chloroplasts of mutants *Atoep16-1;6* and *Atoep16-1;8* in their capability to sequester transA-DHFR. In *Atoep16-1;6* mutant, a 106 kDa crosslink product (CLP2) was formed that consisted of transA-DHFR (31 kDa) and TOC75 (75 kDa) held together by a mixed disulfide bond. Similar to the plastids from mutant *Atoep16-1;6*, a fraction of transA-DHFR was taken up and processed via a TOC75-dependent pathway by chloroplasts isolated from mutant *Atoep16-1;8* (see Samol *et al.*, 2011a, enclosed in the Appendix B). These results support the hypothesis that chloroplasts from line *Atoep16-1;6* and *Atoep16-1;8* take up pPORA by a default pathway and not via the PTC complex as it was shown previously for wild-type chloroplasts (Reinbothe *et al.*, 2004). The presence or absence of Pchlde did not affect the import of transA-DHFR into the plastids of mutants *Atoep16-1;6* and *Atoep16-1;8* (see Figure S.4, enclosed in the Appendix A).

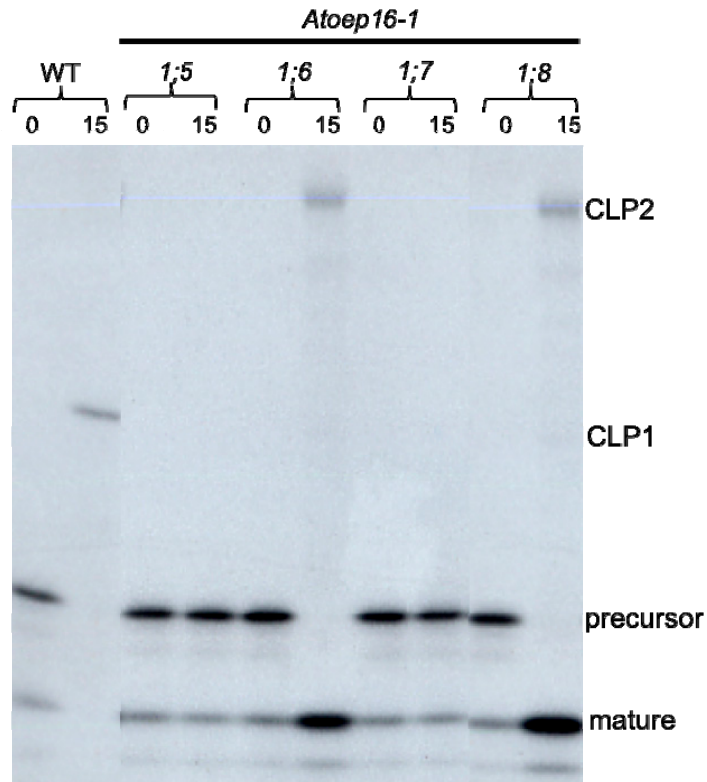


Figure 3.15 *In vitro* import and crosslinking of DTNB-activated ^{35}S -transA-DHFR determined with plastids isolated from wild-type and mutants *Atoep16-1;5-8*.

In vitro import and crosslinking was carried out using ^{35}S -TransA-DHFR molecules that had been derivatized with DTNB and chloroplasts that had been isolated from 14 d-old light-grown *Atoep16-1;5-8* mutant and wild-type seedlings. The autoradiograms show precursor and mature protein levels in plastids before (lanes 0) and after (lanes 15) 15 min of incubation. CLP1 (47 kDa) is caused by the formation of a mixed disulfide bond between transA-DHFR (31 kDa) and AtoEOP16-1 (16 kDa); this product was detectable only in wild-type chloroplasts. CLP2 (106 kDa) results from the formation of a mixed disulfide bond between transA-DHFR (31 kDa) and TOC75 (75 kDa); this CLP was found in chloroplasts isolated from mutants *Atoep16-1;6* and *Atoep16-1;8*.

In contrast to these findings, no higher molecular mass crosslink products were found in chloroplasts of mutants *Atoep16-1;5* and *Atoep16-1;7*. The small amount of mature protein present after 15 min is similar to that at time zero (Figure 3.15), suggesting that some artificial processing of the precursor occurred during sample handling. Nevertheless, chemical crosslinking of transB-DHFR (see Figure S.4, enclosed in the Appendix A) was similar in plastids of all four *Atoep16-1;1-8* mutant lines, where 106 kDa crosslinking products were formed, designated CLP2, that consisted of TOC75 (75 kDa) and transB-DHFR (31 kDa). All four types of mutant plastids imported indistinguishable levels of transB-DHFR (see Figure S,4, enclosed in the Appendix A).

3.2.4.2 Differential *in vivo* import of transA-GFP into plastids

In order to confirm the results of the *in vitro* import experiments, transient expression assays were performed in 3 w-old light-grown *Arabidopsis* plants. TransA was fused to the jellyfish green fluorescent protein (GFP) by genetic engineering and the DNA construct was transformed into leaf epidermis cells of wild-type and *Atoep16-1;5-8* mutant plants. To allow for Pchl_a synthesis, leaf tissues, obtained after transformation, were placed in darkness for 24 h. Then, GFP fluorescence was monitored by confocal laser scanning microscopy. Figure 3.16 shows that transA-GFP was differentially imported into the plastids of mutants *Atoep16-1;5-8*. GFP fluorescence remained largely confined to the cytosol and only little amounts of transA-GFP were imported into the plastids of mutants *Atoep16-1;5* and *Atoep16-1;7*. By contrast, plastids of mutants *Atoep16-1;6* and *Atoep16-1;8* imported significant amounts of the precursor. These findings were consistent with our previous *in vitro* import studies and highlighted the operation of different default import pathways of pPORA *in planta*.

Together, the *in vitro* and *in vivo* import data offer an explanation why no mature PORA protein accumulated *in planta* in mutants *Atoep16-1;5* and *Atoep16-1;7*.

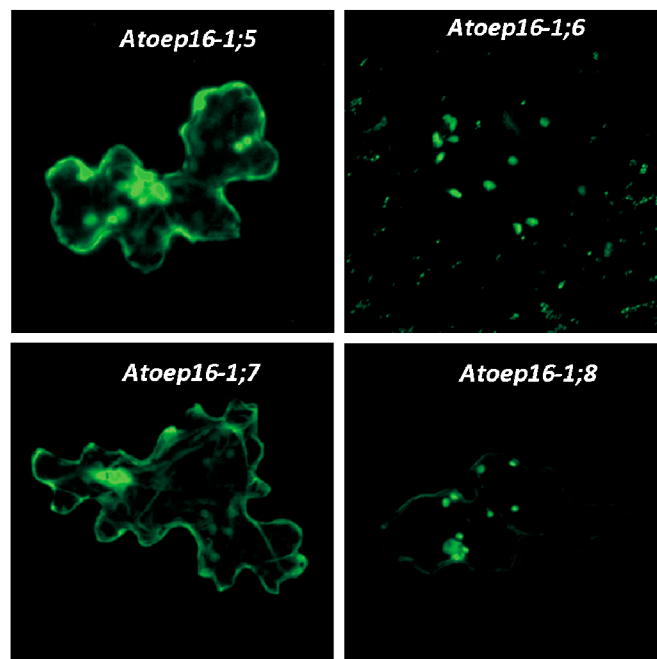


Figure 3.16 *In vivo* import of TransA-GFP into the plastids of mutants *Atoep16-1;5-8*.

In vivo import of TransA-GFP into plastids of 3 w-old light-grown plants of mutants *Atoep16-1;5-8* was analyzed after transforming leaf epidermis cells with a respective DNA construct. GFP fluorescence was collected between 505 nm 530 nm, using an excitation wavelength of 488 nm. Courtesy of Stephan Pollmann, University of Bochum, Germany.

3.2.5 Is the *Atoep16-1* mutation responsible for the photobleaching phenotype?

Among the four *Atoep16-1* null mutants identified in this study, two families were found which respond differentially to light stress: one family comprises *Atoep16-1;5* and *Atoep16-1;6* and exhibits a conditional cell death phenotype. The other family comprising *Atoep16,1-7* and *Atoep16-1;8* mutants, show unimpaired greening. We could argue then if AtOEP16-1 protein prevents a cell death phenotype under a non permissive dark-to-light shift conditions. To explore this possibility, we performed *in planta*-transformation/complementation tests of *Atoep16-1;6* mutant. We have preferentially chosen this line for several reasons. The first is that *Atoep16-1;6* line exhibits bleaching phenotype after illumination of dark-grown seedlings. If AtOEP16-1 prevents cell death phenotype, dark-grown *Atoep16-1;6* complemented line should be able to green, similarly to wild-type, after subsequent exposition to strong white light. The second and very exciting reason is that despite the presence of PORA protein in *Atoep16-1;6* line, we detected highly reduced levels of photoactive Pchl_a-F655. *In vitro* import and crosslinking studies demonstrated that transA-DHFR entered both Pchl_a-free and Pchl_a-containing mutant plastids (see a submitted publication of Samol *et al.*, 2009, enclosed in the Appendix B). In addition, the assays showed that transA-DHFR enters the plastids via a default import pathway involving TOC75 and not PTC complex as it was shown in wild type. It seems that during pPORA import in this mutant, precursor does not interact with the pigment. Otherwise, Pchl_a-F655 should have accumulated to the same extent as in wild-type plants and the establishment of larger complexes LHPP with PORB in etioplasts should occur. Complementation of *Atoep16-1;6* line would then depict if the correct ratios of both Pchl_a species are essential for pPORA import via PTC complex.

3.2.5.1 Complementation test

Gateway[®] technology (Invitrogen) was used to create the following constructs containing the full-length *AtOEP16-1* cDNA under the control of the cauliflower mosaic virus 35S promoter: 35S::OEP16, 35S::GFP::OEP16 and 35S::OEP16::YFP (Yellow Fluorescent Protein). For construction of the 35S::OEP16::YFP clone, a modified *AtOEP16-1* cDNA was used that was devoid of the STOP codon. The cloning was made to generate translational fusions where GFP and YFP were hooked up to either the NH₂-terminus or COOH-terminus of AtOEP16-1, respectively.

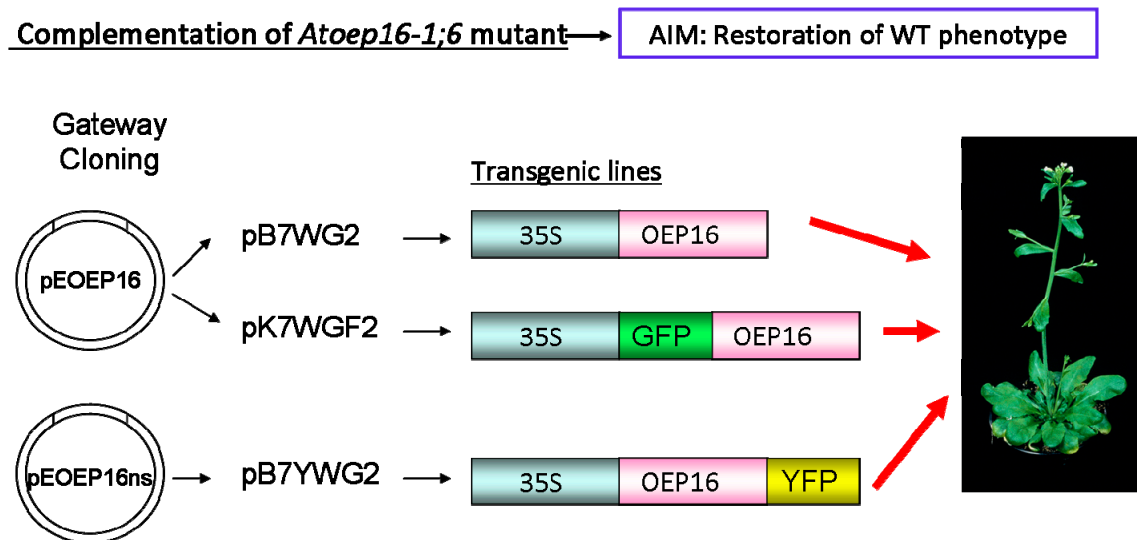


Figure 3.17 Experimental design underlying the complementation assay.

Gateway® technology was used to generate the following three DNA constructs (35S::OEP16, 35S::GFP::OEP16 and 35S::OEP16::YFP). The generated cDNAs encode the indicated fusion proteins consisting of the full length *AtOEP16-1* protein and the GFP and YFP reporter proteins.

The various cDNAs were cloned into the donor vector pDONR221 to yield the entry clones pEOEP16 and pEOEP16_no_STOP, respectively. The final fusion products were generated via the LR reaction in the Gateway compatible binary T-DNA destination vectors pB7WG2, pK7WGF2 and pB7YWG2. The resulting expression vectors, referred to as p35S-OEP16, p35S-GFP-OEP16 and p35S-OEP16-YFP, respectively, were transferred into homozygous *Atoep16-1;6* mutant plants via *Agrobacterium*-mediated transformation (Figure 3.17). Selection of the first, second and third generations of transgenic plants (T1, T2 and T3) was performed under sterile conditions using seeds on MS medium containing kanamycin sulfate (35S::GFP::OEP16) or ammonium glufosinate (35S::OEP16 or 35S::OEP16::YFP). Transformants containing the fluorescent proteins GFP and YFP (35S::GFP::OEP16 and 35S::OEP16::YFP) were inspected under an epifluorescence microscope. Positive, antibiotic-resistant plants (in contrast to untransformed seedlings that rapidly die) were transferred onto soil and, after 2 w, they were selected for the presence of the correct construct by a PCR-based approach. Subsequent photobleaching tests were carried out with individuals of the T3 generation, composed exclusively of the homozygous transformants. These tests should reveal whether or not the reintroduction of the wild-type *AtOEP16-1* gene restored normal greening.

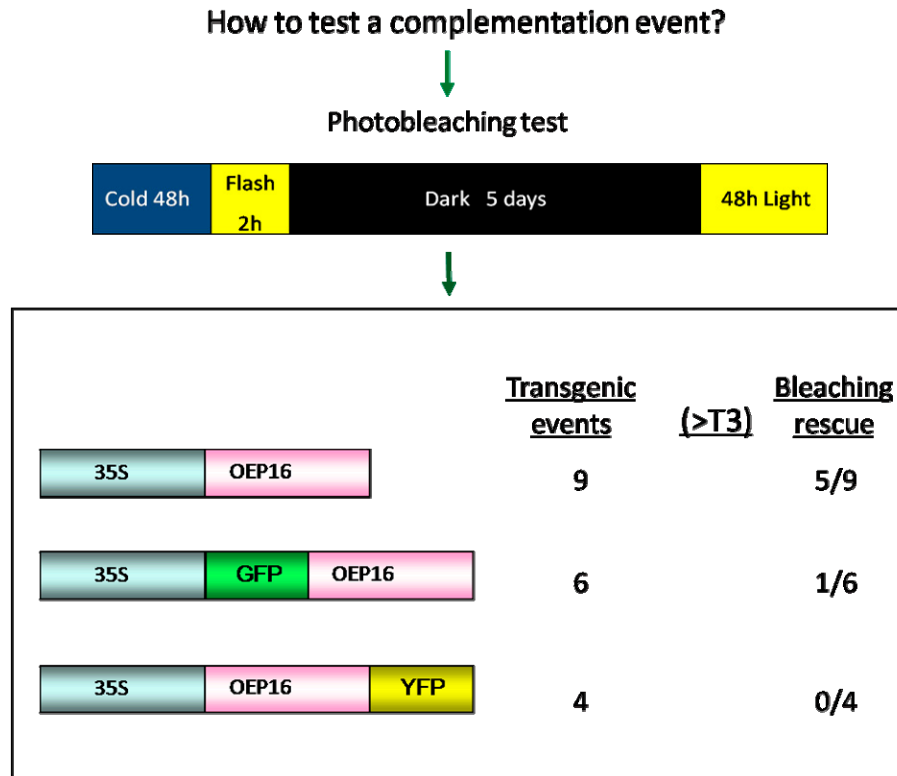


Figure 3.18 How to score successful complementation events.

Plants coming from the third generation of homozygous transformants were grown for 5 d in darkness and exposed to white light ($210\mu\text{E}/\text{m}^2$). Then seedling viability was assessed by the greening test outlined in Figure. 3.2. First numbers give independent families raised for the different constructs, whereas the ratios specify in how many of these lines a functional complementation was achieved that rescued normal greening. While 5 families of transformed 35S::OEP16 plants exhibited wild-type phenotypes and greened normally, only one family of transgenic 35S::GFP::OEP16 plants could be obtained that was viable. For 35S::OEP16::YFP, none of the produced 4 lines allowed for functional complementation.

We identified five families of T3 *Atoep16-1;6 35S::OEP16* and one family of T3 *Atoep16-1;6 35S::GFP::OEP16* plants where successful complementation revealed a bleaching rescue (Figure 3.18). An example for a successful complementation of mutant *Atoep16-1;6* with 35S::OEP16 is made by line *Atoep16-1;6 35S::OEP16 E_6*. This line is composed of 100% homozygous plants, as shown by its herbicide resistance (Figure 3.19 b). After growth in the dark for 5 d and subsequent high light exposure ($210\mu\text{E}/\text{m}^2$), seedlings of *Atoep16-1;6 35S::OEP16 E_6* looked like the wild-type and were fully viable (Figure 3.19 c). These results indicated that the introduced *AtOEP16-1* gene had restored normal greening. Indeed, no red fluorescence indicative of the presence of free Pchl_{ide} molecules was seen in etiolated *Atoep16-1;6 35S::OEP16 E_6* seedlings, but was easily detectable in the *Atoep16-1;6* mother generation. Subsequent exposure of *Atoep16-1;6 35S::OEP16 E_6* seedlings to strong continuous white light (see above) for 48 h or longer periods confirmed

the restoration of normal greening (Figure 3.19 d). Immunoblotting revealed that the introduced *AtOEP16-1* gene was expressed to high levels and gave rise to AtOEP16-1 protein (Figure 3.19 e).

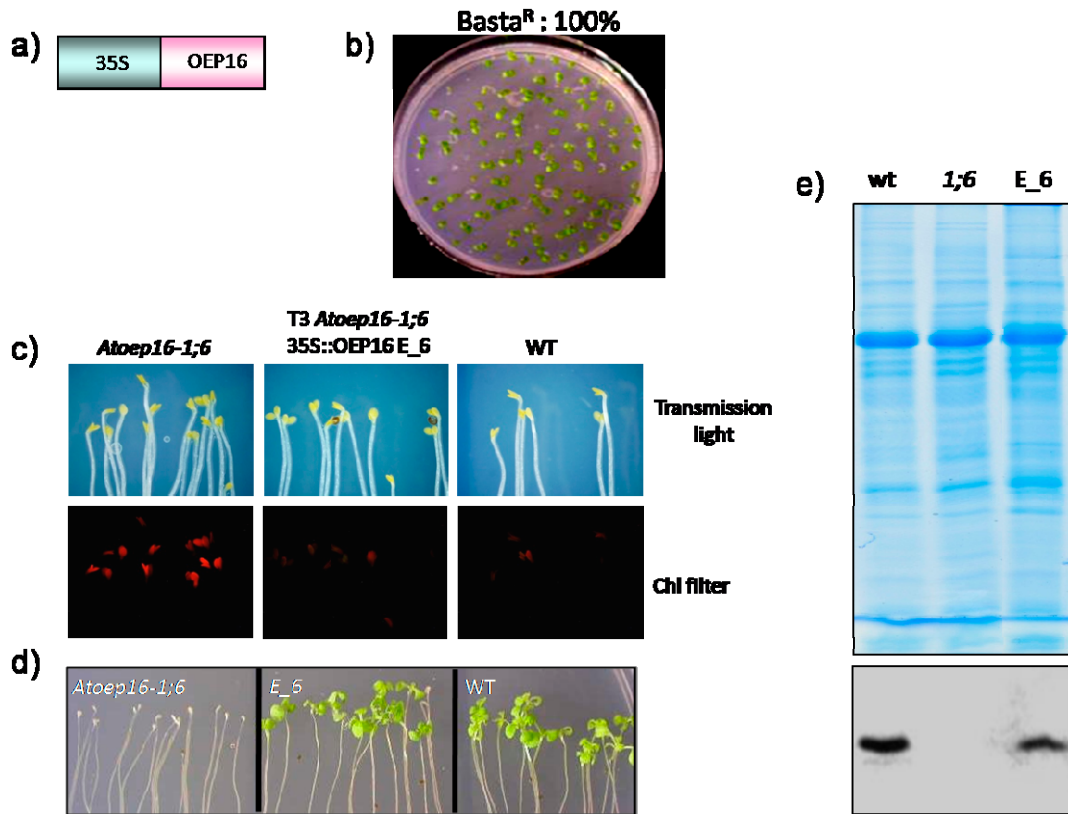


Figure 3.19 Detailed expression analysis of AtOEP16-1 in the 35S::OEP16-expressing line *Atoep16-1;6*.

a) Recall on the structure of the generated 35S::OEP16 fusion protein construct. **b)** Selection of BASTA-resistant plants corresponding to line *T3 Atoep16-1;6 35S::OEP16 E_6*. Seeds were sown on MS medium containing glufosinate ammonium [5 µg/mL]. Note that all plants survived these conditions, demonstrating that they were all homozygous for the transgene. **c)** Phenotypic analysis of line *T3 Atoep16-1;6 35S::OEP16 E_6* and wild-type after growth in darkness for 5 d without **(c)** or with **(d)** a subsequent exposure to strong white light (210 µE/m²) for 48 h. **e)** Detection of AtOEP16-1 in line *T3 Atoep16-1;6 35S::OEP16 E_6* but not in untransformed *Atoep16-1;6* seedlings by Western blotting. Total protein was extracted from mature, green plants, separated on a 15% SDS-PAGE gel and probed with anti-AtOEP16-1 antibody that had been raised from the bacterially expressed and purified *Arabidopsis* AtOEP16-1 protein. The Coomassie stain (upper panel) and Western blot (lower panel) show leaf protein corresponding to 40 µg of bovine serum albumin.

As mentioned before, the generated fluorescent proteins contained their fluorophores at either the NH₂-terminus (GFP) or COOH-terminus (YFP) of AtOEP16-1. Transformants expressing the fusion proteins were used to prove the role and localization of AtOEP16-1 *in planta* and to gain first insights into the insertion mechanism of the AtOEP16-1 protein into the outer envelope membrane of chloroplasts. Figure 3.20 shows results obtained for a representative complemented T3 line: *Atoep16-1;6 35S::GFP::OEP16 D_8*. Similar to the results reported before for *Atoep16-1;6 35S::OEP16 E*, both the reduction of red Pchl_a fluorescence during etiolation and normal green appearance without detectable signs of photooxidative damage after illumination; emphasized that GFP fused to AtOEP16-1 at its NH₂-terminus does not affect the proper compartmentalization and function of AtOEP16 *in planta*.

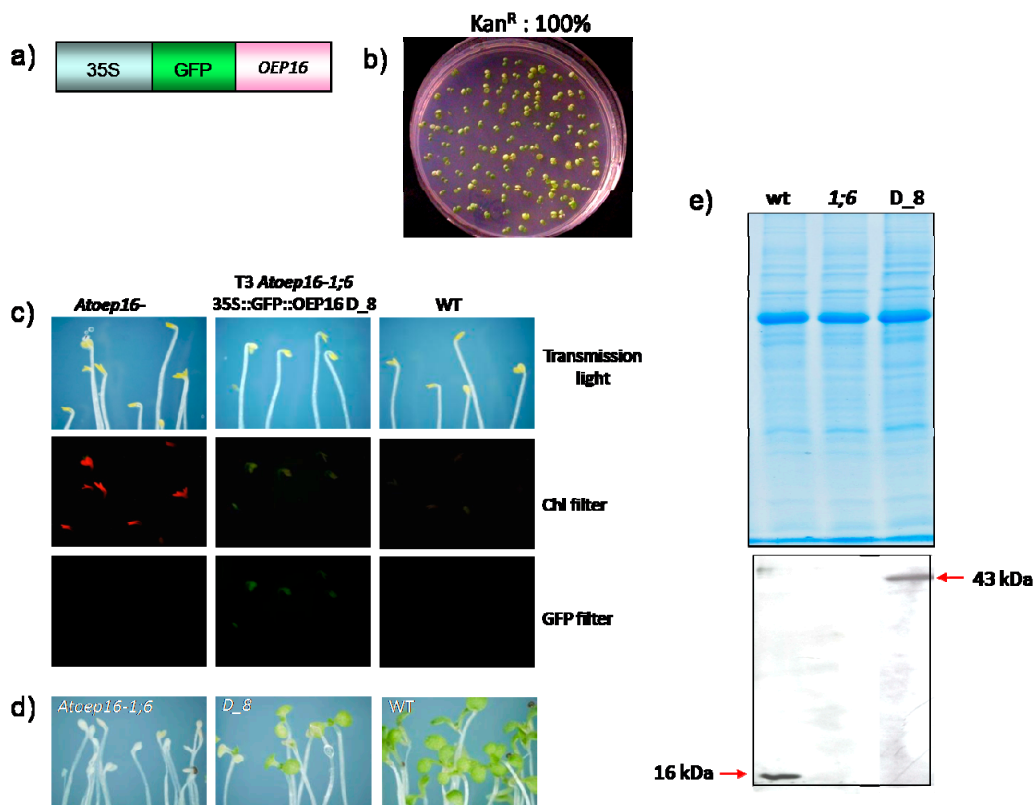


Figure 3.20 Complementation of *Atoep16-1;6* with 35S::GFP::OEP16

As Figure 3.19, but depicting the results obtained for *Atoep16-1;6* transformed with the 35S::GFP::OEP16 construct (a). Note that 100% of the produced plants are resistant to kanamycin sulfate [50 µg/mL](b). The transformants do not show red Pchl_a autofluorescence and they do not bleach after the dark-to-light transfer (c and d). In e), accumulation of the introduced GFP-OEP16-1 fusion protein was confirmed by Western blotting. Total protein (40 µg protein per lane) was probed with *Arabidopsis* anti-AtOEP16-1 antiserum.

In contrast to these results, complementation of mutant *Atoep16-1;6* with the YFP fusion protein did not allow to regenerate plants that were viable during de-etiolation. In spite of the presence of the AtOEP16-1 fusion protein in transformed T3 *Atoep16-1;6* mutant seedlings (Figure 3.21 e), all analyzed transgenic plants, accumulated high levels of red-fluorescing Pchl_{ide} and died after the dark-to-light shifts, similarly to untransformed *Atoep16-1;6* seedlings (Figure 3.21 c, d). Together, these findings unveiled that AtOEP16-1 either cannot enter the outer envelope or attains a nonfunctional state in the presence of the bulky YFP reporter protein.

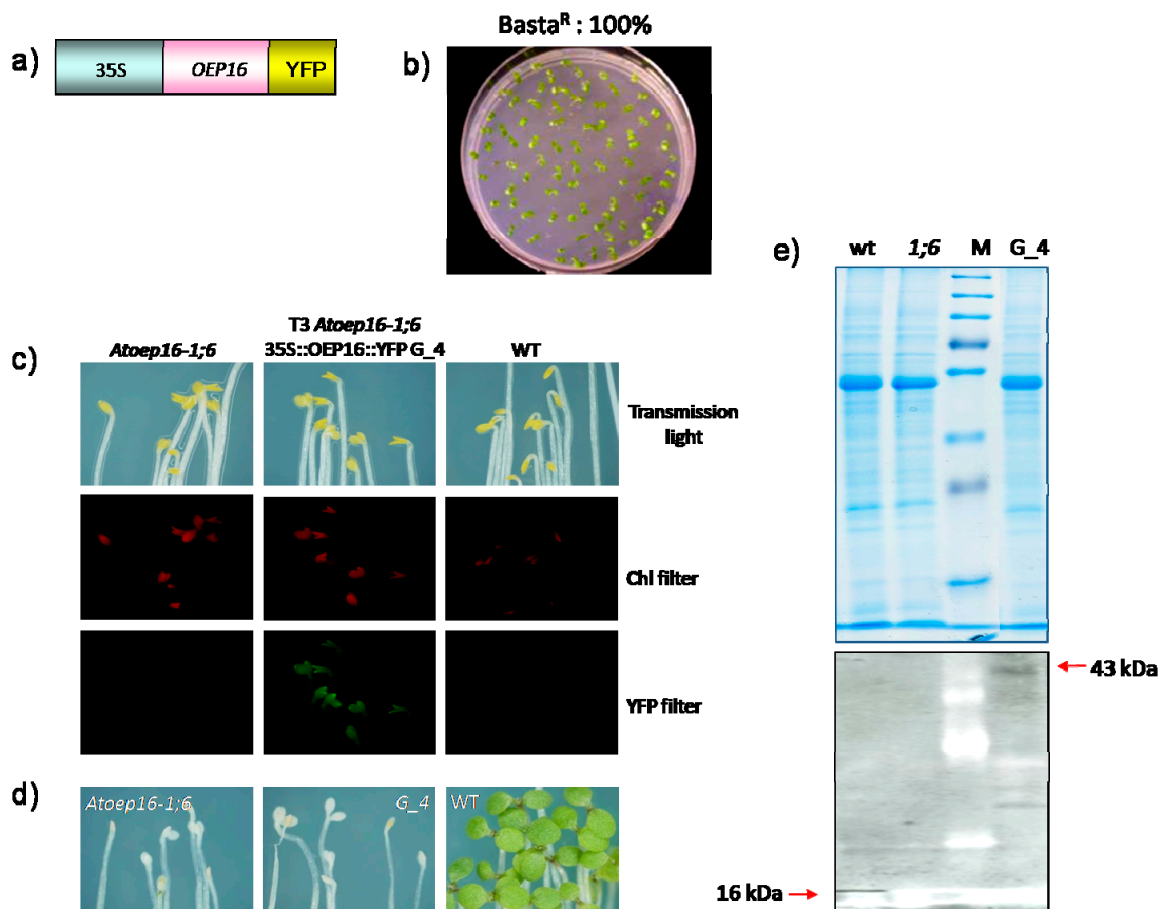


Figure 3.21 Lack of functional complementation in *Atoep16-1;6* transformed with 35S::OEP16::YFP.

As Figure. 3.19, but demonstrating that expression of 35S::OEP16::YFP (a) does not restore normal greening. Despite the fact that 100% of the T3 seedlings of line *Atoep16-1;6* 35S::OEP16::YFP G₄ were resistant to glufosinate ammonium [5 µg/mL](b), the offspring of the transformants overproduced Pchl_{ide} in the dark and died upon illumination (c and d). Even in the presence of OEP16-1-YFP fusion protein on Western blots (40 µg of total leaf protein loaded per lane, probed with homologous anti-AtOEP16-1 serum, (e), the seedlings died after the dark-to-light shift. Lane “M” shows migration of electrophoresis marker proteins.

3.2.5.2 Localization of AtOEP16-1 in plastids

Confocal laser scanning microscopy was used to study the localization of the 35S::GFP::OEP16 and 35S::OEP16::YFP fusion proteins in the generated transgenic lines. Figure 3.22 depicts representative images taken for lines T3 *Atoep16-1;6* 35S::GFP::OEP16 D_8. Clearly, GFP fluorescence in the 35S::GFP::OEP16 transformants co-localized with the red autofluorescence of Chl in chloroplasts of mesophyll cells as well as guard cells of stomata (Figure 3.22 a, b). This result is consistent with previous localization studies (Pohlmeyer et al., 1997; Reinbothe *et al.*, 2004 a+b). In the transformants expressing AtOEP16-1-YFP, however, YFP fluorescence was detectable only at the outmost “edges” of the chloroplast (Figure 3.22 c), suggesting that AtOEP16-1-YFP bound to, but was not imported into the outer envelope membrane. These findings are well consistent with the seedling viability tests reported previously that had shown the failure of AtOEP16-1-YFP to confer photoprotection onto etiolated seedlings during greening.

To conclude, the complementation data supported the role of AtOEP16-1 in the photoprotection mechanism of etiolated plants. It seems likely that re-expression of AtOEP16-1 in *Atoep16-1;6* plants could restore Pchl_{ide}-dependent import of pPORA via the PTC complex. As a result, PORA-Pchl_{ide} *b*-NADPH complexes would be formed that could further assemble with PORB-Pchl_{ide} *a*-NADPH complexes to establish LHPP and photoactive Pchl_{ide} in the prolamellar body of etioplasts. However, to test this hypothesis additional experiments showing accumulation of LHPP complexes still need to be performed.

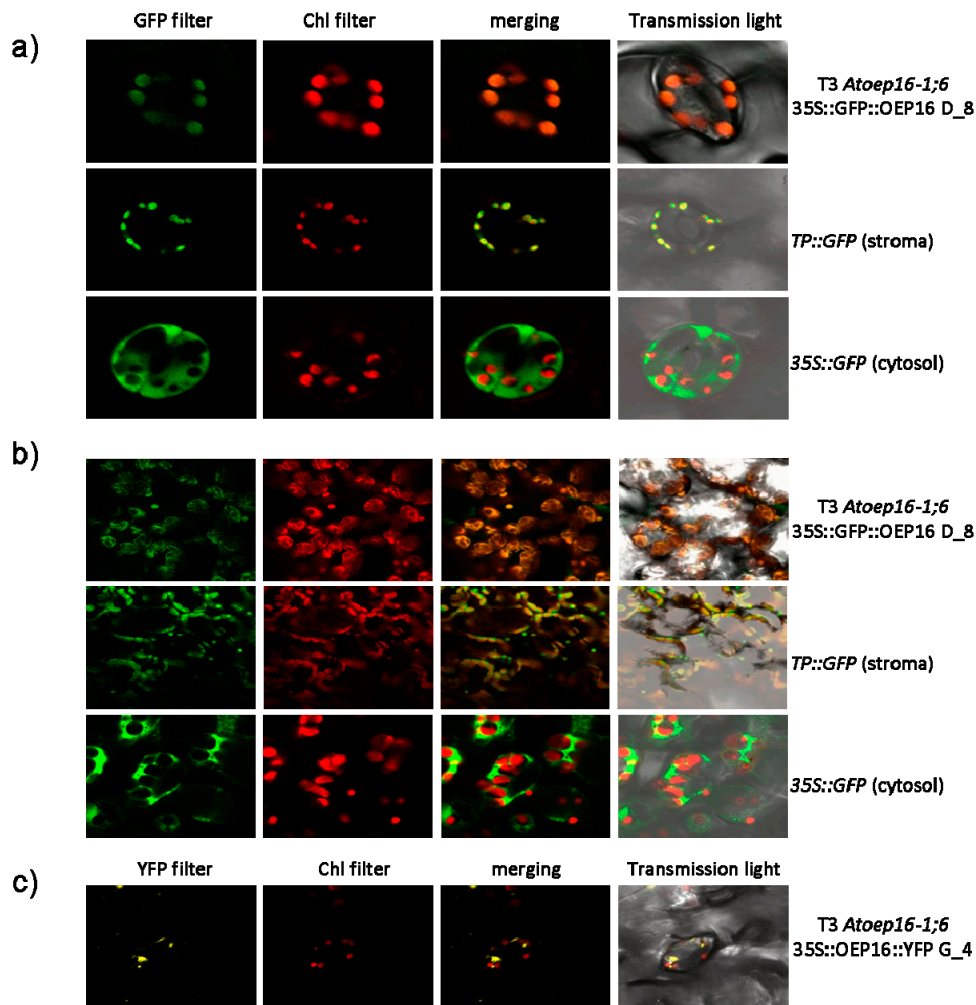


Figure 3.22 Cyto-localization of GFP and YFP in the generated transformants.

The different transformants were analyzed with regard to the localization of the GFP and YFP reporter proteins, using confocal laser scanning microscopy. Co-localization of GFP and Chl fluorescences was observed in guard cells of stomata (**a**) and in mesophyll cells (**b**) in line T3 *Atoep16-1;6* 35S::GFP::OEP16 D_8. As control we used transgenic plants expressing 35S::GFP. This construct gave rise to an entirely cytosolic and nuclear localization of green GFP fluorescence. As further positive control, we used transgenic plants expressing a DNA construct coding for a chimeric precursor consisting of the transit peptide of the small subunit of ribulose-1,5-bisphosphate carb-oxylase/oxygenase and GFP (*TP::GFP*), kindly provided by Dr. Norbert Rolland (PCV, CEA-Grenoble). Plants expressing this construct contained almost all of the GFP fluorescence in their chloroplasts. **c**) Analysis of the T3 of *Atoep16-1;6* transformed with the 35S::OEP16::YFP construct revealed no co-localization of YFP and Chl fluorescences, highlighting that the introduced reporter protein was most likely not correctly targeted to the outer envelope membranes of chloroplasts. For imaging acquisition, GFP was excited at a wavelength of 488 nm, in combination with a 493 nm-573 nm emission filter. For collecting YFP fluorescence, excitation and emission wavelengths of 514 nm and 520 nm-550 nm, respectively, were used.

3.3 Identification of translation as target of singlet oxygen action in *Atoep16-1;5-8, flu* and *tig^{d12}* seedlings

Mutants *Atoep16-1;5* and *1:6* have a conditional cell death phenotype and thus at first glance resemble *flu* of *Arabidopsis* (Figure 3.23). The FLU protein is impaired in the negative feedback loop inhibiting the excess Pchl_a accumulation in the dark. The FLU protein interacts with glutamyl-tRNA reductase (Meskauskiene and Apel, 2002, Goslings *et al.*, 2004) and this interaction is impaired in *flu* plants (Meskaskiene *et al.*, 2001). Two major effects have been observed for *flu* plants subjected to non-permissive dark-to-light shifts: growth inhibition and cell death (op den Camp *et al.*, 2003). When *flu* seedlings are germinated in alternate dark-light cycles, they display a miniature phenotype. By contrast, etiolated plants died when illuminated. Cell death occurred also in mature plants after an 8 h-dark shift and subsequent irradiation (op den Camp *et al.*, 2003). To explain these results, cytotoxic singlet oxygen effects including lipid peroxydations and membrane destruction, and the operation of specific, genetically determined signalling cascades were invoked (op den Camp *et al.*, 2003; Wagner *et al.*, 2004, Danon *et al.*, 2005). Transcriptome analyses identified a larger number of genes that differentially respond to singlet oxygen (op den Camp *et al.*, 2003). Among the genes that were down-regulated by singlet oxygen were those for photosynthetic proteins (op den Camp *et al.*, 2003). Genes that were up-regulated by singlet oxygen include *BONZAI (BON) 1* and *BONI-ASSOCIATED PROTEIN (BAP) 1*, the *ENHANCED DISEASE SUSCEPTIBILITY (EDS) 1* gene, and genes encoding enzymes involved in the biosynthesis of ethylene and jasmonic acid (JA), two key components of stress signalling in higher plants (Wasternack, 2007; Balbi and Devoto, 2008; Kendrick and Chang, 2008). op den Camp *et al.* (2004) found that singlet oxygen gives rise to 13-hydro(per)xy octadecatrienoic acid (13-HPOT) accumulation in mature *flu* plants. 13-HPOT is an intermediate in the biosynthetic pathway of JA. Przybyla *et al.* (2008) reported that irradiated *flu* plants produce large amounts of JA and octadecaphytodienoic acid (OPDA) and suggested that JA may be required for cell death propagation/manifestation, whereas OPDA would counteract the establishment of the cell death phenotype. Wagner *et al.* (2004) and Kim *et al.* (2008) demonstrated that cell death execution is suppressed in the *executer (exe) 1* and *exe2* mutants of *A. thaliana*, but only if low levels of singlet oxygen accumulate and trigger limited cytotoxic effects. EXECUTER 1 and 2 are membrane proteins of chloroplasts of unknown function (Kim *et al.*, 2008).

In our subsequent work we asked whether the molecular events leading to cell death in etiolated *Atoep16-1;5* and *1;6* seedlings after illumination would be the same as in *flu* plants. Hereby we focussed on translation because it is a main site of regulation in all eukaryotic cells (Dufner and Thomas, 1999; Kozma and Thomas, 2002). For comparison, mutants *Atoep16-1;7* and *1;8* were used that do not show photooxidative damage and cell death.

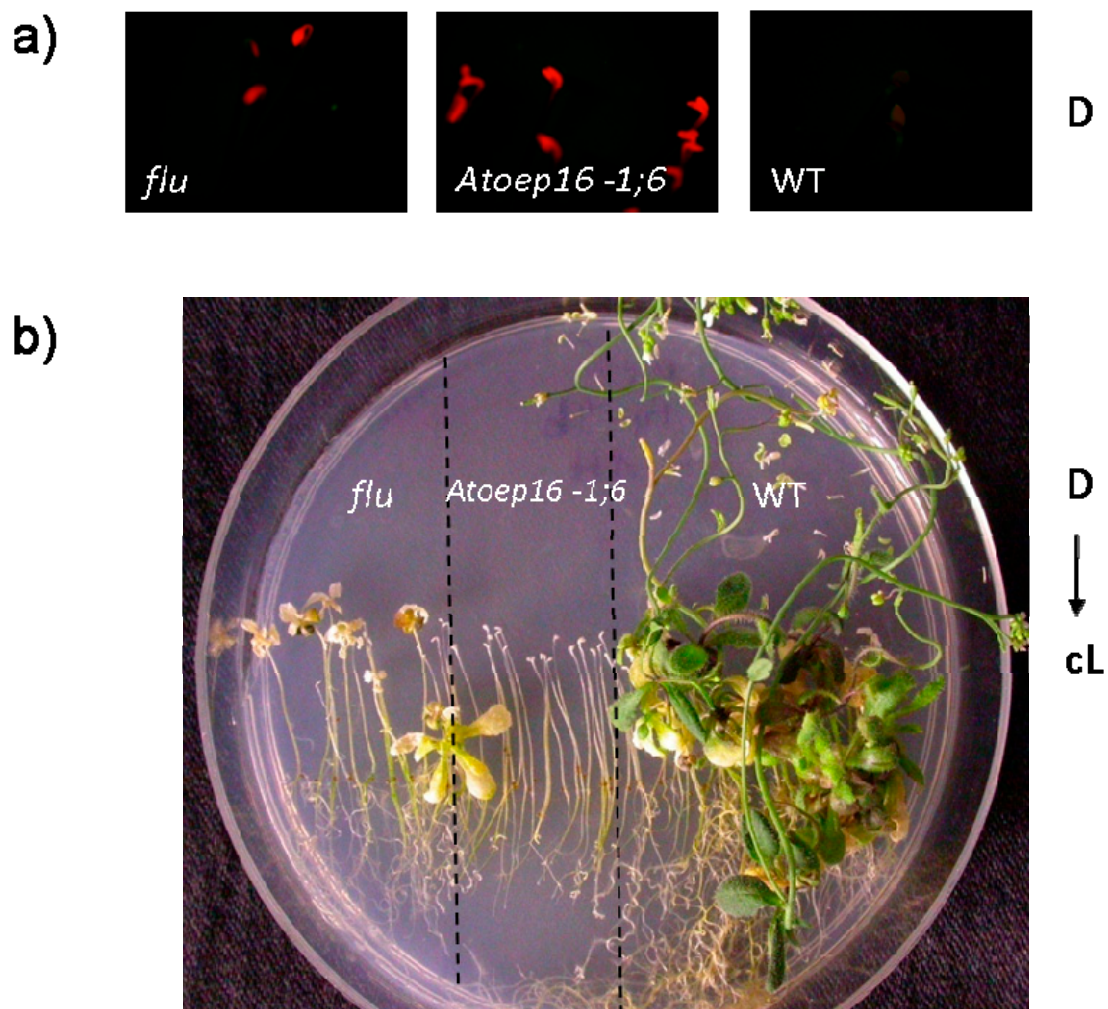


Figure 3.23 Phenotype of *Atoep16-1;6* and *flu*.

a) *flu*, *Atoep16-1;6* and wild-type seeds were sown on MS medium and further cultivated in the dark for 5 d. Then, their pigment fluorescence emission was viewed under blue light (400 nm-450 nm). **b)** After 4 w of growth under continuous white light ($210 \mu\text{mol}/\text{m}^2\text{s}$), the seedling phenotypes were scored by visual inspection. A photo of Petri dish shows that *flu* and *Atoep16-1;6*, but not the wild-type, died after irradiation.

3.3.1 Comparison of *Atoep16-1;5-8* with *flu*

3.3.1.1 *In vitro* protein synthesis

In a first set of experiments we asked whether *Atoep16-1;5* and *1;6* would express stress messengers that are detectable by *in vitro*-translation. Total RNA was extracted from 5 d-old, dark-grown seedlings and from dark-grown seedlings that had been irradiated for 2 h under photobleaching conditions prior to harvest. The messenger fraction was translated into protein in a wheat germ system using ^{35}S -methionine as tracer. When the patterns of produced polypeptides were compared for the 4 different *Atoep16-1;5-8* mutant seedlings, no major differences were found. No new polypeptide species were detected nor were any of detectably absent in all four mutants (Figure 3.24), as would be expected if *Atoep16-1;5* and *Atoep16-1;6* would follow the same cell death pathway as *flu* (op den Camp *et al.*, 2003). Thus, unlike in *flu*, gene expression appeared to be largely controlled by posttranscriptional mechanisms in short-term-irradiated *Atoep16-1;5* and *Atoep16-1;6* seedlings.

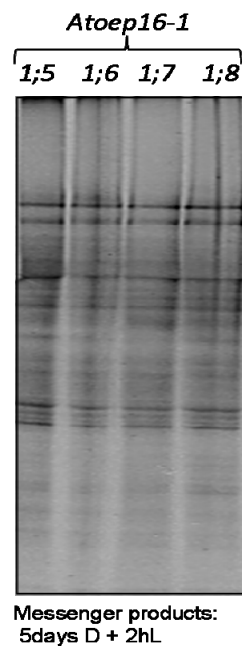
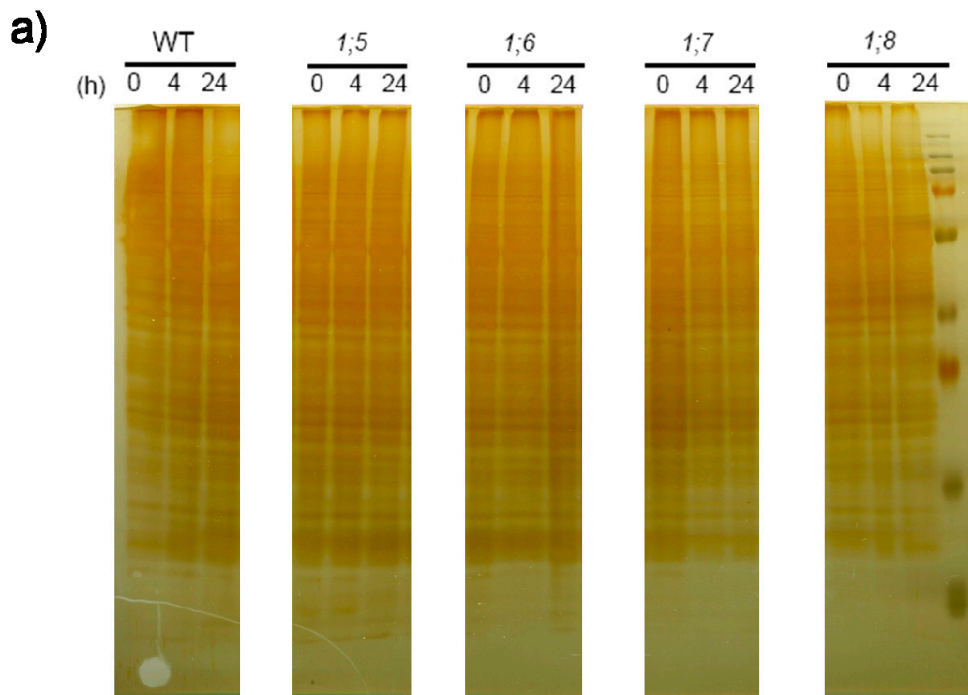


Figure 3.24 Pattern of proteins synthesized *in vitro* using RNA from mutants *Atoep16-1;5-8*.

RNA was extracted from mutants *Atoep16-1;5-8* that had been grown in the dark for 5 d and subsequently exposed to white light for 2 h. RNA was translated into protein in a wheat germ cell-free system, using ^{35}S -methionine as tracer. After SDS-PAGE on a 10-20% polyacrylamide gradient, proteins were detected by autoradiography.

3.3.1.2 *In vivo* protein synthesis during greening and in response to photooxidative stress

We next analyzed the pattern of *in vivo*-labelled proteins. Radiolabelling was carried out with ^{35}S -methionine in 5 d-old dark-grown *Atoep16-1;5-8* seedlings that had been irradiated for 4 h and 24 h with strong white light ($125 \mu\text{mol}/\text{m}^2\text{s}$). Figure 3.25 illustrates that all four *Atoep16-1;5-8* mutants accumulated very similar protein patterns in the dark. Also, all four mutants began to synthesize photosynthetic proteins (Figure 3.25). However, only seedlings of mutants *Atoep16-1;7* and *1;8* pursued synthesizing these proteins at later time points of illumination. In mutants *Atoep16-1;5* and *1;6* an arrest of protein synthesis was seen after 24 h of white light treatment. Instead of accumulating Chl, *Atoep16-1;5* and *1;6* mutant seedlings died (see Figures 3.3, 3.12 and 3.13). By contrast, seedlings of mutants *Atoep16-1;7* and *Atoep16-1;8* greened normally (see Figures 3.3, 3.12 and 3.13). Autoradiography (Figure 3.25 b) shows a severe decrease of total protein synthesis in the cotyledons of *Atoep16-1;5* and *Atoep16-1;6*. This result is in clear contrast to findings reported for *flu* plants, where early stress protein synthesis occurred under light stress conditions (op den Camp *et al.*, 2004, also see Figure S3 in Samol *et al.*, 2011a, enclosed in the Appendix B). Therefore we tentatively assumed that the cell death mechanism in *Atoep16-1;5* and *Atoep16-1;6* must be different from that triggered in *flu* plants .



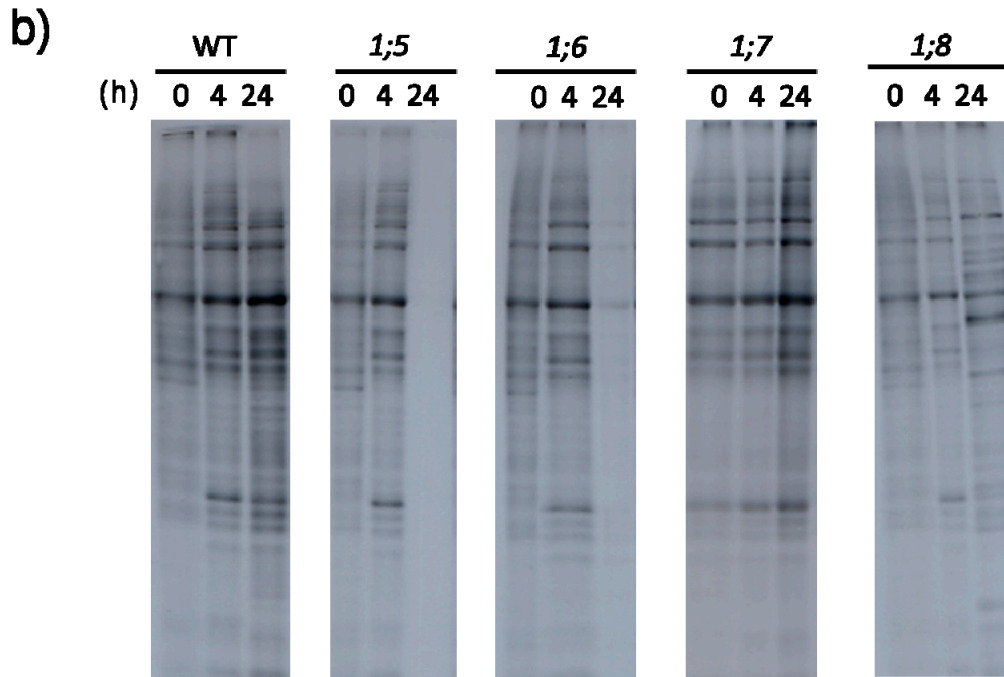


Figure 3.25 Pattern of proteins synthesized in mutants *Atoep16-1;5-8* and wild-type *in vivo*.

a) Pattern of silver stained total proteins in wild-type (WT) and *Atoep16-1;5-8* mutant seedlings in the dark (0 h) and after a subsequent exposure to white light (125 $\mu\text{mol/m}^2\text{s}$) for 4 h and 24 h. **b)** As in (a), but depicting the patterns of ^{35}S -labelled total proteins in a replicate gel. Protein detection was made by SDS-PAGE and autoradiography.

Because *Atoep16-1;6* is virtually identical with *flu* in expressing PORA and accumulating excessive amounts of Pchl ide , we wanted to compare the differences in protein synthesis between both mutants under similar stress conditions to those used by op den Camp *et al.*, (2004). Plants were grown for 14 d in continuous white light, transferred to darkness for 8 h, and re-illuminated for variable periods. According to previous work on *flu* (op den Camp *et al.*, 2003), such treatment was expected to activate the genetic component of singlet oxygen-dependent signalling but without provoking cytotoxic effects.

To corroborate this point, a polysome profiling approach was taken. RNP material was extracted from 2 w-old *flu* and *Atoep16-1;6* seedlings grown under continuous white light that had been transferred to darkness for 8 h, and re-illuminated with white light for 4 h and 24 h. Then, RNP material was resolved on continuous sucrose density gradients. After identifying the 40S and 80S ribosomal subunits as well as polysomal fractions by absorbance measurements at 255 nm, protein in each of the different fractions was

separated by SDS-PAGE and subjected to Western blotting using antisera against the light-harvesting Chl *a/b* binding protein of photosystem II (LHCII), the small subunit of ribulose-1,5-bisphosphate carboxylase/oxygenase (SSU) and allene oxide synthase (AOS). While the former are photosynthetic proteins, AOS is a stress protein known to be activated upon singlet oxygen formation in the *flu* mutant (op den Camp *et al.*, 2004). As shown in Figure 3.26, *flu* plants indeed reacted to singlet oxygen production with an early reprogramming of protein synthesis. From the distribution of the determined proteins in the 40S, 60S and polysomal fractions, an early drop in translation initiation could be deduced for *LHCB2* and *RBCS* transcripts, which was at variance with the pursued translation initiation found for *AOS* transcripts. At later periods, singlet oxygen production affected *LHCB2*, *RBCS* and *AOS* transcripts that were all restricted to the 40S fraction. In marked contrast to *flu*, *Atoep16-1;6* plants reacted to the non-permissive dark-to-light shift with no early synthesis of stress proteins (Fig. 3.26, panel d). These findings highlighted that the early reprogramming of translation in response to singlet oxygen is different in *flu* and *Atoep16-1;6* plants (see also Figure S3 in Samol *et al.*, 2011a, enclosed in the Appendix B).

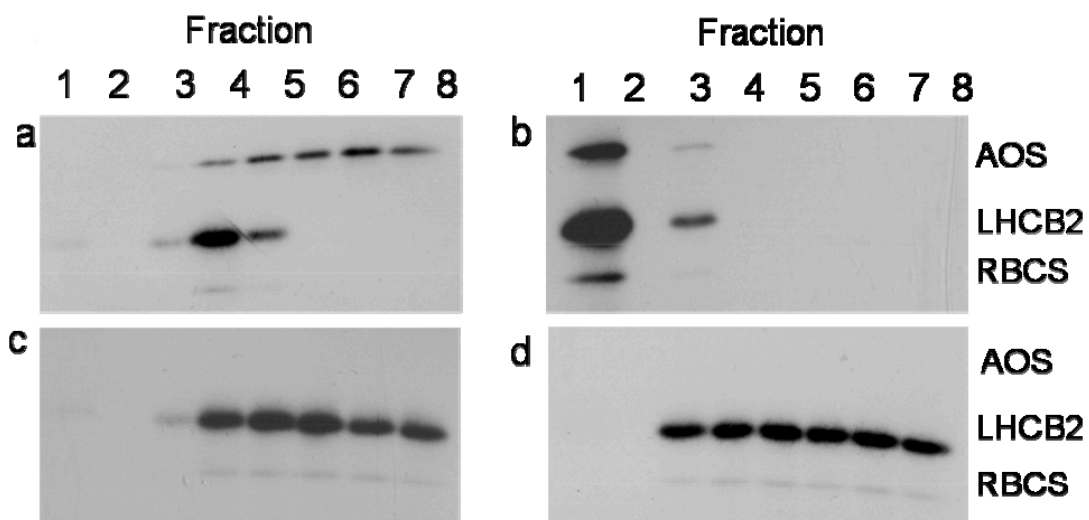


Figure 3.26 Protein synthesis in wild-type, *flu* and *Atoep16-1;6* plants after a non-permissive 8 h dark-to-light shift.

Plants were grown under continuous white light for 2 w and subsequently shifted for 8 h to darkness. Then, the plants were reilluminated. **A)** Polysomal synthesis of light-harvesting chlorophyll *a/b* binding protein of photosystem II, LHCb2, and the small subunit of ribulose-1,5-bisphosphate carboxylase/ oxygenase, RBCS, as well as allene oxide synthase (AOS) in *flu* (**a** and **b**), wild-type (**c**) and *Atoep16-1;6* (**d**) plants detected 4 h (**a**, **c** and **d**) and 24 h (**b**) after the non-permissive dark-to-light shift. Fraction 1 contained the 40S ribosomal subunit, fraction 2 contained the 60S ribosomal subunit, and fractions 3-8 contained cytoplasmic polysomes of increasing size. Proteins from each of the different fractions were separated by SDS-PAGE and subjected to Western blotting using the indicated antisera.

3.4 Porphyrin-based cell death in barley: the *tigrina*^{d12} mutant

To gain further insights into the mechanism of translational control, we decided to study the *tig*^{d12} mutant of barley (von Wettstein *et al.*, 1974). *tig*^{d12} is orthologous to *flu* (Lee *et al.*, 2003) and was used because of its easy of cultivation, greater leaf mass and documented advantages to perform biochemical experiments, if compared with *Arabidopsis*. In addition, the barley genome is currently being sequenced and many of the known mutants may later allow identifying new functions related to the mechanism of ROS action and cell death control.

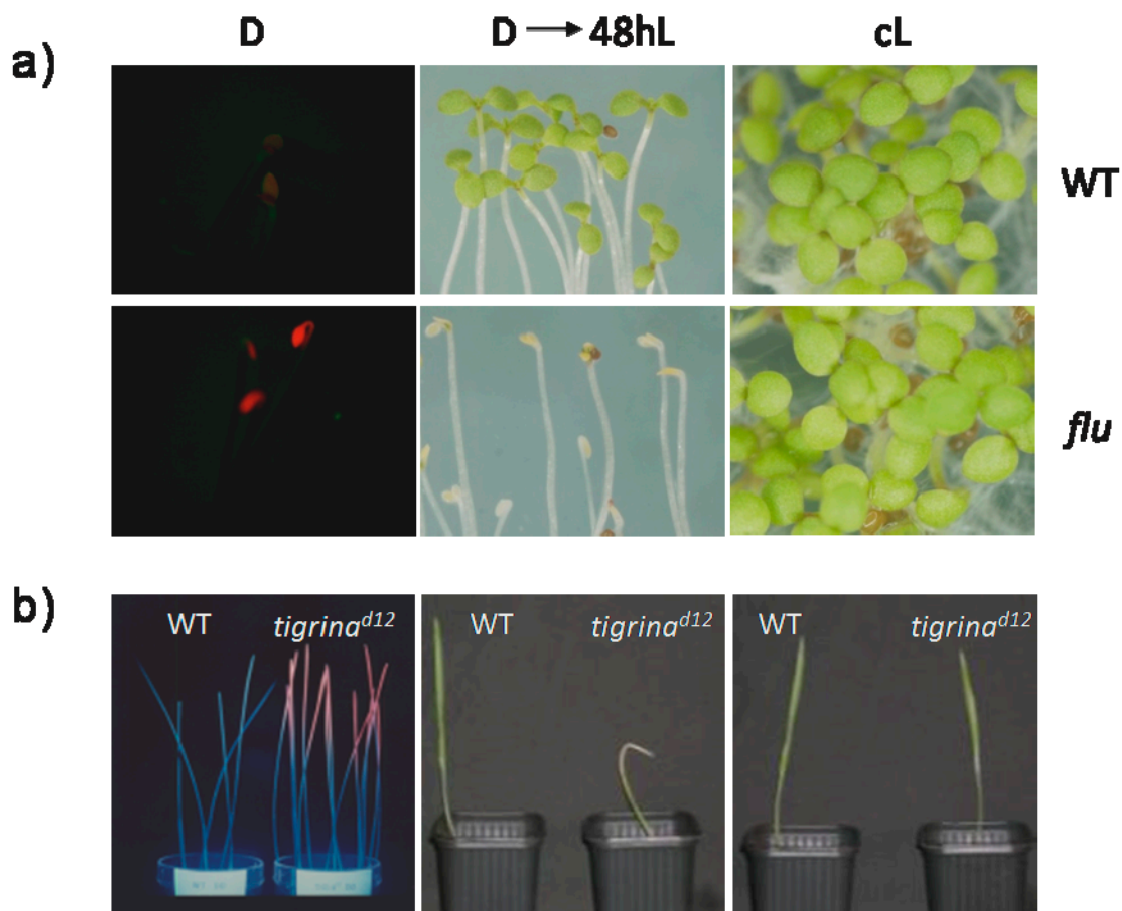


Figure 3.27 Phenotype of *flu* in *Arabidopsis* and its ortholog, *tigrina*^{d12}, in barley.

a) Phenotype of *flu* and wild-type *Arabidopsis* seedlings after growth for 5 d in darkness (D), after a subsequent shift to white light (125 $\mu\text{mol}/\text{m}^2\text{s}$) for 48 h (D → 48hL), and after growth for 5 d in continuous white light (cL). **b)** As in (a), but showing the phenotypes of wild-type and *tig*^{d12} seedlings after growth in the dark, subsequent irradiation, and under continuous white light conditions. Note the similar red fluorescences of free Pchl_a molecules in the dark in *flu* and *tig*^{d12} seedlings and their cell death after subsequent irradiation.

Similar to *flu*, dark-grown *tig^{d12}* seedlings exhibited a strong red fluorescence of Pchl_a under blue light. After illumination, etiolated *tig^{d12}* seedlings bleached and died (Figure 3.27). As *flu*, *tig^{d12}* seedlings looked normal and performed photosynthetic function when grown in continuous white light. However, *tig^{d12}* seedlings developed transverse-striped leaves with green and white sectors under alternate light/dark cycles. Free Pchl_a synthesized in the dark triggered singlet oxygen production and photooxidative damages during subsequent light periods, whereas the pigment was continuously converted to chlorophyllide by virtue of PORB in leaf sectors emerging during the light period (von Wettstein *et al.*, 1974).

3.4.1 Effect of light and singlet oxygen on protein synthesis in etiolated *tig^{d12}* seedlings

tig^{d12} and wild-type seedlings were grown in the dark for 5 d and exposed to white light of 125 $\mu\text{mol}/\text{m}^2\text{s}$ for various time periods. *In vivo*-labelling of proteins with ³⁵S-methionine was carried out for 2 h prior to harvest as described before for *Arabidopsis*. Proteins were extracted and precipitated with trichloroacetic acid, washed with acetone and ethanol and analyzed by SDS-gel electrophoresis. Coomassie blue-staining revealed similar patterns of proteins for light-adapted *tig^{d12}* and wild-type seedlings. By contrast, the protein patterns were slightly different for etiolated seedlings where several proteins were detectable in *tig^{d12}* but not in wild-type seedlings. These differences became even more pronounced when etiolated seedlings were exposed to white light. Then the labeling patterns were very distinct. The changes in protein expression seem to be due to alterations in protein synthesis rather than changes in protein stability. These effects are illustrated in Figure 3.28, showing that after 2 h of irradiation a number of proteins appeared in *tig^{d12}* that were not labelled in wild-type plants. On the other hand, several bands decreased in intensity on the autoradiograms in irradiated *tig^{d12}* seedlings, including SSU (small subunit) and LSU (large subunit) of ribulose-1,5-bisphosphate carboxylase/oxygenase (Rubisco) and LHCII (major light-harvesting chlorophyll *a/b* protein complex of photosystem II). After 12 h of white light exposure, synthesis of SSU and LSU and most other labelled proteins was undetectable in *tig^{d12}* versus wild-type seedlings, suggesting a block of synthesis of these proteins to occur in response to the generation of singlet oxygen (Figure 3.29).

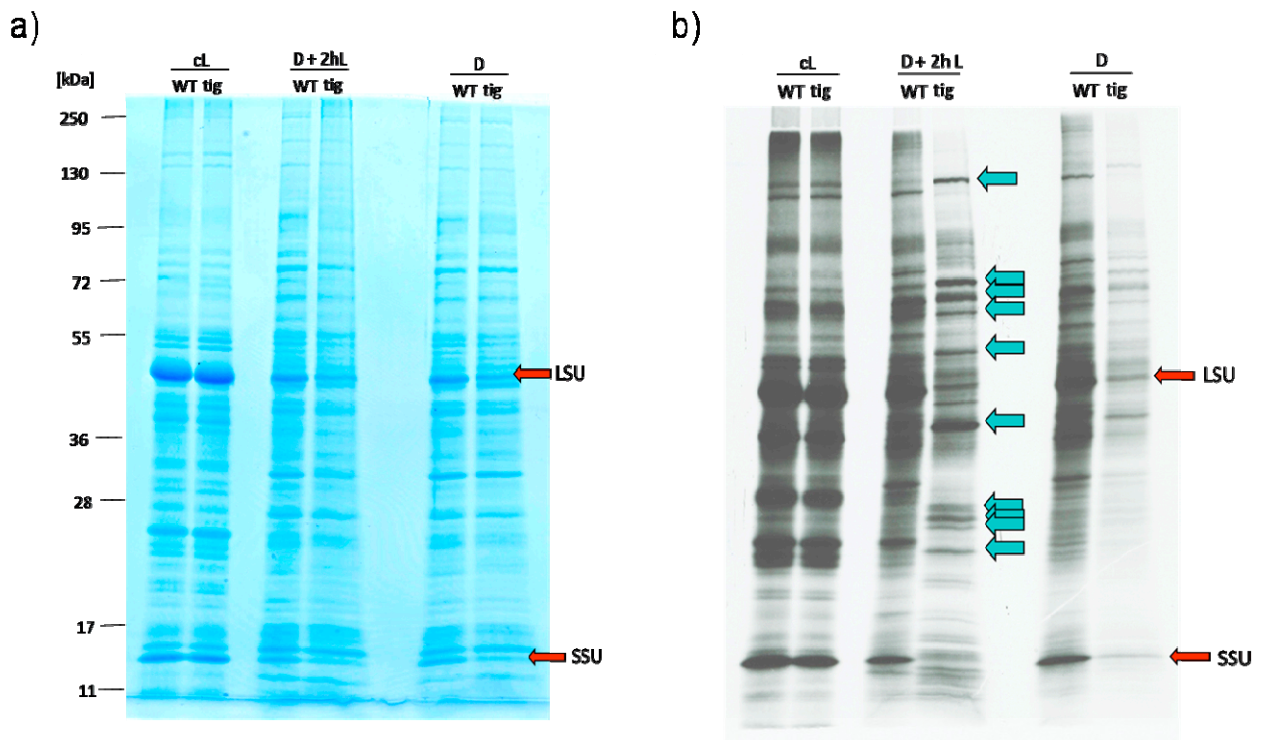


Figure 3.28 Changes in the protein patterns of etiolated and irradiated *tigrina*^{d12} and wild-type seedlings.

a) Patterns of Coomassie-stained proteins in 5 d-old, dark-grown *tig*^{d.12} and wild-type seedlings (D) and in etiolated *tig*^{d.12} and wild-type seedlings after white light exposure ($125 \mu\text{mol}/\text{m}^2\text{s}$) for 2 h prior to seedling harvest (D+2h L). For comparison, the pattern of proteins is shown for *tig*^{d.12} and wild-type seedlings that had been cultivated in continuous white light for 5 d (cL). **b)** Autoradiogram showing ³⁵S-methionine-labelled proteins corresponding to those in **(a)**. Positions of molecular mass standards are highlighted. LSU and SSU define the large and small subunits of ribulose-1,5-bisphosphate carboxylase/oxygenase.

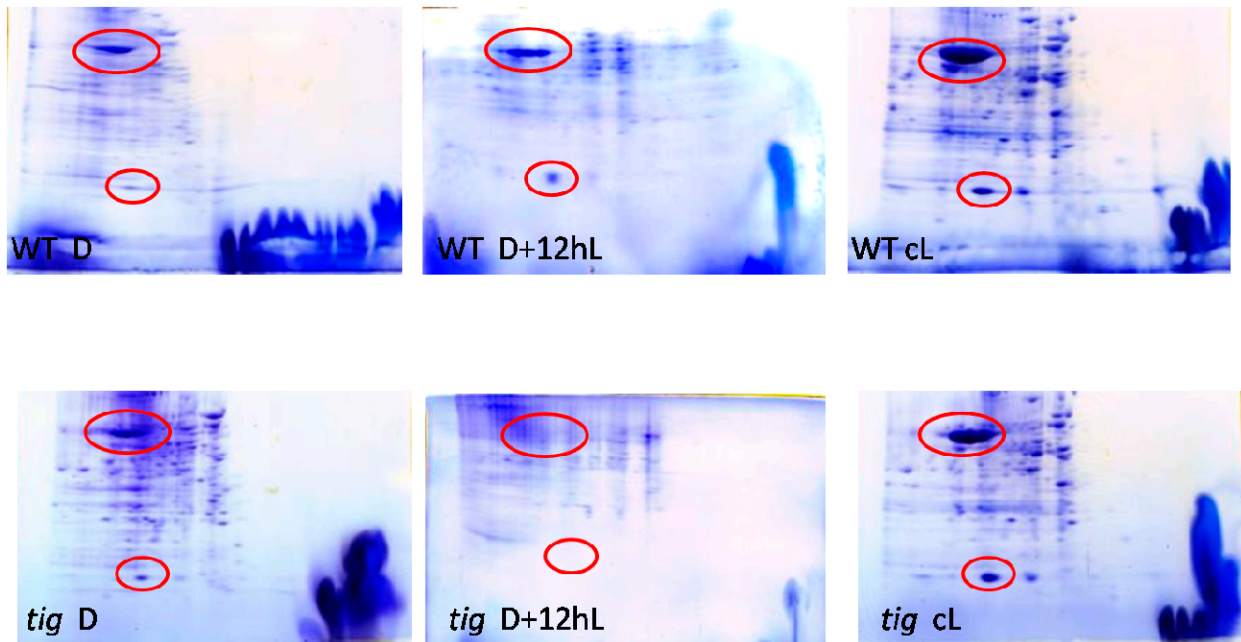


Figure 3.29 Two-dimensional pattern of total leaf proteins in *tigrina*^{d12} and wild-type seedlings.

Protein was extracted from 5 d-old, dark-grown *tig*^{d12} and wild-type seedlings (D) and etiolated *tig*^{d12} and wild-type seedlings that had been exposed to white light of 125 $\mu\text{mol}/\text{m}^2\text{s}$ for 12 h prior to seedling harvest (D+12hL). After 2D-electrophoresis, including isoelectric focusing in the first dimension (from left to right) and SDS-PAGE in the second dimension (from top to bottom), proteins were stained with Coomassie blue. For comparison, the pattern of proteins was analyzed for *tig*^{d12} and wild-type seedlings that had been cultivated in continuous white light for 5 d (cL). Red circles enclose the large and small subunits of ribulose-1,5-bisphosphate carboxylase/oxygenase.

3.4.2 A detailed expression analysis of photosynthetic and stress proteins

Immunoblotting was used to identify individual proteins in the polypeptide patterns. Antibodies were obtained from Agrisera, Sweden, and tested for their cross-reactivity. This approach allowed to identify components of PSII, such as PsbO (subunit of oxygen evolving complex of PSII reaction centre; 33 kDa) and PsbE (essential component for PSII assembly, involved in electron transport mechanisms that help to protect PSII from photodamage; 9,25 kDa), see Figure 3.30. These proteins did not seem to strongly react to singlet oxygen in irradiated *tig*^{d12} seedlings. By contrast, singlet oxygen production depressed accumulation of proteins that normally bind chlorophyll, such as D1 (38 kDa)

and D2 (49,4 kDa), which together form the core reaction centre of PSII. Neither protein accumulated to detectable levels in irradiated *tig^{d12}*, in contrast with wild-type seedlings.

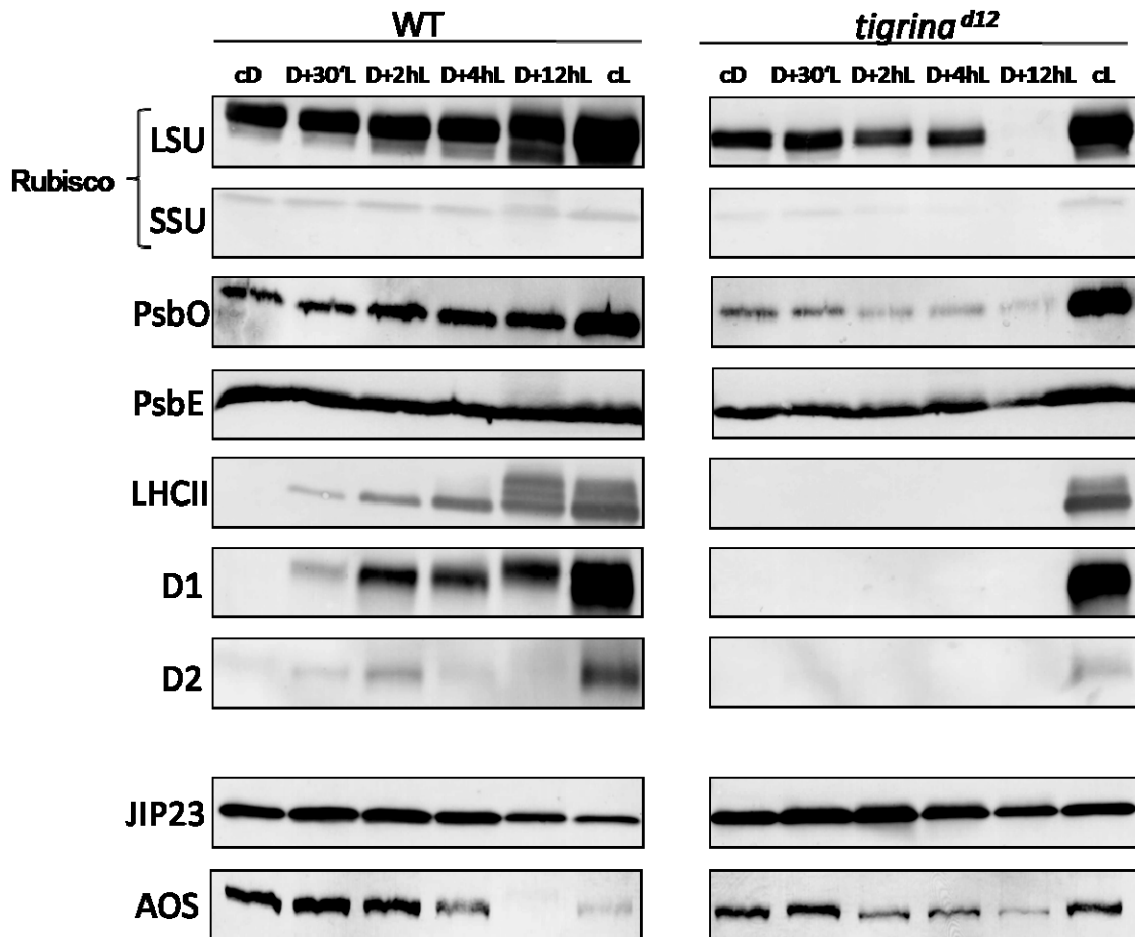


Figure 3.30 Expression of photosynthetic proteins in wild-type (WT) and *tigrina^{d12}* (*tig^{d12}*) seedlings after illumination.

Western blot analysis were carried out to detect abundant photosynthetic proteins in 5 d-old, etiolated *tig^{d12}* and wild-type plants (cD) and in seedlings that had been subjected to irradiation for 30 min (D+30'L), 2 h (D+2hL), 4 h (D+4hL) and 12 h (D+12hL), respectively, with white light of 125 $\mu\text{mol}/\text{m}^2\text{s}$. As control, protein extracts were prepared from plants that had been grown for 5 d under continuous white light (cL). After SDS-PAGE and transfer onto nitrocellulose membranes, the blots were probed with antisera against the indicated proteins. Abbreviations: LSU and SSU, large and small subunits of ribulose-1,5-bisphosphate carboxylase/oxygenase; PSBO and PSBE, the O- and E-subunits of photosystem II; LHCII, light-harvesting chlorophyll *a/b* binding protein 2 of photosystem II; D1 and D2, reaction centre polypeptides of photosystem II; JIP23, jasmonate-induced 23 kDa protein; AOS, allene oxide synthase.

After 12 h of illumination of etiolated plants, numerous stress proteins were found in *tig*^{d12} seedlings. Among them were protein known to play key roles in stress and defense responses, such as JIP23 (jasmonate induced protein of 23 kDa), allene oxide synthase (AOS; 58,2 kDa) and leaf thionins, small fungitoxic proteins localized in the plant cell wall that accumulate in etiolated plants and reappear in illuminated plants in response to pathogens and adverse conditions (Bohlmann *et al.*, 1988). However, their increase in abundance was only slightly elevated over that in wild-type plants, presumably because of their high expression level already in etiolated seedlings. When etiolated *tig*^{d12} seedlings were exposed to white light for periods longer than 24 h, total protein synthesis ceased and was no longer detectable (not shown).

3.4.3 Decrease of nucleus-encoded photosynthetic transcripts in *tig*^{d12} upon light stress

In order to determine whether the observed differences in the *in vivo*-labelling patterns of proteins in *tig*^{d12} versus wild-type plants were caused by corresponding changes of their respective mRNAs, *in vitro*-translation experiments were carried out. A rabbit reticulocyte lysate was programmed with mRNA extracted from 5 d-old etiolated *tig*^{d12} and wild-type plants that had been exposed to white light for 2 h. Figure 3.31 a) shows that this approach did not reveal gross differences in the patterns of translatable mRNAs for irradiated *tig*^{d12} and wild-type plants. This result, which is in clear contrast to those found at the protein level, suggested a posttranscriptional model of control. Northern blot analyses showed that *RBCS* mRNA was reduced in amount in mutant as compared to wild-type plants, both in the dark and after illumination (Figure 3.31 b). However, this reduction was much lower than that found in the *in vivo* labelling protein pattern (see Figure 3.28). For *LHCB2*, transcript levels were drastically reduced and were in most experiments below the limit of detection. This result demonstrated that expression of this protein is most likely controlled at transcriptional level (Figures 3.31 and 3.30, respectively).

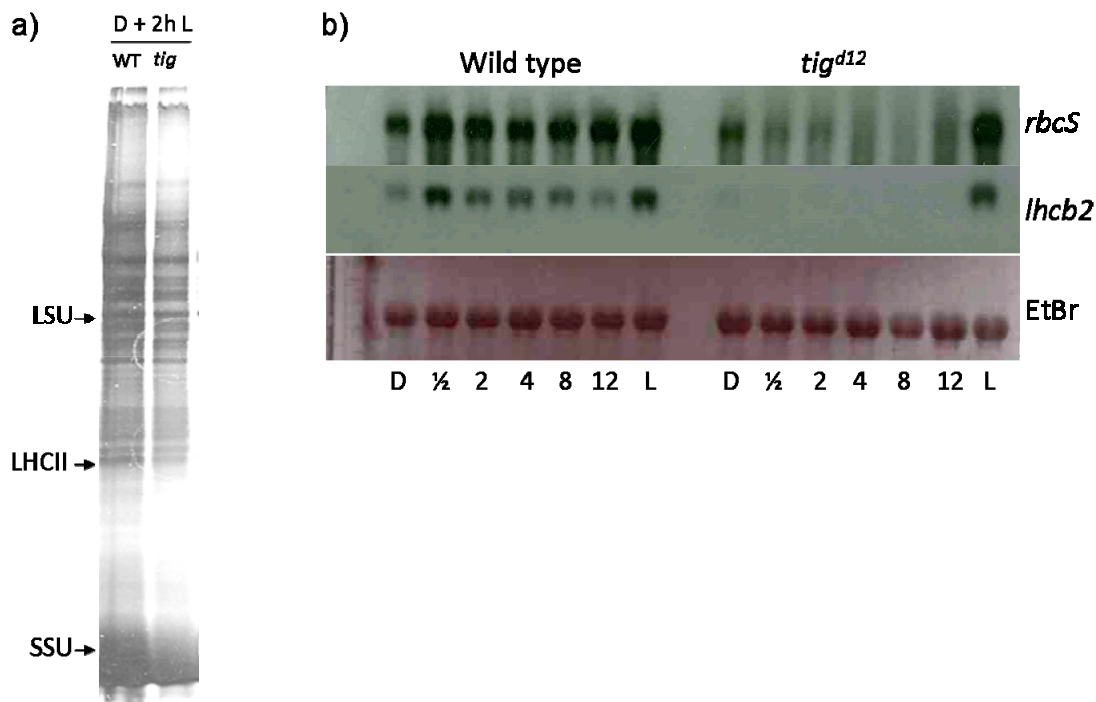


Figure 3.31 RNA expression in etiolated wild-type and *tigrina*^{d12} seedlings after 2 h of irradiation.

a) Patterns of polypeptides translated in a rabbit reticulocyte lysate from RNA of 2 h-irradiated *tig*^{d12} and wild-type plants. LSU (RBCL) and SSU (RBCS) mark the large and small subunits of ribulose-1,5-bisphosphate carboxylase/oxygenase. **b)** Northern blot analysis of *RBCS* and *LHCB2* transcript levels in dark-grown and irradiated *tig*^{d12} and wild-type plants after different periods of illumination. The lower part shows the ethidium bromide (EtBr)-stained 28S rRNA used as loading control.

3.4.4 Analysis of polysomal mRNAs in *tig*^{d12} and wild type-seedlings in response to light stress

The drastic reduction in RBCS synthesis *in vivo* and only moderate reduction in the level of its respective messenger *in vitro* in *tig*^{d12} seedlings suggested a posttranscriptional mode of control. In order to further examine this possibility, we analyzed the polysomal association of photosynthetic and stress transcripts in *tig*^{d12} and wild-type seedlings that had been grown in darkness for 5 d and exposed to strong white light (210 $\mu\text{E}/\text{m}^2$) for 2 h and 24 h, respectively. Polysomes were isolated and subjected to sucrose density gradient centrifugation. After centrifugation and subsequent fractionation, RNP material was recovered by ethanol precipitation and used for Northern hybridization. In parallel, RBCS,

THIONIN and ACTIN protein levels present in the different polysomal fractions were quantified by Western blotting, using large-scale polysome preparations.

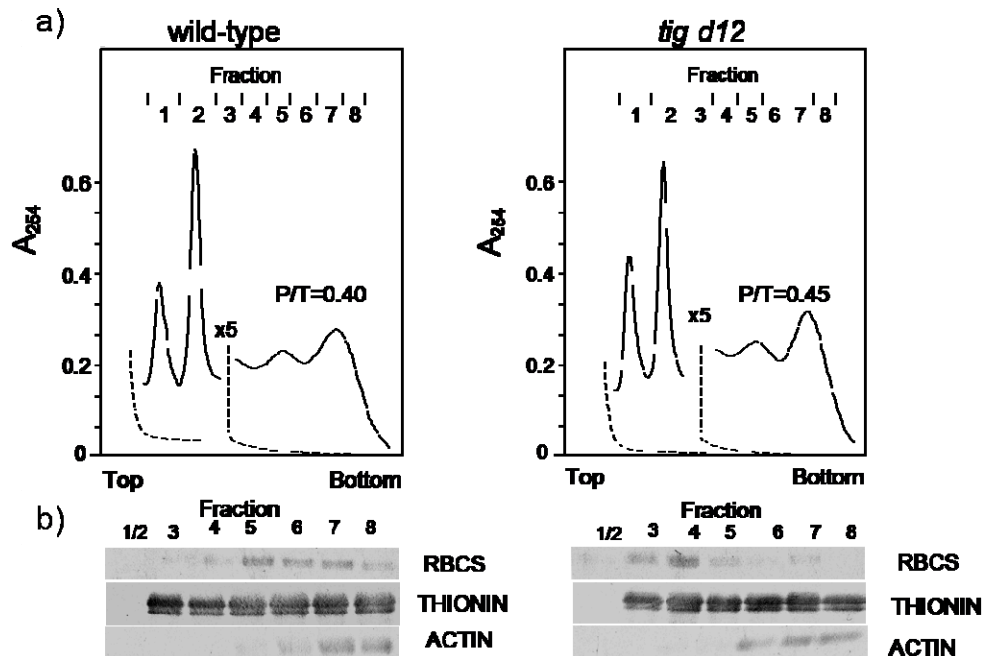


Figure 3.32 Polysome binding of photosynthetic messengers in *tigrida*^{d12} and wild-type plants.

Wild-type and *tigrida*^{d12} plants were sown on vermiculite and grown in the dark for 5 d, before being exposed for 2h to white light (125 $\mu\text{E}/\text{m}^2$). RNP material was extracted from leaf tissues of either plant source and resolved on sucrose step gradients. Absorbance readings were recorded at 254 nm (a). The different fractions represent polysomes of increasing size (fractions 3-8) as well as the 40S and 60S ribosomal subunits (fractions 1 and 2, respectively). (b) Western blot used to determine RBCS, THIONIN and ACTIN protein levels in the different polysomal as well as 40S and 60S fractions. The P/T ratios, defining the amount of ribosomes in polysomes relative to the total amount of RNP material, are indicated. Courtesy of Dhriti Khandal and Steffen Reinbothe.

Figure 3.32 a) shows absorbance profiles of RNP material at 255 nm that had been extracted from etiolated *tigrida*^{d12} and wild-type plants after 2 h of irradiation. Based on the absorbance readings, no major differences were observed in the polysome profiles. However, upon analyzing individual polysomal fractions by Western blotting, a massive reduction in polysome binding of *RBCS* transcripts was found for irradiated *tigrida*^{d12} seedlings. *RBCS* transcripts were confined to smaller polysomes in irradiated *tigrida*^{d12} plants as compared

with wild-type seedlings (Figure 3.32 b). This result suggested a depression in translation initiation to occur in *tig^{d12}* plants in response to light stress. When the illumination period was extended to 24 h, a large decay of polysomes was observed in *tig^{d12}* but not in wild-type plants (Figure 3.33 a, fractions 3-8). Northern-blot analysis confirmed that *RBCS* and *THIONIN* transcripts were present in the 40S ribosomal fractions of *tig^{d12}* seedlings (Figure 3.33 b), highlighting that extended light stress in *tig^{d12}* plants had caused ribosome dissociation into the ribosomal subunits.

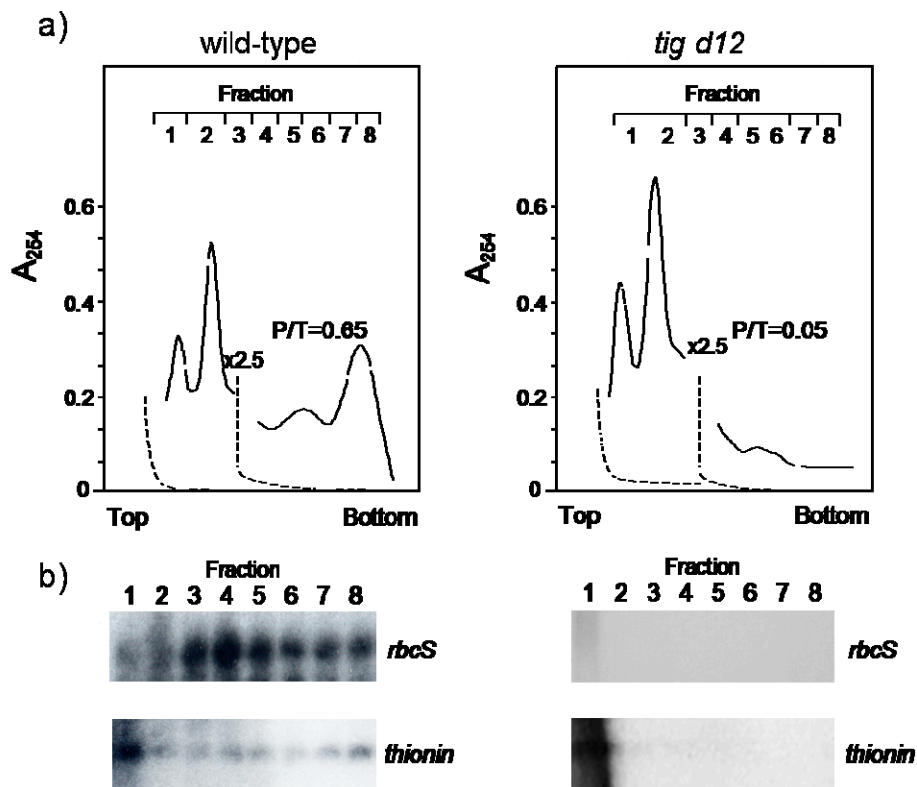


Figure 3.33 Dissociation of 80S cytoplasmic ribosomes in long-term irradiated *tigrina^{d12}* versus wild-type plants.

a) Wild-type and *tig^{d12}* plants were grown in the dark for 5 d and exposed to white light ($125 \mu\text{E}/\text{m}^2$) for 24 h. Then, RNP material was extracted and separated on sucrose gradients as described. Absorbance readings were recorded at 254 nm. The polysome profiles and calculated P/T ratios show a massive decline in the level of polysomes (fractions 3-8) and a respective increase in the amount of the 40S and 60S ribosomal subunits (fractions 1 and 2). **b)** Northern hybridization was used to detect and quantify *RBCS* and *THIONIN* transcript levels in the different polysomal as well as 40S and 60S fractions. Courtesy of Dhriti Khandal and Steffen Reinbothe.

Chapter 4 Discussion

Many functions of chloroplasts rely on thousands of nuclear-encoded proteins, which need to be imported from the cytosol through specialized import machineries located in the outer and inner envelope surrounding plastids. OEP16 is a protein of 16 kDa located in the outer envelope of different plastid types (etioplasts, proplastids, amyloplasts and chloroplasts) of roots, shoots and leaves. OEP16, initially isolated from pea chloroplasts, was shown to play a role of a specific channel for amino acids and amines (Pohlmeyer *et al.*, 1997). In addition, this protein was found to interact with pPORA during its Pchlide dependent import into isolated chloroplasts and etioplasts of barley (Reinbothe *et al.*, 2004 a+b). This finding emphasized the role of OEP16 in photomorphogenesis, since PORA is a key enzyme of Chl synthesis, catalyzing the light-dependent reduction of Pchlide to Chlide. Recently, genes coding for putative homologs of pea OEP16 were identified in *Arabidopsis* designated as *AtOEP16-1*, *AtOEP16-2*, *AtOEP16-3*, *AtOEP16-4* (Drea *et al.*, 2006, Murcha *et al.*, 2007). According to sequence analyses, *AtOEP16-1* shares high amino acid sequence identity with pea OEP16 (PsOEP16, 63%) and barley OEP16-1 (HvOPE16-1, 52%). The aim of the present work was to study the role of *AtOEP16-1* in *planta* and we used a reverse genetics approach to do so.

4.1 Role of *AtOEP16-1* in *planta*

In *Arabidopsis* *AtOEP16-1* is encoded by *At2g28900*. A respective T-DNA insertion line was identified in the mutant collection of the Salk Institute (Salk_018024.50.90.X). Homozygous *AtOep16-1* seedlings (Pollmann *et al.*, 2007) obtained after two backcrosses with the wild-type were isolated and further characterized. Analysis of the offspring of the generated homozygous seed stock provided seedlings that exhibited a conditional cell death phenotype associated with the de-etiolation response. When *AtOep16-1* seeds were germinated in the dark and subsequently exposed to white light, the newborn seedlings did not green but instead they died. Because of import defects of pPORA, Pchlide accumulated in a free, non-protein bound form and operated as photosensitizer that triggered singlet oxygen production and cell death. In electron micrographs, drastic reductions in the size and ultrastructure of the prolamellar body were seen. This result is in line with previous studies that had shown that PORA is a major constituent of the prolamellar body (Dehesh *et al.*, 1985; Reinbothe *et al.*, 2003 a+b). In most cases, etiolated seedlings entirely lacked these

paracrystalline structures and contained ghost-like areas, called plastoglobules. Plastoglobules are metabolite carriers with many roles in chloroplasts, but little is known about their function in etioplasts during greening. It is attractive to hypothesize that plastoglobules in plastids of mutant *Atoep16-1* may be involved in sequestering carotenoids and other compounds that could not be assembled into the prolamellar bodies. Etiolated *Atoep16-1* seedlings did not contain larger PORA:PORB supracomplexes indicative of the presence of LHPP nor did they express photoactive Pchl_a F655. Only one main pigment peak was found in low temperature measurements, emitting at approximately 630 nm and, therefore, consisting mostly of unassembled PORB-Pchl_a-NADPH ternary complexes and free, non-protein-bound pigment molecules (Pollmann *et al.*, 2007).

The phenotype of Pollmann's *Atoep16-1* can be compared and contrasted with that of other mutants defective in key components of the TOC and TIC machineries operating in import of nucleus-encoded proteins into chloroplasts and other plastid types. Bauer *et al.* (2001) identified three receptor components of the TOC machinery, TOC159, TOC130 and TOC120, that all share the presence of conserved membrane anchor and GTP binding domains. TOC159, TOC130 and TOC120 differ by the length of their cytosolically exposed domains that are implicated in binding the presequences of nucleus-encoded plastid proteins during import. Pull-down assays showed that while TOC159 bound precursors to photosynthetic proteins, TOC120 and TOC130 did not and therefore they were concluded to be responsible for the import of other, non-photosynthetic proteins (Bauer *et al.*, 2001). In addition, co-immunoprecipitation showed that TOC159 did not interact with the transit peptide of PORA (Smith *et al.*, 2004), supporting previous studies which had suggested a TOC159-independent pathway of pPORA import (Reinbothe *et al.*, 1995, 2000). A fourth member of the same receptor family was discovered, TOC90, with as yet unknown function during plant development (Hiltbrunner *et al.*, 2004).

Arabidopsis mutants that lack TOC159, designated *ppi2*, are seedling lethal (Bauer *et al.*, 2001). *ppi2* seedlings are unable to establish photosynthetically active chloroplasts because of the import defect for photosynthetic proteins. Although no data was present in the paper by Bauer *et al.* (2001), it is likely that etiolated *ppi2* mutant seedlings are impaired also in the switch from skotomorphogenesis to photomorphogenesis that relies on the activity of PORB and its assembly with PORA into LHPP, as well as other proteins constituting the prolamellar body. In contrast to *toc159 (ppi2)*, *toc120* and *toc130* knock-out seedlings

showed none or only weak phenotypes, underscoring their role in import of non-photosynthetic proteins (Jarvis *et al.*, 1998; Ivanova *et al.*, 2004; Kubis *et al.*, 2004).

TOC159 normally cooperates with TOC75 and TIC33/34 in the recognition, binding and translocation of transit sequence-containing cytosolic precursors of plastid proteins (see Bedard and Jarvis, 2005; Hofmann and Theg, 2005; Kessler and Schnell, 2006, for reviews). As mentioned in the Introduction (§1), TOC75 establishes a hydrophilic translocation channel through which the majority of the cytosolic precursors are transported across the outer envelope (Hinnah *et al.*, 1997, 2002). In *Arabidopsis*, TOC75 is encoded by three genes of which two have different expression patterns and presumed functions (Baldwin *et al.*, 2005). Unlike *ppi2* which is seedling lethal, knock-out of *TOC75-III* gave rise to embryo lethality (Kovacheva *et al.*, 2005). Similarly, mutation in *TIC110* caused an embryo-lethal phenotype (Inaba *et al.*, 2005). TIC110 acts as multifunctional component of the inner envelope translocase (Kessler and Blobel, 1996; Heins *et al.*, 1998; Inaba *et al.*, 2003). In clear contrast to these phenotypes, loss-of-function mutation in *TIC40* and the *Clp C-type Hsp93* were not lethal (Chou *et al.*, 2003; Constan *et al.*, 2004; Ivanova *et al.*, 2004; Kovacheva *et al.*, 2005). Together, these results are suggestive of only partial functional redundancies between different members of the same subfamily of TOC and TIC proteins. By contrast, our results show that *AtOEP16-1* plays a unique role for plant de-etiolation and that the other members of the *AtOEP16* family cannot take over this role in the *Atoep16-1* mutant.

4.2 Salk T-DNA insertion in the gene *Atoep16-1* contains different mutants

The results published by Pollmann *et al* (2007) are at variance with data put forth by Philippar *et al* (2007). Our laboratory and that of Philippar *et al.* (2007) used apparently the same *Atoep16-1* T-DNA insertion mutant stock of *Arabidopsis*, purchased from the Salk Institute (Salk_018024.50.90.X), but obtained strikingly different results. Our studies (Pollmann *et al* (2007) unveiled a conditional seedling lethal phenotype of *Atoep16-1* that is caused by excessive accumulation of free Pchl_{ide} molecules in the dark. The conditional cell death phenotype of *Atoep16-1* described by Pollmann (2007) is reminiscent of the one described by Meskauskiene *et al* (2001) for *flu*. In addition, our findings showed that

mutant *Atoep16-1* is impaired in plastid import of pPORA, confirming previous *in vitro* crosslinking results which had demonstrated a role of OEP16-1 protein in the substrate-dependent transport of pPORA into barley, *Arabidopsis* and pea chloroplasts (Reinbothe *et al.*, 2004 a+b). Kim and Apel (2004) elegantly confirmed that pPORA import is substrate-dependent *in planta*, but only in the cotyledons of etiolated seedlings and not in mature green leaves of light-grown *Arabidopsis* plants. Our results are suggestive of the operation of a default import pathway that governs the substrate-independent import route into leaf mesophyll chloroplasts (see below).

In contrast to our results, work of Philippar *et al* (2007) revealed no differences in pPORA import and content between the *Atoep16-1* mutant they used and wild-type seedlings. Moreover, neither a conditional cell death phenotype during plant de-etiolation nor a change in etioplast ultrastructure was observed in electron micrographs. Together these differences suggested that the mutants used in our studies and those of Philippar *et al.* (2007) were not the same, despite the fact that they originated from the same mutant seed stock provided by the Salk Institute.

In order to solve this issue, we re-screened the original seed stock obtained from the Salk Institute for the presence of additional *Atoep16-1* mutants. We discovered that this seed stock contains several independent knock-out mutants. Based on the autofluorescence of Pchl_a accumulated in etiolated seedlings and the capability of the seedlings to green or not after subsequent illumination, two families of *Atoep16-1* mutants showing distinct features were identified. The first mutant family of plants comprising *Atoep16-1;5* and *Atoep16-1;6* showed high red Pchl_a autofluorescence in the dark and died after illumination. By contrast, the second family comprising *Atoep16-1;7* and *Atoep16-1;8* included plants with weak Pchl_a autofluorescence in the dark and normal greening. Each family was tested with regard to the presence of PORA protein by Western-blotting and each segregated into a PORA-containing and PORA-free line. Collectively, these studies resulted in the identification of four independent *Atoep16-1* knock-out mutants that were named *Atoep16-1;5*, *Atoep16-1;6*, *Atoep16-1;7* and *Atoep16-1;8*. Because all four mutants contained only one detectable T-DNA fragment on Southern-blot, we suppose that other, small mutations undetectable by DNA gel blot hybridization may be present in some of the mutants and responsible for the different phenotypes obtained. It has been observed that T-DNA insertion lines tend to partially lose their DNA insertions, giving rise to small DNA rearrangements at the original insertion site (see below). These exogenic mutations may be

implicated in revealing bleaching (hiding greening) or in revealing greening (hiding bleaching). However, the complementation assays demonstrated a cell death rescue of mutant *Atoep16-1;6* and disproved that these exogenic mutations are responsible for the cell death phenotype.

Mutant *Atoep16-1;5* exhibited the strongest phenotype. It lacked PORA protein and overaccumulated Pchlde in the dark. *In vitro* and *in vivo* import data demonstrated that plastids isolated from mutant *Atoep16-1;5* could not import the transA-DHFR and transA-GFP model precursors to the same extent as wild-type seedlings. In fact, import of these precursors was largely impaired and was in most experiments undetectable, explaining why etiolated *Atoep16-1;5* seedlings did not accumulate PORA *in vivo*.

After a detailed analysis of the *in vivo* states of Pchlde by low temperature spectroscopy only photoinactive Pchlde-F631 was found, whereas photoactive Pchlde-F655 was missing. Photoactive Pchlde-F655 has been generally considered to be the major Pchlde form that leads to the formation of Chlide during greening (Litvin *et al.*, 1993). Photoactive Pchlde-F655 is thought to be due to the unique properties of PORA bound with Pchlde *b* and NADPH to form ternary complexes that further assemble with PORB–Pchlde *a*-NADPH into larger LHPP complexes. As shown previously, LHPP is involved in light-harvesting and energy dissipation during greening (Reinbothe *et al.*, 1999, 2003 a+b). Since neither Pchlde-F655 nor PORA were detectable in mutant *Atoep16-1;5*, we suppose that operational larger PORA:PORB supracomplexes were absent in the dark. The lack of these complexes would explain why mutant *Atoep16-1;5*, similar to Pollmann's mutant *Atoep16-1*, rapidly died during greening. Indeed tetrazolium staining unravelled that an average of only 35% of 5 d-old, dark-grown seedlings remained viable after 4 h of irradiation at 125 $\mu\text{mol}/\text{m}^2\text{s}$. Most likely, free, non-protein bound Pchlde molecules in the bulk of Pchlde-F631 acted as photosensitizer and produced singlet oxygen. DanePy measurements confirmed mass generation of singlet oxygen in irradiated *Atoep16-1;5* seedlings, similar to that observed in irradiated *flu* seedlings. Taken together, we conclude that mutant *Atoep16-1;5* is virtually identical to mutant *Atoep16-1* described previously by Pollmann *et al.* (2007). However, it must be noted that Pollmann's *Atoep16-1* and *Atoep16-1;5* mutants were obtained from the offspring of independent homozygous plants that had been backcrossed twice and once, respectively.

Mutant *Atoep16-1;6* displayed a weaker cell death phenotype than mutant *Atoep16-1;5*. It accumulated high amounts of red-fluorescing Pchlde in the dark and bleached after subsequent exposure to high white light. However, cell death progression seemed to be delayed if compared with that measured for *Atoep16-1;5* seedlings. Tetrazolium staining identified a greater percentage of seedlings that survived after 4 h of illumination of 5 d-old etiolated plants, increasing up to 60%, when compared to *Atoep16-1;5* mutant seedlings of the same age. In spite of this conditional cell death phenotype, PORA protein was detectable in *Atoep16-1;6* plants. However, low temperature spectroscopic analysis revealed only the presence of photoinactive Pchlde-F631 and low, in most cases undetectable levels of photoactive Pchlde-F655. Thus, the majority of the pigment was present in a free form, not bound to POR proteins in mutant *Atoep16-1;6*. Similar to mutant *Atoep16-1;5*, most of the incoming light could not be harvested in the normal manner and provoked singlet oxygen production from excited pigment molecules. Direct proof for this interpretation is provided by the DanePy measurements that demonstrated singlet oxygen generation in irradiated *Atoep16-1;6* seedlings. However, the fluorescence quenching of DanePy and thus produced singlet oxygen levels were lower than those observed for irradiated *Atoep16-1;5* and *flu* seedlings. The trace amounts of photoactive Pchlde-F655 present in etiolated *Atoep16-1;6* seedlings may be the cause of this lowered rate of singlet oxygen release.

Import and crosslinking studies demonstrated that transA-DHFR entered both Pchlde-free and Pchlde-containing mutant plastids. This result suggests that import did not require the presence of Pchlde. *In vitro* and *in planta* import assays additionally showed that pPORA is likely taken up by the plastids via a default import pathway involving TOC75. As shown previously, multiple versions of the TOC machinery exist that differ by an interchange of receptor and regulatory components and exhibit different precursor specificities (Jarvis *et al.*, 1998; Bauer *et al.*, 2000; Ivanova *et al.*, 2004).

Mutant *Atoep16-1;7* did not show a cell death phenotype. In dark-grown seedlings, no red fluorescing Pchlde molecules were found and the fluorescence levels were as low as those in the wild-type. Astonishingly, no PORA protein could be detected on Western blots. However, during low-temperature fluorescence spectroscopy we found drastically reduced amounts of photoinactive Pchlde-F631. Although no photoactive Pchlde-F655 was detected, the plants greened normally. It is likely that mutant *Atoep16-1;7* synthesized Chl by a pathway that was previously attributed to the action of PORB (Lebedev *et al.*, 1995). This LHPP-independent route was discovered in the *det340* mutant of *Arabidopsis* that does

not accumulate PORA because of constitutive activation of phytochrome signaling in the dark (Lebedev *et al.*, 1995). In contrast to *det340*, however, we did not observe an increased sensibility of etiolated *Atoep16-1;7* seedlings to high light intensities. This result may be explained by the rather low level of Pchl_{ide} F-631 *in planta*, allowing the establishment of a Pchl_{ide}-to-PORB homeostasis that permits normal greening. Unlike *Atoep16-1;7*, *det340* contains ca. 12-15-fold increased levels of Pchl_{ide}-F631 *in vivo* (Lebedev *et al.*, 1995). Last but not least, it cannot be excluded that the ROS-quenching mechanisms were differentially expressed in irradiated *Atoep16-1;7* and *det340* seedlings. According to numerous studies, various compounds operate in the photoprotection mechanisms of chloroplasts, such as carotenoids, ascorbate and vitamins B6 and E (α -tocopherol), (Ehrenshaft *et al.*, 1999; Wagner *et al.*, 2004; Danon *et al.*, 2005; Laloi *et al.*, 2007).

Mutant *Atoep16-1;8* is similar to the mutant isolated by Philippar *et al.* (2007). Mutant *Atoep16-1;8* contained wild-type levels of PORA and Pchl_{ide}-F655. These findings strongly suggest that functional LHPP complexes were present and prevented photooxidative damages during greening. How such complexes may be established is unclear, given that our *in vitro* and *in vivo* import data demonstrated a default pathway not involving the PTC complex described previously (Reinbothe *et al.*, 2004 a+b). Crosslinking studies showed that transA-DHFR enters the plastids in a TOC75-mediated manner. It is tempting to speculate that there may be some, as yet unknown mechanisms to assemble PTC52 with TOC and TIC components and build PTC-like complexes in the plastid envelopes. As mentioned in the Introduction (§1), PTC52 is part of a small gene family of proteins, including PAO, CAO and TIC55, that share conserved and unique domains.

4.3 Is the lack of AtOEP16-1 protein responsible for photobleaching?

From a purely simplistic view, one could argue that the conditional cell death phenotype observed in mutants *Atoep16-1;5* and *Atoep16-1;6* is unrelated to the absence of AtOEP16-1. In line with such interpretation would be the identification of mutants *Atoep16-1;7* and *Atoep16-1;8* that did not show any phenotype. To illuminate this issue, complementation studies were carried out for mutant *Atoep16-1;6*. Using several independent transformants

we could show that re-expressing AtOEP16-1 protein depresses the accumulation of free Pchlde molecules in the dark and restores normal greening. These results confirm that the photobleaching phenotype is indeed linked to the *Atoep16-1* mutation. From the *in vitro* import and crosslinking as well as low temperature data we assume that reintroducing AtOEP16-1 protein might restore the substrate-dependent import of pPORA, LHPP assembly and the establishment of photoactive Pchlde-F655 that together allowed normal greening. However, this conclusion needs to be verified in further work. In addition to complementation assays, the RNAi approach could be also important for phenotypical studies, since no other *Arabidopsis* mutants of *AtOEP16-1* gene are available apart from the SALK Institute and other public resources.

What are the reasons for the suppression of the cell death phenotype in mutants *Atoep16-1;7* and *Atoep16-1;8*? We assume that additional mutations may be present in mutants *Atoep16-1;7* and *Atoep16-1;8* that affected the establishment of the cell death phenotype. It has been observed that T-DNA lines containing multiple insertions tend to lose some or all of their foreign DNAs in subsequent generations. DNA arrangements provoked by the insertion and loss of such supplementary T-DNA copies (Latham *et al.*, 2006) could be the reason for the complex genetic background observed in mutants *Atoep16-1;7* and *Atoep16-1;8*. For example, when mutant *Atoep16-1;7* was crossed with *flu* a resulting double mutant *flu:Atoep16-1;7* regained the conditional cell death phenotype (see Figure A.3 enclosed in the appendix A). This finding is reminiscent of results reported for a suppressor of *flu* which contains a second-site mutation in the *HY1* gene encoding heme oxygenase (Goslings *et al.*, 2004). In the isolated suppressor, heme overproduction led to a depression of Pchlde synthesis at the level of glutamyl-tRNA reductase (Meskauskiene *et al.*, 2001) and thereby prevented cell death initiation (Goslings *et al.*, 2004). However, the identity of these additional mutations in *Atoep16-1;7* and *Atoep16-1;8* mutants, remains to be determined by map-based cloning and whole-genome sequencing approaches. Until more detailed studies are performed, we still cannot entirely exclude that such second-site mutations provoked cell death properties in *Atoep16-1* mutant background.

Obviously, there are different plastid import pathways for pPORA whose operation is dependent on plant developmental state and age. One pathway operates in the cotyledons of dark-grown seedlings (Reinbothe *et al.*, 1995; Kim and Apel, 2004; Schemenewitz *et al.*, 2007). This pathway is Pchlde-dependent and involves the PTC complex. The second pathway is operational in light-adapted plants. It takes place independently on Pchlde and

involves the TOC and TIC machineries (Reinbothe *et al.*, 1995; Kim and Apel, 2004; Schemenewitz *et al.*, 2007).

Biochemical evidence suggests that cytosolic HSP70 and 14:3:3 proteins may be key players in regulating the targeting of pPORA to these different pathways. In etiolated seedlings, no HSP70 and 14:3:3 protein complexes bind and direct the precursor to the TOC and TIC machineries (Schemenewitz *et al.*, 2007). By contrast, binding of HSP70 and 14:3:3 proteins to the mature region of pPORA provoked a substrate-independent import pathway of pPORA *in vitro* (Schemenewitz *et al.*, 2007). The operation of this pathway could be responsible for the Pchl_{ide}-independent import of pPORA into the chloroplasts of leaf mesophyll cells described by Kim and Apel (2004).

Evidence for the existence of a third import pathway for pPORA can be deduced from the results of the present study. We used transA-DHFR precursor proteins to demonstrate Pchl_{ide}-independent import of these model precursors. Plastids isolated from mutants *Atoep16-1;6* and *Atoep16-1;8* imported the chimeric precursors presumably via a TOC75-dependent route. Because neither model precursor contains the 14:3:3 recognition motif that is normally present in the mature region of the PORA polypeptide, the import pathway followed in mutants *Atoep16-1;6* and *Atoep16-1;8* cannot rely on the presence of respective guidance complexes consisting of HSP70 and 14:3:3 proteins (May and Soll, 2000; Schemenewitz *et al.*, 2007). However, Qbadou *et al.* (2006) have shown that there is a second type of targeting complex comprising HSP990 that could be involved in directing pPORA to the TOC and TIC import machineries. We are likely to support the hypothesis that second site mutations in the regulatory circuits that establish the functional protein import complexes in the envelope membranes and control the activity of cytosolic targeting factors, which guide the precursors to the “correct” import machinery, could be responsible for the operation of altered plastid import pathways of pPORA in mutant *Atoep16-1;6* and *Atoep16-1;8*.

4.4 Are the cell death regulatory mechanisms in mutants

Atoep16-1;5 and 1;6 the same as in flu?

Mutants *Atoep16-1;5* and *Atoep16-1;6* show a conditional cell death phenotype that is very similar to that of *flu* plants. We therefore asked whether cell death regulation operating in *Atoep16-1;6* would be comparable to the singlet oxygen-dependent pathway reported for the *flu* mutant (Meskauskiene *et al.*, 2001; op den Camp *et al.*, 2004; Wagner *et al.*, 2004; Danon *et al.*, 2005). As outlined in the Introduction (§ 1), FLU is a nucleus-encoded protein that plays a key role during the negative feedback control of Chl biosynthesis in the dark, regulating the accumulation of Pchl_{ide} in *Arabidopsis* and other angiosperms. Inactivation of *flu* causes growth arrest and/or cell death, depending on the amount of singlet oxygen produced from free, photoexcitable Pchl_{ide} molecules. While etiolated *Atoep16-1;5* and *Atoep16-1;6* seedlings share similar cell death symptoms with *flu* seedlings after irradiation, no growth inhibition was observed for mature green *Atoep16-1;5* and *Atoep16-1;6* plants. Similar to *flu*, etiolated *Atoep16-1;5* and *Atoep16-1;6* seedlings accumulated high amounts of Pchl_{ide} in the dark. The excess of Pchl_{ide} was not present in a functional, PORA-bound state and acted as a photosensitizer after subsequent illumination, generating singlet oxygen. DanePy fluorescence quenching demonstrated that mutant *Atoep16-1;5* generates similar amounts of singlet oxygen as *flu*, while in mutant *Atoep16-1;6* lower levels of singlet oxygen were formed. These differences may explain why mutant *Atoep16-1;6* had a weaker phenotype than mutant *Atoep16-1;5*.

In irradiated *flu* seedlings, singlet oxygen was proposed to act primarily as cytotoxin. By contrast, singlet oxygen liberated in light-adapted *flu* plants that had been subjected to a non-permissive 8 h dark-to-white light shift was suggested to function as a signal which activates changes in gene expression (see Kim *et al.*, 2008, for review). *Transcriptome* profiling analyses identified genes that were up-regulated or down-regulated by singlet oxygen. Among them were stress response genes such as *BONZAI1* and *EDS1* that have documented roles in defence against biotic and abiotic cues, as well as genes encoding key enzymes of ethylene and jasmonates synthesis and signalling. By contrast, genes that were down-regulated in response to singlet oxygen comprised genes encoding components of the photosynthetic apparatus (op den Camp *et al.*, 2003).

A major clue for understanding the differences in cell death regulation between *Atoep16-1;6* and *flu* plants was provided by the *in vitro* and *in vivo* protein synthesis experiments. *In vitro* translation did not reveal gross alterations in the pattern of translatable messengers in dark-grown seedlings after 2 h of illumination. In all four *Atoep16-1;5-8* mutant types, indistinguishable messenger products were found and no stress messengers accumulated in *Atoep16-1;5* and *1;6* that at first glance may be expected if these mutants followed the same cell death pathway as *flu* plants. Nevertheless, *in vivo* labelling of proteins identified differences of how the four *Atoep16-1;5-8* mutant types responded to illumination. While all four mutants began synthesizing photosynthetic proteins during the early hours (4 h) of greening, only mutants *Atoep16-1;7* and *Atoep16-1;8* pursued translating photosynthetic proteins. Mutants *Atoep16-1;5* and *Atoep16-1;6* were unable to do so and ceased protein synthesis after 24 h. Polysome profiling studies unveiled that mutants *Atoep16-1;5* and *Atoep16-1;6* are unable to recruit stress messengers for translation. In fact, no *AOS* transcripts used as a model messenger were detectable in the analyzed polysomal fractions. By contrast, light-adapted *flu* plants efficiently translated the *AOS* messenger, as indicated by the preferential polysomal binding of this transcript versus photosynthetic transcripts after the non-permissive dark-to-light shift. Thus, the normal early reprogramming of translation detected for *flu* plants was abrogated in *Atoep16-1;6* plants. Nevertheless, at later stages of the singlet oxygen-dependent response, protein synthesis declined to similar extents in *flu* and *Atoep16-1;6* plants. In the *flu* orthologous mutant of barley, *tig^{d12}* that was used as a reference, the same early as well as later effects on translation, were observed (see Appendix B).

Until recently it was unresolved whether there is one cell death pathway that is activated by porphyrin excitation and singlet oxygen production or whether there are more. Our results clearly show that there must be more than one pathway and that the early and late effects on translation are separable. Thus, *Atoep16-1;6* and *flu* plants, which are virtually identical with regard to their phenotypic properties (Pchl_a overproduction, presence of PORA), represent exciting new tools to step into these mechanisms in more details.

4.5 Reduced carotenoid content leads to enhanced light sensitivity in irradiated *Atoep16-1;5* and *Atoep16-1;6* seedlings

Carotenoids are bound to LHC proteins and act as powerful quenchers of both excited triplet states of porphyrins (Chl, Pchl_a, others) as well as singlet oxygen. We therefore analyzed the actual composition and concentration of carotenoids in mutants *Atoep16-1;5* and *Atoep16-1;6* (photobleaching mutants) and compared them with those in mutants *Atoep16-1;7* and *Atoep16-1;8* (non-photobleaching mutants). This approach appeared to be especially promising because mutants *Atoep16-1;5* and *Atoep16-1;6* cannot synthesize photosynthetic proteins upon persisting light stress.

Our HPLC analyses showed that high white light stress leads to drastic reductions in the violaxanthin, β -carotene and lutein contents in irradiated *Atoep16-1;5* and *Atoep16-1;6* versus *Atoep16-1;5* and *Atoep16-1;6* seedlings. Mutants *Atoep16-1;5* and *1;6* accumulated higher levels of zeaxanthin when compared to mutants *Atoep16-1;7*, *1;8* and the wild-type. Nevertheless, the amount of synthesized zeaxanthin seemed insufficient to compensate for the loss of violaxanthin, lutein and β -carotene levels in irradiated *Atoep16-1;5* and *1;6* seedlings such that no photoprotection occurred.

There are several possibilities to explain these results. Since β -carotene normally binds to PSII core complexes and xanthophylls to LHC proteins in PSII-LHCII supercomplexes, the process of photosynthesis and Chl synthesis may be drastically disturbed in mutants *Atoep16-1;5* and *1;6* under high light stress. Accordingly to Dall'Osto *et al.* (2007), α -branch (lutein) and β -branch (zeaxanthin, violaxanthin and neoxanthin) xanthophylls play different and complementary roles in antenna protein assembly and in the mechanisms of photoprotection. It was reported that a lack of lutein increases the sensitivity to light (Dall'Osto *et al.*, 2006) and even if it is present, it is not able alone to sustain single oxygen scavenging, thus causing rapid bleaching of Chl bound to LHC proteins. Since xanthophylls are needed for the folding of LHC proteins *in vitro* (Plumley *et al.*, 1987), it may be highly possible that a strong decrease in their availability in mutants *Atoep16-1;5* and *Atoep16-1;6* led to a decreased content in LHC proteins. Reduction in LHC proteins could prevent assembly of functional light-harvesting complexes, as a result of which pigment bleaching would occur. Protein denaturation and other hazardous effects caused by singlet oxygen would trigger cell death. The fact that mutants *Atoep16-1;7* and *Atoep16-1;8* greened

normally and were well protected against photooxidative damage may be in part explained by the work of Croce *et al.*, 1999 on the *in vitro* reconstitution of recombinant LHC proteins. The authors showed that the resistance to photobleaching of reconstituted LHC proteins was maximal in the presence of more than a single type of xanthophyll species, particularly by combinations of lutein and violaxanthin. Consistent with such interpretation would be the higher levels of these two xanthophylls in mutants *Atoep16-1;7* and *Atoep16-1;8* versus wild-type plants. In addition, increased levels of β -carotene were found in mutants *Atoep16-1;7* and *Atoep16-1;8*, when compared with mutants *Atoep16-1;5* and *Atoep16-1;6*, that could contribute to the stabilization of PSII core complexes. Taken together, our HPLC analyses underscore that drastic metabolic changes occur in response to light in etiolated *Arabidopsis* seedlings and that these are differentially affected in the *Atoep16-1;5-8* mutants. Also, similar effects have been observed in the *flu* orthologue, *tig^{d12}*, (see Appendix B), suggesting a common metabolic response of etiolated angiosperm seedlings to singlet oxygen that now can be further dissected by *metabolomics* approaches.

Chapter 5 Conclusion

In summary, the results presented in this work show that AtOEP16-1 plays an important role in the photoprotection mechanism of etiolated *Arabidopsis* plants. For the moment, we cannot exclude that second site mutations present in *Atoep16-1* mutants could also prevent greening. On the other hand, complementation studies suggest that the absence of AtOEP16-1 results in a conditional cell death phenotype which is linked to the absence of functional PORA protein. PORA is normally part of larger complexes dubbed LHPP in the prolamellar bodies of etioplasts. These complexes are involved in light trapping and light energy dissipation. If these processes are disturbed, as found in mutants *Atoep16-1* described by Pollmann (2007), *Atoep16-1;5* and *Atoep16-1;6*, seedling bleaching and cell death occur. Despite the fact that some default import pathways are activated in mutant *Atoep16-1;6*, probably no functional LHPP complexes can be formed. It could be that suppressor mutations are present in mutants *Atoep16-1;7* and *Atoep16-1;8* that prevented photooxidative damage. While mutant *Atoep16-1;7* accumulates drastically reduced levels of Pchl_a and presumably greens by an entirely PORB-dependent pathway and without PORA, mutant *Atoep16-1;8* is seemingly unaffected in the import and assembly process of pPORA. In this mutant, normal levels of PORA and photoactive Pchl_a-F655 are present, permitting normal greening. However, the targeting pathway of pPORA did not involve the PTC complex and led to the default import of pPORA through a third, as yet, uncharacterized, Pchl_a-independent pathway. It is attractive to hypothesize that the suppressor mutation(s) presumably present in *Atoep16-1;8* affected the targeting pathway of pPORA to the different import pathways. Post-import pigment binding by an as-yet undetermined mechanism, then would be needed to allow for the formation of LHPP or LHPP-like structures permitting normal seedling greening. Nevertheless, not the entirely normal greening process is suggested by our HPLC profiling experiments which unveiled altered compositions and levels of carotenoids in mutant *Atoep16-1;8*. On the other hand, more detailed gene expression and polysome profiling studies revealed that cell death regulation in *Atoep16-1;6* is not identical to that observed in *flu* plants. Mutant *Atoep16-1;6* appears to be defective in translating total proteins in the early hours of the singlet oxygen response. Nevertheless, mutants *Atoep16-1;6* and *flu* share the same late, singlet oxygen-dependent depression of translation which leads to ribosome decay. These two responses can now be dissected by other tools, such as *transcriptomics*, *proteomics* and *metabolomics* approaches.

Chapter 6 Version abrégée en français

« Implications de la protéine OEP16 dans la photoprotéction d'*Arabidopsis thaliana* lors du stress lumineux »

6.1 Introduction

Les plantes sont exposées en permanence à une large variété de facteurs de stress dans leur environnement naturel. De manière remarquable, ces stress abiotiques (déficit hydrique, chaleur, fortes intensités de lumière, UV) et biotiques (pathogènes : bactériens et fongiques ; insectes) causent de profonds changements dans l'expression des gènes du plaste et du noyau. Ils provoquent de plus une chlorose qui implique des perturbations de l'appareil photosynthétique ainsi que du métabolisme de la chlorophylle. Au cours de la germination des Angiospermes, les plantules étiolées sont particulièrement sensibles à un excès d'énergie lumineuse. C'est en effet le moment où elles ont besoin de basculer d'un métabolisme hétérotrophe, en l'absence de chlorophylle, à une croissance phototrophe.

Lorsque les plantes germent à l'obscurité ou dans la pénombre, leurs plastes doivent faire face au double défi de récolter le peu de lumière disponible et de se préparer à une exposition brutale à une lumière intense. Les proplastides se différencient alors en étioplastes avant de devenir, à la lumière, des chloroplastes. La première étape vers la différenciation en chloroplastes est dépendante de la lumière et d'une enzyme : la NADPH protochlorophyllide oxydoréductase (POR). Des travaux antérieurs de Reinbothe *et al.* (1995) ont montré qu'il existe deux isoformes de la POR, appelées PORA et PORB. Elles sont associées sous forme d'un supra-complexe avec le NADPH, leurs pigments – protochlorophyllide *a* (Pchl *a*) et Pchl *b* (les précurseurs des chlorophylles *a* et *b*, respectivement) – et avec des lipides du corps prolamellaire. L'organisation de ce supra-complexe permet aux jeunes plantes de collecter l'énergie lumineuse et, en même temps, d'éponger l'excès d'énergie. Ce nouveau complexe collecteur de lumière est appelé LHPP pour Light Harvesting POR Protochlorophyllide (Reinbothe *et al.*, 1999). L'analyse approfondie de la structure du LHPP, ainsi que de son rôle pendant la skotomorphogenèse (développement à l'obscurité) ou lors de la transition vers la photomorphogenèse (développement à la lumière), sont en cours d'étude, à l'aide d'approches biochimiques et génétiques.

Les protéines PORA et PORB sont codées par des gènes nucléaires et traduites dans le cytosol avant d'être importées dans les plastes afin de s'y assembler en oligomères. Récemment, il a été mis en évidence un système original d'importation de PORA au sein du chloroplaste : le PTC (Protochlorophyllide dependant Translocon Complex ; Reinbothe *et al.*, 2004a, 2004b). Ce système, qui traverse à la fois les membranes externe et interne de l'enveloppe du plaste, est dépendant de la présence de Pchl *b*, substrat de PORA. Plusieurs approches biochimiques conjointes ont permis d'identifier les protéines majeures du complexe PTC. Certaines sont spécifiques de ce translocon, en particulier PTC52, qui présente une activité Pchl *a* oxygénase *in vitro*, et PTC16/OEP16, une protéine de 16 kDa qui forme un canal hydrophile dans la membrane externe du plaste. Cette dernière a fait l'objet de ce travail de thèse et les résultats obtenus seront résumés dans cette partie.

6.2 Le fond génétique complexe du mutant *Atoep16-1* (chapitre 3.1)

6.2.1 Identification du mutant *Atoep16-1* chez *A.thaliana* (chapitre 3.1.1.)

La protéine OEP16 appartient à une famille de transporteurs d'acides aminés présente chez les bactéries libres et chez leurs descendants endosymbiotiques, mitochondriaux et chloroplastiques (Rassow *et al.*, 1999). Il a été démontré que l'OEP16 des chloroplastes de petit pois forme un canal hydrophile dans la membrane externe permettant le transport des acides aminés (Pohlmeyer *et al.*, 1997 ; Steinkamp *et al.*, 2000). La protéine PTC16 de 16 kDa de l'orge a, par la suite, été mise en évidence dans l'enveloppe externe du plaste par pontage chimique. Celle-ci interagit avec le précurseur de PORA (pPORA) au cours de son import post-traductionnel (Reinbothe *et al.*, 2004 a+b). La purification de la protéine et le séquençage des peptides dérivés ont permis de montrer que cette protéine d'orge est l'orthologue d'OEP16 chez *Arabidopsis* (Reinbothe *et al.*, 2004 a+b). Ces résultats élargissent donc la fonction proposée pour OEP16 à la translocation de macromolécules spécifiques.

Chez *Arabidopsis*, on distingue 4 gènes qui codent OEP16 : *AtOEP16-1* à *AtOEP16-4* (Reinbothe *et al.*, 2004; Philippar *et al.*, 2007). Des quatre OEP16, *AtOEP16-1* (At2g28900) présente la meilleure identité (52%) avec la séquence de la protéine OEP16 de l'orge (*HvOep16-1*). *AtOEP16-1* contient 6 exons et 5 introns. Une approche de génétique inverse a été utilisée pour isoler *Atoep16-1* (At2g28900), mutant dépourvu de protéine OEP16-1.

Nous avons mis en évidence que le mutant KO *Atoep16-1* montre un phénotype léthal conditionnel lors de la germination en condition d'étiollement (Pollmann *et al.*, 2007), qui ressemble au phénotype d'un autre mutant: *fluorescent (flu)* (Meskauskiene *et al.*, 2001). L'observation au microscope à épifluorescence des cotylédons de plantules étiolées a révélé une hyper accumulation de Pchl_a dans *Atoep16-1* par rapport au sauvage. Les plantes *Atoep16-1* cultivées à la lumière continuent de se développer normalement et ressemblent au sauvage. Par ailleurs, des plantes *Atoep16-1*, cultivées à l'obscurité pendant 5 jours puis exposées à une lumière forte, blanchissent et meurent. Ce phénomène s'explique par le fait que l'excitation de Pchl_a libre (non liée à la protéine PORA) entraîne la formation d'oxygène singulet, qui déclenche un programme de mort cellulaire (PCD). Outre l'absence de protéine PORA chez le mutant *Atoep16-1*, nous avons démontré par des essais d'import *in vivo*, que les chloroplastes dépourvus d'*AtOEP16-1* sont capable d'importer uniquement transB-GFP (le peptide de transit de la protéine pPORB; transB; fusioné avec la GFP), alors que les chloroplastes sauvages peuvent importer, en plus de transB-GFP, un transgène transA-GFP (le peptide de transit de la protéine pPORA; transA; fusioné avec la protéine Green Fluorescent Protein).

6.2.2 Re-criblage du stock d'origine de mutant *Atoep16-1* de la collection SALK (chapitre 3.1.2)

Contrairement aux résultats obtenus par notre laboratoire (Pollmann *et al.*, 2007), l'étude du mutant *Atoep16-1*, menée par Philippar et collaborateurs (2007), n'a pas révélé de phénotype de photoblanchiment. Les auteurs ont par ailleurs détecté la présence de PORA dans le mutant, suggérant l'existence d'un fond génétique complexe chez ce dernier.

Suite à ces divergences, nous avons re-criblé le stock d'origine du mutant *Atoep16-1* disponible dans la collection de l'Institut SALK. Des analyses de descendance nous ont

permis d'isoler 4 lignées de mutants *Atoep16-1* présentant des combinaisons différentes de phénotypes de photoblanchiment et de présence/absence de protéine PORA. Nous avons nommé ces lignées *Atoep16-1;5*, *Atoep16-1;6*, *Atoep16-1;7* et *Atoep16-1;8*. À l'obscurité, les cotylédons des lignées *Atoep16-1;5* et *Atoep16-1;6* accumulent des quantités élevées de Pchl_{id}e, comme l'indique l'augmentation spécifique de la fluorescence rouge. Au contraire, les mutants *Atoep16-1;7* et *Atoep16-1;8* présentent un niveau de fluorescence de la Pchl_{id}e comparable au sauvage. Quand les plantes étiolées sont exposées à une lumière forte, les mutants *Atoep16-1;5* et *Atoep16-1;6* blanchissent alors que les mutants *Atoep16-1;7* et *Atoep16-1;8* peuvent verdier normalement. Les expériences d'immunoblotting ont montré que les mutants *Atoep16-1;5* et *Atoep16-1;7* sont dépourvus de protéine PORA, alors qu'on détecte cette protéine chez les mutants *Atoep16-1;6* et *Atoep16-1;8*.

Malgré ces différences, les 4 lignées sont dépourvues de protéine AtOEP16 et contiennent une seule insertion de l'ADN-T (ADN de Transfert). Cette dernière est composée de deux ADN-T en position « head-to-tail » introduits dans le locus *AtOEP16-1*. De plus, les analyses de séquençage ont révélé que ni le gène *FLU* ni *PORA* ne sont affectés par des mutations ponctuelles chez les 4 mutants *Atoep16-1;5-8*.

6.3 Caractérisation physiologique des quatre mutants *Atoep16-1;5-8* (chapitre 3.2)

6.3.1 Analyses de fluorescence de la Pchl_{id}e à basse température chez les mutants *Atoep16-1;5-8* (chapitre 3.2.1)

L'augmentation excessive de la fluorescence de la Pchl_{id}e chez les mutants *Atoep16-1;5* et *Atoep16-1;6* suggère la présence de Pchl_{id}e libre, non liée aux protéines POR, qui ne peut pas être convertie en Chl_{id}e, et qui par conséquent devient source de production d'oxygène singulet qui déclenche la mort cellulaire. Nous avons effectué des analyses spectroscopiques à basse température afin d'identifier l'état fonctionnel des pigments *in planta*. Chez le sauvage, deux formes de Pchl_{id}e, chacune possédant un spectre spécifique, peuvent être détectées. Il s'agit de la Pchl_{id}e-F655, aussi appelée forme photo-active, et la Pchl_{id}e-F631, une forme photo-inactive (Lebedev and Timko, 1998). La Pchl_{id}e-F655 peut

être converti en Chlide en 1 msec de flash de lumière blanche. Sa présence indique la formation de complexes LHPP au sein des corps prolamellaires des étiooplastes (Reinbothe *et al.*, 1999 and 2003). La Pchlide-F631 comprend les molécules de Pchlide libre et celles contenues dans les complexes PORA-Pchlide *b* (Reinbothe *et al.*, 1999 and 2003).

Les analyses de fluorescence à basse température ont révélé que les mutants *Atoep16-1;5-8* ont un ratio Pchlide-F655 / Pchlide-F631 différent du type sauvage. Nous avons détecté une quantité largement supérieure de Pchlide-F631 chez le mutant *Atoep16-1;5* par rapport au sauvage, alors que la Pchlide-F655 n'a pas été détectée chez ce mutant. En comparant les spectres des mutants *Atoep16-1;6* étiolés avec ceux du sauvage, nous avons observé des quantités élevées de Pchlide-F631 et des niveaux réduits de Pchlide-F655 chez le mutant. Chez le mutant *Atoep16-1;7*, nous n'avons détecté que des traces de la Pchlide-F631. Contrairement aux spectres de la Pchlide détectés chez les mutants *Atoep16-1;5-7*, ceux du mutant *Atoep16-1;8* sont similaires au sauvage avec les deux formes de Pchlide (photo-active et photo-inactive).

L'ensemble de ces résultats suggèrent que la lignée nommée *Atoep16-1;5* dans la présente étude correspond à la lignée *Atoep16-1* initialement identifiée par Pollmann *et al.* (2007), et que la lignée nommée *Atoep16-1;8* correspond à celle décrite par Philippar et collaborateurs (2007).

6.3.2 Viabilité des plantules *Atoep16-1;5-8* (chapitre 3.2.2.2)

La viabilité des mutants *Atoep16-1;5-8* a été mise en évidence par coloration au tétrazolium (TTC) des plantules développées à l'obscurité pendant 5j et ensuite exposées à une lumière forte pendant 30 min, 2h et 4h. Cette coloration permet de distinguer les plantules viables qui sont colorés en rouge et les plantules ayant des cellules mortes qui ne se colorent pas.

Après plusieurs tests, effectués sur une centaine de plantules de type sauvage et de chaque lignée mutante (expérience réalisée en triplicat), nous avons démontré que le mutant *Atoep16-1;5* possède un phénotype de photoblanchiment plus sévère que le mutant *Atoep16-1;6*. La mort cellulaire chez le mutant *Atoep16-1;5* se manifeste le plus rapidement (après 4h d'illumination, seulement 35% des plantules étiochées restent viables, alors que 60% de plantules viables sont retrouvées chez le mutant *Atoep16-1;6*). Cependant, les plantules les plus résistantes au stress lumineux sont celles des lignées non-

photoblanchissantes : *Atoep16-1;7* et *Atoep16-1;8*, chez lesquelles la viabilité est respectivement de 95% et de 86%, après 4h de stress lumineux.

6.3.3 La production d'oxygène singulet chez les plantules *Atoep16-1;5-8* (chapitre 3.2.3)

Les observations de plantules étiolées âgées de 5j au microscope, sous lumière bleue, ont montré une forte fluorescence rouge de la Pchl_a chez les mutants *Atoep16-1;5* et *Atoep16-1;6*, suggérant la présence de molécules libres de Pchl_a, non liées aux protéines POR. Puisque l'illumination des tétrapyrroles libres entraîne la formation d'oxygène singulet (Wagner *et al.*, 2004), nous avons mesuré la production de cette espèce réactive de l'oxygène chez les mutants *Atoep16-1;5-8* par des mesures de fluorescence DanePy (Hideg *et al.*, 1998). Les mutants *Atoep16-1;5* et *Atoep16-1;6* produisent des quantités importantes d'oxygène singulet, ce qui se manifeste par une réduction de la fluorescence DanePy par rapport au sauvage. Cette réduction de la fluorescence chez le mutant *Atoep16-1;5* est comparable avec celle retrouvée chez le mutant *flu*. Chez le sauvage et les mutants *Atoep16-1;7* ou *Atoep16-1;8*, aucune réduction de la fluorescence DanePy n'est détectable, ce qui indique l'absence de la formation d'oxygène singulet.

6.3.4 L'import des protéines dans les chloroplastes des mutants *Atoep16-1;5-8* (chapitre 3.2.4)

Dans ce chapitre, nous avons mis en évidence par des études d'import *in vitro* et *in vivo*, que les mutants *Atoep16-1;5-8* sont affectés dans l'import de la protéine PORA via le complexe PTC. Les mutants *Atoep16-1;5* et *Atoep16-1;7*, chez lesquels nous ne détectons pas de protéine PORA, ne sont pas capables d'importer la protéine PORA dans les plastes. Dans les essais de « crosslinking » avec le transA-DHFR, nous avons mis en évidence qu'aucun produit n'est formé chez ces mutants. Dans les études d'import *in vivo* avec transA-GFP nous avons observé que la fluorescence de la GFP est largement restreinte au cytosol et seulement des traces de transA-GFP sont détectables à l'intérieur des plastes. En revanche, les mutants *Atoep16-1;6* et *Atoep16-1;8* qui expriment la protéine PORA, importent la protéine transA-DHFR à l'intérieur des plastes. Néanmoins, ce transport ne se déroule pas via le complexe PTC, préalablement décrit et retrouvé chez le sauvage

(Reinbothe *et al.*, 2004), mais via une protéine de 75 kDa, faisant partie du complexe TOC. Les études d'import *in vitro* ont confirmé l'import de transA-GFP dans les plastes. Ensemble de ces études démontre pourquoi la protéine PORA n'est pas retrouvée chez les mutants *Atoep16-1;5* et *Atoep16-1;7*.

6.3.5 La mutation *Atoep16-1* est-elle responsable du phénotype de photoblanchiment (chapitre 3.2.5) ?

Parmi les quatre lignées *Atoep16-1*, nous avons identifié deux familles qui répondent différemment au stress lumineux. Une famille comprend les mutants *Atoep16-1;5* et *Atoep16-1;6* qui montrent un phénotype létal conditionnel, et l'autre famille comprend *Atoep16-1;7* et *Atoep16-1;8* qui verdissent normalement. Ces observations nous amènent à la question suivante : « la mutation du gène *AtOEP16-1* est-elle effectivement la cause du photoblanchiment ? ». Afin d'y répondre, nous avons entrepris un test de complémentation du mutant *Atoep16-1*.

L'étude du mutant *Atoep16-1;6* possédant un transgène 35S-OEP16 a démontré que les plantes complémentées peuvent devenir résistantes à l'effet néfaste de la lumière forte et ressemblent au sauvage. Ce résultat confirme que l'absence de la protéine AtOEP16-1 est la cause du photoblanchiment en conditions de stress lumineux. De plus, des fusions traductionnelles entre les protéines GFP et YFP et les extrémités N-terminales ou C-terminales d'AtOEP16-1, respectivement, ont été introduites dans les plantes mutantes *Atoep16-1;6*. L'observation, au microscope confocal, des cellules des plantes transformées avec le transgène GFP-AtOEP16-1 a révélé une localisation plastidiale d'AtOEP16-1 et une restauration du verdissement normal. En revanche, nous n'avons trouvé aucune restauration du phénotype de photoblanchiment chez le mutant *Atoep16-1;6* transformé avec la fusion AtOEP16-1-YFP. L'observation au microscope confocal a révélé une fluorescence au niveau de l'enveloppe des chloroplastes suggérant que le transgène AtOEP16-1-YFP ne peut pas être importé à l'intérieur des plastes.

6.4 Identification de la traduction en tant que cible de l'action de l'oxygène singulet chez les mutants *Atoep16-1;5-8*, *flu* and *tig^{d12}* (chapitre 3.3)

Suite à la complexité inattendue du fond génétique des mutants SALK *Atoep16-1*, nous avons effectué des études pour identifier les relais conduisant au phénomène de mort cellulaire programmée, provoquée par le stress lumineux. Les modifications de la traduction dans ce type de stress ont fait l'objet d'une attention particulière.

Les comparaisons des produits messagers traduits *in vitro* après 2h de stress lumineux sur les mutants *Atoep16-1;5-8* étiolés pendant 5j, n'ont révélé aucune différence majeure entre les lignées. Contrairement aux observations reportées pour le mutant *flu*, la régulation de l'expression des gènes lors du stress lumineux est probablement effectuée au niveau post-traductionnel et non au niveau transcriptionnel, comme cela était trouvé pour le mutant *flu*.

Des radiomarquages des protéines *in vivo* ont été effectués pour les différentes lignées d'*Atoep16-1* étiolées pendant 5j et exposées à la lumière durant périodes de longueurs différentes. Ces analyses ont révélé que les profils de polypeptides, synthétisés lors des premières 4h de stress lumineux, sont similaires pour les quatre mutants *Atoep16-1;5-8*. Au contraire, quand le stress lumineux est prolongé jusqu'à 24h, nous avons observé un arrêt total de la synthèse des protéines chez les mutants photoblanchissants *Atoep16-1;5* et *Atoep16-1;6*; alors que la synthèse protéique se déroule normalement chez les mutants verdissants *Atoep16-1;7* et *Atoep16-1;8*. Ainsi, nous n'avons pas détecté de synthèse des protéines photosynthétiques lors du stress lumineux chez les mutants *Atoep16-1;5* et *Atoep16-1;6* (ayant un phénotype conditionnel létal), contrairement à ce que l'on pourrait attendre si la régulation de la mort cellulaire se déroule de la même manière que chez le mutant *flu*.

Puisque le phénotype du mutant *Atoep16-1;6* ressemble à celui du mutant *flu* en ce qui concerne la présence de la protéine PORA, nous avons comparé la synthèse des protéines chez ces deux mutants, soumis à un stress lumineux similaire à celui décrit par op den Camp *et al.* (2004). Des analyses de profils de polysomes et des protéines associées ont été effectuées chez des plantes *Atoep16-1;6*, *flu* ou sauvages préalablement cultivées pendant 14j sous lumière continue, transférées à l'obscurité pendant 8h, puis ré-illuminées pendant

4h ou 24h. Nos expériences ont confirmé que la synthèse des protéines de stress, accompagnée d'une réduction de la synthèse générale des protéines, se déroule pendant les premières heures du stress lumineux chez le mutant *flu*. Contrairement à ce dernier, le mutant *Atoep16-1;6* ne synthétise pas de protéines de stress au cours des 4h de ré-illumination, et son profil protéique est similaire à celui du sauvage. Cependant, après 24h de ré-illumination, nous avons détecté une réduction significative de la synthèse protéique chez les deux mutants *flu* et *Atoep16-1;6*. Ces résultats suggèrent que *flu* et *Atoep16-1;6* reprogramment différemment la traduction seulement pendant les premières heures du stress lumineux.

Afin de comprendre plus en détails les mécanismes du contrôle traductionnel pendant le stress lumineux, nous avons étudié le mutant *tigrina*^{*d12*} (*tig*^{*d12*}) de l'orge (von Wettstein *et al.*, 1974) duquel le gène muté est orthologue de *flu* chez *Arabidopsis* (Lee *et al.*, 2003). L'utilisation de l'orge représente des avantages en biochimie par rapport à *Arabidopsis* en raison de la quantité plus importante de biomasse. De plus, le séquençage de son génome est en cours et beaucoup de mutants déjà disponibles pourront permettre l'identification de nouvelles fonctions, liées à l'action des espèces réactives de l'oxygène et au contrôle de la mort cellulaire.

Des radiomarquages de protéines *in vivo* effectués chez des plantes *tig*^{*d12*} d'abord étioilées puis illuminées, ainsi que des analyses par électrophorèse 2D, nous ont permis de découvrir que les régulations de la traduction des protéines de stress et de celles impliquées dans la photosynthèse sont inverses. Les analyses d'immunoblotting nous ont permis d'identifier les protéines spécifiques impliquées dans ces régulations. Parmi les protéines photosynthétiques dont la synthèse est diminuée lors du stress lumineux se trouvent les protéines du photosystème II (PSII) : D1, D2, Rubisco, LHCII, PsbO, PsbE. En revanche, les protéines de stress dont la synthèse est augmentée lors du stress lumineux sont JIP23 ou AOS. Elles sont impliquées dans la biosynthèse de l'acide jasmonique ou dans les réponses de défense pendant l'infection par des pathogènes, respectivement. Des expériences de traduction *in vitro* nous ont permis d'identifier les ARN messagers de *LHCII* comme cible de régulation au niveau transcriptionnel, la Rubisco étant régulée majoritairement au niveau post-traductionnel. L'analyse de fractions polysomales et de leurs transcrits associés dans les mutants *tig*^{*d12*} étioilés et illuminés pendant des périodes de durées variables, a clairement démontré que l'initiation de la traduction fait également l'objet de ce type de régulation.

6.5 Conclusions générales

Nos résultats montrent que la protéine *AtOEP16-1* joue un rôle important dans les mécanismes de photoprotection de plantes d'*Arabidopsis* développées à l'obscurité. Son absence conduit à la sensibilité de ces plantes au stress lumineux et provoque un phénotype conditionnel léthal que nous attribuons à l'absence de la protéine PORA fonctionnelle dans les complexes LHPP. PORA fait partie des complexes LHPP qui coopèrent au sein des corps prolamellaires des étiooplastes. Ces complexes sont impliqués dans la capture de la lumière ainsi que dans la dissipation de l'excès de l'énergie lumineuse. Si ces complexes sont perturbés, comme c'est le cas dans les mutants *Atoep16-1* (initialement décrit par Pollmann *et al* (2007)), *Atoep16-1;5* et *Atoep16-1;6*, les plantules blanchissent, ce qui conduit à la mort cellulaire. Malgré l'existence d'une voie alternative pour l'import de PORA trouvé chez *Atoep16-1;6*, les complexes fonctionnels LHPP ne peuvent pas être formés. Nos données suggèrent qu'il existe des mutations supplémentaires qui empêchent la révélation de ce phénotype et de la mort cellulaire chez les mutants *Atoep16-1;7* et *Atoep16-1;8*. Le mutant *Atoep16-1;7* présente une faible accumulation de Pchl_a à l'obscurité et verdit probablement grâce à la présence de la protéine PORB. Par ailleurs, le mutant *Atoep16-1;8* est affecté dans l'import de pPORA via le complexe PTC, mais contient toutefois la protéine PORA ainsi que de la Pchl_a photo-active F-655. Nous supposons qu'une autre mutation suppressive existe chez ce mutant, affectant la voie d'import de pPORA via le complexe PTC. L'import de pPORA se produirait de manière alternative, par le biais d'une, troisième voie, indépendante de la Pchl_a. Cette nouvelle voie d'import permettrait, dans ce mutant, l'assemblage des complexes LHPP qui permettent le verdissement. Nos études détaillées de *Atoep16-1;6* ont révélé l'existence de mécanismes de régulation de la mort cellulaire différents de ceux identifiés chez le mutant *flu*. Le mutant *Atoep16-1;6* semble être affecté dans la traduction des protéines de stress lors des premières heures de formation de l'oxygène singulet pendant le stress lumineux. Cependant, les mutants *Atoep16-1;6* et *flu* présentent les mêmes effets d'arrêt de la traduction pendant le stress de long terme. L'étude de ces deux types de réponses, par des approches combinées de transcriptomique, protéomique et métabolomique, fournira un éclairage nouveau sur la régulation de la mort cellulaire chez les plantes.

REFERENCES

- Akita, M., Nielsen, E. and Keegstra, K.**, 1997. Identification of Protein Transport Complexes in the Chloroplastic Envelope Membranes via Chemical Cross-Linking. *J. Cell Biol.*, 136(5): 983-994.
- Alawady, A. and Grimm, B.**, 2005. Tobacco Mg protoporphyrin IX methyltransferase is involved in inverse activation of Mg porphyrin and protoheme synthesis. *The Plant journal : for cell and molecular biology*, 41(2): 282-90.
- Aldridge, C., Maple, J. and Møller, S.G.**, 2005. The molecular biology of plastid division in higher plants. *Journal of Experimental Botany*, 56(414): 1061-77.
- Apel, K.**, 1981. The protochlorophyllide holochrome of barley (*Hordeum vulgare* L.): phytochrome-induced decrease of translatable mRNA coding for the NADPH:protochlorophyllide oxidoreductase. *Eur. J. Biochem.*, 120: 89-93.
- Apel, K., Santel, H.J., Redlinger, T.E. and Falk, H.**, 1980. The protochlorophyllide holochrome of barley. Isolation and characterization of the NADPH:protochlorophyllide oxidoreductase. *Eur J Biochem*, 111: 251-258.
- Armstrong, G.A.**, 1998. Greening in the dark: light-independent chlorophyll biosynthesis from anoxygenic photosynthetic bacteria to gymnosperms. *J. Photochem. Photobiol. B: Biol.*, 43: 87-100.
- Armstrong, G.A., S., R., Frick, G., Sperling, U. and Apel, K.**, 1995. Identification of NADPH: protochlorophyllide oxidoreductases A and B: a branched pathway for light-dependent chlorophyll biosynthesis in *Arabidopsis thaliana*. *Plant Physiol.*, 108: 1505-1517.
- Balbi, V. and Devoto, A.**, 2008. Jasmonate signalling network in *Arabidopsis thaliana*: crucial regulatory nodes and new physiological scenarios. *The New Phytologist*, 177(2): 301-18.
- Baldi, P., Grossi, M., Pecchioni, N., Valè, G. and Cattivelli, L.**, 1999. High expression level of a gene coding for a chloroplastic amino acid selective channel protein is correlated to cold acclimation in cereals. *Plant Molecular Biology*, 41(2): 233-43.

- Baldwin, A., Wardle, A., Patel, R., Dudley, P., Park, S., Twell, D., Inoue, K. and Jarvis, P., 2005.** A molecular-genetic study of the Arabidopsis Toc75 gene family. *Plant Physiology*, 138(2): 715-33.
- Bartsch, S., Monnet, J., Selbach, K., Quigley, F., Gray, J., von Wettstein, D., Reinbothe, S. and Reinbothe, C., 2008.** Three thioredoxin targets in the inner envelope membrane of chloroplasts function in protein import and chlorophyll metabolism. *Proceedings of the National Academy of Science of the United States of America*, 105(12): 4933-8.
- Baskin, C.C. and Baskin, J.M., 1998.** *Seeds: ecology, biogeography, and evolution of dormancy and germination.* Academic Press, San Diego, CA, US. .
- Bauer, J., Chen, K., Hiltbunner, A., Wehrli, E., Eugster, M., Schnell, D. and Kessler, F., 2000.** The major protein import receptor of plastids is essential for chloroplast biogenesis. *Nature*, 403(6766): 203-207.
- Bauer, J., Hiltbrunner, A. and Kessler, F., 2001.** Molecular biology of chloroplast biogenesis: gene expression, protein import and intraorganellar sorting. *Cell. Mol. Life Sci.*. 58: 420–433.
- Baumgartner, B., Rapp, J. and Mullet, J., 1989.** Plastid Transcription Activity and DNA Copy Number Increase Early in Barley Chloroplast Development. *Plant Physiology*, 89(3): 1011-1018.
- Beale, S., 1990.** Biosynthesis of the Tetrapyrrole Pigment Precursor, delta-Aminolevulinic Acid, from Glutamate. *Plant Physiology*, 93(4): 1273-1279.
- Beale, S. and Weinstein, J., 1990.** Tetrapyrrole metabolism in photosynthetic organisms. HA Dailey, ed, *Biosynthesis of Heme and Chlorophylls.* McGraw-Hill, New York: 287-391.
- Bedard, J. and Jarvis, P., 2005.** Recognition and envelope translocation of chloroplast preproteins. *J. Exp. Bot.*, 56(419): 2287-2320.
- Bhattacharya, D., Yoon, H.S. and Hackett, J.D., 2004.** Photosynthetic eukaryotes unite: endosymbiosis connects the dots. *BioEssays*, 26: 50-60.

Birnboim, H. and Doly, J., 1979. A rapid alkaline extraction procedure for screening recombinant plasmid DNA. *Nucleic Acids Res.*, 7(6): 1513-1523.

Bisanz-Seyer, C., Li, Y.-F., Seyer, P. and Mache, R., 1989. The components of the plastid ribosome are not accumulated synchronously during early development of pinach plants. *Plant Molecular Biology* 12: 201-211.

Bohlmann, H., Clausen, S., Behnke, S., Giese, H., Hiller, C., Reimann-Philipp, U., Schrader, G., Barkholt, V. and Apel, K., 1988. Leaf-specific thionins of barley - a novel class of cell wall proteins toxic to plant-pathogenic fungi and possible involvement in the defence mechanism of plants. *EMBO J.*, 7: 1559-1565.

Bölter, B., May, T. and Soll, J., 1998. A protein import receptor in pea chloroplasts, Toc86, is only a proteolytic fragment of a larger polypeptide. *FEBS Lett.*, 441: 59–62.

Bréhélin, C., Kessler, F. and van Wijk, K.J., 2007. Plastoglobules: versatile lipoprotein particles in plastids. *Trends in Plant Science*, 12(6): 260-266.

Caliebe, A., Grimm, R., Kaiser, G., Lübeck, J., Soll, J. and Heins, L., 1997. The chloroplastic protein import machinery contains a Rieske-type iron-sulfur cluster and a mononuclear iron-binding protein. *EMBO J.*, 16: 7342-7350.

Cavalier-Smith, T., 2000. Membrane heredity and early chloroplast evolution. *Trends in Plant Science*, 5: 174-182.

Cavalier-Smith, T., 2006. Cell evolution and earth history: stasis and revolution. *Phil. Trans. Roy. Soc. Lond. B.*, 361: 969-1006.

Chen, K., Chen, X. and Schnell, D.J., 2000. Initial binding of preproteins involving the Toc159 receptor can be bypassed during protein import into chloroplasts. *Plant Physiol.*, 122: 813–822.

Chen, K., Chen, X. and Schnell, D.J., 2000. Initial binding of preproteins involving the Toc159 receptor can be bypassed during protein import into chloroplasts. *Plant Physiol.*, 122: 813–822.

- Chou, M.-L., Fitzpatrick, L.M., Tu, S.-L., Budziszewski, G., Potter-Lewis, S., Akita, M., Levin, J.Z., Keegstra, K. and Li, H-M.,** 2003. Tic40, a membrane-anchored co-chaperone homolog in the chloroplast protein translocon. *The EMBO Journal*, 22: 2970–2980.
- Cline, K., Werner-Washburne, M., Andrews, J. and Keegstra, K.,** 1984. Thermolysin Is a Suitable Protease for Probing the Surface of Intact Pea Chloroplasts. *Plant Physiol.*, 75(3): 675-678.
- Clough, S. and Bent, A.,** 1998. Floral dip: a simplified method for *Agrobacterium*-mediated transformation of *Arabidopsis thaliana*. *The Plant Journal* 16(6): 735-43.
- Constan, D., Froehlich, J.E., Rangarajan, S. and Keegstra, K.,** 2004. A Stromal Hsp100 Protein Is Required for Normal Chloroplast Development and Function in *Arabidopsis*. *Plant Physiol.*, 136(3): 3605-3615.
- Croce, R., Weiss, S. and Bassi, R.,** 1999. Carotenoid-binding sites of the major light-harvesting complex II of higher plants. *J Biol Chem*, 274: 29613 - 29623.
- Dall'Osto, L., Cazzaniga, S., North, H., Marion-Poll, A. and Bassi, R.,** 2007. The *Arabidopsis aba4-1* Mutant Reveals a Specific Function for Neoxanthin in Protection against Photooxidative Stress. *Plant Cell*, 19(3): 1048-1064.
- Dall'Osto, L., Lico, C., Alric, J., Giuliano, G., Havaux, M. and Bassi, R.,** 2006. Lutein is needed for efficient chlorophyll triplet quenching in the major LHCII antenna complex of higher plants and effective photoprotection in vivo under strong light. *BMC Plant Biology*, 6(1): 32.
- Danon, A., Miersch, O., Felix, G., op den Camp, R. and Apel, K.,** 2005. Concurrent activation of cell death-regulating signalling pathways by singlet oxygen in *Arabidopsis thaliana*. *Plant J.*, 41: 68-80.
- Dehesh, K. and Ryberg, M.,** 1985. The NADPH-protochlorophyllide oxidoreductase is the major protein constituent of prolamellar bodies in wheat (*Triticum aestivum* L.). *Planta*, 164(3): 396-399.

Delwiche, C.F., 1999. Tracing the Thread of Plastid Diversity through the Tapestry of Life. *American Naturalist*, 154(4): 164-177.

Deschamps, P., Colleoni, C., Nakamura, Y., Suzuki, E., Putaux, J.-L., Buleon, A., Haebel, S., Ritte, G., Steup, M., Falcon, L.I., Moreira, D., Loffelhardt, W., Raj, J.N., Plancke, C., d'Hulst, C., Dauvillee, D. and Ball, S., 2008. Metabolic Symbiosis and the Birth of the Plant Kingdom. *Mol Biol Evol*, 25(3): 536-548.

Drea, S., Lao, N., Wolfe, K. and Kavanagh, T., 2006. Gene duplication, exon gain and neofunctionalization of OEP16-related genes in land plants. *The Plant Journal*, 46(5): 723-735.

Dreyfuss, B.W. and Thornber, J.P., 1994. Assembly of the light-harvesting complexes (LHCs) of photosystem II. Monomeric LHCIIb complexes are intermediates in the formation of oligomeric LHC IIb complexes. *Plant Physiol.*, 106: 829-839.

Dufner, A. and Thomas, G., 1999. Ribosomal S6 kinase signalling and the control of translation. *Exp. Cell Res.*, 253: 100-109.

Dyall, S.D., Brown, M.T. and Johnson, P.J., 2004. Ancient invasions: from endosymbionts to organelles. *Science*, 304(5668): 253-7.

Eckhardt, U., Grimm, B. and Hörtensteiner, S., 2004. Recent advances in chlorophyll biosynthesis and breakdown in higher plants. *Plant Molecular Biology*, 56(1): 1-14.

Ehrenshaft, M., Chung, K.-R., Jenns, A.E. and Daub, M.E., 1999. Functional characterization of SOR1, a gene required for resistance to photosensitizing toxins in the fungus *Cercospora nicotianae*. *Current Genetics*, 34(6): 478-485.

Esen, A., 1978. A simple method for quantitative, semiquantitative, and qualitative assay of protein. *Analytical Biochemistry*, 89(1): 264-73.

Frick, G., Su, Q., Apel, K. and Armstrong, G.A., 2003. An *Arabidopsis* *porB porC* double mutant lacking light-dependent NADPH:protochlorophyllide oxidoreductases B and C is highly chlorophyll-deficient and developmentally arrested. *Plant J.*, 25: 141-153.

- Goslings, D., Meskauskiene, R., Kim, C., Lee, K.P., Nater, M. and Apel, K., 2004.** Concurrent interactions of heme and FLU with Glu tRNA reductase (HEMA1), the target of metabolic feedback inhibition of tetrapyrrole biosynthesis, in dark- and light-grown Arabidopsis plants. *The Plant Journal*, 40(6): 957-967.
- Granick, S., 1950.** The structural and functional relationships between heme and chlorophyll. *Harvey Lect.*, 44: 220-245.
- Gray, J., Wardzala, E., Yang, M., Reinbothe, S., Haller, S. and Pauli, F., 2004.** A small family of LLS1-related non-heme oxygenases in plants with an origin amongst oxygenic photosynthesizers. *Plant Molecular Biology*, 54(1): 39-54.
- Gutensohn, M., Schulz, B., Nicolay, P. and Flugge, U.-I., 2000.** Functional analysis of the two Arabidopsis homologues of Toc34, a component of the chloroplast protein import apparatus. *Plant J.*, 23(6): 771-783.
- Hardtke, C. and Deng, X., 2000.** The cell biology of the COP/DET/FUS proteins. Regulating proteolysis in photomorphogenesis and beyond? *Plant Physiology*, 124(4): 1548-57.
- Havaux, M., 2003.** Spontaneous and thermoinduced photon emission: new methods to detect and quantify oxidative stress in plants. *Trends in Plant Science*, 8: 409 - 413.
- Heins, L., Collison, I. and Soll, J., 1998.** The protein translocation apparatus of chloroplast envelopes. *Trends Plant Sci.*, 3: 56-61.
- Hideg, E., Kálai, T., Hideg, K. and Vass, I., 1998.** Photoinhibition of photosynthesis in vivo results in singlet oxygen production detection via nitroxide-induced fluorescence quenching in broad bean leaves. *Biochemistry*, 37(33): 11405-11.
- Hiltbrunner, A., Granig, K., Alvarez-Huerta, M., Infanger, S., Bauer, J. and Kessler, F., 2004.** AtToc90, a New GTP-Binding Component of the Arabidopsis Chloroplast Protein Import Machinery. *Plant Molecular Biology*, 54(3): 427-440.
- Hinnah, S.C., Hill, K., Wagner, R., Schlicher, T. and Soll, J., 1997.** Reconstitution of a chloroplast protein import channel. *EMBO J.*, 16(24): 7351-7360.

- Hinnah, S.C., Wagner, R., Sveshnikova, N., Harrer, R. and Soll, J., 2002.** The Chloroplast Protein Import Channel Toc75: Pore Properties and Interaction with Transit Peptides. *Biophysical Journal*, 83(2): 899-911.
- Hirsch, S., Muckel, E., Heemeyer, F., von Heijne, G. and Soll, J., 1994.** A receptor component of the chloroplast protein translocation machinery. *Science*, 266: 1989-1992.
- Hofmann, N.R. and Theg, S.M., 2005.** Chloroplast outer membrane protein targeting and insertion. *Trends in Plant Science*, 10(9): 450-457.
- Holm, M., Ma, L., Qu, L. and Deng, X., 2002.** Two interacting bZIP proteins are direct targets of COP1-mediated control of light-dependent gene expression in Arabidopsis. *Genes and Development*, 16(10): 1247-59.
- Holtorf, H., Reinbothe, S., Reinbothe, C., Berezina, B. and Apel, K., 1995.** Two routes of chlorophyllide synthesis that are differentially regulated by light in barley (*Hordeum vulgare* L.). *Proceedings of the National Academy of Sciences of the United States of America*, 92(8): 3254-3258.
- Huang, L., Bonner, B. and Castelfranco, P., 1989.** Regulation of 5-Aminolevulinic Acid (ALA) Synthesis in Developing Chloroplasts : II. Regulation of ALA-Synthesizing Capacity by Phytochrome. *Plant Physiology*, 90(3): 1003-1008.
- Inaba, T., Alvarez-Huerta, M., Li, M., Bauer, J., Ewers, C., Kessler, F. and Schnell, D.J., 2005.** Arabidopsis Tic110 Is Essential for the Assembly and Function of the Protein Import Machinery of Plastids. *Plant Cell*, 17(5): 1482-1496.
- Inaba, T., Li, M., Alvarez-Huerta, M., Kessler, F. and Schnell, D.J., 2003.** atTic110 Functions as a Scaffold for Coordinating the Stromal Events of Protein Import into Chloroplasts. *J. Biol. Chem.*, 278(40): 38617-38627.
- Ivanova, Y., Smith, M.D., Chen, K. and Schnell, D.J., 2004.** Members of the Toc159 import receptor family represent distinct pathways for protein targeting to plastids. *Molecular Biology of the Cell*, 15(7): 3379–3379.
- Jackson-Constan, D. and Keegstra, K., 2001.** Arabidopsis Genes Encoding Components of the Chloroplastic Protein Import Apparatus. *Plant Physiol.*, 125(4): 1567-1576.

Jarvis, P., Chen, L.-J., Li, H.-m., Peto, C.A., Fankhauser, C. and Chory, J., 1998. An Arabidopsis Mutant Defective in the Plastid General Protein Import Apparatus. *Science*, 282(5386): 100-103.

Jelic, M., Soll, J. and Schleiff, E., 2003. Two Toc34 Homologues with Different Properties. *Biochemistry*, 42(19): 5906-5916.

Jelic, M., Sveshnikova, N., Motzkus, M., Hörth, P., Soll, J. and Schleiff, E., 2002. The Chloroplast Import Receptor Toc34 Functions as Preprotein-Regulated GTPase. *Biological Chemistry*, 383(12): 1875-1883.

Keegstra, K. and Cline, K., 1999. Protein import and routing systems of chloroplasts. *Plant Cell*, 11: 557–570.

Keegstra, K., Olsen, L.J. and Theg, S.M., 1989. Chloroplastic Precursors and their Transport Across the Envelope Membranes. *Annual Review of Plant Physiology and Plant Molecular Biology*, 40(1): 471-501.

Kendrick, M. and Chang, C., 2008. Ethylene signaling: new levels of complexity and regulation. *Current Opinion in Plant Biology*, 11(5): 479-485.

Kendrick, R. and Kronenberg, G., 1994. *Photomorphogenesis in Plants*. Kluwer Academic Publishers: Dordrecht, The Netherlands.

Kessler, F. and Blobel, G., 1996. Interaction of the protein import and folding machineries in the chloroplast. *Proceedings of the National Academy of Sciences of the United States of America*, 93: 7684-7689.

Kessler, F., Blobel, G., Patel, H.A. and Schnell, D.J., 1994. Identification of two GTP-binding proteins in the chloroplast protein import machinery. *Science*, 266: 1035-1039.

Kessler, F. and Schnell, D., 2006. The Function and Diversity of Plastid Protein Import Pathways: A Multilane GTPase Highway into Plastids. *Traffic*, 7(3): 248-257.

Kessler, F. and Vidi, P.-A., 2007. *Plastoglobule Lipid Bodies: their Functions in Chloroplasts and their Potential for Applications*, *Green Gene Technology*, pp. 153-172.

Kim, C. and Apel, K., 2004. Substrate-dependent and organ-specific chloroplast protein import in planta. *The Plant Cell*, 16(1): 88-98.

Kim, C., Ham, H. and Apel, K., 2005. Multiplicity of different cell- and organ-specific import routes for the NADPH-protochlorophyllide oxidoreductases A and B in plastids of *Arabidopsis* seedlings. *The Plant Journal*, 42(3): 329-40.

Kim, C., Meskauskiene, R., Apel, K. and Laloi, C., 2008. No single way to understand singlet oxygen signalling in plants. *EMBO Rep.*, 9: 435-439.

Kleffmann, T., Russenberger, D., von Zychlinski, A., Christopher, W., Sjölander, K., Gruissem, W. and Baginsky, S., 2004. The *Arabidopsis thaliana* Chloroplast Proteome Reveals Pathway Abundance and Novel Protein Functions. *Current Biology*, 14(5): 354-362.

Kouranov, A., Chen, X., Fuks, B. and Schnell, D.J., 1998. Tic20 and Tic22 Are New Components of the Protein Import Apparatus at the Chloroplast Inner Envelope Membrane. *J. Cell Biol.*, 143(4): 991-1002.

Kouranov, A. and Schnell, D., 1997. Analysis of the interactions of preproteins with the import machinery over the course of protein import into chloroplasts. *The Journal of Cell Biology*, 139(7): 1677-85.

Kouranov, A., Wang, H. and Schnell, D.J., 1999. Tic22 Is Targeted to the Intermembrane Space of Chloroplasts by a Novel Pathway. *J. Biol. Chem.*, 274(35): 25181-25186.

Kovacheva, S., Bedard, J., Patel, R., Dudley, P., Twell, D., Rios, G., Koncz, C. and Jarvis, P., 2005. In vivo studies on the roles of Tic110, Tic40 and Hsp93 during chloroplast protein import. *Plant J.*, 41(3): 412-428.

Kozma, S.C. and Thomas, G., 2002. Regulation of cell size in growth, development and human disease: PI3K, PKB and S6K. *BioEssays*, 24(1): 65-71.

Kubis, S., Patel, R., Combe, J., Bedard, J., Kovacheva, S., Lilley, K., Biehl, A., Leister, D., Rios, G., Koncz, C. and Jarvis, P., 2004. Functional Specialization amongst the *Arabidopsis* Toc159 Family of Chloroplast Protein Import Receptors. *Plant Cell*, 16(8): 2059-2077.

- Küchler, M., Decker, S., Hörmann, F., Soll, J. and Heins, L.,** 2002. Protein import into chloroplasts involves redox-regulated proteins. *The EMBO Journal*, 21(22): 6136-45.
- Kühlbrandt, W., Wang, D.N. and Fujiyoshi, Y.,** 1994. Atomic model of plant light harvesting complex by electron crystallography. *Nature*, 367: 614-621.
- Laloi, C., Stachowiak, M., Pers-Kamczyc, E., Warzych, E., Murgia, I. and Apel, K.,** 2007. Cross-talk between singlet oxygen- and hydrogen peroxide-dependent signaling of stress responses in *Arabidopsis thaliana*. *Proceedings of the National Academy of Sciences*, 104(2): 672-677.
- Latham, J.R., Wilson, A.K. and Steinbrecher, R.A.,** 2006. The mutational consequences of plant transformation. *J Biomed Biotechnol*: Article ID 25376, Pages 1–7.
- Lebedev, N. and Timko, M.P.,** 1998. Protochlorophyllide photoreduction. *Photosynthesis Research*, 58(1): 5-23.
- Lebedev, N., van Cleve, B., Armstrong, G. and Apel, K.,** 1995. Chlorophyll Synthesis in a Deetiolated (det340) Mutant of *Arabidopsis* without NADPH-Protochlorophyllide (PChlide) Oxidoreductase (POR) A and Photoactive PChlide-F655. *Plant Cell*, 7(12): 2081-2090.
- Lee, K.P., Kim, C., Lee, D.W. and Apel, K.,** 2003. TIGRINA d, required for regulating the biosynthesis of tetrapyrroles in barley, is an ortholog of the FLU gene of *Arabidopsis thaliana*. *FEBS Letters*, 553(1-2): 119-124.
- Litvin, F., Belyaeva, O. and Ignatov, N.,** 1993. The mechanism of final stages of chlorophyll and pheophytin biosynthesis and problem of photosystem II reaction center biogenesis. *Biofizika*, 38: 919-939.
- Lyndon, R.F. and Robertson, E.S.,** 1976. The quantitative ultrastructure of the pea shoot apex in relation to leaf initiation. *Protoplasma*, 87: 387–402.
- Martin, W. and Herrmann, R.G.,** 1998. Gene Transfer from Organelles to the Nucleus: How Much, What Happens, and Why? *Plant Physiology*, 118: 9–17.
- Martin, W. and Müller, M.,** 1998. The hydrogen hypothesis for the first eukaryote. *Nature*, 392: 37-41.

Martin, W., Rujan, T., Richly, E., Hansen, A., Cornelsen, S., Lins, T., Leister, D., Stoebe, B., Hasegawa, M. and Penny, D., 2002. Evolutionary analysis of Arabidopsis, cyanobacterial, and chloroplast genomes reveals plastid phylogeny and thousands of cyanobacterial genes in the nucleus. *Proceedings of The National Academy of Sciences of The United States of America* 99: 12246-12251.

Martin, W., Stoebe, B., Goremykin, V., Hapsmann, S., Hasegawa, M. and Kowallik, K.V., 1998. Gene transfer to the nucleus and the evolution of chloroplasts. *Nature*, 393(6681): 162-5.

May, T. and Soll, J., 2000. 14-3-3 Proteins Form a Guidance Complex with Chloroplast Precursor Proteins in Plants. *Plant Cell*, 12(1): 53-64.

McCormac, A., Fischer, A., Kumar, A., Soll, D. and Terry, M., 2001. Regulation of HEMA1 expression by phytochrome and a plastid signal during de-etiolation in *Arabidopsis thaliana*. *The Plant Journal* 25: 549-561.

McFadden, G.I. and van Dooren, G.G., 2004. Evolution: red algal genome affirms a common origin of all plastids. *Curr Biol*, 14: 514-516.

Meskauskiene, R. and Apel, K., 2002. Interaction of FLU, a negative regulator of tetrapyrrole biosynthesis, with the glutamyl-tRNA reductase requires the tetratricopeptide repeat domain of FLU. *FEBS Letters*, 532(1-2): 27-30.

Meskauskiene, R. and Apel, K., 2002. Interaction of FLU, a negative regulator of tetrapyrrole biosynthesis, with the glutamyl-tRNA reductase requires the tetratricopeptide repeat domain of FLU. *FEBS Letters*, 532(1-2): 27-30.

Meskauskiene, R., Nater, M., Goslings, D., Kessler, F., op den Camp, R. and Apel, K., 2001. FLU: A negative regulator of chlorophyll biosynthesis in *Arabidopsis thaliana*. *Proceedings of the National Academy of Sciences of the United States of America*, 98(22): 12826-12831.

Miras, S., Salvi, D., Ferro, M., Grunwald, D., Garin, J., Joyard, J. and Rolland, N., 2002. Non canonical transit peptide for import into the chloroplast. *J. Biol. Chem.*: M207477200.

Miras, S., Salvi, D., Piette, L., Seigneurin-Berny, D., Grunwald, D., Reinbothe, C., Joyard, J., Reinbothe, S. and Rolland, N., 2007. Toc159- and Toc75-independent Import of a Transit Sequence-less Precursor into the Inner Envelope of Chloroplasts. *J. Biol. Chem.*, 282(40): 29482-29492.

Møller, S., Ingles, P. and Whitelam, G., 2002. The cell biology of phytochrome signalling. *New Phytologist* 154: 553-590.

Moreira, D., Le Guyader, H. and Philippe, H., 2000. The origin of red algae and the evolution of chloroplasts. *Nature*, 405(6782): 32-3.

Morita, M. and Tasaka, M., 2004. Gravity sensing and signaling. *Current Opinion in Plant Biology*, 7(6): 712-8.

Murcha, M.W., Elhafez, D., Lister, R., Tonti-Filippini, J., Baumgartner, M., Philippar, K., Carrie, C., Mokranjac, D., Soll, J. and Whelan, J., 2007. Characterization of the Preprotein and Amino Acid Transporter Gene Family in Arabidopsis. *Plant Physiol.*, 143(1): 199-212.

Nagy, F. and Schäfer, E., 2002. Phytochromes control photomorphogenesis by differentially regulated, interacting signaling pathways in higher plants. *Annu Rev Plant Biol.*, 53: 329–355.

Ni, M., Tepperman, J. and Quail, P., 1999. Binding of phytochrome B to its nuclear signalling partner PIF3 is reversibly induced by light. *Nature*, 400(6746): 781-4.

Nielsen, E., Akita, M., Davila-Aponte, J. and Keegstra, K., 1997. Stable association of chloroplastic precursors with protein-translocation complexes containing proteins from both envelope membranes and a stromal Hsp100 molecular chaperone. *EMBO J.*, 16: 935–946.

Oosawa, N., Masuda, T., Awai, K., Fusada, N., Shimada, H., Ohta, H. and Takamiya, K.I., 2000. Identification and light-induced expression of a novel gene of NADPH-protochlorophyllide oxidoreductase isoform in Arabidopsis thaliana. *FEBS Lett.*, 474: 133-136.

op den Camp, R., Przybyla, D., Ochsenein, C., Laloi, C., Kim, C., Danon, A., Wagner, D., Hideg, E., Göbel, C., Feussner, I., Nater, M. and Apel, K., 2003. Rapid

induction of distinct stress responses after the release of singlet oxygen in Arabidopsis. *The Plant Cell*, 15(10): 2320-32.

op den Camp, R., Przybyla, D., Ochsenein, C., Laloi, C., Kim, C., Danon, A., Wagner, D., Hidég, E., Göbel, C., Feussner, I., Nater, M. and Apel, K., 2004. Rapid induction of distinct stress responses after the release of singlet oxygen in Arabidopsis. *Plant Cell*, 15: 2320-2332.

Oster, U., Tanaka, R., Tanaka, A. and Rüdiger, W., 2000. Cloning and functional expression of the gene encoding the key enzyme for chlorophyll b biosynthesis (CAO) from Arabidopsis thaliana. *The Plant Journal*, 21(3): 305-10.

Oyama, T., Shimura, Y. and Okada, K., 1997. The Arabidopsis HY5 gene encodes a bZIP protein that regulates stimulus-induced development of root and hypocotyl. *Genes and Development*, 11: 2983-2995.

Palmer, J.D., 2003. The symbiotic birth and spread of plastids: how many times and whodunit? *Journal of Phycology*, 39(1): 4-12.

Palsson, L.O., Spangfort, M.D., Gulbinas, V. and Gillbro, T., 1994. Ultrafast chlorophyll b to chlorophyll a excitation energy transfer in the isolated light harvesting complex, LHCII, of green plants: implications for the organisation of chlorophylls. *FEBS Lett.*, 339: 134-138.

Peeters, N. and Small, I., 2001. Dual targeting to mitochondria and chloroplasts. *Biochimica et Biophysica Acta (BBA) - Molecular Cell Research*, 1541(1-2): 54-63.

Perry, S.E. and Keegstra, K., 1994. Envelope Membrane Proteins That Interact with Chloroplastic Precursor Proteins. *Plant Cell*, 6(1): 93-105.

Philippar, K., Geis, T., Ilkavets, I., Oster, U., Schwenkert, S., Meurer, J. and Soll, J., 2007. Chloroplast biogenesis: The use of mutants to study the etioplast-chloroplast transition. *Proceedings of the National Academy of Sciences*, 104(2): 678-683.

Plumley, F. and Schmidt, G., 1987. Reconstitution of chlorophyll a/b light-harvesting complexes: Xanthophyll-dependent assembly and energy transfer. *Proceedings of the National Academy of Science of the United States of America.*, 84(1): 146-150.

Pohlmeier, K., Soll, J., Steinkamp, T., Hinnah, S. and Wagner, R., 1997. Isolation and characterization of an amino acid-selective channel protein present in the chloroplastic outer envelope membrane. *Proceedings of the National Academy of Sciences of the United States of America*, 94(17): 9504-9509.

Pollmann, S., Springer, A., Buhr, F., Lahroussi, A., Samol, I., Bonneville, J.-M., Tichtinsky, G., von Wettstein, D., Reinbothe, C. and Reinbothe, S., 2007. A plant porphyria related to defects in plastid import of protochlorophyllide oxidoreductase A. *Proceedings of the National Academy of Sciences*, 104(6): 2019-2023.

Przybyla, D., Göbel, C., Imboden, A., Feussner, I., Hamberg, M. and Apel, K., 2008. Enzymatic, but not non-enzymatic $1O_2$ -mediated peroxidation of polyunsaturated fatty acids forms part of the EXECUTER1-dependent stress response program in the flu mutant of *Arabidopsis thaliana*. *Plant J.*, 54: 236-248.

Qbadou, S., Becker, T., Mirus, O., Tews, I., Soll, J. and Schleiff, E., 2006. The molecular chaperone Hsp90 delivers precursor proteins to the chloroplast import receptor Toc64. *EMBO J.*, 25: 1836-1847.

Quail, P., 2000. Phytochrome-interacting factors. *Seminars in Cell and Development Biology*, 11(6): 457-66.

Rassow, J., Dekker, P.J.T., van Wilpe, S., Meijer, M. and Soll, J., 1999. The preprotein translocase of the mitochondrial inner membrane: function and evolution. *Journal of Molecular Biology*, 286(1): 105-120.

Reed, J., Nagpal, P., Poole, D., Furuya, M. and Chory, J., 1993. Mutations in the gene for the red/far-red light receptor phytochrome B alter cell elongation and physiological responses throughout *Arabidopsis* development. *Plant Cell*, 5: 147-157.

Reinbothe, C., Bartsch, S., Eggink, L., Hooper, J., Brusslan, J., Andrade-Paz, R., Monnet, J. and Reinbothe, S., 2006. A role for chlorophyllide a oxygenase in the regulated import and stabilization of light-harvesting chlorophyll a/b proteins. *Proc Natl Acad Sci U S A*, 103(12): 4777-82.

Reinbothe, C., Buhr, F., Pollmann, S. and Reinbothe, S., 2003. In Vitro Reconstitution of Light-harvesting POR-Protochlorophyllide Complex with Protochlorophyllides a and b. *J. Biol. Chem.*, 278(2): 807-815.

Reinbothe, C., Lebedev, N. and Reinbothe, S., 1999. A protochlorophyllide light-harvesting complex involved in de-etiolation of higher plants. *Nature*, 397(6714): 80-84.

Reinbothe, C., Pollmann, S., Desvignes, C., Weigele, M., Beck, E. and Reinbothe, S., 2004. LHPP, the light-harvesting NADPH:protochlorophyllide (Pchl) oxidoreductase:Pchl complex of etiolated plants, is developmentally expressed across the barley leaf gradient. *Plant Science*, 167(5): 1027-1041.

Reinbothe, S., Krauspe, R. and Parthier, B., 1990. In-vitro transport of chloroplast proteins in a homologous Euglena system with particular reference to plastid leucyl-tRNA synthetase. *Planta*, 181(2): 176-183.

Reinbothe, S., Mache, R. and Reinbothe, C., 2000. A second, substrate-dependent site of protein import into chloroplasts. *Proceedings of the National Academy of Science of the United States of America*, 97(17): 9795-800.

Reinbothe, S., Quigley, F., Gray, J., Schemenewitz, A. and Reinbothe, C., 2004. Identification of plastid envelope proteins required for import of protochlorophyllide oxidoreductase A into the chloroplast of barley. *Proceedings of the National Academy of Sciences of the United States of America*, 101(7): 2197-2202.

Reinbothe, S., Quigley, F., Springer, A., Schemenewitz, A. and Reinbothe, C., 2004. The outer plastid envelope protein Oep16: Role as precursor translocase in import of protochlorophyllide oxidoreductase A. *Proceedings of the National Academy of Sciences of the United States of America*, 101(7): 2203-2208.

Reinbothe, S., Reinbothe, C., Heintzen, C., Seidenbecher, C. and Parthier, B., 1993. A methyl jasmonate-induced shift in the length of the 5' untranslated region impairs translation of the plastid *rbcL* transcript in barley. *EMBO J.*, 12: 1505-1512.

Reinbothe, S., Reinbothe, C., Holtorf, H. and Apel, K., 1995. Two NADPH:Protochlorophyllide Oxidoreductases in Barley: Evidence for the Selective

Disappearance of PORA during the Light-Induced Greening of Etiolated Seedlings. *Plant Cell*, 7(11): 1933-1940.

Reinbothe, S., Reinbothe, C., Neumann, D. and Apel, K., 1996. A plastid enzyme arrested in the step of precursor translocation in vivo. *Proceedings of the National Academy of Science of the United States of America*, 93(21): 12026-30.

Reinbothe, S., Reinbothe, C. and Parthier, B., 1993. Methyl jasmonate represses translation initiation of a specific set of mRNAs in barley. *The Plant Journal*, 4(3): 459-467.

Reinbothe, S., Reinbothe, C. and Parthier, B., 1993. Methyl jasmonate-regulated translation of nuclear-encoded chloroplast proteins in barley (*Hordeum vulgare* L. cv. salome). *J. Biol. Chem.*, 268(14): 10606-10611.

Reinbothe, S., Runge, S., Reinbothe, C., van Cleve, B. and Apel, K., 1995. Substrate-dependent transport of the NADPH:protochlorophyllide oxidoreductase into isolated plastids. *The Plant Cell*, 7(2): 161-72.

Reumann, S., Inoue, K. and Keegstra, K., 2005. Evolution of the general protein import pathway of plastids (review). *Mol Membr Biol.*, 22(1-2): 73-86.

Ryberg, M. and Sundqvist, C., 1991. Structural and functional significance of pigment-protein complexes of chlorophyll precursors. In: H. Scheer (Editor), *Chlorophylls*. CRC Press, Boca Raton, pp. 587-612.

Sambrook, J. and Russell, R., 2001. *Molecular Cloning A Laboratory Manual* (3rd ed.). Cold Spring Harbor Laboratory Press.

Sanger, F., Nicklen, S. and Coulson, A., 1977. DNA sequencing with chain-terminating inhibitors. *Proceedings of the National Academy of Science of the United States of America*, 74(12): 5463-5467.

Schemenewitz, A., Pollmann, S., Reinbothe, C. and Reinbothe, S., 2007. A substrate-independent, 14:3:3 protein-mediated plastid import pathway of NADPH:protochlorophyllide oxidoreductase A. *Proceedings of the National Academy of Sciences*, 104(20): 8538-8543.

Scheumann, V., Schoch, S. and Rüdiger, W., 1998. Chlorophyll a formation in the chlorophyll b reductase reaction requires reduced ferredoxin. *The Journal of biological chemistry*, 273(52): 35102-8.

Schnell, D.J., Blobel, G., Keegstra, K., Ko, K. and Soll, J., 1997. A consensus nomenclature for the protein-import components of the chloroplast envelope. *Trends Cell Biol.*, 7: 303-304.

Schnell, D.J., Kessler, F. and Blobel, G., 1994. Isolation of components of the chloroplast protein import machinery. *Science*, 266: 1007-1012.

Schulz, R., Steinmüller, K., Klaas, M., Forreiter, C., Rasmussen, S., Hiller, C., and Appel, K., 1989. Nucleotide sequence of a cDNA coding for the NADPH-protochlorophyllide oxidoreductase (PCR) of barley (*Hordeum vulgare* L.) and its expression in *Escherichia coli*. *Mol. Gen. Genet.* 217 : 335-361.

Simkin, A.J., 2002. Etude de l'expression des gènes de la biosynthèse des caroténoïdes et de la surexpression hétérologue d'une protéine chez la tomate, PhD Thesis, Laboratoire Plastes et Differentiation Cellulaire, Université Joseph Fourier, Grenoble.

Smith, M., Rounds, C., Wang, F., Chen, K., Afithile, M. and Schnell, D., 2004. atToc159 is a selective transit peptide receptor for the import of nucleus-encoded chloroplast proteins. *The Journal of Cell Biology*, 165(3): 323-34.

Spano, A. and Timko, M., 1991. Isolation, characterization and partial amino acid sequence of a chloroplast-localized porphobilinogen deaminase from pea (*Pisum sativum* L.). *Biochimica et Biophysica Acta*, 1076(1): 29-36.

Stahl, T., Glockmann, C., Soll, J. and Heins, L., 1999. Tic40, a New "Old" Subunit of the Chloroplast Protein Import Translocon. *J. Biol. Chem.*, 274(52): 37467-37472.

Stern, D., Higgs, D. and Yang, J., 1997. Transcription and translation in chloroplasts. *Trends in Plant Science*, 2: 308-315.

Szabó, I., Bergantino, E. and Giacometti, G.M., 2005. Light and oxygenic photosynthesis: energy dissipation as a protection mechanism against photo-oxidation. *EMBO Rep.*, 6: 629-634.

- Tranel, P., Froehlich, J., Goyal, A. and Keegstra, K.**, 1995. A component of the chloroplastic protein import apparatus is targeted to the outer envelope membrane via a novel pathway. *The EMBO Journal*, 14(11): 2436-46.
- Verhoeven, A.S., Aadams, W.W. and Demmig, A.B.**, 1996. Close relationship between the state of the xanthophyll cycle pigments and photosystem II efficiency during recovery from winter stress. *Physiologia Plantarum*, 96: 567-576.
- Villarejo, A., Buren, S., Larsson, S., Dejardin, A., Monne, M., Rudhe, C., Karlsson, J., Jansson, S., Lerouge, P., Rolland, N., von Heijne, G., Grebe, M., Bako, L. and Samuelsson, G.**, 2005. Evidence for a protein transported through the secretory pathway en route to the higher plant chloroplast. *Nat Cell Biol.*, 7: 1224–1231.
- von Wettstein, D., Kahn, A., Nielsen, O.F. and Gough, S.**, 1974. Genetic regulation of chlorophyll synthesis analyzed with mutants in barley. *Science*, 184: 800-802.
- Vothknecht, U.C.**, 1996. Expression of catalytically active barley glutamyl tRNA^{Glu} reductase in *Escherichia coli* as a fusion protein with glutathione S-transferase. *Proceedings of the National Academy of Sciences of the United States of America*, 93(17): 9287–9291.
- Vothknecht, U.C. and Westhoff, P.**, 2001. Biogenesis and origin of thylakoid membranes. *Biochimica et Biophysica Acta*, 1541(1-2): 91-101.
- Wagner, D., Przybyla, D., op den Camp, R., Kim, C., Landgraf, F., Lee, K.P., Wursch, M., Laloi, C., Nater, M. and Apel, K.**, 2004. The genetic basis of singlet oxygen-induced stress responses of *Arabidopsis thaliana*. *Science*, 306: 1183-1185.
- Wasternack, C.**, 2007. Jasmonates: An Update on Biosynthesis, Signal Transduction and Action in Plant Stress Response, Growth and Development. *Ann Bot*, 100(4): 681-697.
- Whitelam, G., Johnson, E., Peng, J., Carol, P., Anderson, M., Cowl, J. and Harberd, N.**, 1993. Phytochrome A null mutants of *Arabidopsis* display a wild-type phenotype in white light. *Plant Cell*, 5: 757-768.
- Witty, M., Wallace-Cook, A., Albrecht, H., Spano, A., Michel, H., Shabanowitz, J., Hunt, D., Timko, M. and Smith, A.**, 1993. Structure and expression of chloroplast-

localized porphobilinogen deaminase from pea (*Pisum sativum* L.) isolated by redundant polymerase chain reaction. *Plant Physiology*, 103(1): 139-47.

Wu, C., Seibert, F.S. and Ko, K., 1994. Identification of chloroplast envelope proteins in close physical proximity to a partially translocated chimeric precursor protein. *J Biol Chem*, 269: 32264–32271.

Yoon, H.S., Hackett, J.D., Ciniglia, C., Pinto, G. and Bhattacharya, D., 2004. A molecular timeline for the origin of photosynthetic eukaryotes. *Mol Biol Evol*, 21: 809–818.

APPENDIX A

A. 1 Primer list

Table A.1. A list of primers used in this study.

Name	Gene	Sequence (5' to 3' end)	Utilization
AtOEP16-F	<i>AtOEP16</i>	5'- AACGAACTGAGAAGCGGTTGC	genotyping
AtOEP16-R	<i>AtOEP16</i>	5'- ATCCACCGTTAAAAGCCCTT	genotyping
AtFLU-F	<i>AtFLU</i>	5'- TCCCTTTCCTTGTCGCTCCTT	genotyping
AtFLU-R	<i>AtFLU</i>	5'- ATTTGACATAGCCGGGCATCA	genotyping
AtPORA-F	<i>AtPORA</i>	5'- GATAATGGCGTGACAGAGACTT	genotyping
AtPORA-R	<i>AtPORA</i>	5'- GAATCAGCCAAAACACAACACTACTAA	genotyping
LBa1	T-DNA (Salk)	5'- TGGTTCACGTAGTGGGCCATCG	Genotyping of <i>Atoep16-1</i> and <i>flu</i> mutants, T-DNA probe for Southern-blot on <i>Atoep16-1</i>
OEP16 Fgw	<i>AtOEP16</i>	5'- AAAAAGCAGGCTTCCGGAGGTCGGCCATGCCTTCAAGCACATTCTC	Gateway cloning of <i>AtOEP16-1</i> cDNA
OEP16 Rgw	<i>AtOEP16</i>	5'- AGAAAGCTGGGTGACTAGTATGATCAGTAGAAATAATGATTGTT	Gateway cloning of <i>AtOEP16-1</i> cDNA
OEP16 Rgw_no Stop	<i>AtOEP16</i>	5'- AGAAAGCTGGGTGACTAGTGTAGAAATAATGATTGTTAACGAA	Gateway cloning of <i>AtOEP16-1</i> cDNA
AttB1	Gateway adapter	5'- GGGGACAAGTTTGTACAAAAAAGCAGGCT	Gateway cloning of <i>AtOEP16-1</i> cDNA
AttB2	Gateway adapter	5'- GGGGACCACCTTTGTACAAGAAAGCTGGGT	Gateway cloning of <i>AtOEP16-1</i> cDNA
35S F	35S promoter	5'- CGCACAATCCCCTATCCTT	genotyping
M13 R	35S terminator	5'- GGAAACAGCTATGACCATG	
YFP R	<i>YFP</i>	5'- GCTGAACTTGTGGCCGTTA	genotyping
NPTII-F	Kanamycin resistance	5'- CGGTTCTTTTTGTCAAGACC	T-DNA probe, Southern-blot on <i>Atoep16-1</i>
NPTII-R	Kanamycin resistance	5'- CAATATCACGGGTAGCCAAC	T-DNA probe, Southern-blot on <i>Atoep16-1</i>
LBGT1-F		5'- ACTTAATAACACATTGCGGACG	T-DNA probe, Southern-blot on <i>Atoep16-1</i>
TransA-F	transit peptide of the pPORA	5'-GAGAGAGGATCCCAAGCTCACCGTCATCCATGGCT	Precursor molecules for crosslinking and import assays
TransA-R	transit peptide of the pPORA	5'-TATGCCGGATCCGCTCGGCGACGGTCTCGA	Precursor molecules for crosslinking and import assays
TransB-F	transit peptide of the pPORA	5'-TATGAGAGAGGATCCTGCTCGCCGGCTCAGATGGCT	Precursor molecules for crosslinking and import assays
TransB-R	transit peptide of the pPORA	5'-TATGAGAGAGGATCCGGCCGGCGACGCCGGGGTTGC	Precursor molecules for crosslinking and import assays

A. 2. Overexpression and purification of 6His-tag-AtOEP16-1 protein

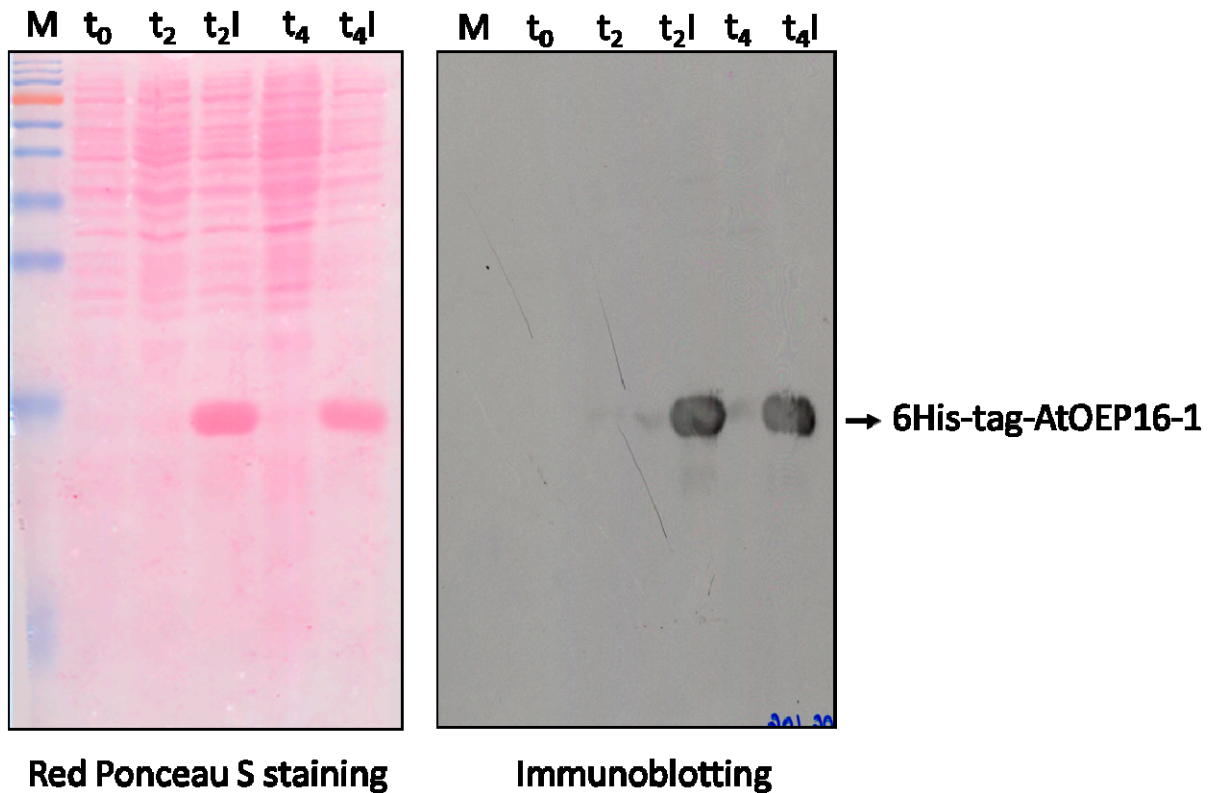


Figure A.2.1. Overexpression of 6His-tag-AtOEP16-1 protein.

Pilot expression of 6His-tag-AtOEP16-1 protein in *E.coli* BL21-TM bacteria grown in LB medium at 37°C with shaking until the OD₆₀₀ reached 0,6 (t₀) and continued for 2 h and 4 h with the addition of L-arabinose into the culture medium (t₂I, t₄I) or not (t₂, t₄). M: protein marker.

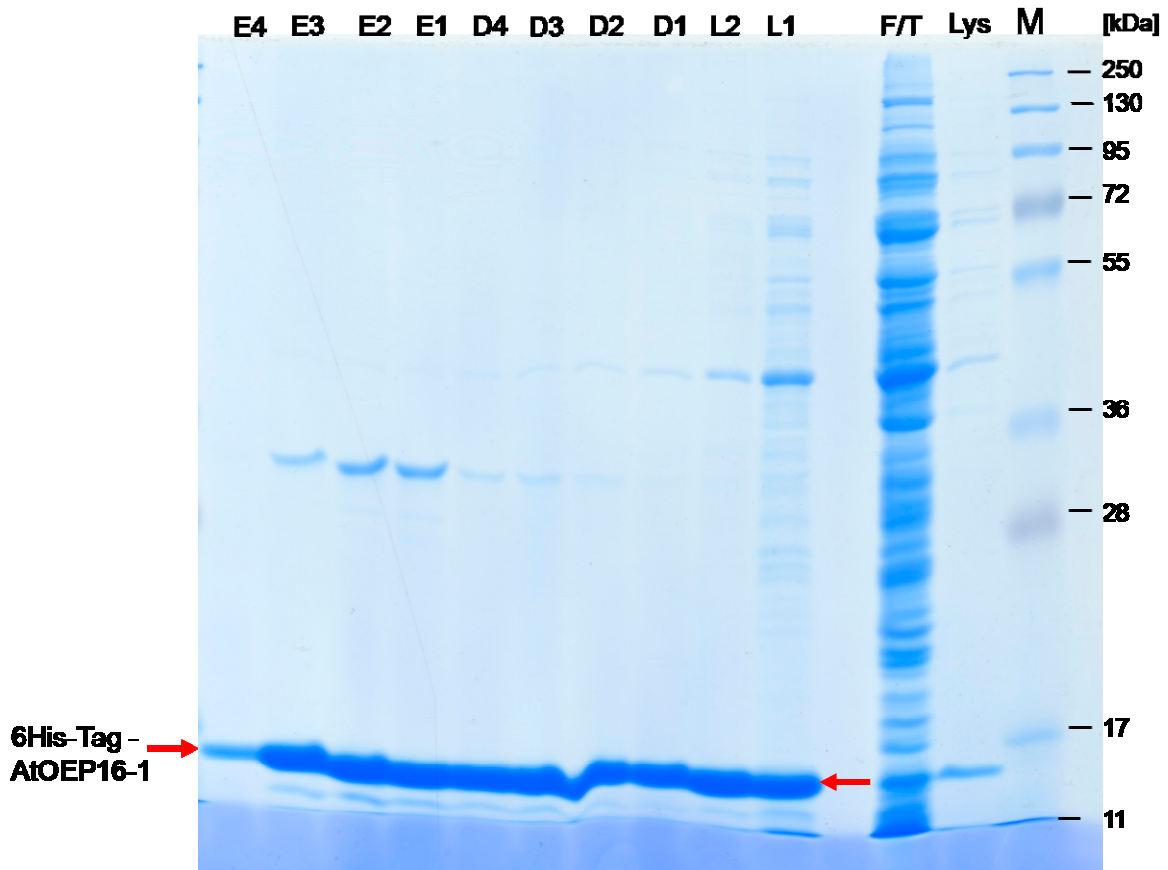


Figure A.2.2. Purification of 6His-tag-AtOEP16-1 recombinant protein.

Purification of recombinant fusion protein 6His-tag-AtOEP16-1 using the procedure of batch purification under denaturing conditions based on a nickel-chelating resin Ni-NTA (adapted from the protocol of the QIAexpressionist-Qiagen). 20 μ g of proteins of each purification step was loaded per each vial on 15% polyacrylamide SDS gel stained with Blue Coomassie. **M**: protein marker, **L**: lysis extract, **F/T**: flow-through, **L1** and **L2**: subsequent washings with L solution, **D1-D4**: subsequent washings with D solution, **E1-E4**: subsequent elutions with E solution. 6His-tag-AtOEP16-1 as a single band of increased intensity was finally cut and sent to Interchim enterprise for rabbit immunization and collection of produced antisera.

A. 3. Phenotypic analysis of double mutant *Atoep16-1;7/flu*

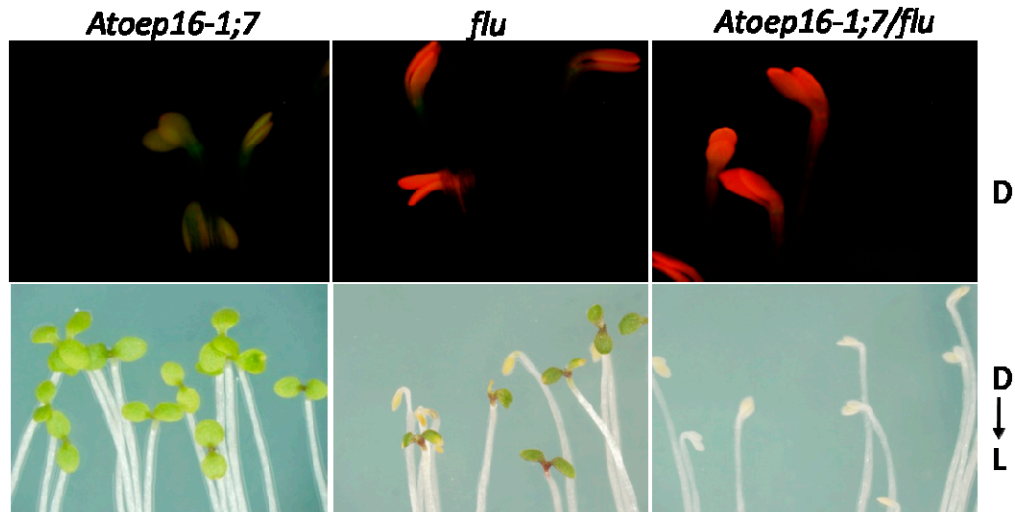


Figure A.3. Phenotypic analysis of *flu*, *Atoep16-1;7* and *Atoep16-1;7/flu* double mutants.

Phenotypic analysis of seedlings of *Atoep16-1;7*, *flu* and a double mutant *Atoep16-1;7/flu*, grown for 5 d in the dark (D), after a non-permissive dark-to-light shift for 24h (D→L). Note the red Pchl_a fluorescence under blue light shown in the upper panels and seedlings phenotypes observed under white light presented in the lower panels.

A.4. *In vitro* import of transA-DHFR and transB-DHFR into isolated *Atoep16-1* mutant plastids.

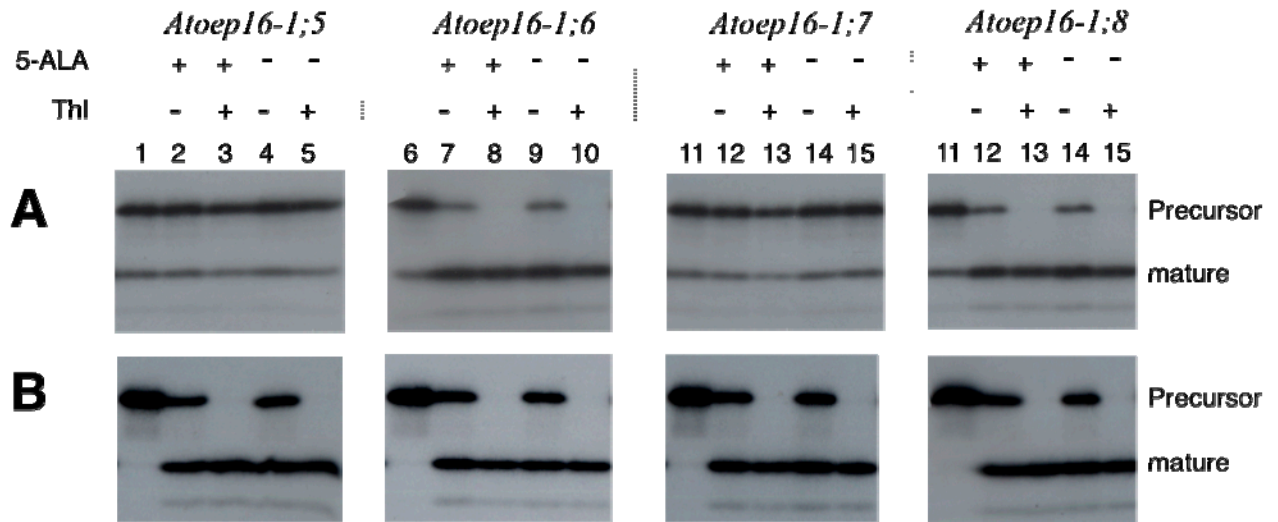


Figure A.4. *In vitro*-import of ^{35}S -transA-DHFR (A) and ^{35}S -transB-DHFR (B) into chloroplasts isolated from the 4 different *Atoep16-1* mutants.

Import was studied with Percoll/sucrose-purified chloroplasts that had been fed 5-aminolevulinic acid (5-ALA) to induce intraplastidic Pchlide synthesis or mock-incubated with phosphate buffer. All import assays were conducted in the dark for 15 min and contained 2.5 mM Mg-ATP and 0.1 mM Mg-GTP. After import, the assays were treated with (+) or without (-) thermolysin (Thl)(Cline et al., 1984). Proteins were precipitated with trichloroacetic acid. After SDS-PAGE, the gel was subjected to autoradiography. Note that a fraction of ^{35}S -transA-DHFR is artificially processed at time point zero.

APPENDIX B

Publications

Pollmann et al., 2007

Khandal et al., 2009

Reinbothe et al., 2009

Samol et al., 2011a

Samol et al., 2011b

A plant porphyria related to defects in plastid import of protochlorophyllide oxidoreductase A

Stephan Pollmann^{*†}, Armin Springer^{*‡}, Frank Buhr^{*‡}, Abder Lahroussi^{*}, Iga Samol^{*}, Jean-Marc Bonneville^{*}, Gabrielle Tichtinsky^{*}, Diter von Wettstein^{*§¶}, Christiane Reinbothe^{*}, and Steffen Reinbothe^{*¶}

^{*}Université Joseph Fourier et Centre National de la Recherche Scientifique Unité Mixte de Recherche 5575, CERMO, BP53, F-38041 Grenoble Cedex 9, France; [†]Lehrstuhl für Pflanzenphysiologie, Universität Bayreuth, Universitätsstrasse 30, D-95447 Bayreuth, Germany; and [§]Department of Crop and Soil Sciences, Washington State University, Pullman, WA 99164-6420

Contributed by Diter von Wettstein, December 12, 2006 (sent for review November 11, 2006)

The plastid envelope of higher plant chloroplasts is a focal point of plant metabolism. It is involved in numerous pathways, including tetrapyrrole biosynthesis and protein translocation. Chloroplasts need to import a large number of proteins from the cytosol because most are encoded in the nucleus. Here we report that a loss-of-function mutation in the outer plastid envelope 16-kDa protein (*oep16*) gene causes a conditional seedling lethal phenotype related to defects in import and assembly of NADPH:protochlorophyllide (Pchl) oxidoreductase A. In the isolated knockout mutant of *Arabidopsis thaliana*, excess Pchl accumulated in the dark operated as photosensitizer and provoked cell death during greening. Our results highlight the essential role of the substrate-dependent plastid import pathway of precursor Pchl oxidoreductase A for seedling survival and the avoidance of developmentally programmed porphyria in higher plants.

cell death | greening | plastid biogenesis | protein translocation

In plants, light provides an important environmental signal and trigger for the production of photosynthetically active chloroplasts (1, 2). In dark-grown angiosperms, plastid development is arrested at a state that leads only to the formation of so-called etioplasts. These organelles are devoid of chlorophyll and are incapable of photosynthetic function. Once dark-grown plants break through the soil after germination and reach the sunlight, they begin to synthesize chlorophyll and assemble the photosynthetic apparatus. The synthesis of chlorophyll from protochlorophyllide (Pchl) is, in angiosperms, a light-dependent reaction and an essential step for the establishment of photosynthetically active chloroplasts. In barley, it is catalyzed by two closely related light-activated enzymes, NADPH:Pchl oxidoreductases A and B (PORA and PORB) (3), which form supramolecular light-harvesting structures designated LHPP in the prolamellar body of etioplasts (4, 5). Dark-stable PORA:PORB-Pchl-NADPH supracomplexes are poised such that absorption of a photon by Pchl *b* bound to PORA leads to energy transfer onto PORB-bound Pchl *a* and its subsequent reduction, resulting in the formation of Chl *a* (4, 5). Like other free tetrapyrroles, Pchl not bound to POR could operate as a photosensitizer (6–8). Angiosperm plants, therefore, have evolved efficient mechanisms to keep the level of these potentially phototoxic compounds low and thereby avoid porphyrias (9–12). One such mechanism is feedback control of Pchl synthesis by heme and Pchl (10, 11). Another factor is the fluorescent (FLU) protein, which depresses Pchl synthesis in darkness (12). After LHPP's dissociation, which is induced by light and correlates with the dispersal of the prolamellar body (13), PORA gains activity as a Pchl *b*-reducing enzyme such that another part of the light energy is quenched in a nonhazardous way (4, 5).

Being encoded in the nucleus, PORA and PORB are synthesized as larger precursors (pPORA and pPORB) and are imported into the plastids through specific protein translocon complexes in the outer and inner envelope membranes (14–18).

Whereas pPORB enters the plastids via the general protein import apparatus comprising the presequence receptor TOC159 and translocation channel protein TOC75 (17, 18), pPORA uses a Pchl-dependent translocon named the PTC complex, which is distinctive from the general protein import site (14, 17). Among the identified PTC proteins was a 16-kDa protein related to a group of amino acid and preprotein transporters found in free-living bacteria and endosymbiotic mitochondria and chloroplasts (14, 17). Several lines of evidence verified that the identified barley *PTC16* gene is an ortholog of the previously characterized pea and *Arabidopsis OEP16* (At2g28900) gene (17).

In the present work a reverse genetic approach was taken to dissect the function of the *Arabidopsis OEP16* (At2g28900) gene *in planta*. Using a knockout line of *Arabidopsis thaliana* that is deficient in the *OEP16* gene we demonstrate that PTC16/OEP16 is involved in pPORA import. Interestingly, dark-grown *Atoep16* plants resembled etiolated *flu* plants and accumulated free Pchl. After a dark-to-light shift, this pigment operated as photosensitizer and caused rapid bleaching and cell death. Our results underscore the essential role of the substrate-dependent import pathway of pPORA, which couples protein translocation to pigment biosynthesis in the plastid envelope, for Pchl homeostasis and cell viability during seedling de-etiolation.

Results and Discussion

At2g28900 (*AtOEP16*) contains six exons and five introns (Fig. 1A), and we used reverse genetics to determine its role in *Arabidopsis*. A respective *Arabidopsis* mutant was obtained from the Salk Institute Genomic Analysis Laboratory collection (19) carrying a T-DNA insertion SALK_024018 that disrupts the *AtOEP16* locus (Fig. 1A and C). Sequencing of the T-DNA/*AtOEP16* junction established that the insertion disrupted the gene 6 bp upstream of the 3' end of exon 2. We refer to this line as *Atoep16-1* throughout the rest of the article. DNA gel blot analyses yielded a single T-DNA hybridizing band in genomic DNA isolated from light-grown homozygous *Atoep16-1* plants that had been digested with two different restriction enzymes (Fig. 1B), demonstrating that *Atoep16-1* contained a single T-DNA insertion in the genome. Expression studies showed that

Author contributions: S.P., J.-M.B., G.T., C.R., and S.R. designed research; S.P., A.S., F.B., A.L., I.S., C.R., and S.R. performed research; D.v.W., C.R., and S.R. analyzed data; and S.R. wrote the paper.

The authors declare no conflict of interest.

Abbreviations: Pchl, protochlorophyllide; pPORA/B, precursor Pchl oxidoreductases A and B; DHFR, dihydrofolate reductase; 5-ALA, 5-aminolevulinic acid; trans A, transit peptide of pPORA.

[†]Present address: Lehrstuhl für Pflanzenphysiologie, Ruhr-Universität Bochum, Universitätsstrasse 150, D-44801 Bochum, Germany.

[¶]To whom correspondence may be addressed. E-mail: diter@wsu.edu or steffen.reinbothe@ujf-grenoble.fr.

This article contains supporting information online at www.pnas.org/cgi/content/full/0610934104/DC1.

© 2007 by The National Academy of Sciences of the USA

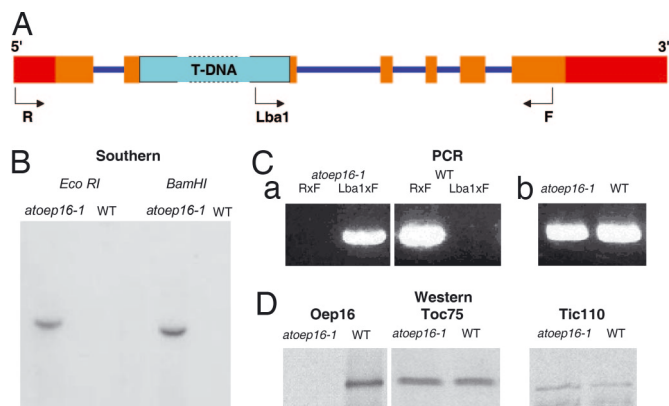


Fig. 1. Description of the *Atoep16-1* T-DNA insertion line (SALK_024018.50.90.X). (A) Diagram of the *Atoep16-1:1* gene and respective T-DNA insertion. 5' and 3' untranslated regions are in red, exons are in ochre, and introns are in violet. The 4.5-kb T-DNA insertion (not drawn to scale) is shown in turquoise. R, F, and Lba1 mark primers used for PCR analyses. (B) DNA gel blot analysis of the *Atoep16-1* line. Genomic DNA (10 μ g) from homozygous *Atoep16-1* or wild-type plants was digested with EcoRI and BamHI, respectively, and the filter-bound DNA fragments were hybridized to a DNA probe corresponding to the kanamycin-resistance gene of the T-DNA using standard procedures. (C) Confirmation of the T-DNA insertion by PCR using the following primers. (a) Lba1, 5'-ATGGTTCACGTAGTGGCCATCG-3'; R (reverse primer), 5'-ATCCACCGTTAAAGCCCTT-3'; F, (forward primer), 5'-AACGAAGTGAAGCGGTTGC-3'. (b) Primers specific for the adenine phosphoryl transferase gene of wild-type and *Atoep16-1* plants. (D) Western blot analysis of OEP16 protein expression in chloroplasts of *Atoep16-1* and wild-type plants. Protein was prepared from isolated chloroplasts and subjected to Western blotting using antisera against OEP16 and the 75- and 110-kDa proteins of the outer and inner envelope membrane translocases of chloroplasts TOC75 and TIC110, respectively.

neither *OEP16* transcript nor OEP16 protein was detectable in *Atoep16-1* plants, and thus the mutant was null with respect to the *Atoep16-1:1* gene (Fig. 1D).

Depending on the growth conditions, *Atoep16-1* seedlings exhibited different phenotypes (Fig. 2). If grown in darkness and exposed to white light, the mutant rapidly bleached and finally died (Fig. 2B). In plants kept under continuous white light right from the beginning of germination, no phenotype was detectable, and the plants looked like the wild type (Fig. 2, compare C and F). Etiolated *Atoep16-1* plants examined under blue light with a Leica MZ12 fluorescence microscope showed a strong red fluorescence indicative of the presence of free porphyrin pigments in darkness (Fig. 2A, compare with the wild type shown in D). These results were reminiscent of findings reported for the *flu* mutant of *Arabidopsis* that contains elevated levels of red-fluorescing Pchl*d* in darkness (12). Pchl*d* is present in a free form in etiolated *flu* plants, which triggers singlet oxygen formation and cell death upon illumination (12). When dark-grown *Atoep16-1* seedlings were exposed to white light, very similar defects were observed, including bleaching and cell death (Fig. 2B versus E). However, the time courses shown in Fig. 2G revealed some differences in cell death progression (Fig. 2G). We assumed that this difference may be reflective of the actual level and/or composition of free porphyrin pigment(s) in *Atoep16-1* versus *flu* plants. Pigment analyses (20) indeed showed that whereas *flu* plants accumulate ≈ 8.5 -fold-higher levels of total Pchl*d* than wild-type plants, *Atoep16-1* plants contained only ≈ 4.5 -fold-higher pigment levels. Interestingly, the composition of pigments was also altered in *Atoep16-1* versus *flu* and wild-type plants (Fig. 2H). Whereas *Atoep16-1* plants accumulated Pchl*d*, *flu* plants contained elevated levels of Pchl*a* [Fig. 2H; for details of pigment identification, see supporting information (SI) Fig. 8].

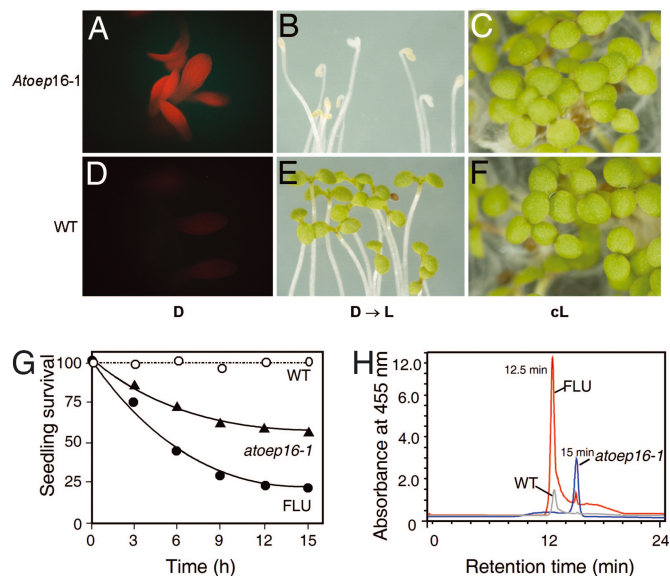


Fig. 2. Growth-dependent cell death phenotype of the *Atoep16-1* mutant. (A–F) *Atoep16-1* (A–C) and wild-type (D–F) plants were grown in the dark (A and D) under a nonpermissive dark-to-light shift (B and E) or under permissive continuous white light (C and F) and inspected under a microscope. Accumulation of free, red-fluorescing Pchl*d* was monitored under blue light (400–500 nm) (A and D). Free, excited Pchl*d* molecules present in etiolated *Atoep16-1* (A) but not in wild-type (D) plants caused photooxidative damages, as a result of which the seedlings died (B versus E, respectively). (G) Seedling survival rates of wild-type (open circles), *Atoep16-1* (triangles), and *flu* (filled circles) plants during a nonpermissive dark-to-light shift. Of a number of 300 seedlings in three independent experiments, the indicated percentages survived, whereas the remainder died as a result of pigment-sensitized photooxidation. (H) Pigment accumulation in etiolated wild-type (gray line), *Atoep16-1* (blue line), and *flu* (red line) plants. The different peaks were identified as Pchl*b* (peak eluting at 12.5 min) and Pchl*a* (peak eluting at 15 min) by using synthetic standards and absorbance measurements as well as mass spectrometry (SI Fig. 8).

OEP16 is a transmembrane channel protein of the outer plastid envelope membrane implicated in amino acid (21) and/or polypeptide transport (17). When we performed radioisotope-labeling studies with 14 C-glutamate, 14 C-glutamine, and 14 C-glycine, and isolated chloroplasts and etioplasts (22), no difference in amino acid uptake was found for *Atoep16-1* versus

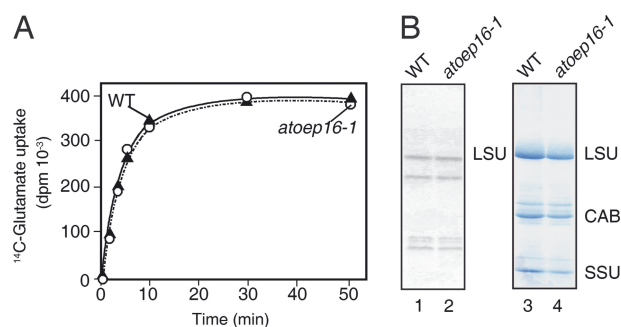


Fig. 3. Amino acid uptake into *Atoep16-1* and wild-type chloroplasts. (A) Isolated chloroplasts were incubated with 14 C-glutamate for various time intervals, and uptake of radioactivity was determined. (B) After labeling isolated chloroplasts with [35 S]methionine for 5 min (lanes 1 and 2) or 20 min (data not shown), protein was extracted and precipitated with trichloroacetic acid, separated by SDS/PAGE, and detected by either autoradiography (lanes 1 and 2) or Coomassie staining (lanes 3 and 4). LSU and SSU, large and small subunits of ribulose-1,5-bisphosphate carboxylase/oxygenase; CAB, chlorophyll *a/b*-binding protein of photosystem II.

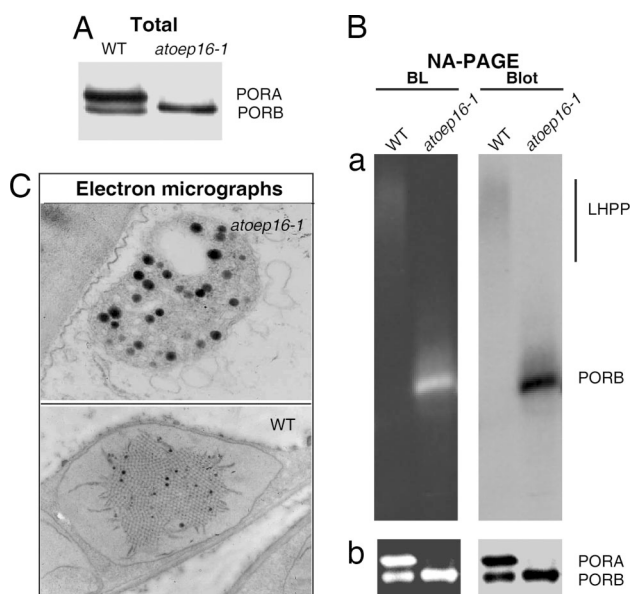


Fig. 6. POR expression in etiolated *Atoep16-1* and wild-type seedlings. (A) PORA and PORB protein levels in *Atoep16-1* and wild-type etioplasts determined by SDS/PAGE and Western blotting. (B) Detection of light-dissociable PORA:PORB-Pchl ide -NADPH suprastructures indicative of LHPP in solubilized membrane fractions of *Atoep16-1* and wild-type etioplasts before (a) and after (b) a 1-msec flash of white light. Protein detection was made by non-denaturing, analytical PAGE (NA-PAGE) and blue light (BL)-induced pigment autofluorescence (Left) and protein gel blot (Blot) analysis (Right) using a POR antiserum. (C) Transmission electron micrographs of *Atoep16-1* and wild-type etioplasts. Black dots represent plastoglobules formed in excess in *Atoep16-1* versus wild-type etioplasts.

plants (Fig. 6 A and B). Electron microscopy highlighted a complete lack of the prolamellar body in *Atoep16-1* as compared with wild-type etioplasts (Fig. 6C). Together, these findings conclusively showed that PORA, as part of larger complexes in the prolamellar body, played an essential role for plant survival

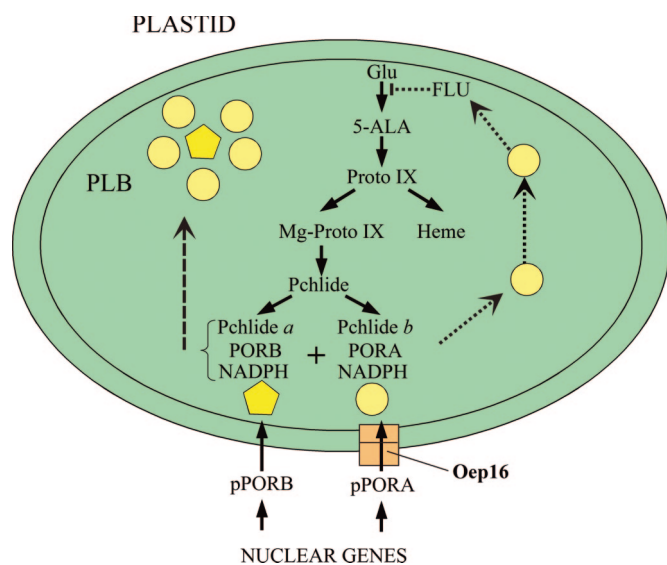


Fig. 7. Working model of pPORA import, LHPP assembly, and FLU-mediated regulation of Chl biosynthesis. Yellow circles and pentagons illustrate PORA-Pchl ide *b*-NADPH and PORB-Pchl ide *a*-NADPH ternary complexes, respectively. The ochre box highlights Oep16 as part of the Ptc complex. Proto IX, protoporphyrin IX.

during seedling de-etiolation and greening. Free Pchl ide not bound to the PORA, by contrast, operated as photosensitizer and, by triplet-triplet interchange, provoked singlet oxygen production and cell death. Similar observations have been made for photobleached *flu* plants (12). In a sense, these findings are reminiscent of genetically inherited porphyrias in humans where perturbations in heme metabolism trigger cell death, including nuclear condensation, chromatin separation, DNA breakdown, and release of cytochrome *c* from mitochondria into the cytosol (25). However, porphyrin-dependent, plastid-dependent cell death in plants also exhibits unique properties, as illustrated by recent work of Wagner *et al.* (26) on the *executer* mutant of *Arabidopsis*.

Our results suggest the working model described in Fig. 7, explaining the possible interaction of OEP16, PORA, and FLU during greening. Accordingly, PORA-Pchl ide *b*-NADPH ternary complexes not assembled into PORA:PORB suprastructures after import through OEP16 could provide the link to the FLU protein and help fine-tune the size of the prolamellar body. In wild-type plants, PORA would sense the amount of Pchl ide , and once enough LHPP is made, excess PORA-Pchl ide *b*-NADPH ternary complexes could bind to and block the activity of the FLU protein, thereby inhibiting glutamyl-tRNA reductase. By contrast, this negative feedback would no longer operate in the OEP16-deficient *Atoep16-1* mutant line because of the lack of imported PORA. It is clear that the intimate interaction of all players is required for successful greening. Any change in Pchl ide homeostasis has deleterious effects on plant growth.

Materials and Methods

Plant Growth. Seeds of the *Atoep16* line (SALK_024018) were obtained from the Salk Institute Genomic Analysis Laboratory collection (19). Seeds were germinated on half-concentrated Murashige-Skoog-agar medium on Petri dishes for 4.5 days. To trigger photooxidative damages, dark-grown seedlings were exposed to white light at 125 $\mu\text{E}\cdot\text{m}^{-2}$. Alternatively, seeds were germinated on soil and grown to maturity in continuous white light.

Pigment Measurements. High-performance liquid chromatography of acetone-extracted pigments was carried out by using a C18 reverse-phase silica gel column (Hypersil ODS, 5 μm ; Shandon HPLC, Cheshire, U.K.) and synthetic Pchl ides *a* and *b* as standards (5, 20). Pigments were detected and quantified at 455 nm, the Soret band of Pchl ide *b* (5, 20).

Analysis of Amino Acid Uptake into Isolated Plastids. Uptake of ^{14}C amino acids into isolated chloroplasts was monitored by using the filter paper disk method of Mans and Novelli (22). Pulse-labeling of chloroplast protein with [^{35}S]methionine (1.87 MBq per 50- μl assay, 37 TBq/mmol; Amersham Pharmacia, Uppsala, Sweden) was carried out according to Mullet *et al.* (23). Protein was extracted with trichloroacetic acid, depleted of chlorophyll, and washed and run on 10–20% SDS/polyacrylamide gradients (27). Protein detection was made by Coomassie staining and autoradiography or by Western blotting (28).

Protein Import Assay *in Vitro* and *in Planta*. Protein import into isolated *Arabidopsis* chloroplasts and etioplasts was studied as described by using cDNA-encoded, wheat germ-translated ^{35}S precursors (24). Briefly, ^{35}S precursors were synthesized from corresponding cDNA clones by coupled transcription/translation and incubated with isolated, energy-depleted *Arabidopsis* plastids from wild-type and *Atoep16-1* plants. Plastids were treated with thermolysin (29) after import to degrade unimported precursors. Chemical cross-linking of 5,5'-dithiobis(2-nitrobenzoic acid)-derivatized ^{35}S -transA-DHFR, consisting of the transit peptide of pPORA (transA) and a cytosolic dihydro-

folate reductase (DHFR) reporter protein of mouse, was carried out as described (17).

TransA-GFP derivatives were produced as described in *SI Methods*. Transient expression of TransA-GFP derivatives in *Arabidopsis* leaf epidermis cells was performed after ballistic bombardment by using a pneumatic particle inflow gun according to Finer *et al.* (30). The conditions of bombardment were adjusted to helium pressure of 6.5 bar, at a 12-cm target distance, with a disperse grid at 7 cm, using 1 μm of gold microcarriers (Bio-Rad, Hercules, CA). After bombardment, the plantlets were kept under sterile conditions and incubated for 24 h in darkness. Confocal laser scanning microscopy was carried out by using a LSM 510 Meta microscope (Zeiss, Jena, Germany) with krypton/argon laser excitation at 488 nm and an emission

wavelength window from 505 to 530 nm. LSM 510 Meta software release 3.2 (Zeiss, Oberkochen, Germany) and Photoshop 7 (Adobe Systems, San Jose, CA) were used for image acquisition and processing. Nondenaturing, analytical PAGE was carried out as described (31).

Miscellaneous. Electron microscopy was carried out by using ultrathin sections of leaf tissues prepared from etiolated plants using a Zeiss 109 electron microscope.

We are indebted to L. Reinbothe for editorial work. This work was supported by a Chaire d'Excellence research project grant from the French Ministry of Research (to C.R.). This is scientific paper no. 1201-06 from the College of Agricultural, Human, and Natural Resource Sciences of Washington State University.

1. von Wettstein D, Gough S, Kannangara CG (1995) *Plant Cell* 7:1039–1057.
2. Kirk JTO, Tilney-Basset RAE (1978) *The Plastids: Their Chemistry, Structure, Growth, and Inheritance* (Elsevier North-Holland Biomedical Press, Amsterdam).
3. Holtorf H, Reinbothe S, Reinbothe C, Bereza B, Apel K (1995) *Proc Natl Acad Sci USA* 92:3254–3258.
4. Reinbothe C, Lebedev N, Reinbothe S (1999) *Nature* 397:80–84.
5. Reinbothe S, Pollmann S, Reinbothe C (2003) *J Biol Chem* 278:807–815.
6. Rebeiz CA, Nandihalli UB, Velu J (1990) *Photochem Photobiol* 52:1099–1117.
7. Matringe M, Camadro JM, Labbe P, Scalla R (1989) *Biochem J* 260:231–235.
8. Mock H-P, Keetman U, Kruse E, Rank B, Grimm B (1998) *Plant Physiol* 116:107–116.
9. Beale SI, Weinstein JD (1990) in *Biosynthesis of Heme and Chlorophyll*, ed Dailey HA (McGraw-Hill, New York), pp 287–391.
10. Pontoppidan B, Kannangara CG (1994) *Eur J Biochem* 225:529–537.
11. Vothknecht UC, Kannangara CG, von Wettstein D (1998) *Phytochemistry* 47:513–519.
12. Meskauskiene R, Nater M, Gosling D, Kessler F, op den Camp R, Apel K (2001) *Proc Natl Acad Sci USA* 98:12826–12831.
13. Kahn A (1968) *Plant Physiol* 43:1781–1785.
14. Reinbothe S, Quigley F, Gray J, Schemenewitz A, Reinbothe C (2004) *Proc Natl Acad Sci USA* 101:2197–2202.
15. Reinbothe S, Runge S, Reinbothe C, van Cleve B, Apel K (1995) *Plant Cell* 7:161–172.
16. Reinbothe S, Reinbothe C, Holtorf H, Apel K (1995) *Plant Cell* 7:1933–1940.
17. Reinbothe S, Quigley F, Springer A, Schemenewitz A, Reinbothe C (2004) *Proc Natl Acad Sci USA* 101:2203–2208.
18. Aronsson H, Sohr K, Soll J (2000) *Biol Chem* 381:1263–1267.
19. Alonso JM, Stepanova AN, Leisse TJ, Kim CJ, Chen H, Shinn P, Stevenson DK, Zimmerman J, Barajas P, Cheuk R, *et al.* (2003) *Science* 301:653–657.
20. Reinbothe S, Pollmann S, Reinbothe C (2003) *J Biol Chem* 278:800–806.
21. Pohlmeier K, Soll J, Steinkamp T, Hinnah S, Wagner R (1997) *Proc Natl Acad Sci USA* 94:9504–9509.
22. Mans RJ, Novelli GD (1960) *Biochem Biophys Res Commun* 3:540–543.
23. Mullet JE, Klein RR, Grossman AR (1986) *Eur J Biochem* 155:331–338.
24. Reinbothe S, Pollmann S, Springer A, James RJ, Tichtinsky G, Reinbothe C (2005) *Plant J* 42:1–12.
25. Moore MR, McColl KEL, Rimington C, Goldberg SA (1990) *Disease of Porphyrin Metabolism* (Plenum, New York).
26. Wagner D, Przybyla D, Op den Camp R, Kim C, Landgraf F, Lee KP, Wursch M, Laloi C, Nater M, Apel K (2004) *Science* 306:1183–1185.
27. Laemmli UK (1970) *Nature* 227:680–685.
28. Towbin M, Staehelin T, Gordon J (1979) *Proc Natl Acad Sci USA* 76:4350–4354.
29. Cline K, Werner-Washburne M, Andrews J, Keegstra K (1984) *Plant Physiol* 75:675–678.
30. Finer JJ, Vain P, Jones MW, McMullen MD (1992) *Plant Cell Rep* 11:323–328.
31. Reinbothe S, Krauspe R, Parthier B (1990) *J Plant Physiol* 137:81–87.

Corrections

BIOPHYSICS AND COMPUTATIONAL BIOLOGY

Correction for “Site-directed spin labeling of a genetically encoded unnatural amino acid,” by Mark R. Fleissner, Eric M. Brustad, Tamás Kálai, Christian Altenbach, Duilio Cascio, Francis B. Peters, Kálmán Hideg, Peter G. Schultz, and Wayne L. Hubbell, which appeared in issue 51, December 22, 2009, of *Proc Natl Acad Sci USA* (106:21637–21642; first published December 7, 2009; 10.1073/pnas.0912009106).

The authors request that Sebastian Peuker be added to the author list between Kálmán Hideg and Peter G. Schultz and be credited with designing research and performing research. The online version has been corrected. The corrected author and affiliation lines, author contributions, and related footnotes appear below.

Mark R. Fleissner^{a,1}, Eric M. Brustad^{b,1,2}, Tamás Kálai^c, Christian Altenbach^a, Duilio Cascio^d, Francis B. Peters^b, Kálmán Hideg^e, Sebastian Peuker^e, Peter G. Schultz^{b,3}, and Wayne L. Hubbell^{a,3}

^aJules Stein Eye Institute and Department of Chemistry and Biochemistry, University of California, Los Angeles, CA 90095; ^bDepartment of Chemistry and the Skaggs Institute for Chemical Biology, The Scripps Research Institute, La Jolla, CA 92037; ^cInstitute of Organic and Medicinal Chemistry, University of Pécs, H-7624 Pécs, Hungary; ^dUCLA-DOE Institute for Genomics and Proteomics, University of California, Los Angeles, CA 90095-1570; and ^eCAESAR Research Center, Ludwig-Erhard-Allee 2, 53175 Bonn, Germany

Author contributions: M.R.F., E.M.B., S.P., P.G.S., and W.L.H. designed research; M.R.F., E.M.B., D.C., F.B.P., and S.P. performed research; T.K., C.A., and K.H. contributed new reagents/analytic tools; M.R.F., E.M.B., C.A., D.C., P.G.S., and W.L.H. analyzed data; and M.R.F., E.M.B., K.H., P.G.S., and W.L.H. wrote the paper.

www.pnas.org/cgi/doi/10.1073/pnas.1000908107

PHYSICS

Correction for “Onset of frictional slip by domain nucleation in adsorbed monolayers,” by Marco Reguzzoni, Mauro Ferrario, Stefano Zapperi, and Maria Clelia Righi, which appeared in issue 4, January 26, 2010, of *Proc Natl Acad Sci USA* (107:1311–1316; first published December 24, 2009; 10.1073/pnas.0909993107).

The authors note that, due to a printer’s error, the affiliation for Stefano Zapperi appeared incorrectly. It should have appeared as Institute for Scientific Interchange Foundation. The corrected affiliation line appears below. Additionally, the authors note that equation 8 appeared incorrectly in part. The corrected equation appears below.

^aConsiglio Nazionale delle Ricerche, Istituto Nazionale per la Fisica della Materia-S3 and Dipartimento di Fisica, Università di Modena e Reggio Emilia, Via G. Campi 213/A, I-41100, Modena, Italy; and ^bInstitute for Scientific Interchange Foundation, Viale San Severo 65, 10133 Turin, Italy

$$x - L/2 = \frac{a\sqrt{2B}}{\pi\sqrt{V_0\rho}} \frac{\log[\tan(\pi u/2a)]\sin(\pi u/a)}{\sqrt{1 - \cos(2\pi u/a)}}$$

www.pnas.org/cgi/doi/10.1073/pnas.1000842107

www.pnas.org

PLANT BIOLOGY

Correction for “A plant porphyria related to defects in plastid import of protochlorophyllide oxidoreductase A,” by Stephan Pollmann, Armin Springer, Frank Buhr, Abder Lahroussi, Iga Samol, Jean-Marc Bonneville, Gabrielle Tichtinsky, Diter von Wettstein, Christiane Reinbothe, and Steffen Reinbothe, which appeared in issue 6, February 6, 2007, of *Proc Natl Acad Sci USA* (104:2019–2023; first published January 29, 2007; 10.1073/pnas.0610934104).

The undersigned authors wish to note that: “We have been associated with part of the experimental work described therein, yet now disagree with the title and main conclusion of the article. (i) Among the backcrossed lines homozygous for oep16-1 T-DNA insertion that we reanalyzed after publication, one did not show a bleaching phenotype during de-etiolation. Another line showed bleaching of etiolated seedlings upon light exposure, yet displayed wildtype levels of the PORA protein by Western blotting, in its processed form (e.g., mature, imported into etioplasts). The flu-like bleaching phenotype in part of the descent of this oep16-1 mutant stock therefore appears unlinked with the lack of OEP16-1 expression or with a defect in PORA import, in accordance with the recent report of Pudelski et al. (2009) [PNAS 106:12201–12206]. (ii) We were never granted access to the complete set of original data, in particular to those supporting Figs. 2G, 4 C and D, and 6B. Therefore, we wonder about the quality of the underlying work and have expressed doubts concerning what is concluded from these pictures. It must also be made clear that the flu mutant used is not a published allele but contains a T-DNA insertion (SALK_002383) and displays a weak phenotype.”

Jean-Marc Bonneville
Gabrielle Tichtinsky

www.pnas.org/cgi/doi/10.1073/pnas.1001005107

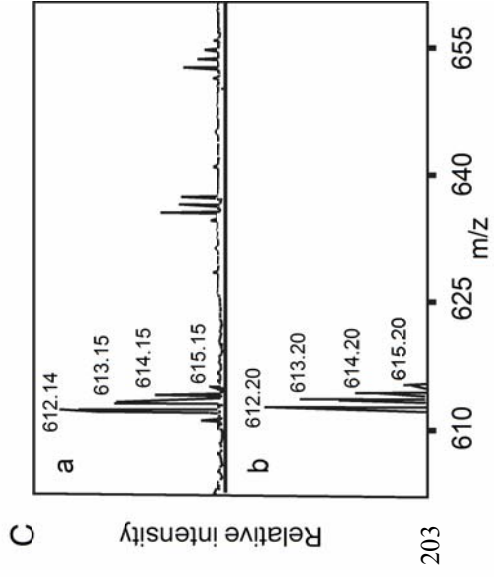
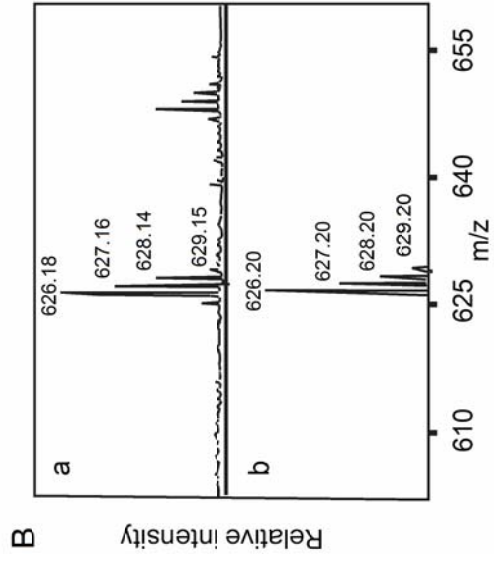
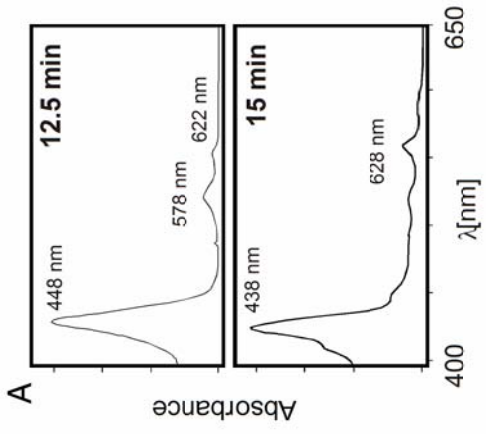
PLANT BIOLOGY

Correction for “A plant porphyria related to defects in plastid import of protochlorophyllide oxidoreductase A,” by Stephan Pollmann, Armin Springer, Frank Buhr, Abder Lahroussi, Iga Samol, Jean-Marc Bonneville, Gabrielle Tichtinsky, Diter von Wettstein, Christiane Reinbothe, and Steffen Reinbothe, which appeared in issue 6, February 6, 2007, of *Proc Natl Acad Sci USA* (104:2019–2023; first published January 29, 2007; 10.1073/pnas.0610934104).

The undersigned authors wish to note that: “We confirm that we are confident in the data and conclusions in the published article.”

Stephan Pollmann
Armin Springer
Frank Buhr
Abder Lahroussi
Iga Samol
Diter von Wettstein
Christiane Reinbothe
Steffen Reinbothe

www.pnas.org/cgi/doi/10.1073/pnas.1001007107



Singlet oxygen-dependent translational control in the *tigrina-d.12* mutant of barley

Dhriti Khandal^a, Iga Samol^a, Frank Buhr^a, Stephan Pollmann^b, Holger Schmidt^c, Stephan Clemens^c, Steffen Reinbothe^a, and Christiane Reinbothe^{c,1}

^aUniversité Joseph Fourier, CERMO, PO Box 53, F-38041 Grenoble Cedex 9, France; ^bLehrstuhl für Pflanzenphysiologie, Ruhr-Universität Bochum, Universitätsstrasse 150, D-44801 Bochum, Germany; and ^cLehrstuhl für Pflanzenphysiologie, Universität Bayreuth, Universitätsstrasse 30, D-95447 Bayreuth, Germany

Edited by Diter von Wettstein, Washington State University, Pullman, WA, and approved May 29, 2009 (received for review April 2, 2009)

The *tigrina* (*tig*)-*d.12* mutant of barley is impaired in the negative control limiting excess protochlorophyllide (Pchl_{id}) accumulation in the dark. Upon illumination, Pchl_{id} operates as photosensitizer and triggers singlet oxygen production and cell death. Here, we show that both Pchl_{id} and singlet oxygen operate as signals that control gene expression and metabolite accumulation in *tig-d.12* plants. In vivo labeling, Northern blotting, polysome profiling, and protein gel blot analyses revealed a selective suppression of synthesis of the small and large subunits of ribulose-1,5-bisphosphate carboxylase/oxygenase (RBCs and RBCLs), the major light-harvesting chlorophyll *a/b*-binding protein of photosystem II (LHCB2), as well as other chlorophyll-binding proteins, in response to singlet oxygen. In part, these effects were caused by an arrest in translation initiation of photosynthetic transcripts at 80S cytoplasmic ribosomes. The observed changes in translation correlated with a decline in the phosphorylation level of ribosomal protein S6. At later stages, ribosome dissociation occurred. Together, our results identify translation as a major target of singlet oxygen-dependent growth control and cell death in higher plants.

cell death | photooxidative stress | ribosome structure | S6 phosphorylation | ribosome dissociation

The biosynthesis of chlorophyll (Chl) is a light-dependent reaction in angiosperms (1). Several independent mechanisms regulate the activity of the C5 pathway leading to Chl. The first regulatory circuit operates at the level of 5-aminolevulinic acid (5-ALA) synthesis. Expression of key enzymes of 5-ALA synthesis is depressed in dark-grown plants (2, 3). Moreover, a negative feedback loop exerted by heme and protochlorophyllide (Pchl_{id}) at the level of glutamyl-tRNA reductase (4, 5) reduces 5-ALA synthesis in the dark. Another factor was recently identified to be the FLUORESCENT (FLU) protein (6).

The *tigrina* (*tig*)-*d.12* locus of barley is orthologous to the *flu* locus in *Arabidopsis thaliana* (7, 8). The *tig-d.12* is a conditional cell death mutant. When *tig-d.12* plants are grown in continuous white light, they are fully viable and do not show any signs of damage. However, *tig-d.12* seedlings develop transverse-striped leaves with green and white sectors under alternate light/dark cycles. Free Pchl_{id} synthesized in the dark operates as photosensitizer and, by triplet-triplet interchange, provokes singlet oxygen production and photooxidative damages during subsequent light periods, whereas the pigment is continuously converted to chlorophyllide by virtue of the NADPH:protochlorophyllide oxidoreductase in leaf sectors emerging during the light period (7). Similarly, etiolated *tig-d.12* seedlings accumulate excessive amounts of Pchl_{id} and die rapidly when illuminated (7). Cell death triggered in *flu* and, presumably, also in *tig-d.12* plants is a combined effect of the cytotoxic properties of singlet oxygen and the operation of a genetic pathway involving the *EXECUTER 1* and *EXECUTER 2* genes (9, 10). Transcription of singlet oxygen-responsive genes has been reported previously (11). Whether translation also may contribute to singlet oxygen-triggered growth control and cell death was thus far undetermined, and this motivated us to perform the current study. In animals and humans, translation is a major target for cell size and

growth control as well as programmed cell death and apoptosis (12–14). In the present work, we report on changes in transcript accumulation, translation, and metabolite profiles in *tig-d.12* plants in response to singlet oxygen.

Results

Pchl_{id}-Dependent and Singlet Oxygen-Dependent Changes in Protein Synthesis in *tig-d.12* and Wild-Type Plants. Seedlings of *tig-d.12* and wild-type were grown in the dark for 5 days and exposed to white light of approximately 125 micro-Einsteins ($\approx 125 \mu\text{E}$) $\text{m}^{-2} \text{sec}^{-1}$ for variable periods. To see whether or not *tig-d.12* plants would respond to illumination with the generation of singlet oxygen, DanePy measurements were carried out (15–17). The DanePy reagent is a dansyl-based singlet oxygen sensor whose green fluorescence is quenched upon reacting with singlet oxygen. Fig. 1 shows that irradiation of etiolated *tig-d.12* plants gave rise to generation of singlet oxygen. Singlet oxygen production was linear for at least 1 h in *tig-d.12* plants, and then it reached a plateau. The linear relationship between singlet oxygen generation and time in the early period of irradiation excluded the possibility that the nitroxide radicals formed from DanePy were partly reduced and transformed into inactive states in the samples (17). At later stages, DanePy may be converted into an inactive state or disintegrate spontaneously. On the other hand, singlet oxygen production may cease because of the destruction of Pchl_{id} operating as a photosensitizer. It has been reported that photooxidative stress easily leads to a rapid pigment bleaching (18). In wild-type seedlings, no singlet oxygen production was measurable over the time course of the experiment (Fig. 1).

Next, pulse labeling of protein with [³⁵S]methionine was carried out for 2 h before seedling harvest. Fig. 2 shows that already in the dark, differences occurred in the polypeptide patterns of wild-type and *tig-d.12* plants. Reductions in the synthesis and accumulation were observed for the large and small subunits of ribulose-1,5-bisphosphate carboxylase/oxygenase (RBCL and RBCS gene products). These differences were further enhanced upon illumination. After 2 h of irradiation, a number of proteins were synthesized in *tig-d.12* plants that were weakly labeled in wild-type plants (Fig. 2). Protein gel blot analyses revealed that Chl-binding proteins, such as LHCB2, D1, and D2, which encode major components of photosystem II, did not accumulate in irradiated *tig-d.12* seedlings (Fig. 3). By contrast, stress-induced proteins, such as allene oxide synthase (AOS), a key enzyme of jasmonic acid (JA) biosynthesis, and other, major jasmonate-induced proteins, such as JIP5 (thionin)

Author contributions: C.R. designed research; D.K., I.S., F.B., S.P., H.S., S.C., S.R., and C.R. performed research; D.K., I.S., F.B., S.P., H.S., S.C., and S.R. analyzed data; and C.R. wrote the paper.

The authors declare no conflict of interest.

This article is a PNAS Direct Submission.

¹To whom correspondence should be addressed. E-mail: christiane.reinbothe@uni-bayreuth.de.

This article contains supporting information online at www.pnas.org/cgi/content/full/0903522106/DCSupplemental.

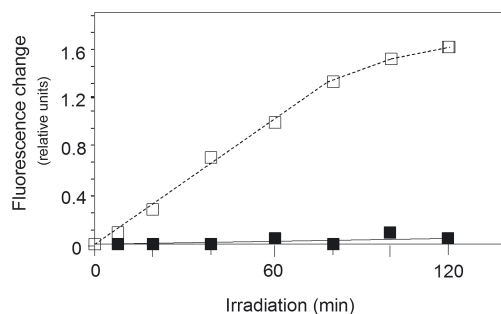


Fig. 1. Singlet oxygen production in dark-grown *tig-d.12* and wild-type seedlings after irradiation. The *tig-d.12* and wild-type seedlings were grown in the dark for 5 days. Then, DanePy was applied to the leaf tissues by infiltration. For estimation of singlet oxygen levels on an equal leaf surface area, singlet oxygen trapping was measured as relative fluorescence quenching at the 532-nm emission maximum of DanePy. The curves show fluorescence quenching in leaf tissues of irradiated *tig-d.12* (□) and wild-type (■) seedlings.

and JIP23, were present both in *tig-d.12* and wild-type plants, although their amounts were different after 12 h of greening (Fig. 3). When etiolated *tig-d.12* seedlings were exposed to white light for periods longer than 24 h, total protein synthesis dropped to undetectable levels (data not shown).

Metabolite Profiles of *tig-d.12* and Wild-Type Plants. In order to gain insight into singlet oxygen-dependent changes in gene expression, a metabolite-profiling approach was taken. Methanol extracts were prepared from *tig-d.12* and wild-type plants and subjected to ultraperformance liquid chromatography/electrospray ionization/quadrupole time-of-flight mass spectrometry (UPLC-ESI-QTOF-MS) analyses. This profiling approach is capable of resolving several hundred to a few thousand features (mass-retention time pairs)—i.e., metabolites or their

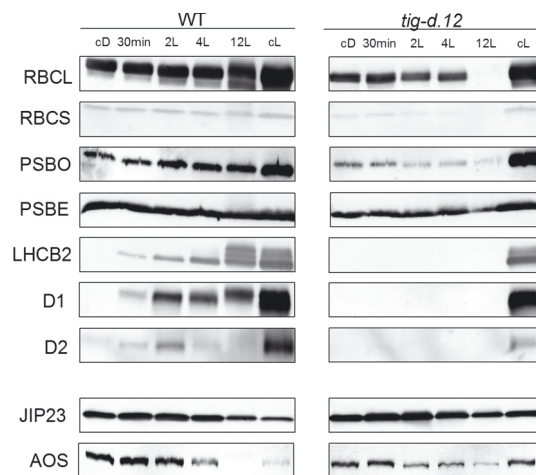


Fig. 3. Western blot analysis of abundant photosynthetic proteins in etiolated *tig-d.12* and wild-type plants after different lengths of irradiation with white light of $125 \mu\text{E m}^{-2} \text{sec}^{-1}$. RBCL and RBCS, large and small subunits of ribulose-1,5-bisphosphate carboxylase/oxygenase, respectively; PSBO and PSBE, O and E subunits of photosystem II, respectively; LHCB2, light-harvesting chlorophyll *a/b*-binding protein 2 of photosystem II; D1 and D2, reaction center polypeptides of photosystem II; JIP23, jasmonate-induced 23-kDa protein; AOS, allene oxide synthase.

mass fragments—in one run (19–21). Studies carried out for *A. thaliana* have shown that this method can resolve known classes of *Arabidopsis* secondary metabolites, such as indole-derived compounds (e.g., indole acetic acid derivatives), degradation products of glucosinolates (sulfinyl nitriles and isothiocyanates), phenylpropanoids (sinapoylmalate), and flavonoids, as well as their glycosides (e.g., kaempferol-3-*O*- α -L-rhamnopyranosid-7-*O*- α -L-rhamnopyranosid) (19). The individual metabolite pro-

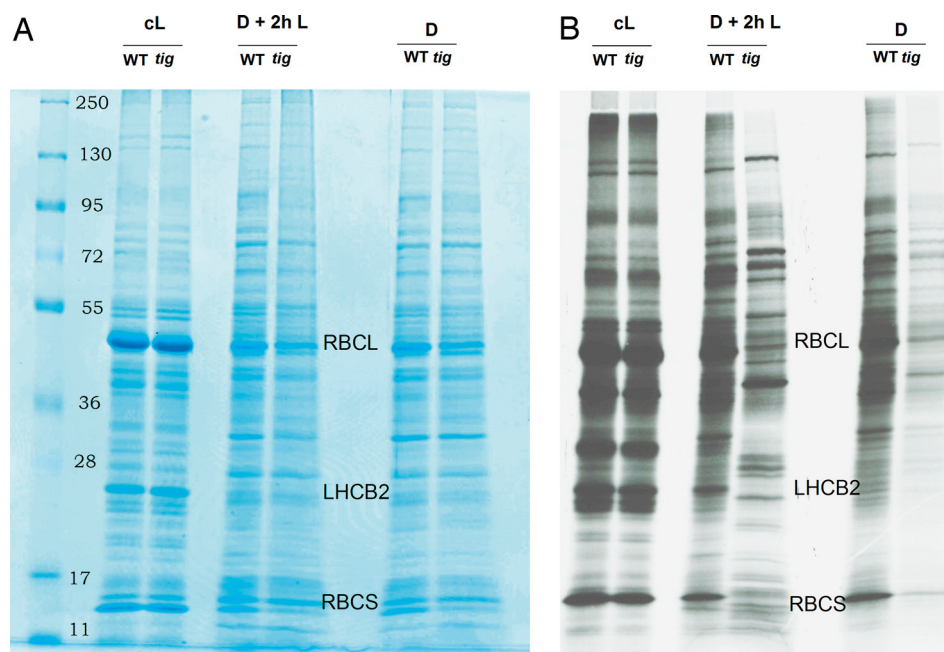


Fig. 2. Pchl_a- and singlet oxygen-dependent changes in the protein patterns of etiolated and irradiated *tig-d.12* and wild-type plants. (A) Pattern of Coomassie-stained proteins in dark-grown *tig-d.12* and wild-type seedlings (D) and in etiolated *tig-d.12* and wild-type seedlings that had been exposed to white light of $125 \mu\text{E m}^{-2} \text{sec}^{-1}$ for 2 h before harvest (D + 2h L). For comparison, the pattern of proteins is shown for *tig-d.12* and wild-type seedlings that had been cultivated in continuous white light for 5 days (cL). (B) As in A, but depicting the patterns of [³⁵S]methionine-labeled proteins. Positions of molecular mass markers are highlighted. RBCL and RBCS designate the large and small subunits of ribulose-1,5-bisphosphate carboxylase/oxygenase; LHCB2 designates the light-harvesting chlorophyll *a/b*-binding protein 2 of photosystem II.

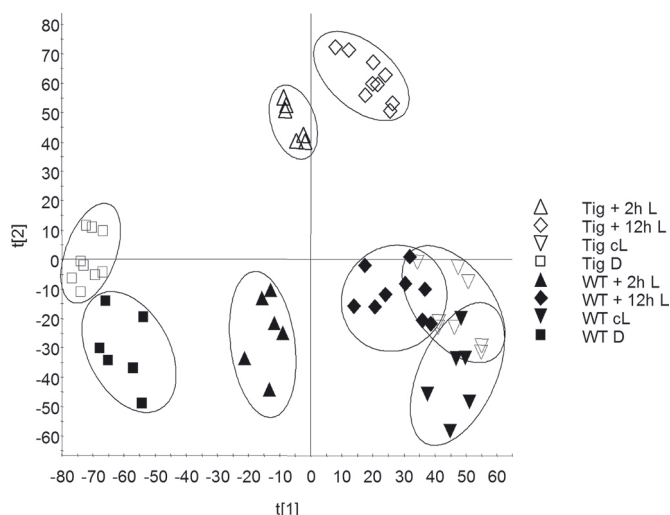


Fig. 4. Compilation of changes in the metabolite levels of etiolated *tig-d.12* and wild-type seedlings after irradiation. PCA (scores plot) of the metabolite profiles obtained in the positive ionization mode, illustrating the overall metabolic differences between *tig-d.12* and wild-type plants, depending on the light conditions.

files obtained for barley wild-type and *tig-d.12* plants were compared by principal component analysis (PCA), a data reduction and visualization technique (22). Fig. 4 and Fig. S1 depict the overall similarity/dissimilarity of the respective entities for etiolated, irradiated, and light-grown *tig-d.12* and wild-type seedlings. A pairwise orthogonal partial least-squares to latent structures analysis of *tig-d.12* and wild-type samples allowed the identification of markers that significantly contribute to the separation of the groups (cL, D, and 2-h L). The entries were sorted according to their covariance (magnitude) and correlation (reliability) (23). In summary, the metabolite profiles of *tig-d.12* plants grown under continuous light closely resembled those of the corresponding wild-type plants. However, marked differences occurred between dark-grown *tig-d.12* and wild-type plants. These differences were further pronounced when etiolated *tig-d.12* and wild-type seedlings were irradiated.

Depression of Nucleus-Encoded Photosynthetic Transcripts in *tig-d.12* Versus Wild-Type Plants. To assess whether the observed large differences in the in vivo-labeling pattern of proteins in *tig-d.12* versus wild-type plants were caused by corresponding changes of their respective mRNAs, in vitro translation experiments were carried out. A rabbit reticulocyte lysate was programmed with mRNA prepared from etiolated *tig-d.12* and wild-type plants that had been exposed to white light for 2 h. Fig. 5A shows that this approach did not reveal gross differences in the patterns of translatable mRNAs for irradiated *tig-d.12* and wild-type plants. Northern blot analyses showed that *RBCS* mRNA was reduced in amount in mutant compared with wild-type plants both in the dark and after illumination (Fig. 5B). In either case, this reduction in *RBCS* synthesis was much lower than that measured in vivo (compare with Fig. 2). *LHCB2* transcript levels were drastically reduced and were in most experiments below the limit of detection, and no *LHCB2* protein accumulated in irradiated *tig-d.12* seedlings (Figs. 3 and 5). When light-grown *tig-d.12* plants were subjected to a nonpermissive 12-h dark to 12-h light shift, reductions in the synthesis of *RBCS* and *LHCB2* similar to those reported for etiolated plants were observed, whereas only little changes were detectable in the pattern of in vitro-translatable mRNAs (Fig. S2). DanePy measurements con-

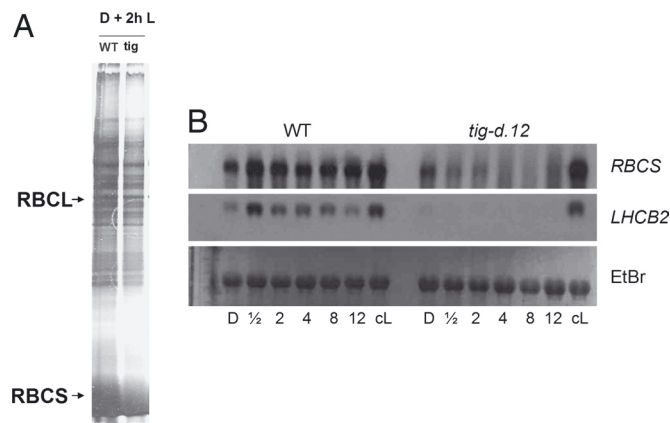


Fig. 5. mRNA levels in etiolated *tig-d.12* and wild-type plants after a 2-h light shift. (A) Patterns of polypeptides translated in a rabbit reticulocyte lysate from RNA of 2-h irradiated *tig-d.12* and wild-type plants. RBCL and RBCS mark the large and small subunits of ribulose-1,5-bisphosphate carboxylase/oxygenase, respectively. (B) Northern blot analysis of *RBCS* and *LHCB2* transcript levels in dark-grown and irradiated *tig-d.12* and wild-type plants after different periods of illumination. The lower part shows the ethidium bromide (EtBr)-stained 28S rRNA used as loading control.

firmed singlet oxygen production in response to the 12-h dark to 12-h light shift (Fig. S3).

Polysome Binding of Stress and Defense Versus Photosynthetic Messengers in *tig-d.12* and Wild-Type Plants.

The drastic reduction in *RBCS* synthesis in vivo and only moderate reduction in the level of its respective messenger in vitro in *tig-d.12* seedlings subjected to nonpermissive dark-to-light shifts suggested a posttranscriptional mode of control. To explore this possibility, polysomes were isolated from etiolated and illuminated *tig-d.12* and wild-type plants and were subjected to sucrose density gradient centrifugation. Ribonucleoprotein (RNP) material contained in the different fractions was recovered by ethanol precipitation and used for Northern blot hybridization and in vitro translation. In parallel, *RBCS*, *AOS*, thionin, and actin protein levels present in the different polysomal fractions were quantified by Western blotting using large-scale polysome preparations. Thionins are small fungitoxic proteins localized in the plant cell wall that accumulate in etiolated plants and reappear in illuminated plants in response to pathogens and adverse conditions (24). *AOS* encodes a key enzyme of JA biosynthesis; its expression is induced after abiotic and biotic stress (summarized in ref. 25).

Fig. 6A shows absorbance profiles of RNP material that had been extracted from etiolated *tig-d.12* and wild-type plants after 2 h of irradiation. Based on the absorbance readings, no major difference was apparent in the polysome profiles. However, upon analyzing individual polysomal fractions by Western blotting, a massive reduction in polysome binding of *RBCS* transcripts was found for *tig-d.12* seedlings. *RBCS* transcripts, in fact, were confined to smaller polysomes in irradiated *tig-d.12* plants compared with wild-type seedlings (Fig. 6B). This result suggested a depression in translation initiation to occur in *tig-d.12* plants in response to singlet oxygen. Similarly, *RBCS* transcript binding to polysomes was reduced in 4.5-day-old, light-grown *tig-d.12* plants that had been subjected to a 12-h dark to 12-h light shift (Fig. S4). This effect correlated with the observed drop in *RBCS* synthesis but was at variance with the unchanged level of translatable *RBCS* mRNA in vitro (Fig. S2). Both etiolated and light-adapted *tig-d.12* seedlings reacted to nonpermissive conditions causing singlet oxygen production with similar dissociations of their 80S cytoplasmic polysomes into the respective ribosomal subunits when the illumination period was extended to 24 h (Fig. 7 and Fig. S5).

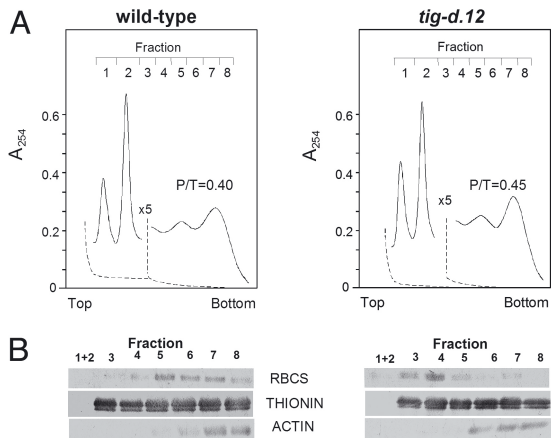


Fig. 6. Polysome profiles of dark-grown *tig-d.12* and wild-type plants after a 2-h white light exposure. RNP material was extracted from irradiated *tig-d.12* and wild-type seedlings and resolved on sucrose gradients. (A) Absorbance readings at 254 nm of polysomes (fractions 3–8) and the 40S and 60S ribosomal subunits (fractions 1 and 2). A 5-fold decrease in full-scale absorbance is indicated by a break in the absorbance tracing of each profile. Dashed lines represent baselines. The top of the gradients is to the left. Note that absorbance at the top of the gradient is not included because of the high absorbance of Triton X-100. (B) Western blot used to determine RBCS, THIONIN, and ACTIN protein levels in the different polysomal fractions. The P/T ratios are given.

S6 Dephosphorylation in *tig-d.12* and Wild-Type Plants. Ribosomal protein S6 is a major mediator of translational control and changes its phosphorylation state under a variety of adverse conditions in animals and plants (26–28). To determine whether singlet oxygen may trigger changes in S6 phosphorylation, pulse-labeling studies were carried out with [³²P]phosphate. Leaf tissues were incubated with [³²P]phosphate; then, ribosomes were isolated, and their phosphoprotein pattern was analyzed by 1D and 2D SDS/PAGE. Fig. 8 shows the phosphory-

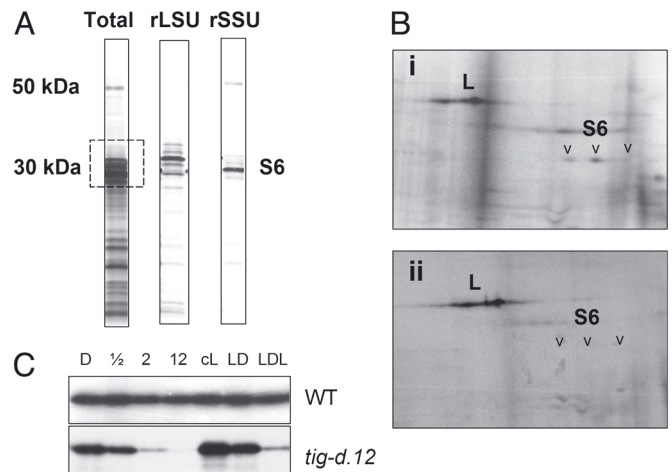


Fig. 8. Ribosomal protein S6 dephosphorylation in irradiated *tig-d.12* plants. (A) 1D pattern of ³²P-labeled proteins present in total ribosomes (Total) and in large (rLSU) and small (rSSU) ribosomal subunits isolated from 5-day-old, dark-grown wild-type plants. (B) 2D pattern of ribosomal ³²P-labeled proteins in dark-grown wild-type seedlings (Bi) and *tig-d.12* seedlings (Bii) after a 4-h period of irradiation. The autoradiogram shows ³²P-labeled proteins of the molecular mass range boxed in A. Arrowheads mark ribosomal protein S6 isoforms. (C) S6 dephosphorylation in dark-grown *tig-d.12* and wild-type (WT) plants after various periods of irradiation (in hours) and in light-adapted plants before (cL) and after a 12-h dark (LD) and subsequent 12-h light (LDL) shift.

lation status of ribosomal protein S6 for etiolated wild-type and *tig-d.12* plants after different periods of irradiation. The results revealed a decline in the phosphorylation of S6 in *tig-d.12* but not wild-type plants (Fig. 8 B and C). When light-grown *tig-d.12* seedlings were exposed to a 12-h dark to 12-h light shift, a similar decline in the phosphorylation level of S6 became apparent (Fig. 8C, LDL).

Discussion

In the present work, changes occurring at the transcript, translational, and metabolite levels in response to Pchl_{ide} and singlet oxygen were analyzed for the *tig-d.12* mutant of barley. We show that dark-grown *tig-d.12* seedlings synthesize a pattern of polypeptides and metabolites that is distinct from that of wild-type plants. Lower levels of *RBCS* and *LHCB2* transcripts were found on Northern blots. It is likely that Pchl_{ide} operated as a signal that affected the expression of nuclear genes. Also, other tetrapyrroles have documented effects on transcription of nucleus-encoded genes for plastid proteins (29–34).

Once illuminated, Pchl_{ide} accumulating in dark-grown *tig-d.12* seedlings operated as a photosensitizer and provoked generation of singlet oxygen. Both Pchl_{ide} synthesis and singlet oxygen production appear to be confined to the plastid compartment in irradiated *tig-d.12* plants and *flu* (11) plants, suggesting the presence of intermediates that leave the plastid to control gene expression in the nucleocytoplasmic space. Given that the plastid envelope is a site of Pchl_{ide} synthesis (35, 36), it seems likely that membrane-derived signals, such as oxygenated fatty acid derivatives, including JA (see below), function in the complex signaling network controlling protein synthesis at 80S ribosomes. As shown here, polysomes isolated from etiolated *tig-d.12* plants that had been irradiated for 2 h contained fewer *RBCS* transcripts than polysomes from wild-type plants. These *RBCS* transcripts were confined to smaller polysomes, suggesting a depression of translation initiation occurs in response to singlet oxygen. Because translation initiation is rate-limiting for protein synthesis under most physiological conditions (37, 38), we exclude an effect of singlet oxygen on translation elongation of *RBCS* transcripts in irradiated

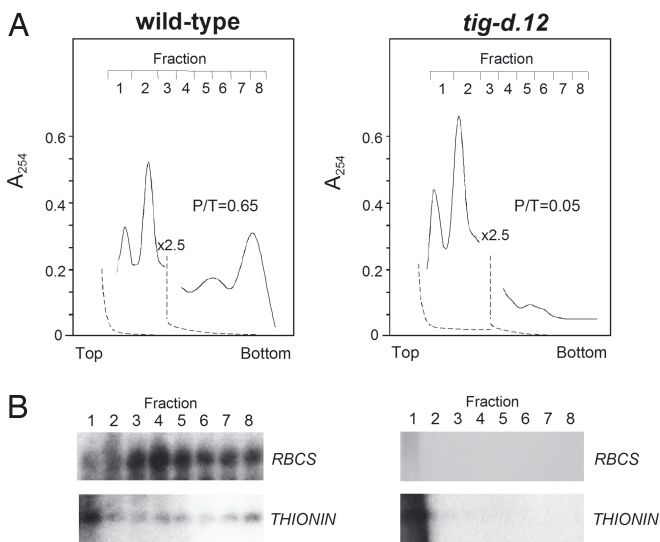


Fig. 7. Polysome profiles of dark-grown *tig-d.12* and wild-type plants after a 24-h white light shift. RNP material was extracted from irradiated *tig-d.12* and wild-type seedlings and resolved in sucrose gradients. (A) Absorbance tracings at 254 nm of polysomes (fractions 3–8) and the 40S and 60S ribosomal subunits (fractions 1 and 2). A 2.5-fold decrease in full-scale absorbance is indicated by a break in the absorbance tracing of each profile. Dashed lines represent baselines. The top of the gradients is to the left. Note that absorbance at the top of the gradient is not included because of the high absorbance of Triton X-100. (B) Northern blot analysis used to determine *RBCS* and *THIONIN* transcript levels in the different polysomal fractions. P/T ratios are indicated.

tig-d.12 plants. In line with this view, *THIONIN* and *AOS* transcripts were equally distributed to small and large polyosomes and gave rise to protein.

Singlet oxygen is both a powerful cytotoxin and a potent signaling compound (6, 9–11, 39, 40). Pioneering work performed by Apel and coworkers (see ref. 41 for review) for the *flu* mutant has provided valuable insights into the complexity of cell death regulation by singlet oxygen and other reactive oxygen species. Transcriptome analyses identified genes that differentially responded to singlet oxygen and hydrogen peroxide (11, 42). Among the genes specifically induced by singlet oxygen were those for ERF/AP2, MYB, WRKY and other transcription factors, calmodulin-like proteins, and the ENHANCED DISEASE SUSCEPTIBILITY 1 and BONZAI 1 proteins, 2 key components operating in defense signaling and growth control (11, 43). Genes that were down-regulated by singlet oxygen included those for components operating in auxin synthesis and transport, as well as constituents of the photosynthetic apparatus (11).

The results presented in this work add to the understanding of singlet oxygen action in higher plants and reveal its role in the regulation of translation. We show that singlet oxygen can provoke a rapid dephosphorylation of ribosomal protein S6. Whether this is a direct effect caused by the cytotoxicity of singlet oxygen or an indirect effect caused by the operation of specific signaling pathways is unknown. Precedents for photodynamic regulation of protein synthesis exist in the literature. For example, Yang and Hooper (44) reported on a Ca²⁺-dependent, 14-kDa surface protein in the bacterium *Arthrobacter photogonimus* that was inactivated under photodynamic conditions provoking the generation of singlet oxygen. The 14-kDa protein operates as repressor of the light-inducible *lipA* gene (45). Removal of the 14-kDa protein constitutively activated *lipA* expression in the dark (44). For irradiated *tig-d.12* plants, two possible explanations of how singlet oxygen may act on translation are (i) inhibition of S6 and upstream TOR or NPDK1 kinases, or (ii) activation of protein phosphatases dephosphorylating S6. Both reactions are prone to adverse conditions (46–48) and may involve Ca²⁺ and calmodulin-like proteins to be explored in future work.

A third, remarkable result of this study is the demonstration of ribosome dissociation occurring in *tig-d.12* plants in response to singlet oxygen. This result is reminiscent of our previous findings for leaf tissues of barley treated with the methyl ester of JA, methyl jasmonate (49–51). Endogenous JA accumulates under various stress conditions, such as heat shock, UV light exposure, and desiccation, as well as in response to wounding and bacterial and fungal pathogens (see ref. 25 for review). Singlet oxygen rapidly activates the expression of JA biosynthetic genes, such as those for lipoxygenase, AOS, and allene oxide cyclase, and thereby boosts JA generation in *flu* plants (52, 53). It is therefore attractive to suppose a role of JA in reprogramming translation in response to singlet oxygen. Work is underway to dissect the mechanism of singlet oxygen-dependent translational control in higher plants.

Materials and Methods

Plant Growth. The *tig-d.12* mutant has been described previously (7). *Tig-d.12* and wild-type seeds were germinated on moist vermiculite under the follow-

ing conditions. In a first set of experiments, seedlings were grown in the dark for 5 days and exposed to white light (125 μE m⁻² sec⁻¹), provoking singlet oxygen production. In a second set of experiments, seedlings were germinated for 4.5 days in continuous white light and subsequently subjected to a 12-h dark shift before being reilluminated. As controls, wild-type seedlings were treated identically.

Singlet Oxygen Measurements. Singlet oxygen generation was measured with the DanePy method developed by Hideg et al. (15) and Kálai et al. (16, 17). Fluorescence emission spectroscopy was performed at an excitation wavelength of 330 nm and collecting fluorescence emission between 515–550 nm using a spectrometer (model LS50; Perkin-Elmer).

Protein Analyses. Pulse labeling of protein was carried out with [³⁵S]methionine (37 TBq/mmol; Amersham-Pharmacia) for 2 h before seedling harvest. After extraction, leaf protein was precipitated with trichloroacetic acid and subjected to SDS/PAGE on 10–20% polyacrylamide gradients (46, 47). Immunodetection of electrophoretically resolved proteins (54) was carried out by using an enhanced chemiluminescence system (Amersham-Pharmacia) and the indicated antisera that were obtained from Agrisera.

RNA Analyses. Total RNA was prepared from leaf segments by phenol/chloroform/isoamyl alcohol extraction (49). After precipitation with lithium chloride, high-molecular mass RNAs were translated into polypeptides in a rabbit reticulocyte system or wheat germ system. Assays for 1D and 2D polyacrylamide gel electrophoresis contained 11.2 MBq L-[³⁵S]methionine (37 TBq mmol⁻¹; Amersham-Pharmacia). For Northern blotting, RNA was separated on agarose gels and transferred onto nitrocellulose membranes (BA-45; Schleicher and Schuell) before being hybridized with [³²P]dATP-labeled and [³²P]dCTP-labeled cDNA probes under high-stringency conditions (49).

Polysome Isolation and Analysis. Polysomes were isolated by Mg²⁺ precipitation and sucrose density gradient centrifugation as described previously (49). Details on the buffers and conditions used can be found in the *SI Methods*. After centrifugation at 60,000 rpm in a Beckman Spinco L75 centrifuge, rotor Ti 60, for 1 h at 4 °C, the gradient was harvested from bottom to top in a modified Beckman harvesting device, with continuous monitoring of the absorbance at 254 nm (2138 Uvicord S; LKB). After integration of the areas below the curves, the ratio of polysomes to total ribosome (P/T) was calculated as follows: (area of polysomes)/(area of polysomes + ribosomal subunits + monosomes). From the arbitrarily defined gradient fractions, each corresponding to 10 drops (≈0.35 mL), the RNAs were recovered by ethanol precipitation and subsequently used for Northern blot hybridization or in vitro translation (see above). In parallel assays, protein was extracted from the polysomal fractions with trichloroacetic acid and washed extensively with ethanol and diethyl ether. All of these operations were performed at 4 °C. Ribosomal protein phosphorylation was studied as described by Scharf and Nover (46) and Nover and Scharf (47) by using [³²P]phosphate as tracer. The 2D electrophoresis of ³²P-labeled ribosomal proteins included isoelectric focusing in the first dimension and SDS/PAGE on 10–20% polyacrylamide gradients in the second dimension. Basic ribosomal proteins were separated by the Kaltschmidt-Wittmann technique that is described in ref. 46.

Metabolite Profiling. Plant material was essentially extracted as described previously and subjected to UPLC-ESI-QTOF-MS analyses (19–21). Signals from 0.5 to 16 min within 80 to 1,000 Da were taken into account. Based on these discriminatory markers (i.e., mass–retention time pairs), PCA and partial least-squares to latent structures were performed.

ACKNOWLEDGMENTS. We are grateful to K. Kálai and E. Hideg (Institute for Plant Biology, Biological Research Centre, Hungarian Academy of Sciences, Szeged, Hungary) for a gift of the DanePy reagent. This study was supported by the Chaire d'Excellence program of the French Ministry of Research (C.R.).

1. von Wettstein D, Gough S, Kannangara CG (1995) Chlorophyll biosynthesis. *Plant Cell* 7:1039–1057.
2. Batschauer A, Apel K (1984) An inverse control by phytochrome of the expression of two nuclear genes in barley (*Hordeum vulgare* L.). *Eur J Biochem* 143:593–597.
3. Huq E, et al. (2004) Phytochrome-interacting factor 1 is a critical bHLH regulator of chlorophyll biosynthesis. *Science* 305:1937–1941.
4. Pontoppidan B, Kannangara CG (1994) Purification and partial characterisation of barley glutamyl-tRNA(Glu) reductase, the enzyme that directs glutamate to chlorophyll biosynthesis. *Eur J Biochem* 225:529–537.
5. Vothknecht U, Kannangara CG, von Wettstein D (1998) Barley glutamyl tRNA(Glu) reductase: Mutations affecting haem inhibition and enzyme activity. *Phytochemistry* 47:513–519.
6. Meskauskiene R, et al. (2001) FLU: A negative regulator of chlorophyll biosynthesis in *Arabidopsis thaliana*. *Proc Natl Acad Sci USA* 98:12826–12831.
7. von Wettstein D, Kahn A, Nielsen OF, Gough S (1974) Genetic regulation of chlorophyll synthesis analyzed with mutants in barley. *Science* 184:800–802.
8. Lee KP, Kim C, Lee DW, Apel K (2002) TIGRINA d, required for regulating the biosynthesis of tetrapyrroles in barley, is an ortholog of the FLU gene of *Arabidopsis thaliana*. *FEBS Lett* 553:119–124.

9. Wagner D, et al. (2004) The genetic basis of singlet oxygen-induced stress responses of *Arabidopsis thaliana*. *Science* 306:1183–1185.
10. Lee KP, Kim C, Landgraf F, Apel K (2007) *EXECUTER1*- and *EXECUTER2*-dependent transfer of stress-related signals from the plastid to the nucleus of *Arabidopsis thaliana*. *Proc Natl Acad Sci USA* 104:10270–10275.
11. op den Camp RG, et al. (2004) Rapid induction of distinct stress responses after the release of singlet oxygen in *Arabidopsis*. *Plant Cell* 15:2320–2332.
12. Bommer UA, Thiele BJ (2004) The translationally controlled tumour protein (TCTP). *Int J Biochem Cell Biol* 36:379–385.
13. Kozma SC, Thomas G (2002) Regulation of cell size in growth, development and human disease: PI3K, PKB and S6K. *BioEssays* 24:65–71.
14. Dufner A, Thomas G (1999) Ribosomal S6 kinase signalling and the control of translation. *Exp Cell Res* 253:100–109.
15. Hideg E, Kálai T, Hideg K, Vass I (1998) Photoinhibition of photosynthesis in vivo results in singlet oxygen production: Detection via nitroxide-induced fluorescence quenching in broad bean leaves. *Biochemistry* 37:11405–11411.
16. Kálai T, Hankovszky O, Hideg E, Jeko J, Hideg K (2002) Synthesis and structure optimization of double (fluorescent and spin) sensor molecules. *ARKIVOC* iii:112–120.
17. Kálai T, Hideg E, Vass I, Hideg K (1998) Double (fluorescent and spin) sensor for detection of reactive oxygen species in the thylakoid membranes. *Free Radical Biol Med* 24:649–652.
18. Reinbothe S, Reinbothe C, Apel K, Lebedev N (1996) Evolution of chlorophyll biosynthesis: The challenge to survive photooxidation. *Cell* 86:703–705.
19. von Roepenack-Lahaye E, et al. (2004) Profiling of *Arabidopsis* secondary metabolites by capillary liquid chromatography coupled to electrospray ionization quadrupole time-of-flight mass spectrometry. *Plant Physiol* 134:548–559.
20. Böttcher C, von Roepenack-Lahaye EV, Willscher E, Scheel D, Clemens S (2007) Evaluation of matrix effects in metabolite profiling based on capillary liquid chromatography electrospray ionization quadrupole time-of-flight mass spectrometry. *Anal Chem* 79:1507–1513.
21. Böttcher C, et al. (2008) Metabolome analysis of biosynthetic mutants reveals a diversity of metabolic changes and allows identification of a large number of new compounds in *Arabidopsis*. *Plant Physiol* 147:2107–2120.
22. Wiklund S, et al. (2007) Visualization of GC/TOF-MS-based metabolomics data for identification of biochemically interesting compounds using OPLS class models. *Anal Chem* 80:115–122.
23. Fiehn O, et al. (2000) Metabolite profiling for plant functional genomics. *Nat Biotechnol* 18:1157–1161.
24. Bohlmann H, et al. (1988) Leaf-specific thionins of barley - a novel class of cell wall proteins toxic to plant-pathogenic fungi and possible involvement in the defence mechanism of plants. *EMBO J* 7:1559–1565.
25. Wasternack C (2007) Jasmonates: An update on biosynthesis, signal transduction and action in plant stress response, growth and development. *Ann Bot (London)* 100:681–697.
26. Thomas G (2002) The S6 kinase signalling pathway in the control of development and growth. *Biol Res* 35:305–313.
27. Dennis PB, Fumagalli S, Thomas G (1999) Target of rapamycin (TOR): Balancing the opposing forces of protein synthesis and degradation. *Curr Opin Genet* 9:49–54.
28. Menand B, Meyer C, Robaglia C (2004) Plant growth and the TOR pathway. *Curr Top Microbiol Immunol* 279:97–113.
29. Strand A, Asami T, Alonso A, Ecker JR, Chory J (2003) Chloroplast to nucleus communication triggered by accumulation of Mg-protoporphyrin IX. *Nature* 423:79–83.
30. Mochizuki N, Brusslan JA, Larkin R, Nagatani A, Chory J (2001) *Arabidopsis genomes uncoupled 5 (GUN5)* mutant reveals the involvement of Mg-chelatase H subunit in plastid-to-nucleus signal transduction. *Proc Natl Acad Sci USA* 98:2053–2058.
31. Larkin RM, Alonso JM, Ecker JR, Chory J (2003) *GUN4*, a regulator of chlorophyll synthesis and intracellular signalling. *Science* 299:902–906.
32. Koussevitzky S, et al. (2007) Signals from chloroplasts converge to regulate nuclear gene expression. *Science* 316:715–719.
33. Moulin M, McCormac AC, Terry MJ, Smith AG (2008) Tetrapyrrole profiling in *Arabidopsis* seedlings reveals that retrograde plastid nuclear signaling is not due to Mg-protoporphyrin IX accumulation. *Proc Natl Acad Sci USA* 105:15178–15183.
34. Mochizuki N, Tanaka R, Tanaka A, Masuda T, Nagatani A (2008) The steady-state level of Mg-protoporphyrin IX is not a determinant of plastid-to-nucleus signaling in *Arabidopsis*. *Proc Natl Acad Sci USA* 105:15184–15189.
35. Joyard J, Block M, Pineau B, Albrieux C, Douce R (1990) Envelope membranes from mature spinach chloroplasts contain a NADPH:protochlorophyllide reductase on the cytosolic side of the outer membrane. *J Biol Chem* 265:21820–21827.
36. Pineau B, Gerard-Hirne C, Douce R, Joyard J (1993) Identification of the main species of tetrapyrrolic pigments in envelope membranes from spinach chloroplasts. *Plant Physiol* 102:821–828.
37. Vassart G, Dumont JE, Cantraine FRL (1971) Translational control of protein synthesis: a simulation study. *Biochim Biophys Acta* 247:471–485.
38. Lodish HF (1976) Translational control of protein synthesis. *Annu Rev Biochem* 45:39–73.
39. Kochevar I (2004) Singlet oxygen signalling: From intimate to global. *Sci STKE* 221:pe7.
40. MAUGH TH (1973) Singlet oxygen: A unique microbicidal agent in cells. *Science* 182:44–45.
41. Kim C, Meskauskiene R, Apel K, Laloi C (2008) No single way to understand singlet oxygen signalling in plants. *EMBO Rep* 9:435–439.
42. Laloi C, et al. (2007) Cross-talk between singlet oxygen- and hydrogen peroxide-dependent signaling of stress responses in *Arabidopsis thaliana*. *Proc Natl Acad Sci USA* 104:672–677.
43. Gadjev I, et al. (2006) Transcriptomic footprints disclose specificity of reactive oxygen species signaling in *Arabidopsis*. *Plant Physiol* 141:436–445.
44. Yang H, Hooper JK (1999) Regulation of *lipA* gene expression by cell surface proteins in *Arthrobacter photogonimos*. *Curr Microbiol* 38:92–95.
45. Hooper JK, Phinney DG (1988) Induction of a light-inducible gene in *Arthrobacter photogonimos* sp. by exposure of cells to chelating agents and pH5. *Biochim Biophys Acta* 950:234–237.
46. Scharf KD, Nover L (1982) Heat-shock-induced alterations of ribosomal protein phosphorylation in plant cell cultures. *Cell* 30:427–437.
47. Nover L, Scharf KD (1984) Synthesis, modification and structural binding of heat-shock proteins in tomato cell cultures. *Eur J Biochem* 139:303–313.
48. Bailey-Serres J, Freeling M (1990) Hypoxic stress-induced changes in ribosomes of maize seedling roots. *Plant Physiol* 94:1237–1243.
49. Reinbothe S, Reinbothe C, Parthier B (1993) Methyl jasmonate-regulated translation of nuclear-encoded chloroplast proteins in barley (*Hordeum vulgare* L. cv. Salome). *J Biol Chem* 268:10606–10611.
50. Reinbothe S, Reinbothe C, Parthier B (1993) Methyl jasmonate represses translation initiation of a specific set of mRNAs in barley. *Plant J* 4:459–467.
51. Reinbothe S, et al. (1994) JIP60, a methyl jasmonate-induced ribosome-inactivating protein involved in plant stress reactions. *Proc Natl Acad Sci USA* 91:7012–7016.
52. Danon A, Miersch O, Felix G, op den Camp RG, Apel K (2005) Concurrent activation of cell death-regulating signalling pathways by singlet oxygen in *Arabidopsis thaliana*. *Plant J* 41:68–80.
53. Przybyla D, et al. (2008) Enzymatic, but not non-enzymatic ¹O₂-mediated peroxidation of polyunsaturated fatty acids forms part of the *EXECUTER1*-dependent stress response program in the *flu* mutant of *Arabidopsis thaliana*. *Plant J* 54:236–248.
54. Towbin M, Staehelin T, Gordon J (1979) Electrophoretic transfer of proteins from polyacrylamide gels to nitrocellulose sheets: Procedure and some applications. *Proc Natl Acad Sci USA* 76:4350–4354.

Supporting Information

Khandal et al. 10.1073/pnas.0903522106

SI Methods

Polysome Isolation. For preparative assays, 500 g of leaf material was used. For analytical assays, 25 g of leaf material was used. Leaf material was ground under liquid nitrogen until a fine powder was obtained. After resuspension in buffer A [50 mM Tris·HCl (pH 8.0), 250 mM KCl, 10 mM MgCl₂, 10 mM β-mercaptoethanol, 10 μg/mL cycloheximide, and 200 μg/mL heparin], the thawed cell homogenate was filtered through 2 layers of filter gauze (120-μm and 70-μm mesh). The crude cell extract was differentially centrifuged at 2,000; 4,000; and 12,000 rpm for 5 min each in a Sorvall RC-5B centrifuge using an HB6 rotor to remove cell debris and organelles. Triton X-100 was added to the final supernatant [1% (vol/vol) final concentration]. The solution was either loaded onto a discontinuous sucrose step gradient consisting of 2 mL of 2 M, 2 mL of 1.75 M, 2 mL of 1.5 M, 4 mL of 1.25 M, 6 mL of 1.0 M, 6 mL of 0.75 M, and 6 mL of 0.5 M sucrose in buffer B [50 mM Hepes/KOH (pH 8.5), 25 mM KCl, 10 mM MgCl₂, 10 mM 2-mercaptoethanol, 10 μg/mL cycloheximide, and 500 μg/mL heparin] or was supplemented with magnesium chloride (0.1 M final concentration) to precipitate ribonucleoprotein material.

Metabolite Profiling. For liquid chromatography (LC), 5 μL of samples were separated on a BEH C18 column (2.1 × 100 mm, 1.7 μm) at 40 °C. The flow was set to 0.5 mL per minute, and solvents were water (A) and acetonitrile (B), both acidified with 0.1% formic acid. The gradient was as follows: 1 min 95% A,

from 1 to 16 min a linear gradient to 95% B, 95% B for 3 min, linear gradient to 95% A in 2 min, and finally 1 min 95% A.

The mass spectrometer was operated in both ESI V+ and V- mode. Source settings were as follows: capillary: 2.5 kV, sampling cone 30, extraction cone 30, ion guide 3.3, source temperature 120 °C, cone gas flow 10 L/h, desolvation gas flow 1,000 L/h. The MS acquisition was performed from 80 to 1,000 Da with a scan time of 0.3 s and an interscan delay of 0.05 s. For accurate mass measurement, a reference compound was infused [lockspray, (D-Ala-2) leucine enkephalin, (M⁺H⁺) = 570.2928 Da, 2 ng/μL, 5 μL per minute], and the sample cone voltage was adjusted to yield approximately 800 counts per second for the lockspray. The lockspray was measured every 1 s for 0.4 s. MS acquisition in the negative mode was performed analogously with the following settings: capillary -2.5 kV, sampling cone 50, extraction cone 6, ion guide 3, source temperature 100 °C, cone gas flow 10 L/h, and desolvation gas flow 1,000 L/h. Runs were recorded and reviewed by using the MassLynx 4.1 software (Waters Corporation). For statistical analysis, the MarkerLynx XS (Waters Corporation) package was used.

Chemicals. Biochanin A, *p*-anisic acid, *N*-(3-indolylacetyl)-L-valine (IAA-Val), and rutin were obtained in highest available purity from SigmaAldrich, whereas formic acid was at LC-MS grade. Methanol and acetonitrile for metabolite extraction and LC were B&J LC-MS grade solvents (Honeywell). Water from a Milli-Q ultrapure water purification system (Millipore) was used for all experiments.



MINIREVIEW

Plant oxylipins: role of jasmonic acid during programmed cell death, defence and leaf senescence

Christiane Reinbothe^{1,2}, Armin Springer¹, Iga Samol² and Steffen Reinbothe²¹ Lehrstuhl für Pflanzenphysiologie, Universität Bayreuth, Germany² Laboratoire de Génétique moléculaires des Plantes, Université Joseph Fourier, Grenoble, France

Keywords

biotic and abiotic stress responses; chloroplast; dys-regulation of chlorophyll metabolism; fluorescent (flu) mutant (*A. thaliana*); gene expression; photooxidative stress; reactive oxygen species (ROS); signalling; singlet oxygen; transcriptional and translational control

Plants are continuously challenged by a variety of abiotic and biotic cues. To deter feeding insects, nematodes and fungal and bacterial pathogens, plants have evolved a plethora of defence strategies. A central player in many of these defence responses is jasmonic acid. It is the aim of this mini-review to summarize recent findings that highlight the role of jasmonic acid during programmed cell death, plant defence and leaf senescence.

Correspondence

C. Reinbothe, Lehrstuhl für Pflanzenphysiologie, Universität Bayreuth, Universitätsstrasse 30, D-95447 Bayreuth, Germany
Fax: +49 921 75 77 442
Fax: +49 921 55 26 34
E-mail: christiane.reinbothe@uni-bayreuth.de

(Received 7 November 2008, revised 29 June 2009, accepted 2 July 2009)

doi:10.1111/j.1742-4658.2009.07193.x

Introduction

Oxygenated fatty acid-derivatives (oxylipins) are central players in a variety of physiological processes in plants and animals. Jasmonic acid (JA), in particular, accomplishes unique roles in plant developmental processes and defence. It has been shown to regulate flower development, embryogenesis, seed germination, fruit ripening and leaf senescence [1–3]. JA is also involved in wound responses and defence [4–7]. Pioneering work from Zenk's group has shown that

several fungal pathogens and elicitors promote JA accumulation in cell cultures of *Petroselinum hortense*, *Eschscholtzia californica*, *Rauvolfia canescens* and *Glycine max* [8,9]. This observation was extended and confirmed for numerous other plant species [10,11]. Interestingly, JA also accumulates when plants are subjected to UV light [12] or elevated temperature [13], underscoring the central role of JA in the deterrence of both biotic and abiotic cues.

Abbreviations

CC, coiled-coiled; Chl, chlorophyll; Chlide, chlorophyllide; *cis*(+)-OPDA, *cis*(+)-12-oxo-phytyldienoic acid; JA, jasmonic acid; JIP, jasmonate-induced protein; LRR, leucine-rich repeat; Me-JA, methyl ester of JA; miRNA, micro RNA; PCD, programmed cell death; Pchlide, protochlorophyllide; RIP, ribosome-inactivating protein; ROS, reactive oxygen species; SA, salicylic acid; TIR, Toll and interleukin-1 receptor.

Recent work has shown that JA is also synthesized in response to singlet oxygen. Singlet oxygen is one prominent form of reactive oxygen species (ROS) that is generated during oxygenic photosynthesis [14,15]. Excited chlorophyll (Chl) molecules in the reaction centres interact with molecular oxygen and, by triplet-triplet interchange, provoke singlet oxygen production. The same mechanism can be elicited by the cyclic, light-absorbing precursors and degradation products of Chl that operate as photosensitizers. Hallmark work performed by Apel and co-workers has led to the discovery of a singlet oxygen-dependent signalling network, that controls growth and cell viability, in which JA and its biosynthetic precursor *cis*-(+)-12-oxo-phytodienoic acid (*cis*-(+)-OPDA) are involved.

Discovery of the *flu* mutant and singlet oxygen-signalling leading to JA

Chl as a component of the photosynthetic machinery absorbs light energy and mediates energy transfer in the course of photosynthesis [16]. However, under unfavourable environmental conditions, excited Chl (or other porphyrin) molecules may interact directly with oxygen to give rise to highly reactive singlet oxygen [17,18]. Like other types of ROS, singlet oxygen has detrimental effects for the plant. To avoid the negative effects of ROS, higher plants have evolved mechanisms so that, under normal growth conditions, an equilibrium is established between the production and scavenging of ROS [19]. Moreover, the biosynthetic pathway leading to Chl is tightly controlled [16,20,21]. When angiosperms grow under dark conditions, Chl biosynthesis halts at the stage of protochlorophyllide (Pchl_{id}), the immediate precursor of chlorophyllide (Chl_{id}). Once a threshold level of Pchl_{id} has been reached, 5-aminolevulinic acid synthesis is shut off. Only after illumination, is Pchl_{id} converted to Chl_{id} and the block in 5-aminolevulinic acid synthesis released [22]. Feedback control of 5-aminolevulinic acid synthesis has been attributed to heme and Pchl_{id} [23,24].

A mutant of *Arabidopsis thaliana*, termed *fluorescent (flu)*, which is impaired in this feedback control was isolated and characterized [25]. The FLU protein interacts with glutamyl-tRNA reductase [26,27] and this interaction is impaired in *flu* plants [25]. The *flu* mutation consequently results in the accumulation of excessive levels of free Pchl_{id} molecules in etiolated seedlings and plants grown under light/dark cycles, where the pigment is resynthesized at the end of the dark period [25]. Once illuminated, these free Pchl_{id} molecules are excited, leading to the production of sin-

glet oxygen that causes damage to membrane structures and changes in the gene expression pattern.

Steps in the *flu*- and singlet oxygen-dependent signalling pathway

Two major effects have been observed for *flu* plants subjected to nonpermissive dark-to-light shifts in which JA may be involved: growth inhibition and cell death [28]. When *flu* seedlings were germinated in alternate dark-light cycles, they displayed a miniature phenotype (Fig. 1). By contrast, etiolated plants died when illuminated. Cell death also occurred in mature plants after an 8 h dark shift and subsequent irradiation [28]. To explain these results, cytotoxic singlet oxygen effects including lipid peroxydation and membrane destruction, and the operation of specific, genetically determined signalling cascades have been proposed [28–31] (for a review see Ref. [32]). *Transcriptome* analyses identified a large number of genes that differentially respond to singlet oxygen [28]. Among the genes that were downregulated by singlet oxygen were those for photosynthetic proteins [28]. Genes that were upregulated by singlet oxygen include *BONZAI (BON) 1* and *BON1-ASSOCIATED PROTEIN (BAP) 1*, the *ENHANCED DISEASE SUSCEPTIBILITY (EDS) 1* gene, and genes encoding enzymes involved in the biosynthesis of ethylene and JA, two key components of stress signalling in higher plants [1–3,33]. op den Camp *et al.* [28] found that singlet oxygen gives rise to 13-hydro(pero)xy octadecatrienoic acid accumulation in mature *flu* plants. 13-Hydro(pero)xy octadecatrienoic acid is an intermediate in the biosynthetic pathway of JA (see Fig. 1 of the accompanying minireview by Böttcher & Pollmann). Przybyla *et al.* [34] later reported that irradiated *flu* plants produce large amounts of JA and OPDA and suggested that JA may be required for cell death propagation/manifestation, whereas OPDA would counteract the establishment of the cell death phenotype (see below). Wagner *et al.* [30] and Kim *et al.* [31] demonstrated that cell death execution is suppressed in the *executer (exe) 1* and *exe2* mutants of *A. thaliana*, but only if low levels of singlet oxygen accumulate and trigger limited cytotoxic effects. EXECUTER 1 and 2 are membrane proteins of chloroplasts of unknown function [30,31].

EDS1 is a central player in the disease response to a variety of pathogens [35] (Fig. 2). Race-specific pathogen resistance is mediated by an interaction between a plant disease resistance (*R*) gene and its corresponding pathogen avirulence (*Avr*) gene [36]. The gene-for-gene interaction triggers defence responses, such as the hypersensitive response, to

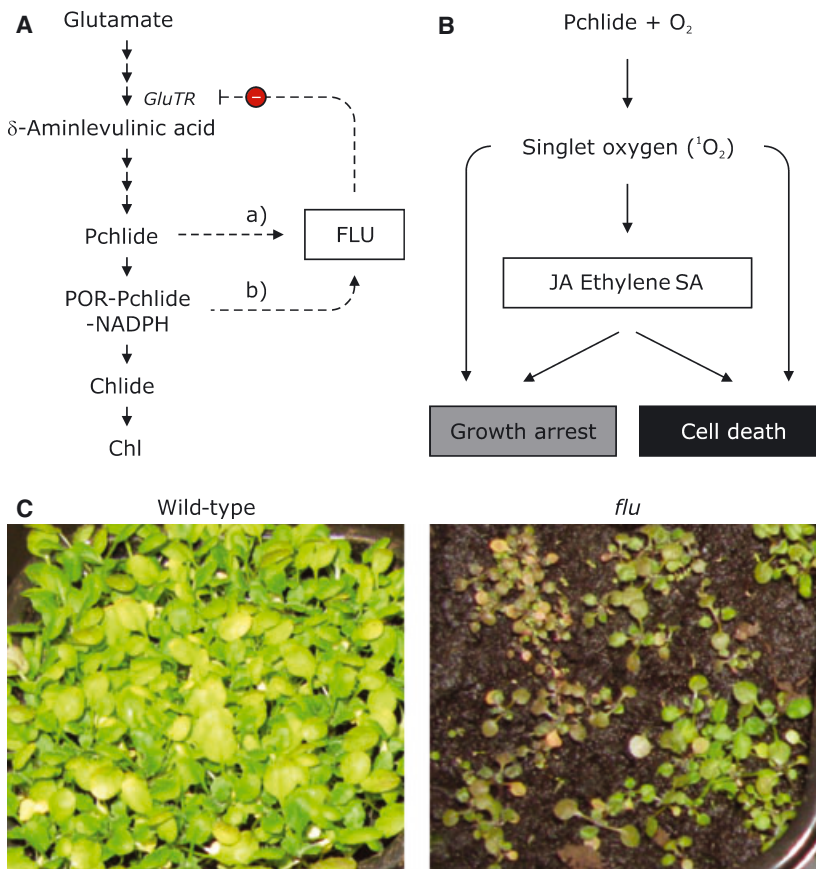


Fig. 1. Singlet oxygen- and JA-dependent signalling in the *fluorescent (flu)* mutant of *Arabidopsis thaliana*. (A) Schematic view of the tetrapyrrole pathway leading to chlorophyll and role of the FLU protein. GluTR, glutamyl-tRNA reductase, the target of FLU; Pchlide, protochlorophyllide; POR, NADPH:Pchlide oxidoreductase; Chl(ide), chlorophyll(ide). The two models designated 'a' and 'b' suggest that either the free pigment or POR-bound Pchlide may provide the signal for the feedback loop. (B) Pchlide-sensitized singlet oxygen production, growth control versus cell death, and the role of JA, ethylene and SA (C) Miniature phenotype of *flu* seedlings after growth in white light and an overnight dark period, followed by cultivation in continuous white light. *flu* seeds were a kind gift from K. Apel (The Boyce Thompson Institute for Plant research, Cornell University, USA).

restrict pathogen growth and reproduction [37]. A number of *R* genes have been cloned and characterized at the molecular level. They mostly encode five families of proteins, with R proteins in the largest family containing nucleotide-binding sites (NB) and leucine-rich repeat (LRR) domains [38,39]. The N-termini of these proteins display either Toll and interleukin-1 receptor-like (TIR) type or coiled-coiled (CC) type structures [38,39].

EDS1 and *PHYTOALEXIN DEFICIENT4 (PAD4)* are required for the function of TIR-NB-LRR proteins, whereas *NONRACE-SPECIFIC DISEASE RESISTANCE1 (NDR1)* is normally required for the CC-NB-LRR proteins; exceptions to this rule have been reported [35]. In addition to their roles in *R*-gene-mediated defence responses, *EDS1*, *PAD4*, and *NDR1* act as amplifiers of cell death [40,41].

EDS1 and *PAD4* interact during defence [42,43], but *EDS1* also forms complexes with the *SENESCENCE-ASSOCIATED GENE (SAG) 101* product [44]. *EDS1*, *PAD4* and *SAG101* share the presence of conserved domains in their C-terminal halves, but unlike *EDS1* and *PAD4*, *SAG101* does not possess the catalytic serine hydrolase triad [44]. It has been proposed that *SAG101* may accomplish a defence regulatory function

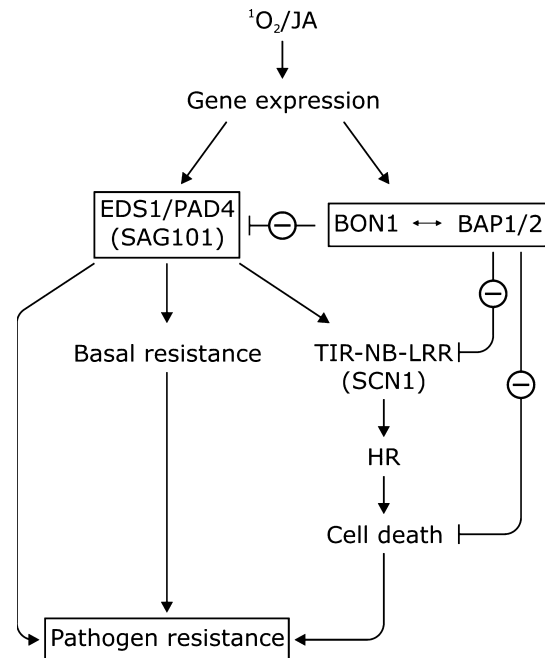


Fig. 2. Role of *EDS1/PAD4/SAG101* and *BON1/BAP1 + 2* in cell death and plant pathogen resistance. Whereas *EDS1*, *PAD4* and *SAG101* are positive regulators of cell death, *BON1*, *BAP1* and *BAP2* operate as negative regulators. HR, hypersensitive response.

that is partially redundant with PAD4 in both TIR–NB–LRR-triggered, *R*-gene-mediated resistance and basal resistance [44].

op den Camp *et al.* [28] found that *BON1* and *BAP1* belong to the very early markers of singlet oxygen-mediated signalling. At first glance, it is therefore somewhat unexpected to find that *BON1*, and also *BAP1* and *BAP2*, have been reported by other groups to operate as negative regulators of cell death [45,46] (Fig. 2). *BON1* belongs to the copine protein family that includes members from protozoa to humans and regulates cell, organ and body size. Copines consist of a so-called C2 N-terminal domain that binds phospholipids [47] and a so-called C-terminal A domain with presumed function as kinase [48]. In mice, one of the copine family members, copine-N, is expressed in neurons, both in the cell bodies and dendrites, and has been suggested to establish a role in synaptic plasticity [49]. Loss-of-function *bon1* mutants in *A. thaliana* have enhanced disease resistance and a dwarf phenotype that are developed in a temperature- and humidity-dependent manner [50,51]. *BON1* interacts with *BAP1* and *BAP2*, which seem to accomplish redundant roles, as judged from yeast two-hybrid system screens and overexpression studies [52]. However, unlike *bap1*, the *bap2* loss-of-function mutant had no apparent growth defects or increased disease resistance. Nevertheless, it displayed an accelerated hypersensitive response to avirulent bacterial pathogens [52]. Deletion of both *BAP1* and *BAP2* caused seedling lethality that could be reverted by *pad4* or *eds1* mutations. Because overexpression of *BAP1* and *BON1* inhibited cell death induced by several *R* genes, a function as a hub in different defence responses has been proposed [52]. This view was corroborated by reports that expressing *BAP1* or *BAP2* in yeast attenuated cell death induced by hydrogen peroxide [52].

BON1 and *BAP1/2* target *SUPPRESSOR OF NPR1*, *CONSTITUTIVE 1*, *SNCI*, a TIR–NB–LRR [53] (Fig. 2). Consequently, the *bap1* and *bon1* phenotypes were reversed by loss-of-function mutations in *SNCI*, but also by loss-of-function mutations in *EDS1*, *PAD4* and by *nahG*, encoding a salicylic acid (SA)-degrading enzyme [45,46]. Together, these results highlight the great complexity of interactions and suggest that *BON1* and *BAP1* act as general negative regulators of the *R* gene *SNCI*.

The *BAP1* and *BON1* genes must have additional roles other than negatively regulating *SNCI* (Fig. 2). This is illustrated by results on the overexpression of *BAP1* in wild-type plants that conferred an enhanced susceptibility to a virulent oomycete in a *SNCI*-independent manner [46]. Furthermore, the loss of function of all *BON1* family members including *BON1*, *BON2* and

BON3 provoked seedling lethality that was largely suppressed by *eds1*, *pad4*, but not by *sncl* or *nahG* [54]. How JA may interfere in this pathway is not yet resolved.

JA-dependent reprogramming of gene expression

JA and its volatile methyl ester, Me-JA, exert two major effects on gene expression in detached leaves of barley and other species, and in whole plants: first, they induce novel abundant proteins designated jasmonat-induced proteins (JIPs); second, they repress the synthesis of photosynthetic proteins [1,3,55–60]. Both nuclear and plastid photosynthetic genes are repressed under the control of JA. Within the chloroplast, rapid Me-JA-induced changes in the processing pattern of *RBCL*, encoding the large subunit of ribulose-1,5-bisphosphate carboxylase/oxygenase, are superimposed by delayed effects on plastid transcription and RNA stabilities [59]. Together, these effects lead to a rapid cessation of ribulose-1,5-bisphosphate carboxylase/oxygenase LSU synthesis and cause a drastic drop of photosynthesis and carbon dioxide fixation rates.

Also, nuclear genes encoding photosynthetic proteins are rapidly switched off by JA [55–58]. Although most of their respective mRNAs remain abundant and functional (as shown by northern hybridization and translation experiments in wheat germ extracts), they are no longer translated into protein [56–58]. Polysome profiling studies have revealed that polysomes isolated from stressed or Me-JA-treated plants efficiently translate stress messengers but not photosynthetic mRNAs [57,58]. Changes in the phosphorylation status of ribosomal protein S6, which is a key player regulating translation [61–63], are likely to contribute to this effect. Such changes have been reported earlier for other adverse conditions [64,65].

A terminal response of excised barley leaves to Me-JA is the rapid dissociation of 80S ribosomes into their subunits. This effect is caused by the interaction of JIP60, a 60 kDa cytosolic protein [66], with 80S plant ribosomes [67,68]. JIP60 shares amino acid sequence homology to that of ribosome-inactivating proteins (RIPs) found in bacteria and plants [69,70]. The N-terminal half of the novel barley RIP is related to both type I and type II RIPs, which are exceptionally potent inhibitors of eukaryotic protein synthesis [71,72]. Both types of RIP catalytically cleave a conserved *N*-glycosyl bond of a specific adenine nucleoside residue in the 28S rRNA [73–76] such that elongation factor II binding can no longer proceed during translation, causing a cessation of protein synthesis [77]. An additional, C-terminal domain is present in JIP60

[67,68] which was discovered to feature another activity. This domain is related to eukaryotic initiation factors of type eIF4 γ [68] and is involved in sustaining stress and defence protein synthesis in terminally staged tissues where JIP60 is proteolytically processed (C Reinbothe, unpublished results). In contrast to barley and other monocots, neither *JIP60* nor any other *RIP*-related genes are detectable in the genome of the model plant *A. thaliana*. Nevertheless, *A. thaliana* responds to stress with the same type of arrest of translation at 80S ribosomes as found for barley plants [60], suggesting a case of convergent evolution involving different proteins.

It is remarkable to note that exactly the same early and late effects on translation as those reported for Me-JA have been observed for the *flu*-orthologue of barley, designated *tigrina-d.12* [78]. The fact that *tigrina-d.12*, like *flu*, accumulates Pchl_{ide} when transferred from light to darkness and uses the pigment as a photosensitizer suggests that singlet oxygen-dependent JA production may provide the signal to reprogramme translation toward stress and defence protein synthesis in the early stage and to shut-down protein synthesis in the terminal stages preceding or correlating with cell death.

Implication of JA in cell death regulation

Plant hormones such as ethylene, SA and JA play important roles in cell death regulation. This is illustrated by studies on *flu*. It has been shown that in mature green *flu* leaves only enzymatic lipid peroxidation contributes to OPDA and JA synthesis [34]. By contrast, fractions of the unsaturated membrane fatty acid α -linolenic acid and α -linoleic acid are converted randomly and nonenzymatically to a variety of products when etiolated plants are irradiated [34]. Thus, in this case, singlet oxygen exerts a cytotoxic effect that superimposes its genetic effect. As mentioned previously, Przybyla *et al.* [34] proposed that cell death may be controlled not only by JA, but also by some of the intermediates of the oxylipin pathway giving rise to JA. Antagonistic effects between JA and OPDA and its C16 carbon skeleton homologue, *dinor*-OPDA, were invoked to explain cell death control [34,79]. However, the induction of several enzymes involved in ethylene biosynthesis and SA action in illuminated *flu* plants points to concurrent signalling pathways that are triggered by singlet oxygen [28]. This was directly proven by studies in which the actual levels of SA and/or ethylene were manipulated pharmacologically or genetically [29,79]. It is also well known that SA depresses JA signalling [80,81].

In contrast to these studies suggesting a positive role of JA in cell death control, JA has been implicated in the containment of ROS-dependent lesion propagation in response to ozone [82–85] (for a review see refs [86,87]). For example, the JA-insensitive *jar1* [88] and *coil* [89] (see minireview by Chini *et al.* [89a]) mutants, as well as the JA-deficient *fad3-fad7-fad8* triple mutant [90] (see minireview by Böttcher & Pollmann [90a]) all showed an increased magnitude of ozone-induced oxidative burst, SA accumulation and cell death. Pretreatment of the ozone-sensitive accession Cyi-O of *A. thaliana* with Me-JA abrogated ozone-induced H₂O₂ accumulation, SA production and defence gene activation [82–84]. Furthermore, *jar1* exhibited a transient spreading cell death phenotype and a pattern of superoxide anion (O₂⁻) accumulation similar to that observed in *rcd1* plants [82]. *RCD1* defines a radical-induced cell death locus that mediates ozone and O₂⁻ sensitivity [82]. Treatment of O₃-exposed *rcd1* mutant plants with JA arrested spreading cell death, suggesting a direct role for JA in lesion containment [82,83]. Similarly, pretreatment of tobacco cells with JA diminished O₃-dependent cellular damage [82–84]. It has been proposed that lesion containment by JA could be achieved through increased ethylene receptor protein synthesis, thereby desensitizing plants to ethylene and halting lesion spread [82–84]. However, no evidence has been obtained for a role of the ethylene receptor LF-ETR (NR) in mediating ozone sensitivity in tomato [91]. Thus, alternative scenarios must be considered. Such scenarios were inspired by work on mutants of *A. thaliana* that constitutively overexpress the thionin (THI2.1) gene, called *cet* mutants [92]. These mutants spontaneously form microlesions [92] but do so by remarkably different mechanisms. Whereas lesion formation in *cet2* and *cet4.1* plants occurred independently of COI1-mediated JA signal(s) and SA, that in *cet3* required both COI1-mediated JA signalling and SA [92]. In SA-depleted transgenic *cet3* plants expressing the bacterial SA hydroxylase NahG, THI2.1 expression was independent of lesion formation. In wild-type plants, NahG-dependent depletion of SA levels, however, abolished hypersensitive response-like cell death symptoms [92]. Taken together, these results emphasize that signals other than SA, JA and ethylene must be involved in the regulation of cell death in *cet* plants [93,94].

JA action on mitochondria links oxidative damage to cell death

Mitochondria play an active role in cell death regulation in animals and plants (Fig. 3). Singlet oxygen-

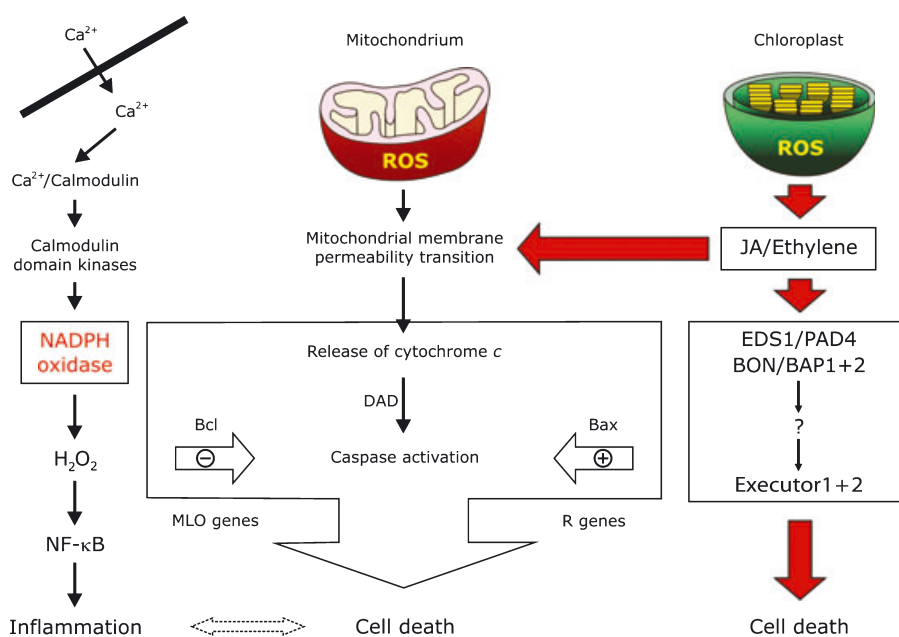


Fig. 3. Central role of JA in cell death regulation in plants. Animals respond to many external factors with a plethora of different cell death pathways of which two are illustrated here: (a) the Ca^{2+} /calmodulin-dependent, NADPH oxidase pathway triggering NF- κ B activation and inflammatory processes; and (b) the activation of the mitochondrial pathway involving membrane permeability transition, release of cytochrome *c* and caspase activation. In plants, a plastid-derived pathway of cell death regulation exists that comprises singlet oxygen and JA that activates specific downstream signalling cascades in the cytosol and in mitochondria. Singlet oxygen generation in chloroplasts in fact triggers changes in gene expression such as the induction of *BON1*, *BAP1* and *BAP2* genes as well as downstream elements that ultimately converge at the *EXECUTER1* and *EXECUTER2* genes. Most of the intermediates in this pathway have not yet been identified and are therefore highlighted with a question mark here.

and JA-mediated cell death in irradiated *flu* plants is likely to be a form of programmed cell death (PCD) [29]. In many aspects it resembles PCD and apoptosis in animals [95–99]. This includes cell condensation, chromatin separation, cleavage of nuclear DNA and the release of cytochrome *c* from the mitochondria to the cytosol. Entry into PCD is dependent upon depression of proapoptotic signals in the mitochondrial membrane [100–103]. Mitochondrial membrane permeability transition and the subsequent release of cytochrome *c* are stimulated by various signals, including (stress-induced) Ca^{2+} fluxes and increased ROS levels. Conversely, loss of mitochondrial transmembrane potential leads to mass generation of ROS and thereby provides a powerful feed-forward loop. Intermediate components include BCL-2-like proteins [104–106]. SA-dependent ROS production triggers an increase in cytosolic Ca^{2+} [107,108] and inhibits mitochondrial functions [109,110]. According to most recent studies, JA itself is able to cause mitochondrial ROS production and mitochondrial membrane permeability transition [111].

Zhang & Xing [111] studied ROS production, alterations in mitochondrial dynamics and function, as well

as photosynthetic activity in response to Me-JA in *A. thaliana* and obtained remarkable results. They found that Me-JA is a powerful inducer of ROS, which first accumulated in mitochondria in periods as short as 1 h after the onset of Me-JA treatment and was followed by a second burst, detectable after 3 h, in chloroplasts. Serious alterations in mitochondrial mobility and, most remarkably, a loss of mitochondrial transmembrane potential occurred. These effects preceded the dramatic decline in photochemical efficiency in chloroplasts [111]. Although the release of cytochrome *c* was not determined, it is likely that JA triggered PCD and apoptosis in a way that is similar to that in animals. Indeed, JA can provoke mitochondrial membrane permeability transition and the release of cytochrome *c* in animal cells [112]. In A549 human lung adenocarcinoma cells, Me-JA operates through the induction of proapoptotic genes of the BCL-2, Bax and Bcl-X families and activation of caspase 3 [113]. It is currently being discussed whether other proapoptotic signals may also contribute to JA-dependent cell death regulation. For example, sphingosine is a well-known proapoptotic molecule [114] that stimulates lysosomal cathepsins B and D involved in the removal of the

prodomains from caspases. Interestingly, the mycotoxin and sphingosine analogue fumonisin-B1 is a powerful inducer of singlet oxygen-dependent PCD in animals and plants [115,116]. Fumonisin-1-induced PCD in plants requires SA, JA and ethylene, similar to cell death triggered by singlet oxygen in *flu* plants [29]. However, an alternative pathway of sphingosine signalling may be inferred from studies on the *accelerated cell death (acd) 11* of *A. thaliana* [116]. ACD11 operates in lipid transfer between membranes and is supposed to negatively regulate PCD and defence *in vivo*. Activation of PCD and defence pathways in *acd11* plants required SA and EDS1 but was not dependent on intact JA or ethylene signalling cascades [116,117], once more emphasizing that multiple cell death pathways are present in higher plants.

Role of JA during leaf senescence

The methyl ester of JA, Me-JA, was discovered by its senescence-promoting activity [118]. It induces rapid Chl breakdown and plastid protein turnover [55–58]. The same effects are found also during natural senescence, and three- to four-fold increases in the JA content [119] have been measured for *A. thaliana* undergoing the senescence programme [120–122].

Transcription factors belonging to the TEOSINTEBRANCHED/CYCLOIDEA/PCF (TCP), WRKY and NAM, ATAF and CUC (NAC) families control leaf senescence and may provide the link to JA signalling (Fig. 4). Members of the WRKY family share the presence of a 60 amino acid motif, the WRKY domain [123]. Studies on *A. thaliana* led to the discovery of two different WRKY proteins designated WRKY6 and

WRKY53 that differentially accumulate during leaf senescence [123,124]. Targets of *AtWRKY6* include calmodulin-response genes and different types of senescence-associated and senescence-induced kinases, called SARK and SIRQ, respectively [125]. SARK and SIRQ share similar structures and consist of an extracellular leucine-rich domain, a transmembrane domain, and a Ser/Thr kinase domain. It has been proposed that both proteins may be membrane-bound and that their activation during senescence may involve intra- and extracellular signals such as plant hormones and light [126]. A WRKY53 partner is EPITHIOSPECIFYING SENESCENCE REGULATOR, ESR/ESP, which is involved in senescence as well as pathogen defence [127]. WRKY53 and ESR/ESP may exert antagonistic effects during leaf senescence by sensing the JA/SA ratio. The role of SA in leaf senescence has been established [128]. WRKY53 expression is induced by SA, whereas ESR/ESP expression is induced by JA. Both proteins interact in the nucleus, providing a potential node for SA- and JA-dependent signalling [127] (Fig. 4).

Another example of a transcription factor family implicated in the control of leaf senescence is established by the TCPs (Fig. 4). TCPs comprise two groups in *A. thaliana*, designated class 1 and class 2 [129,130]. Whereas class 1 TCPs, such as TCP20, operate as positive regulators of growth, class 2 TCPs, such as TB1 and CYC/DICH, function as negative regulators [131,132]. Both types of TCPs bind to the promoter motifs of genes that are essential for expression of the cell-cycle regulator PCNA. For example, p33^{TCP20} binds to GCCCR elements found in the promoters of cyclin *CYCB1;1* and many ribosomal protein genes *in vitro* and *in vivo* [132]. It has been suggested that organ growth rates and the shape in aerial organs are regulated by the balance of positively and negatively acting TCPs [133].

Interestingly, 5 of the 24 TCP genes in *A. thaliana* are targets of micro (mi)RNAs [134] (Fig. 4). miRNAs are ubiquitous regulators of various developmental processes in plants and animals, and act at both the transcriptional and post-transcriptional levels [135,136]. The class 2 TCP genes are represented by CINCINATA (CIN) and JAW-D [137]. CIN controls cell division arrest in the peripheral region of the leaf. *cin* mutants have de-repressed cell growth leading to crinkles and negative leaf curvature [138]. Reduced leaf size is observed in *A. thaliana* and tomato plants in which miR319 control of TCP genes is impaired [138]. It was found that miR319-targeted TCP additionally controls expression of *AtLOX2*, one of the key enzymes involved in JA biosynthesis (see minireview by Böttcher & Pollmann [90a]), both during natural and

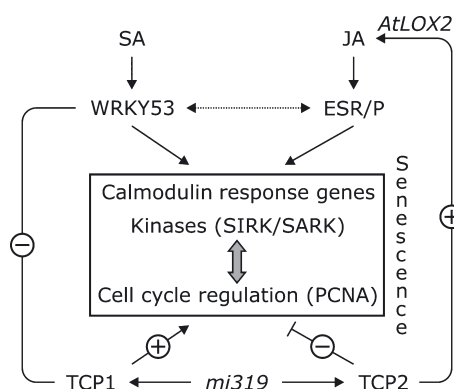


Fig. 4. WRKY and TCP transcription factors control gene expression during senescence. Shown is the network of interactions that positively and negatively regulate leaf senescence. Key targets of control are highlighted. Note that this is a very simplistic cartoon not drawn to comprehension that underscores the role of salicylic acid (SA) and jasmonic acid (JA).

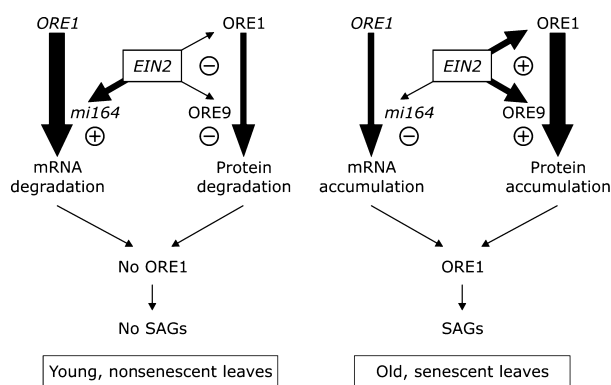


Fig. 5. Implication of ORE1 in cell death control in senescent plants. ORE1 expression is low in young, non-senescent leaf tissues because *EIN2* supports high *mi164* expression that targets *ORE1* transcripts for degradation. At the same time, overall expression of ORE1 is depressed by *EIN2*. In senescent leaves, by contrast, *EIN2* depresses *mi164* expression and thereby allows for ORE1 transcript and protein accumulation. ORE1 may gain access to senescence-associated gene (SAG) promoters by virtue of the action of ORE9 that could target transcriptional repressors for degradation by the 26S proteasome.

dark-induced senescence [133]. Another target of TCPs appears to be WRKY53 that is involved in the onset of early senescence gene expression (see Fig. 4 and above). Schommer *et al.* [133] proposed that mi319-regulated TCPs control leaf senescence by regulating not only JA biosynthesis, but also a second, as-yet unidentified, pathway inhibiting senescence in wild-type plants.

NAC transcription factors control leaf senescence and cell death. Kim *et al.* [139] showed that the *ore* [oresara ('long-living' in Korean)] 1 gene encodes such transcription factor (Fig. 5). *ORE1* is a nuclear gene the expression of which increases during leaf senescence by a complex mechanism involving miRNA164, *ETHYLENE-INSENSITIVE (EIN) 2-34* (a gene that was originally isolated as *ore3-1*), and *ORE1* [139]. *ORE1* transcript levels are low in non-senescent plants because miRNA164 targets the messenger for degradation. At later stages of development, miRNA164 expression declines, allowing for *ORE1* mRNA accumulation (Fig. 5). *EIN2* controls miRNA164 expression, and miRNA164 expression is barely altered with aging in the *ein2-34* mutant. *EIN2* also triggers *ORE1* expression in an aging-dependent mode (Fig. 5). In addition to its role in regulating age-dependent cell death through changes in its expression level and that of *ORE1* over the life span of leaves, miRNA164 seems to affect also other processes, including lateral root development and organ boundary formation in shoot meristem and flower development, because it targets other NAC transcription factors [139].

ORE1 and other transcription factors may bind to the promoters of senescence-associated genes and activate them. However, it is not yet clear whether these promoters are accessible at all stages of plant development or may gain access specifically during the senescence programme. Work performed on another *ore* mutant, *ore9*, suggests a de-repressor model of gene activation [140] (Fig. 5). *ORE9* is an F-box protein which is part of the Skp1-cullin/CDC53-F-box protein complex [141,142]. F-box proteins have been identified in plants and found to function in the regulation of floral organ identity (UFO), JA-regulated defence (COI1; see also minireview by Chini *et al.* [89a]), auxin response (TIR1) and control of the circadian clock (ZTL and FKF1) [89,143–146]. *ORE9* is a likely E3 ubiquitin ligase that may target transcriptional repressors for degradation [139]. E3 enzymes are involved in selecting substrate proteins for ubiquitination and subsequent degradation by the 26S proteasome under a variety of conditions [147,148]. In addition to its role in senescence, *ORE9* participates in regulating processes as diverse as photomorphogenesis [149], shoot branching [150,151] and cell death [152]. For example, *ORE9* operates downstream of the *ENHANCED DISEASE RESISTANCE 1 (EDR1)* gene [152]. *EDR1* encodes a *CTR1*-like kinase that was previously reported to function as a negative regulator of disease resistance to the bacterium *Pseudomonas syringae* and the ascomycete fungus *Erysiphe cichoracearum* and ethylene-induced senescence [153]. The function of *EDR1* in plant disease resistance, stress responses, cell death and ethylene signalling is largely unclear. The *edr1*-mediated ethylene-induced senescence phenotype is suppressed by mutations in *EIN2*, but not by mutations in *PAD4*, *EDS1* or *NPRI* [152]. Together these results suggest that *EDR1* functions at a point of cross-talk between ethylene and SA signalling that impinges on senescence and cell death.

Chl breakdown is a hallmark of natural and JA-induced leaf senescence. It needs to be tightly controlled to avoid photooxidative damage. It involves the selective destabilization of the major light-harvesting Chl *a/b* binding protein complexes associated with photosystem I and photosystem II. Recently, a protein was discovered that operates in regulating LHC stability [154] (see also ref. 155 for a recent review on other *stay-green* mutants). The STAYGREEN PROTEIN from rice, SGR, is absent from mature leaves and is induced specifically during leaf senescence [154]. Rice mutants lacking SGR showed a greater longevity of Chl both under natural and artificial senescence conditions. Conversely, SGR overexpression triggered Chl degradation in developing leaves [154]. Expression of

the SGR homologue SGN1 in *A. thaliana* is reduced in mutants such as *acd2*, encoding pheophorbide *a* oxygenase [156], and *acd1*, encoding red Chl catabolite reductase [157], suggesting the existence of retrograde signalling pathways from senescing chloroplasts that control LHC stability and the release of Chl. It has been shown that plastids transmit information about their structural and functional state to the cytosol and nucleus and thereby trigger adaptive responses [158–161]. Tetrapyrroles belong to the plastid signals identified, but also ROS, redox compounds and plastid constituents are implicated in retrograde signalling during greening, senescence and pathogen defence [162,163]. Although SGR and SGN1 do not have significant homologies to known proteins and do not bind or convert Chl to other products [154], Genevestigator database searches (<https://www.genevestigator.ethz>) [164] suggest their roles in floral organs, during seed maturation, under nitrogen deprivation, in response to osmotic stress and after pathogen attack. It seems likely that SGN1 may be expressed to avoid the undesirable accumulation of free Chl molecules that would operate as photosensitizers and trigger singlet oxygen production and JA signalling.

Key enzymes of Chl breakdown are JA-responsive such as chlorophyllase. In *A. thaliana*, two chlorophyllase genes termed *AtCLH1* and *AtCLH2* have been identified [165] which respond differentially to JA and ethylene as well as pathogens. *AtCLH1* was strongly induced by Me-JA and the phytotoxin coronatine, a structural analogue of JA-Ile from *Pseudomonas* sp. [166], whereas *AtCLH2* did not respond to Me-JA [165,167]. Knockdown of *AtCHL1* by RNA interference was reported to drastically affect plant resistance to the bacterium *Erwinia carotovora* and the fungus *Alternaria brassiciola* [168]. Although *AtCHL1* RNAi plants were resistant to *E. carotovora*, they showed hypersensitivity to *A. brassiciola* [168]. It has been suggested that, by virtue of its chlorophyllase activity, *AtCLH1* may score damages inflicted by bacterial and fungal necrotrophs [168]. It is well known that JA plays a role in the defence of necrotrophs [169–171].

An as yet unknown mechanism triggers the perforation/permeabilization of the plastid envelope in senescent chloroplasts. It is not yet clear whether the implicit membrane destruction is a requirement for senescence progression or just a late consequence of imbalanced fatty acid recycling by salvage reactions. An active scenario is offered by studies on animal cells in which an inducible membrane destruction mechanism operates in the differentiation of reticulocytes and keratinocytes. It involves the selective permeabilization of the outer surroundings of mitochondria,

peroxysomes and the endoplasmic reticulum by arachidonic-type 15-lipoxygenases [172,173]. We hypothesize that some of the 13-LOX enzymes present in chloroplasts [174–176] may play a similar role during senescence and oxygenate α -linolenic acid such that JA would be produced. In non-senescent plants, salvage pathways would re-synthesize α -linolenic acid and thereby avoid undesirable membrane damage. Under senescence conditions, however, membrane fatty acid peroxydation would predominate and initiate programmed organelle destruction. At the same time, JA-dependent signalling would lead to defence gene activation and plant protection, allowing for undisturbed nutrient relocation.

Conclusions

The aspects summarized in this minireview show that JA plays many roles in plants, ranging from defence factors to cell death regulators and, finally, promoters of leaf senescence. The common link between these, at first glance, unrelated processes could be the chloroplast where the first steps of JA biosynthesis take place. Remarkably, components operating in photosynthesis participate in defence and cell death signalling and may also be active in the senescence programme. ROS, including singlet oxygen and H₂O₂, as well as *LSD1* and *EDS1-PAD4/SAG101* appear to be essential components in this signalling network [14,177]. Pigment-sensitized singlet oxygen formation is one source of plastid signalling involving JA-dependent and JA-independent pathways. Nevertheless, porphyrins themselves can operate as cell death factors, even in their unexcited states [178]. Major targets of singlet oxygen, JA and porphyrin action are transcription and translation as well as membrane-bound organelles such as mitochondria and chloroplasts.

Acknowledgements

This work was supported by research project grants of the German Science Foundation (DFG) to SR (RE1387/3-1) and CR (FOR222/3-1).

References

- 1 Liechti R & Farmer EE (2003) The jasmonate biochemical pathway. *Sci STKE* **203**, CM18.
- 2 Balbi V & Devoto A (2008) Jasmonate signalling network in *Arabidopsis thaliana*: crucial regulatory nodes and new physiological scenarios. *New Phytol* **177**, 301–318.
- 3 Wasternack C (2007) Jasmonates: an update on biosynthesis, signal transduction and action in plant stress

- response, growth and development. *Ann Bot (Lond)* **100**, 681–697.
- 4 Farmer EE & Ryan CA (1992) Octadecanoid precursors of jasmonic acid activate the synthesis of wound-inducible proteinase inhibitors. *Plant Cell* **4**, 129–134.
 - 5 Creelman RA, Tierney ML & Mullet JE (1992) Jasmonic acid/methyl jasmonate accumulate in wounded soybean hypocotyls and modulate wound gene expression. *Proc Natl Acad Sci USA* **89**, 4938–4941.
 - 6 Albrecht T, Kehlen A, Stahl K, Knöfel H-D, Sembdner G & Weiler E (1993) Quantification of rapid, transient increases in jasmonic acid in wounded plants using a monoclonal antibody. *Planta* **191**, 86–94.
 - 7 Avdiushko S, Croft KP, Brown GC, Jackson DM, Hamilton-Kemp TR & Hildebrand D (1995) Effect of volatile methyl jasmonate on the oxylipin pathway in tobacco, cucumber, and *Arabidopsis*. *Plant Physiol* **109**, 1227–1230.
 - 8 Gundlach H, Müller M, Kutchan TM & Zenk MH (1992) Jasmonic acid is a signal transducer in elicitor-induced plant cell cultures. *Proc Natl Acad Sci USA* **89**, 2389–2393.
 - 9 Müller MJ, Brodschelm W, Spannagl E & Zenk MH (1993) Signalling in the elicitation process is mediated through the octadecanoid pathway leading to jasmonic acid. *Proc Natl Acad Sci USA* **90**, 7490–7494.
 - 10 Nojiri H, Sugimori M, Yamane H, Nishimura Y, Yamada A, Shibuya N, Kodama O, Murofushi N & Omori T (1996) Involvement of jasmonic acid in elicitor-induced phytoalexin production in suspension-cultured rice cells. *Plant Physiol* **110**, 387–392.
 - 11 Rickauer M, Brodschelm W, Bottin A, Veronesi C, Grimal H & Esquerre-Tugaye MT (1997) The jasmonate pathway is involved in the regulation of different defence responses in tobacco cells. *Planta* **202**, 155–162.
 - 12 Conconi A, Smerdon MJ, Howe GA & Ryan CA (1996) The octadecanoid signalling pathway in plants mediates a response to ultraviolet radiation. *Nature* **383**, 826–829.
 - 13 Herde O, Atzorn R, Fisahn J, Wasternack C, Willmitzer L & Pena-Cortes H (1996) Localized wounding by heat initiates the accumulation of proteinase inhibitor II in abscisic acid-deficient plants by triggering jasmonic acid biosynthesis. *Plant Physiol* **112**, 853–860.
 - 14 Mühlenbock P, Szechynska-Hebda M, Plaszczyca M, Baudo M, Mullineaux PM, Parker JE, Karpinska B & Karpinski S (2008) Chloroplast signalling and LESION SIMULATING DISEASE1 regulate crosstalk between light acclimation and immunity in *Arabidopsis*. *Plant Cell* **20**, 2339–2356.
 - 15 Krieger-Liszkay A & Trebst A (2006) Tocopherol is the scavenger of singlet oxygen produced by the triplet states of chlorophyll in the PSII reaction centre. *J Exp Bot* **57**, 1677–1684.
 - 16 von Wettstein D, Gough S & Kannangara CG (1995) Chlorophyll biosynthesis. *Plant Cell* **7**, 1039–1057.
 - 17 Rebeiz CA, Motanzer-Zouhoor A, Mayasich JM, Tripathy BC, Wu S-M & Rebeiz C (1988) Phytodynamic herbicides: recent development and molecular basis of selectivity. *CRC Crit Rev Plant Sci* **6**, 385–436.
 - 18 Triantaphylidès C, Kruschke M, Hoerberichts FA, Ksas B, Gresser G, Havaux M, Van Breusegem F & Mueller MJ (2008) Singlet oxygen is the major reactive oxygen species involved in photooxidative damage to plants. *Plant Physiol* **148**, 960–968.
 - 19 Foyer CH & Noctor G (2000) Oxygen processing in photosynthesis: regulation and signalling. *New Phytol* **146**, 358–388.
 - 20 Matringe M, Camadro J-M, Labbe P & Scalla R (1989) Protoporphyrinogen oxidase as molecular target for diphenyl ether herbicides. *Biochem J* **260**, 231–235.
 - 21 Mock H-P, Keetman U, Kruse E, Rank B & Grimm B (1998) Defense responses to tetrapyrrole-induced oxidative stress in transgenic plants with reduced uroporphyrinogen decarboxylase or coproporphyrinogen oxidase activity. *Plant Physiol* **116**, 107–116.
 - 22 Reinbothe S & Reinbothe C (1996) The regulation of enzymes involved in chlorophyll biosynthesis. *Eur J Biochem* **237**, 323–343.
 - 23 Pontoppidan B & Kannangara CG (1994) Purification and partial characterisation of barley glutamyl-tRNA(-Glu) reductase, the enzyme that directs glutamate to chlorophyll biosynthesis. *Eur J Biochem* **225**, 529–537.
 - 24 Vothknecht U, Kannangara CG & von Wettstein D (1998) Barley glutamyl tRNAGlu reductase: mutations affecting haem inhibition and enzyme activity. *Phytochemistry* **47**, 513–519.
 - 25 Meskauskiene R, Nater M, Gosling D, Kessler F, op den Camp R & Apel K (2001) FLU: a negative regulator of chlorophyll biosynthesis in *Arabidopsis thaliana*. *Proc Natl Acad Sci USA* **98**, 12826–12831.
 - 26 Meskauskiene R & Apel K (2002) Interaction of FLU, a negative regulator of tetrapyrrole biosynthesis, with the glutamyl-tRNA reductase requires the tetra-tripeptide repeat domain of FLU. *FEBS Lett* **532**, 27–30.
 - 27 Goslings D, Meskauskiene R, Kim C, Lee KP, Nater M & Apel K (2004) Concurrent interactions of heme and FLU with Glu-tRNA reductase (HEMA1), the target of metabolic feedback inhibition of tetrapyrrole biosynthesis, in dark- and light-grown *Arabidopsis* plants. *Plant J* **40**, 957–967.
 - 28 op den Camp R, Przybyla D, Ochsenein C, Laloi C, Kim C, Danon A, Wagner D, Hidég E, Göbel C, Feussner I *et al.* (2004) Rapid induction of distinct stress responses after the release of singlet oxygen in *Arabidopsis*. *Plant Cell* **15**, 2320–2332.
 - 29 Danon A, Miersch O, Felix G, op den Camp R & Apel K (2005) Concurrent activation of cell death-regulating

- signalling pathways by singlet oxygen in *Arabidopsis thaliana*. *Plant J* **41**, 68–80.
- 30 Wagner D, Przybyla D, op den Camp R, Kim C, Landgraf F, Lee KP, Wursch M, Laloi C, Nater M & Apel K (2004) The genetic basis of singlet oxygen-induced stress responses of *Arabidopsis thaliana*. *Science* **306**, 1183–1185.
- 31 Lee KP, Kim C, Landgraf F & Apel K (2007) *EXECUTER1*- and *EXECUTER2*-dependent transfer of stress-related signals from the plastid to the nucleus of *Arabidopsis thaliana*. *Proc Natl Acad Sci USA* **104**, 10270–10275.
- 32 Kim C, Meskauskiene R, Apel K & Laloi C (2008) No single way to understand singlet oxygen signalling in plants. *EMBO Rep* **9**, 435–439.
- 33 Kendrick MD & Chang C (2008) Ethylene signalling: new levels of complexity and regulation. *Curr Opin Plant Biol* **11**, 479–485.
- 34 Przybyla D, Göbel C, Imboden A, Feussner I, Hamburger M & Apel K (2008) Enzymatic, but not non-enzymatic $^1\text{O}_2$ -mediated peroxidation of polyunsaturated fatty acids forms part of the *EXECUTER1*-dependent stress response program in the *flu* mutant of *Arabidopsis thaliana*. *Plant J* **54**, 236–248.
- 35 Wiermer M, Feys B & Parker JE (2005) Plant immunity: the EDS regulatory node. *Curr Opin Plant Biol* **8**, 383–389.
- 36 Flor HH (1971) Current status of the gene-for-gene concept. *Annu Rev Phytopathol* **9**, 275–296.
- 37 Hammond-Kosack KE & Jones JD (1996) Resistance gene-dependent plant defense responses. *Plant Cell* **8**, 1773–1791.
- 38 Dangl JL & Jones JD (2001) Plant pathogens and integrated defence responses to infection. *Nature* **411**, 826–833.
- 39 Martin G, Bogdanove A & Sessa G (2003) Understanding the functions of plant disease resistance proteins. *Annu Rev Plant Biol* **54**, 23–61.
- 40 Clarke JD, Aarts N, Feys BJ, Dong X & Parker JE (2001) Constitutive disease resistance requires *EDS1* in the *Arabidopsis* mutants *cpr1* and *cpr6* and is partially *EDS1*-dependent in *cpr5*. *Plant J* **26**, 409–420.
- 41 Rusterucci C, Aviv DH, Holt BF III, Dangl JL & Parker JE (2001) The disease resistance signaling components *EDS1* and *PAD4* are essential regulators of the cell death pathway controlled by *LSD1* in *Arabidopsis*. *Plant Cell* **13**, 2211–2224.
- 42 Aarts N, Metz M, Holub E, Staskawicz BJ, Daniels J & Parker JE (1998) Different requirements for *EDS1* and *NDR1* by disease resistance genes define at least two *R* gene-mediated signaling pathways in *Arabidopsis*. *Proc Natl Acad Sci USA* **95**, 10306–10311.
- 43 Feys BJ, Moisan LJ, Newman MA & Parker JE (2001) Direct interaction between the *Arabidopsis* disease resistance signaling proteins, *EDS1* and *PAD4*. *EMBO J* **20**, 5400–5411.
- 44 Feys BJ, Wiermer M, Bhat RA, Moisan LJ, Medina-Escobar N, Neu C, Cabral A & Parker JE (2005) *Arabidopsis* *SENESCENCE-ASSOCIATED GENE 101* stabilizes and signals within an *ENHANCED DISEASE SUSCEPTIBILITY1* complex in plant innate immunity. *Plant Cell* **17**, 2601–2613.
- 45 Yang S & Hua J (2004) A haplotype-specific resistance gene regulated by *BONZAI1* mediates temperature-dependent growth control in *Arabidopsis*. *Plant Cell* **16**, 1060–1071.
- 46 Yang H, Li Y & Hua J (2006a) The C2 domain protein *BAP1* negatively regulates defense responses in *Arabidopsis*. *Plant J* **48**, 238–248.
- 47 Creutz CE, Tomsig JL, Snyder SL, Gautier MC, Sjourri F, Beisson J & Cohen J (1998) The copines, a novel class of C2 domain-containing, calcium-dependent, phospholipid binding proteins conserved from *Paramecium* to humans. *J Biol Chem* **273**, 1393–1402.
- 48 Caudell EG, Caudell JI, Tang CH, Yu TK, Ferderick MJ & Grimm EA (2000) Characterization of human copine III as a phosphoprotein with associated kinase activity. *Biochemistry* **39**, 13034–13043.
- 49 Nakayama T, Yaoi T & Kuwajima G (1999) Localization and subcellular distribution of N-copine in mouse brain. *J Neurochem* **72**, 373–379.
- 50 Hua J, Grisafi P, Cheng SH & Fink GR (2001) Plant growth homeostasis is controlled by the *Arabidopsis* *BON1* and *BAP1* genes. *Genes Dev* **15**, 2263–2272.
- 51 Jambunathan N, Siani JM & McNellis TW (2001) A humidity-sensitive *Arabidopsis copine* mutant exhibits precocious cell death and increased disease resistance. *Plant Cell* **13**, 2225–2240.
- 52 Yang H, Yang S, Li Y & Hua J (2007) The *Arabidopsis* *BAP1* and *BAP2* genes are general inhibitors of programmed cell death. *Plant Physiol* **145**, 135–146.
- 53 Li Y, Yang S, Yang H & Hua J (2007) The *TIR-NB-LRR* gene *SNC1* is regulated at the transcript level by multiple factors. *J Mol Plant Microbe Interact* **20**, 1449–1456.
- 54 Yang S, Yang H, Grisafi P, Sanchatjate S, Fink GR, Sun Q & Hua J (2006) The *BON/CPN* gene family represses cell death and promotes cell growth in *Arabidopsis*. *Plant J* **45**, 166–179.
- 55 Weidhase RA, Kramell H, Lehmann J, Liebisch HW, Lerbs W & Parthier B (1987) Methyl jasmonate-induced changes in the polypeptide pattern of senescing barley leaf segments. *Plant Sci* **51**, 177–186.
- 56 Müller-Uri F, Parthier B & Nover L (1988) Jasmonate-induced alteration of gene expression in barley leaf segments analyzed by *in vivo* and *in vitro* protein synthesis. *Planta* **176**, 241–248.

- 57 Reinbothe S, Reinbothe C & Parthier B (1993) Methyl jasmonate represses translation initiation of a specific set of mRNAs in barley. *Plant J* **4**, 459–467.
- 58 Reinbothe S, Reinbothe C & Parthier B (1993) Methyl jasmonate-regulated translation of nuclear-encoded chloroplast proteins in barley. *J Biol Chem* **268**, 10606–10611.
- 59 Reinbothe S, Reinbothe C, Heintzen C, Seidenbecher C & Parthier B (1993) A methyl jasmonate-induced shift in the length of the 5' untranslated region impairs translation of the plastid rbcL transcript in barley. *EMBO J* **12**, 1505–1512.
- 60 Reinbothe S, Mollenhauer B & Reinbothe C (1994) JIPs and RIPs: the regulation of plant gene expression by jasmonates in response to environmental cues and pathogens. *Plant Cell* **6**, 1197–1209.
- 61 Thomas G (2002) The S6 kinase signalling pathway in the control of development and growth. *Biol Res* **35**, 305–313.
- 62 Dennis PB, Fumagalli S & Thomas G (1999) Target of rapamycin (TOR): balancing the opposing forces of protein synthesis and degradation. *Curr Opin Genet* **9**, 49–54.
- 63 Menand B, Meyer C & Robaglia C (2004) Plant growth and the TOR pathway. *Curr Top Microbiol Immunol* **279**, 97–113.
- 64 Nover L & Scharf K-D (1984) Synthesis, modification and structural binding of heat-shock proteins in tomato cell cultures. *Eur J Biochem* **139**, 303–313.
- 65 Bailey-Serres J & Freeling M (1990) Hypoxic stress-induced changes in ribosomes of maize seedlings roots. *Plant Physiol* **94**, 1237–1243.
- 66 Becker W & Apel K (1992) Isolation and characterization of a cDNA encoding a novel jasmonate-induced protein of barley (*Hordeum vulgare* L.). *Plant Mol Biol* **19**, 1065–1067.
- 67 Reinbothe S, Reinbothe C, Lehmann J, Becker W, Apel K & Parthier B (1994) JIP60, a methyl jasmonate-induced ribosome-inactivating protein involved in plant stress reactions. *Proc Natl Acad Sci USA* **91**, 7012–7016.
- 68 Chaudhry B, Muller-Uri F, Cameron-Mills V, Gough S, Simpson D, Skriver K & Mundy J (1994) The barley 60 kDa jasmonate-induced protein (JIP60) is a novel ribosome-inactivating protein. *Plant J* **6**, 815–824.
- 69 Stirpe F & Barbieri L (1986) Ribosome-inactivating proteins up to date. *FEBS Lett* **195**, 1–8.
- 70 Van Damme EJM, Hao Q, Chen Y, Barre A, Vandebusch F, Desmyter S, Rouge P & Peumans WJ (2001) Ribosome-inactivating proteins: a family of plant proteins that do more than inactivate ribosomes. *Crit Rev Plant Sci* **20**, 395–465.
- 71 Coleman WH & Roberts WK (1982) Inhibitors of animal cell-free protein synthesis from grains. *Biochim Biophys Acta* **696**, 239–244.
- 72 Stirpe F, Bailey S, Miller SP & Bodley JW (1988) Modification of ribosomal RNA by ribosome-inactivating proteins from plants. *Nucleic Acids Res* **16**, 1349–1357.
- 73 Endo Y & Tsurugi K (1987) RNA N-glycosidase activity of ricin A chain: mechanism of action of the toxic lectin ricin on eukaryotic ribosomes. *J Biol Chem* **262**, 8128–8130.
- 74 Endo Y, Mitsui K, Motizuki M & Tsurugi K (1987) The mechanism of action of ricin and related toxic lectins on eukaryotic ribosomes: the site and characteristics of the modification in 28S ribosomal RNA caused by the toxins. *J Biol Chem* **262**, 5908–5912.
- 75 Endo Y, Tsurugi K & Lamberts JM (1988) The site of action of six different ribosome-inactivating proteins from plants on eukaryotic ribosomes: the RNA N-glycosidase activity of the proteins. *Biochem Biophys Res Commun* **150**, 1032–1036.
- 76 Roberts WK & Stewart TS (1979) Purification and properties of a translation inhibitor from wheat germ. *Biochemistry* **18**, 2615–2621.
- 77 Brigotti M, Rambelli M, Zamboni M, Montanaro L & Sperti S (1989) Effect of α -sarcin and ribosome-inactivating proteins on the interaction of elongation factors with ribosomes. *Biochem J* **257**, 723–727.
- 78 Khandal D, Samol I, Buhr F, Pollmann S, Schmidt H, Clemens C, Reinbothe S & Reinbothe C (2009) Singlet oxygen-dependent translational control in the *tigrina-d.12* mutant of barley, submitted. *Proc Natl Acad Sci USA*, in press.
- 79 Ochsenbein C, Przybyla D, Danon A, Landgraf F, Göbel C, Imboden A, Feussner I & Apel K (2006) The role of EDS1 (enhanced disease susceptibility) during singlet oxygen-mediated stress responses of *Arabidopsis*. *Plant J* **47**, 445–456.
- 80 Pena-Cortes H, Albrecht T, Prat S, Weiler EW & Willmitzer L (1993) Aspirin prevents wound-induced gene expression in tomato leaves by blocking jasmonic acid biosynthesis. *Planta* **191**, 123–128.
- 81 Doares H, Narvaez-Vasquez J, Conconin A & Ryan CA (1995) Salicylic acid inhibits synthesis of proteinase inhibitors in tomato leaves induced by systemin and jasmonic acid. *Plant Physiol* **108**, 1741–1748.
- 82 Overmyer K, Tuominen H, Kettunen R, Betz C, Langebartels C, Sandermann H & Kangasjärvi J (2000) The ozone-sensitive *Arabidopsis red1* mutant reveals opposite roles for ethylene and jasmonate signaling pathways in regulating superoxide-dependent cell death. *Plant Cell* **12**, 1849–1862.
- 83 Rao MV, Lee H, Creelman RA, Mullet JE & Davis KR (2000) Jasmonic acid signalling modulates ozone-induced hypersensitive cell death. *Plant Cell* **12**, 1633–1646.
- 84 Rao MV, Lee HI & Davis KR (2002) Ozone-induced ethylene production is dependent on salicylic acid, and both salicylic acid and ethylene act in concert to regulate ozone-induced cell death. *Plant J* **32**, 447–456.

- 85 Ahlfors R, Brosché M, Kollist H & Kangasjärvi J (2008) Nitric oxide modulates ozone-induced cell death, hormone biosynthesis and gene expression in *Arabidopsis thaliana*. *Plant J* **58**, 1–12.
- 86 Vranová E, Inzé D & van Breusegem F (2002) Signal transduction during oxidative stress. *J Exp Bot* **53**, 1227–1236.
- 87 Overmyer K, Borsché M & Kangasjärvi J (2003) Reactive oxygen species and hormonal control of cell death. *Trends Plant Sci* **8**, 335–342.
- 88 Staswick PE, Su W & Howell SH (1992) Methyl jasmonate inhibition of root growth and induction of a leaf protein are decreased in an *Arabidopsis thaliana* mutant. *Proc Natl Acad Sci USA* **89**, 6832–6840.
- 89 Xie DX, Feys BF, James S, Nieto-Rostro M & Turner JG (1998) *COI1*: an *Arabidopsis* gene required for jasmonate-regulated defense and fertility. *Science* **280**, 1091–1094.
- 89a Chini A, Boter M & Solano R (2009) Plant oxylipins: COI1/JAZs/MYC2 as the core jasmonic acid-signaling module. *FEBS J* **276**, doi:10.1111/j.7142-4658.2009.07194.x
- 90 McConn M & Browse J (1996) The critical requirement for linolenic acid is pollen development, not photosynthesis, in an *Arabidopsis* mutant. *Plant Cell* **8**, 403–416.
- 90a Böttcher C & Pollman S (2009) Plant oxylipins: Plant responses to 12-oxo-phytodienoic acid are governed by its specific structural and functional properties. *FEBS J* **276**, doi:10.1111/j.1742-4658.2009.07195.x
- 91 Castagna A, Ederli L, Pasqualini S, Mensuali-Sodi A, Baldan B, Donnini S & Ranieri A (2007) The tomato ethylene receptor LE-ETR3 (NR) is not involved in mediating ozone sensitivity: causal relationships among ethylene emission, oxidative burst and tissue damage. *New Phytol* **174**, 342–356.
- 92 Nibbe M, Hilpert B, Wasternack C, Miersch O & Apel K (2002) Cell death and salicylate- and jasmonate-dependent stress responses in *Arabidopsis* are controlled by single *cet* genes. *Planta* **216**, 120–128.
- 93 Xiang C & Oliver DJ (1998) Glutathione metabolic genes coordinately respond to heavy metals and jasmonic acid in *Arabidopsis*. *Plant Cell* **10**, 1539–1590.
- 94 Schenk PM, Kazan K, Wilson I, Anderson JP, Richmond T, Somerville SC & Manners JM (2000) Coordinated plant defense responses in *Arabidopsis* revealed by microarray analysis. *Proc Natl Acad Sci USA* **97**, 11655–11660.
- 95 Danon A, Delorme V, Mailhac N & Gallois P (2000) Plant programmed cell death: a common way to die. *Plant Physiol Biochem* **38**, 647–655.
- 96 Hoerberichts FA & Woltering EJ (2002) Multiple mediators of plant programmed cell death: interplay of conserved cell death mechanisms and plant-specific regulators. *BioEssays* **25**, 47–57.
- 97 Loake G & Grant M (2007) Salicylic acid in plant defence – the players and protagonists. *Curr Opin Plant Biol* **10**, 466–472.
- 98 Noctor G, De Paepe R & Foyer CH (2007) Mitochondrial redox biology and homeostasis in plants. *Trends Plant Sci* **12**, 125–134.
- 99 Green DR & Reed JC (1998) Mitochondria and apoptosis. *Science* **281**, 1309–1312.
- 100 van Doorn WG & Woltering EJ (2005) Many ways to exit? Cell death categories in plants. *Trends Plant Sci* **10**, 117–122.
- 101 Yonekawa H & Akita Y (2008) Protein kinase Cepsilon: the mitochondria-mediated signaling pathway. *FEBS J* **275**, 4005–4013.
- 102 Kawai-Yamada M, Ohori Y & Ucimiya H (2004) Dissection of *Arabidopsis* Bax inhibitor-1 suppressing Bax-, hydrogen peroxide-, and salicylic acid-induced cell death. *Plant Cell* **16**, 21–32.
- 103 Coupe SA, Watson LM, Ryan DJ, Pinkney TT & Eason JR (2004) Molecular analysis of programmed cell death during senescence in *Arabidopsis thaliana* and *Brassica oleracea*: cloning broccoli LSD1, Bax inhibitor and serine palmitoyltransferase homologues. *J Exp Bot* **55**, 59–68.
- 104 Watanabe N & Lam E (2004) Recent advance in the study of caspase-like proteases and Bax inhibitor-1 in plants: their possible roles as regulator of programmed cell death. *Mol Plant Pathol* **5**, 65–70.
- 105 Kabbage M & Dieckman MB (2008) The BAG proteins: a ubiquitous family of chaperone regulators. *Cell Mol Life Sci* **65**, 1390–1402.
- 106 Kawano T, Sahashi N, Takahashi K, Uozumi N & Muto S (1998) Salicylic acid induces extracellular generation of superoxide followed by an increase in cytosolic calcium ion in tobacco suspension culture: the earliest events in salicylic acid signal transduction. *Plant Cell Physiol* **39**, 721–730.
- 107 López MA, Bannenberg G & Castresana C (2008) Controlling hormone signaling is a plant and pathogen challenge for growth and survival. *Curr Opin Plant Biol* **11**, 420–427.
- 108 Xie Z & Chen Z (1999) Salicylic acid induces rapid inhibition of mitochondrial electron transport and oxidative phosphorylation in tobacco cells. *Plant Physiol* **120**, 217–226.
- 109 Lecourieux D, Ranjeva R & Pugin A (2006) Calcium in plant defence-signalling pathways. *New Phytol* **171**, 249–269.
- 110 Ma W & Berkowitz GA (2007) The grateful dead: calcium and cell death in plant innate immunity. *Cell Microbiol* **9**, 2571–2585.
- 111 Zhang L & Xing D (2008) Methyl jasmonate induces production of reactive oxygen species and alterations in mitochondrial dynamics that precede photosynthetic dysfunction and subsequent cell death. *Plant Cell Physiol* **49**, 1092–1111.

- 112 Rotem R, Heyfets A, Fingrut O, Blickstein D, Shaklai M & Flescher E (2005) Jasmonates: novel anticancer agents acting directly and selectively on human cancer cell mitochondria. *Cancer Res* **65**, 1984–1993.
- 113 Kim JH, Lee SY, Oh SY, Han SI, Park HG, Yoo MA & Kang HS (2004) Methyl jasmonate induces apoptosis through induction of Bax/Bcl-XS and activation of caspase-3 via ROS production in A549 cells. *Oncol Rep* **12**, 1233–1238.
- 114 Gilchrist DG (1997) Mycotoxins reveal connections between plants and animals in apoptosis and ceramide signaling. *Cell Death Differ* **4**, 689–698.
- 115 Brodersen P, Petersen M, Pike HM, Olszak B, Skov S, Odum N, Jorgensen LB, Brown RE & Mundy J (2002) Knock-out of *Arabidopsis accelerated cell death 11* encoding a sphingosine transfer protein causes activation of programmed cell death and defense. *Genes Dev* **16**, 490–502.
- 116 Petersen NH, McKinney LV, Pike H, Hofius D, Zakaria A, Brodersen P, Petersen M, Brown RE & Mundy J (2008) Human GLTP and mutant forms of ACD11 suppress cell death in the *Arabidopsis acd11* mutant. *FEBS J* **275**, 4378–4388.
- 117 Petersen NH, Joensen J, McKinney LV, Brodersen P, Petersen M, Hofius D & Mundy J (2009) Identification of proteins interacting with *Arabidopsis ACD11*. *J Plant Physiol* **166**, 661–666.
- 118 Ueda J & Kato J (1980) Isolation and identification of a senescence-promoting substance from wormwood (*Artemisia absinthium* L.). *Plant Physiol* **66**, 246–249.
- 119 He Y, Fukushige H, Hildebrand DF & Gan S (2002) Evidence supporting a role of jasmonic acid in *Arabidopsis* leaf senescence. *Plant Physiol* **128**, 876–884.
- 120 Zentgraf U, Jobst J, Kolb D & Rentsch D (2004) Senescence-related gene expression profiles of rosette leaves of *Arabidopsis thaliana*: leaf age versus plant age. *Plant Biol* **6**, 178–183.
- 121 Buchanan-Wollaston V, Page T, Harrison E, Breeze E, Lim PO, Nam HG, Lin JF, Wu SH, Swidzinski J, Ishizaki K *et al.* (2005) Comparative transcriptome analysis reveals significant differences in gene expression and signalling pathways between developmental and dark/starvation-induced senescence in *Arabidopsis*. *Plant J* **42**, 567–585.
- 122 van der Graaff E, Schwacke R, Schneider A, Desimone M, Flügge UI & Kunze R (2006) Transcription analysis of *Arabidopsis* membrane transporters and hormone pathways during developmental and induced leaf senescence. *Plant Physiol* **141**, 776–792.
- 123 Eulgem T, Rushton PJ, Robatzek S & Somssich IE (2001) The WRKY superfamily of plant transcription factors. *Trends Plant Sci* **5**, 199–206.
- 124 Hinderhofer K & Zentgraf U (2001) Identification of a transcriptional factor specifically expressed at the onset of leaf senescence. *Planta* **213**, 469–473.
- 125 Robatzek S & Somssich IE (2002) Targets of AtWRKY6 regulation during plant senescence and pathogen defense. *Gene Dev* **16**, 1139–1149.
- 126 Yoshida S (2003) Molecular regulation of leaf senescence. *Curr Opin Plant Biol* **6**, 79–84.
- 127 Miao Y & Zentgraf U (2007) The antagonist function of *Arabidopsis* WRKY53 and ESR/ESP in leaf senescence is modulated by the jasmonic and salicylic acid equilibrium. *Plant Cell* **19**, 819–830.
- 128 Morris K, MacKerness SA, Page T, John CF, Murphy AM, Carr JP & Buchanan-Wollaston V (2000) Salicylic acid has a role in regulating gene expression during leaf senescence. *Plant J* **23**, 677–685.
- 129 Kosugi S & Ohashi Y (1997) PCF1 and PCF2 specifically bind to *cis* elements in the rice proliferating cell nuclear antigen gene. *Plant Cell* **9**, 1607–1619.
- 130 Cubas P, Lauter N, Doebley J & Coen E (1999) The TCP domain: a motif found in proteins regulating plant growth and development. *Plant J* **18**, 215–222.
- 131 Kosugi S & Ohashi Y (2002) DNA binding and dimerization specificity and potential targets for the TCP protein family. *Plant J* **30**, 337–348.
- 132 Li C, Potuschak T, Colón-Carmona A, Gutiérrez R & Doermann P (2005) *Arabidopsis* TCP29 links regulation of growth and cell division control pathways. *Proc Natl Acad Sci USA* **102**, 12978–12983.
- 133 Schommer C, Palatik JF, Aggarwal P, Chételat A, Cubas P, Farmer E, Nath U & Weigel D (2008) Control of jasmonate biosynthesis and senescence by miR319 targets. *PLoS Biol* **6**, 1991–2001.
- 134 Jones-Rhoades MW, Bartel DP & Bartel B (2006) MicroRNAs and their regulatory roles in plants. *Annu Rev Plant Biol* **57**, 19–53.
- 135 Mallory AC & Vaucheret H (2006) Functions of microRNAs and related small RNAs in plants. *Nat Genet* **38**(Suppl), S31–S36.
- 136 Nath U, Crawford BC, Carpenter R & Coen E (2003) Genetic control of surface curvature. *Science* **299**, 1404–1407.
- 137 Palatik JF, Allen E, Wu X, Schommer C, Schwab R, Carrington JC & Weigel D (2003) Control of leaf morphogenesis by microRNAs. *Nature* **425**, 257–263.
- 138 Ori N, Cohen AR, Etzioni A, Brand A, Yanai O, Shleizer S, Menda N, Amsellem Z, Efroni I, Pekker I *et al.* (2007) Regulation of LANCEOLATE by miR319 is required for compound-leaf development in tomato. *Nat Genet* **39**, 787–791.
- 139 Kim JH, Woo HR, Kim J, Lim PO, Lee IC, Choi SH, Hwang DH & Nam HG (2009) Trifurcate feed-forward regulation of age-dependent cell death involving miR164 in *Arabidopsis*. *Science* **323**, 1053–1057.

- 140 Woo HR, Chung KM, Park J-H, Oh SA, Ahn T, Hong SH, Jang SK & Nam HG (2001) ORE9, an F-box protein that regulates leaf senescence in *Arabidopsis*. *Plant Cell* **13**, 1779–1790.
- 141 Hellmann H & Estelle M (2002) Plant development: regulation by protein degradation. *Science* **297**, 793–797.
- 142 Schwechheimer C & Calderón Villalobos LIA (2004) Cullin-containing E3 ubiquitin ligases in plant development. *Curr Opin Plant Biol* **7**, 677–688.
- 143 Ruegger M, Dewey E, Gray WM, Hobbie L, Turner J & Estelle M (1998) The TIR1 protein of *Arabidopsis* functions in auxin response and is related to human SKP2 and yeast grr1p. *Genes Dev* **12**, 198–207.
- 144 Samach A, Klenz JE, Kohalmi SE, Risseuw E, Haughn GW & Crosby WL (1999) The UNUSUAL FLORAL ORGANS gene of *Arabidopsis thaliana* is an F-box protein required for normal patterning and growth in the floral meristem. *Plant J* **20**, 433–445.
- 145 Nelson DC, Lasswell J, Rogg LE, Cohen MA & Bartel B (2000) FKF1, a clock-controlled gene that regulates the transition to flowering in *Arabidopsis*. *Cell* **101**, 331–340.
- 146 Somers DE, Schultz TF, Milnamow M & Kay SA (2000) ZEITLUPE encodes a novel clock-associated PAS protein from *Arabidopsis*. *Cell* **101**, 319–329.
- 147 Glickman MH & Ciechanover A (2002) The ubiquitin–proteasome proteolysis pathway: destruction for the sake of construction. *Physiol Rev* **82**, 373–428.
- 148 Vierstra RD (2003) The ubiquitin/26S proteasome pathway, the complex last chapter in the life of many plant proteins. *Trends Plant Sci* **8**, 135–142.
- 149 Shen H, Luong P & Huq E (2007) The F-box protein MAX2 functions as a positive regulator of photomorphogenesis in *Arabidopsis*. *Plant Physiol* **145**, 1471–1483.
- 150 Stirnberg P, van De Sande K & Leyser HM (2002) MAX1 and MAX2 control shoot lateral branching in *Arabidopsis*. *Development* **129**, 1131–1141.
- 151 Stirnberg P, Furner IJ & Ottoline Leyser HM (2007) MAX2 participates in an SCF complex which acts locally at the node to suppress shoot branching. *Plant J* **50**, 80–94.
- 152 Tang D, Christiansen KM & Innes RW (2005) Regulation of plant disease resistance, stress responses, cell death, and ethylene signaling in *Arabidopsis* by the EDR1 protein kinase. *Plant Physiol* **138**, 1018–1026.
- 153 Frye CA & Innes RW (1998) An *Arabidopsis* mutant with enhanced resistance to powdery mildew. *Plant Cell* **10**, 947–956.
- 154 Park S-Y, Yu J-W, Park J-S, Li J, Yoo S-C, Lee S-K, Jeong S-W, Seo HS, Koh H-J, Park Y-I *et al.* (2007) The senescence-induced staygreen protein regulates chlorophyll degradation. *Plant Cell* **19**, 1649–1664.
- 155 Hörtensteiner S (2009) Stay-green regulates chlorophyll and chlorophyll-binding protein degradation during senescence. *Trends Plant Sci* **14**, 155–162.
- 156 Pruzinska A, Tanner G, Anders I, Roca M & Hörtensteiner S (2003) Chlorophyll breakdown: phaeophorbide *a* oxygenase is a Rieske-type iron-sulfur protein, encoded by the *accelerated cell death 1* gene. *Proc Natl Acad Sci USA* **100**, 15259–15264.
- 157 Mach JM, Castillo AR, Hoogstraten R & Greenberg JT (2001) The *Arabidopsis accelerated cell death* gene *ACD2* encodes red chlorophyll catabolite reductase and suppresses the spread of disease symptoms. *Proc Natl Acad Sci USA* **98**, 771–776.
- 158 Larkin RM & Ruckle ME (2008) Integration of light and plastid signals. *Curr Opin Plant Biol* **11**, 593–599.
- 159 Pogson BJ, Woo NS, Förster B & Small ID (2008) Plastid signalling to the nucleus and beyond. *Trends Plant Sci* **13**, 602–609.
- 160 Fernández AP & Strand A (2008) Retrograde signaling and plant stress: plastid signals initiate cellular stress responses. *Curr Opin Plant Biol* **11**, 509–513.
- 161 Woodson JD & Chory J (2008) Coordination of gene expression between organellar and nuclear genomes. *Nat Rev Genet* **9**, 383–395.
- 162 Jelenska J, Yao N, Vinatzer BA, Wright CM, Brodsky JL & Greenberg JT (2007) A J domain virulence effector of *Pseudomonas syringae* remodels host chloroplasts and suppresses defenses. *Curr Biol* **17**, 499–508.
- 163 Caplan JL, Mamillapalli P, Burch-Smith TM, Czymmek K & Dinesh-Kumar SP (2008) Chloroplastic protein NRIP1 mediates innate immune receptor recognition of a viral effector. *Cell* **132**, 449–462.
- 164 Zimmermann P, Hirsch-Hoffmann M, Hennig L & Gruissem W (2004) GENEVESTIGATOR. *Arabidopsis* microarray database and analysis toolbox. *Plant Physiol* **136**, 2621–2632.
- 165 Tsuchiya T, Ohta H, Okawa K, Iwamatsu A, Shimada H, Masuda T & Takamiya K-I (1999) Cloning of chlorophyllase, the key enzyme in chlorophyll degradation: finding of a lipase motif and the induction by methyl jasmonate. *Proc Natl Acad Sci USA* **96**, 15362–15367.
- 166 Weiler EW, Kutchan TM, Gorba T, Brodschelm W, Niesel U & Bublitz F (1994) The *Pseudomonas* phyto-toxin coronatine mimics octadecanoid signalling molecules of higher plants. *FEBS Lett* **345**, 9–13.
- 167 Benedetti CE, Costa CL, Turcinelli SR & Arruda P (1998) Differential expression of a novel gene in response to coronatine, methyl jasmonate, and wounding in the coil mutant of *Arabidopsis*. *Plant Physiol* **116**, 1037–1042.
- 168 Kariola T, Brader G & Tapio E (2005) Chlorophyllase 1, a damage control enzyme, affects the balance between defense pathways in plants. *Plant Cell* **17**, 282–294.

- 169 Feys B, Benedetti CE, Penfold CN & Turner JG (1994) *Arabidopsis* mutants selected for resistance to the phytotoxin coronatine are male sterile, insensitive to methyl jasmonate, and resistant to a bacterial pathogen. *Plant Cell* **6**, 751–759.
- 170 Stintzi A & Browse J (2000) The *Arabidopsis* male-sterile mutant, *opr3*, lacks the 12-oxophytodienoic acid reductase required for jasmonate synthesis. *Proc Natl Acad Sci USA* **97**, 10625–10630.
- 171 Sanders PM, Lee PY, Biesgen C, Boone JD, Beals TP, Weiler EW & Goldberg RB (2000) The *Arabidopsis* *DELAYED DEHISCENCE1* gene encodes an enzyme in the jasmonic acid synthesis pathway. *Plant Cell* **12**, 1041–1061.
- 172 Schewe T, Halangk W, Hiebssch C & Rapoport SM (1975) A lipoxygenase in rabbit reticulocytes which attacks phospholipids and intact mitochondria. *FEBS Lett* **60**, 149–152.
- 173 van Leyen K, Duvolsini RM, Engelhardt H & Wiedmann M (1998) A function for lipoxygenase in programmed organelle degradation. *Nature* **395**, 392–395.
- 174 Bell E, Creelman RA & Mullet JE (1995) A chloroplast lipoxygenase is required for wound-induced jasmonic acid accumulation in *Arabidopsis*. *Proc Natl Acad Sci USA* **92**, 8675–8679.
- 175 Feussner I, Hause B, Vörös K, Parthier B & Wasternack C (1995) Jasmonate-induced lipoxygenase forms are localized in chloroplasts of barley leaves (*Hordeum vulgare* cv. Salome). *Plant J* **7**, 949–957.
- 176 Bachmann A, Hause B, Mauchert H, Garbe E, Vörös K, Weichert H, Wasternack C & Feussner I (2002) Jasmonate-induced lipid peroxidation in barley leaves initiated by distinct 14-LOX forms of chloroplasts. *Biol Chem* **383**, 1645–1657.
- 177 Wormuth D, Baier M, Kandlbinder A, Scheibe R, Hartung W & Dietz KJ (2006) Regulation of gene expression by photosynthetic signals triggered through modified CO₂ availability. *BMC Plant Biol* **6**, 15.
- 178 Hirashima M, Tanaka R & Tanaka A (2009) Light-independent cell death induced by accumulation of pheophorbide *a* in *Arabidopsis thaliana*. *Plant Cell Physiol* **50**, 719–729.

Implication of the *oep16-1* Mutation in a *flu*-Independent, Singlet Oxygen-Regulated Cell Death Pathway in *Arabidopsis thaliana*

Iga Samol¹, Frank Buhr¹, Armin Springer², Stephan Pollmann³, Abder Lahroussi¹, Claudia Rossig¹, Diter von Wettstein^{4,5,*}, Christiane Reinbothe¹ and Steffen Reinbothe^{1,4,*}

¹Laboratoire de Génétique Moléculaire des Plantes et Biologie intégrative et systémique (BISy), Université Joseph Fourier, CERMO, BP53, F-38041 Grenoble cedex 9, France

²Lehrstuhl für Pflanzenphysiologie, Universität Bayreuth, Universitätsstraße 30, D-95447 Bayreuth, Germany

³Lehrstuhl für Pflanzenphysiologie, Ruhr-Universität Bochum, Universitätsstraße 150, D-44801 Bochum, Germany

⁴Department of Crop and Soil Sciences & School of Molecular Biosciences, Washington State University, Pullman WA 99164-6420 USA

⁵Research Center for BioSystems, Land Use and Nutrition, Justus Liebig University, Giessen, Germany

*Corresponding author: Diter von Wettstein, E-mail, diter@wsu.edu; Steffen Reinbothe, E-mail, steffen.reinbothe@ujf-grenoble.fr;

Fax, +1-509-335-8674 (DvW), +33-47651-4805 (SR)

(Received June 3, 2010; Accepted November 8, 2010)

Singlet oxygen is a prominent form of reactive oxygen species in higher plants. It is easily formed from molecular oxygen by triplet–triplet interchange with excited porphyrin species. Evidence has been obtained from studies on the *flu* mutant of *Arabidopsis thaliana* of a genetically determined cell death pathway that involves differential changes at the transcriptome level. Here we report on a different cell death pathway that can be deduced from the analysis of *oep16* mutants of *A. thaliana*. Pure lines of four independent OEP16-deficient mutants with different cell death properties were isolated. Two of the mutants overproduced free protochlorophyllide (Pchl) in the dark because of defects in import of NADPH:Pchl oxidoreductase A (pPORA) and died after illumination. The other two mutants avoided excess Pchl accumulation. Using pulse labeling and poly-some profiling studies we show that translation is a major site of cell death regulation in *flu* and *oep16* plants. *flu* plants respond to photooxidative stress triggered by singlet oxygen by reprogramming their translation toward synthesis of key enzymes involved in jasmonic acid synthesis and stress proteins. In contrast, those *oep16* mutants that were prone to photooxidative damage were unable to respond in this way. Together, our results show that translation is differentially affected in the *flu* and *oep16* mutants in response to singlet oxygen.

Keywords: Chlorophyll biosynthesis • Porphyrin-regulated plastid protein import • NADPH:protochlorophyllide oxidoreductase A (PORA) • Reactive oxygen species • Translation.

Abbreviations: DHFR, dihydrofolate reductase; DTNB, 5,5'-dithiobis(2-nitro)benzoic acid; GFP, green fluorescent protein; MS, Murashige and Skoog; Pchl, protochlorophyllide;

pPORA, NADPH:protochlorophyllide oxidoreductase A precursor; ROS, reactive oxygen species.

Introduction

Reactive oxygen species (ROS) are prominent by-products of aerobic metabolism and potent signaling compounds. They are involved in plant–pathogen interactions and also accumulate in response to abiotic stress (Apel and Hirt 2003, Miller et al. 2008). Singlet oxygen is one form of ROS that has gained wide interest because it is generated during photosynthesis (Mühlenbock et al. 2008). On the other hand, a role for singlet oxygen has been demonstrated for mutants that are impaired in sequestering Chl and its precursor and degradation products in a protein-bound form. This is illustrated by studies on the *flu* mutant of *Arabidopsis thaliana* that is defective in the negative feedback loop inhibiting excess protochlorophyllide (Pchl) synthesis in the dark (Meskauskiene et al. 2001). Etiolated *flu* plants rapidly die when illuminated because of singlet oxygen production (Meskauskiene et al. 2001). Light-adapted *flu* plants respond to non-permissive dark to light shifts with a marked growth inhibition and/or cell death, depending on the amount of singlet oxygen produced by Pchl operating as a photosensitizer (op den Camp et al. 2004, Danon et al. 2005).

Two major effects have been proposed to explain the singlet oxygen-mediated cell death phenotype of *flu* plants: a cytotoxic effect including lipid peroxidations and membrane destruction, and a genetic effect including specific signaling cascades (op den Camp et al. 2004, Wagner et al. 2004, Danon et al. 2005; see Kim et al. 2008, Reinbothe et al. 2010, for a review). Transcriptome analyses identified a large number of genes that differentially respond to singlet oxygen (op den Camp et al.

Plant Cell Physiol. 52(1): 84–95 (2011) doi:10.1093/pcp/pcq176, available online at www.pcp.oxfordjournals.org

© The Author 2010. Published by Oxford University Press on behalf of Japanese Society of Plant Physiologists.

All rights reserved. For permissions, please email: journals.permissions@oup.com

2004). Genes that were up-regulated by singlet oxygen include *BONZAI1*, the enhanced disease susceptibility (*EDS*) 1 gene, and genes encoding enzymes involved in the biosynthesis of ethylene and jasmonic acid, two key components of stress signaling in higher plants (Wasternack 2007, Kendrick and Chang 2008, Reinbothe et al. 2009). On the other hand, genes encoding components of the photosynthetic apparatus were rapidly down-regulated in response to singlet oxygen (op den Camp et al. 2004). Wagner et al. (2004) demonstrated that cell death execution is suppressed in the *executer 1* (*exe1*) mutant of *A. thaliana*, but only if low levels of singlet oxygen accumulate and trigger limited cytotoxic effects. EXECUTER 1 is a membrane protein of chloroplasts of unknown function (Wagner et al. 2004).

It is as yet undetermined how *flu* plants translate the rapid, singlet oxygen-dependent changes at the transcriptome level into protein synthesis. It is also unresolved whether there is one cell death pathway that is activated by porphyrin excitation and singlet oxygen production or whether there are more. In our previous work, we described a conditional cell death mutant of *A. thaliana* that is defective in the *OEP16* gene (Pollmann et al. 2007). *OEP16* forms a small gene family comprising three members, designated *AtOEP16-1* (At2g28900), *AtOEP16-2* (At4g16160) and *AtOEP16-4* (At3g62880), that are all plastid proteins that lack a transit sequence (Murcha et al. 2007, Drea et al. 2006). A fourth relative exists (*AtOEP16-3*; encoded by At2g42210) that appears not to belong to this group and is, unlike the other members, localized in mitochondria (Philippa et al. 2007). *AtOEP16-1* shows the highest protein sequence identity (62%) to *OEP16* from pea (Pohlmeyer et al. 1997, Murcha et al. 2007) and to *HvOEP16-1;1* from barley (52%), which was identified as partner of the cytosolic precursor of NADPH:protochlorophyllide oxidoreductase A (pPORA) during its Pchlde-dependent plastid import (Reinbothe et al. 2004a, Reinbothe et al. 2004b). Two non-exclusive functions currently being considered for the *OEP16-1* protein in the outer envelope of chloroplasts are (i) a voltage-gated, amino acid-selective channel (Philippa et al. 2007) and (ii) an import channel of pPORA (Reinbothe et al. 2004a, Reinbothe et al. 2004b). Knock-out mutants in *A. thaliana* for *AtOEP16-1* (designated *oep16-1;1*, corresponding to At2g28900) have provided different results (Philippa et al. 2007, Pollmann et al. 2007). We found that the absence of *OEP16* correlates with the lack of import of pPORA, aberrant etioplast ultrastructures and the accumulation of free, photoexcitable Pchlde molecules that triggered cell death upon irradiation of dark-grown seedlings (Pollmann et al. 2007). In contrast, Philippa et al. (2007) observed no import defects of pPORA, normal etioplast ultrastructures and unimpaired greening.

The phenotype of the *oep16-1;1* mutant we studied (Pollmann et al. 2007) is very similar to that of *flu* plants (Meskauskiene et al. 2001; op den Camp et al. 2004, Wagner et al. 2004, Danon et al. 2005). We therefore compared the molecular events leading to cell death in etiolated *oep16-1;1* and *flu* plants after illumination, with a focus on translation as

the site of active protein synthesis. For comparison, three additional *oep16-1* mutants were isolated from the original seed stock provided by the Salk Institute that displayed different cell death properties. Two of these mutants have phenotypes with different singlet oxygen production and/or signaling patterns. Together, our results provide evidence for the existence of a second, *flu*-independent singlet oxygen-dependent cell death pathway in *oep16-1* plants.

Results

Identification of *oep16-1* knock-out mutant plants

A PCR-based approach using previous primer combinations (Philippa et al. 2007, Pollmann et al. 2007) was employed to re-screen the original seed stock of the Salk Institute (At2g28900, corresponding to SALK_018024) (Alonso et al. 2001) for *oep16-1* knock-out plants (Fig. 1A). Several independent homozygous *oep16-1* knock-out plants were obtained that were backcrossed once with the wild type. Seeds from individual plants of the offspring of these crosses were propagated further to establish seed stocks. Aliquots from these seed stocks were sown on Murashige and Skoog (MS) medium and germinated in the dark. After 5 d, the seedlings were inspected under blue light using a microscope.

Some seedlings exhibited a strong red Pchlde fluorescence while other seedlings were, like the wild type, not fluorescent (Fig. 1B). Western blotting using isolated etioplasts and POR antiserum showed that among the fluorescent seedlings two subclasses of *oep16-1* mutant plants were present: one subclass lacking PORA, consistent with our previous findings (Pollmann et al. 2007), and another subclass with wild-type PORA protein levels (Fig. 1C, panel a). When etioplasts from seedlings that had not shown pigment autofluorescence under blue light were tested by Western blotting, the same segregation into PORA-containing and PORA-free lines was observed (Fig. 1C, panel a), leading all together to four types of *oep16-1* mutant plants that were designated *oep16-1;5*, *oep16-1;6*, *oep16-1;7* and *oep16-1;8*, and characterized further. Western blotting confirmed that all four mutant types were devoid of *OEP16* protein (Fig. 1C, panel b). In Southern blot analyses, all four lines gave rise to only a single T-DNA band (Fig. 1D).

Low temperature fluorescence analysis of pigments in the different *oep16-1* mutants

The red pigment fluorescence present in etiolated *oep16-1;5* and *oep16-1;6* plants suggested the presence of free, non-photoconvertible Pchlde molecules not bound to POR in planta. In situ fluorescence spectroscopy at 77 K (Lebedev et al. 1995) was used to determine the functional state of Pchlde in the four different *oep16-1* mutants. Pchlde normally gives rise to two spectral pigment species: Pchlde-F631 and Pchlde-F655 (Lebedev and Timko 1998). Pchlde-F655 has been named photoactive Pchlde because it can be converted into chlorophyllide upon a 1 ms flash of white light (Lebedev

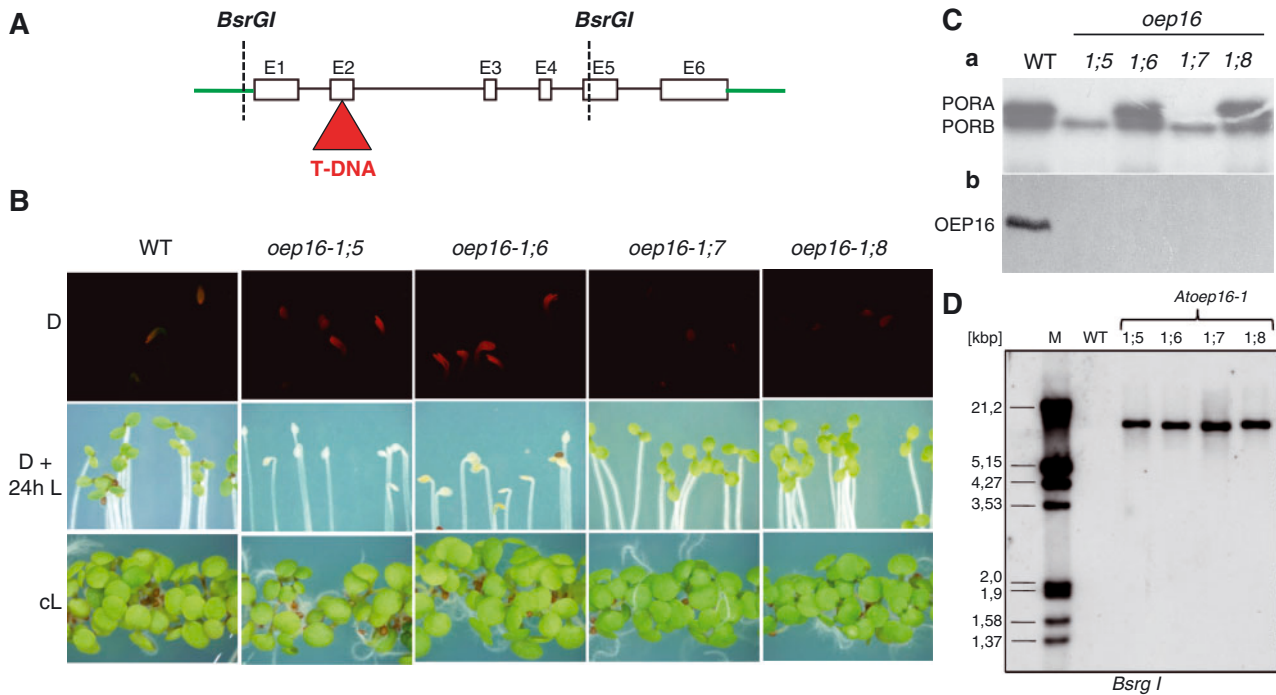


Fig. 1 Identification of *oep16-1* mutants. (A) Schematic presentation of the *OEP16-1* gene and T-DNA insertion. *BsrGI* marks the position of the restriction sites used for the subsequent Southern blot analyses. (B) Phenotypic analysis of four different *OEP16-1* mutants isolated from the SALK seed stock, designated *oep16-1;5*–*oep16-1;8*, and the wild type (WT) after growth in the dark for 5 d (D), after a non-permissive dark to light shift (D + 24 h L) and after growth in continuous white light (cL). The upper panels show fluorescence images after exciting dark-grown seedlings with blue light (400–450 nm) and collecting the emitted fluorescence between 600 and 650 nm. The middle and lower panels depict seedling phenotypes viewed under white light. (C) Western blot analysis of POR-related polypeptides (a) and OEP16 (b) in etioplasts of *oep16-1* mutant seedlings. (D) Southern blot analysis to detect T-DNA insertions in the *OEP16-1* gene in mutants *oep16-1;5*, *oep16-1;6*, *oep16-1;7* and *oep16-1;8*. Positions of size markers are given in kbp.

and Timko 1998); its establishment is an indicator for the presence of functional PORA:PORB–pigment complexes in the prolamellar body of etioplasts (Reinbothe et al. 1999, Reinbothe et al. 2003, Buhr et al. 2008). These complexes are involved in light trapping and energy dissipation once dark-grown seedlings break through the soil after germination (Reinbothe et al. 1999, Reinbothe et al. 2003, Buhr et al. 2008). Pchl_{id}-F631, in contrast, is called photoinactive Pchl_{id} because it cannot be converted immediately to chlorophyll_{id} (Lebedev and Timko 1998). Pchl_{id}-F631 is a mixture of PORA-bound Pchl_{id} *b* and free, non-protein-bound Pchl_{id} molecules (Reinbothe et al. 1999, Reinbothe et al. 2003, Buhr et al. 2008).

Fig. 2 shows that mutant *oep16-1;5* contained large amounts of Pchl_{id}-F631 but no photoactive Pchl_{id}-F655. Etiolated seedlings of mutant *oep16-1;6* contained lower amounts of photoactive Pchl_{id} and reduced levels of photoinactive Pchl_{id}, if compared with mutant *oep16-1;5*. For mutant *oep16-1;7*, a small amount of Pchl_{id}-F631 was present but no Pchl_{id}-F655 was detected, whereas mutant *oep16-1;8* contained both pigment species in ratios that were similar to those in the wild type (**Fig. 2**). Taking into account previous findings, we concluded that mutant *oep16-1;5*

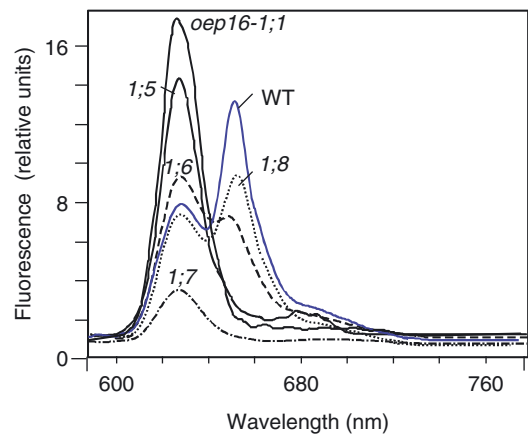


Fig. 2 Low temperature fluorescence analysis at 77K of pigments in 5-day-old, etiolated *oep16-1;5*, *oep16-1;6*, *oep16-1;7* and *oep16-1;8* seedlings. The excitation wavelength was at 440 nm. The two peaks correspond to photoinactive Pchl (Pchl-F631) and photoactive Pchl (Pchl-F655). For comparison, respective fluorescence spectra are included for etiolated wild-type seedlings and seedlings of line *oep16-1;1* isolated by Pollmann et al. (2007). Spectral intensities refer to an equal cotyledon surface area.

may correspond to the line originally described by Pollmann et al. (2007), which was obtained after two subsequent backcrosses with wild-type plants, whereas mutant *oep16-1;8* could be identical to the line identified by Philippar et al. (2007).

Viability of *oep16-1* mutant seedlings

Tetrazolium staining was used to assess seedling viability (Nortin 1966). Seedlings of all four *oep16-1* mutants and of the wild type were grown in the dark for 5 d and subsequently exposed to white light. Whereas all mutant plants were similarly viable in the dark, they responded differentially to illumination. The microscopic images and established seedling survival curves shown in **Fig. 3A and B** demonstrate that cell death was a rapid event ($t_{50} = 4$ h) in mutant *oep16-1;5* and a delayed event ($t_{50} = 8$ h) in mutant *oep16-1;6*. Similar to wild-type seedlings, almost no cell death occurred in mutants *oep16-1;7* and *oep16-1;8* (**Fig. 3A, B**).

The establishment of the cell death phenotype in mutants *oep16-1;5* and *oep16-1;6* is dependent on seedling age and the growth conditions used. Consistent with results reported for the *pif1* mutant of *A. thaliana* (Huq et al. 2004), younger *oep16-1;5* and *oep16-1;6* seedlings were less prone to cell death upon illumination than older seedlings, presumably because of the lower levels of free, non-POR-bound Pchl_{id}e accumulated (Supplementary Fig. S1C). The severity of the cell death phenotype in *oep16-1;5* and *oep16-1;6* seedlings was

thus also dependent on the light intensity (Supplementary Fig. S1A, B). Inclusion of sucrose in the growth medium partially negated the high light effects (data not shown). We explain this finding by the growth-promoting effect of the sugar and the resulting greater capability of the seedlings to sustain a semi-heterotrophic state once the nutrient reserves of the seed have been consumed. On the other hand, sucrose has been reported to affect the polysomal binding of transcripts (Nicolai et al. 2006) as well as the structure and integrity of membranes (Crowe and Crowe 1984). All of these effects could allow for a better stress accommodation.

Singlet oxygen production in *oep16-1* mutant seedlings

The cell death phenotype in *oep16-1;5* and *oep16-1;6* seedlings after irradiation suggested that free, non-photoconvertible Pchl_{id}e molecules not bound to POR operated as a photosensitizer and caused singlet oxygen production. To prove this hypothesis, singlet oxygen measurements were performed with the DanePy reagent which is a dansyl-based singlet oxygen sensor undergoing quenching of its fluorescence upon reacting with singlet oxygen (Hideg et al. 1998, Kálai et al. 2002). DanePy has a broad emission peak at around 530 nm. Upon reacting with singlet oxygen, this peak is reduced, the drop in the amount of fluorescence reflecting the amount of singlet oxygen produced. Thus the greater the amount of fluorescence change, the greater the amount of singlet oxygen

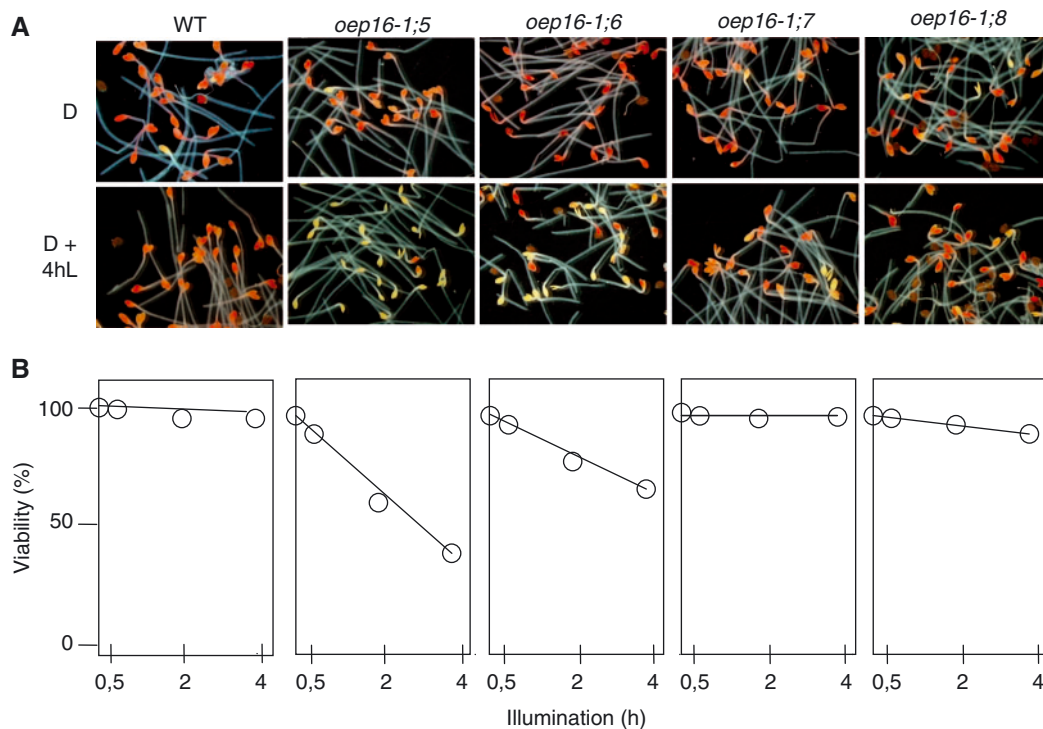


Fig. 3 Seedling viability test on the four types of *oep16-1* mutants and the wild type (WT). (A) Tetrazolium staining of 5-day-old, etiolated *oep16-1;5*, *oep16-1;6*, *oep16-1;7* and *oep16-1;8* seedlings before (D) and after exposure to white light of approximately $75 \mu\text{E m}^{-2} \text{s}^{-1}$ for 4 h (D + 4hL). (B) Seedling viability (in %) as a function of the time of irradiation.

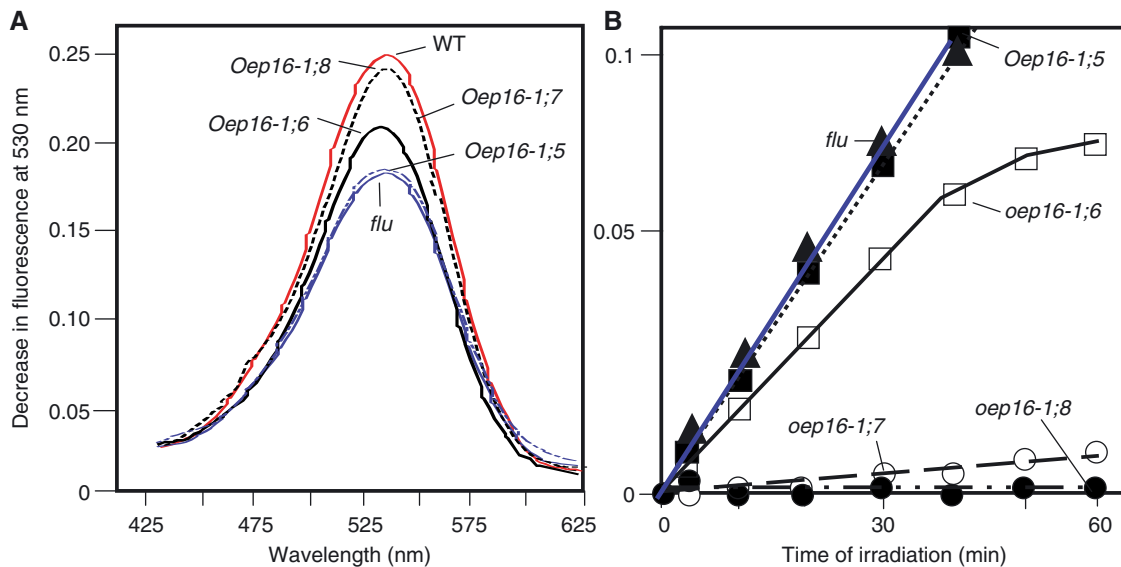


Fig. 4 Singlet oxygen evolution in dark-grown *oep16-1*, *flu* and wild-type seedlings after a 30 min white light shift. (A) DanePy fluorescence emission spectra between 425 and 625 nm at an excitation wavelength of 330 nm obtained for *oep16-1;5* (blue dotted line), *oep16-1;6* (black solid line), *oep16-1;7* (black dashed line) and *oep16-1;8* (black hatched line) vs. *flu* (blue solid line) and wild-type seedlings (red solid line). (B) Time courses of DanePy fluorescence quenching in mutants *oep16-1;5* (dotted line), *oep16-1;6* (solid line), *oep16-1;7* (dashed line) and *oep16-1;8* (hatched line) vs. *flu* seedlings (blue solid line). Spectral intensities refer to an equal cotyledon surface area.

generated in the mutant seedlings. **Fig. 4** shows DanePy fluorescence spectra derived from three independent experiments each comprising 120 etiolated plants that had been infiltrated with DanePy and subsequently exposed to white light of $125 \mu\text{E m}^{-2} \text{s}^{-1}$ for 30 min. As a reference, we used 5-day-old *flu* plants that had been treated identically. **Fig. 4** revealed that mutants *oep16-1;5* and *oep16-1;6* produced significant amounts of singlet oxygen, as evidenced by the quenching of DanePy fluorescence that was collected between 425 and 625 nm. Kinetic measurements demonstrated that singlet oxygen production in mutant *oep16-1;5* was almost indistinguishable from that in *flu*, whereas that in *oep16-1;6* was slightly lower (**Fig. 4A, B**). In wild-type seedlings and seedlings of mutant *oep16-1;7*, there was little DanePy fluorescence quenching, indicative of the generation of a very tiny amount of singlet oxygen. In *oep16-1;8* seedlings, some minor decrease in DanePy fluorescence was observed in two out of three independent experiments, suggesting that some low amounts of singlet oxygen accumulated.

Chloroplast protein import

The finding that mutant *oep16-1;6* did not contain wild-type levels of Pchlde-F655, despite the presence of PORA, suggested that import of pPORA may not proceed via the Pchlde-dependent translocon complex described previously (Reinbothe et al. 2004a, Reinbothe et al. 2004b) but may proceed via another import machinery. To test this hypothesis, *in vitro* import and cross-linking experiments were carried out (Schemenewitz et al. 2007). ^{35}S -labeled transA–DHFR precursor molecules, consisting of the first 67 N-terminal amino

acids of pPORA (henceforth referred to as transA) and a cytosolic dihydrofolate reductase (DHFR) reporter protein of mouse, were activated with 5,5'-dithiobis(2-nitro)benzoic acid (DTNB) (Schemenewitz et al. 2007). Then the precursor was added to chloroplasts that had been isolated from 14-day-old, light-grown *oep16-1;6* plants and energy depleted. Import was assessed under standard conditions in the dark in the presence of 2.5 mM Mg-ATP and 0.1 mM Mg-GTP with chloroplasts that lacked Pchlde (Schemenewitz et al. 2007).

Fig. 5 demonstrates that a significant fraction of [^{35}S]transA–DHFR was imported into Pchlde-free chloroplasts of mutant *oep16-1;6*. Cross-linking gave rise to an ~110 kDa product that consisted of transA–DHFR and TOC75, as demonstrated by immunoprecipitations (data not shown, but see accompanying paper by Samol et al. 2011). Similar to the plastids from mutant *oep16-1;6*, a fraction of transA–DHFR was taken up and processed via a TOC75-dependent pathway by chloroplasts isolated from mutant *oep16-1;8*. In contrast, drastically less precursor import was detectable for chloroplasts of mutants *oep16-1;5* and *oep16-1;7*, and higher molecular mass cross-linked products were not detected (**Fig. 5**). The presence or absence of Pchlde produced by 5-aminolevulinic acid pre-treatment of isolated chloroplasts did not affect this result (Supplementary Fig. S2A). All four types of mutant plastids imported indistinguishable levels of a precursor consisting of the transit peptide of pPORB (transB) and the DHFR (Supplementary Fig. S2B).

To support further the hypothesis that chloroplasts from line *oep16-1;6* take up transA–DHFR by a Pchlde-independent pathway not involving the previously characterized Pchlde-dependent translocon complex (PTC; Reinbothe et al. 2004a,

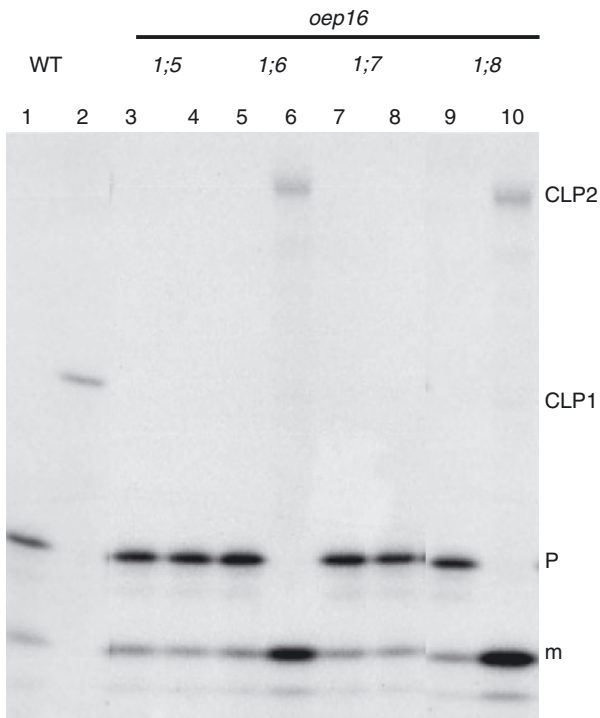


Fig. 5 In vitro import and cross-linking of DTNB-activated [^{35}S]transA-DHFR determined for chloroplasts isolated from wild-type and *oep16* mutant plants. The autoradiogram shows precursor (P) and mature (m) proteins as well as cross-linked products (CLP1 and CLP2) at time zero (lanes 1, 3, 5, 7 and 9) and after 15 min of import (lanes 2, 4, 6, 8 and 10). CLP1 is caused by the formation of a disulfide bond between transA-DHFR and OEP16; this product is only detectable for wild-type chloroplasts. CLP2 resulted from formation of a disulfide bond between transA-DHFR and TOC75; this CLP is found for chloroplasts from mutants *oep16-1;6* and *oep16-1;8*.

Reinbothe et al. 2004b), transient expression and import studies were conducted as described (Finer et al. 1992, Reinbothe et al. 2008). After ballistic bombardment of leaf pavement cells of wild-type and mutant *A. thaliana* plants, the localization of expressed transA-green fluorescent protein (GFP) was followed by confocal laser scanning microscopy. **Fig. 6** depicts fluorescence images for all of the four *oep16-1* mutants described in this study and also shows the respective controls obtained for wild-type plants and seedlings of the *oep16-1;1* mutant described by Pollmann et al. (2007). According to the results, mutants *oep16-1;5* and *oep16-1;7* imported only small amounts of transA-GFP into their plastids, whereas mutants *oep16-1;6* and *oep16-1;8* imported significant levels of the precursor. Confirming previous findings (Pollmann et al. 2007, Reinbothe et al. 2008), the plastids from wild-type plants imported transA-GFP well, whereas the plastids from the *oep16-1;1* mutant were import incompetent.

Protein synthesis during greening and in response to photooxidative stress

op den Camp et al. (2004) have shown that mature *flu* plants accumulate a large number of stress-responsive transcripts

after non-permissive dark to light shifts. At the same time, irradiated *flu* plants rapidly depress photosynthetic gene expression (op den Camp et al. 2004). Whether similar changes would occur in *oep16* plants belonging to the genotypes *1;5* and *1;6* was obviously undetermined and motivated us to perform the following experiments. Pulse labeling of proteins was carried out with [^{35}S]methionine in 5-day-old dark-grown seedlings that had been irradiated for 4 or 24 h. Furthermore, total RNA was extracted from dark-grown and 2 h-irradiated plants and used for in vitro translation and Northern hybridization. When the patterns of polypeptides synthesized in a wheat germ lysate were compared for the four different *oep16* mutants, no major differences were found. No new polypeptide species were detected in mutants nor were any detectably absent (**Fig. 7A** and Supplementary S3A), as would be expected if *oep16-1;5* and *oep16-1;6* followed the same cell death pathway as *flu* (op den Camp et al. 2004).

Fig. 7B and Supplementary Figs. S3B and S4 show that all four *oep16* mutants synthesized very similar protein patterns in the dark but responded differentially to illumination. Seedlings of mutants *oep16-1;5* and *oep16-1;6* began synthesizing photosynthetic proteins after a few hours of illumination but stopped translating these proteins after approximately 24 h of illumination. Instead of accumulating Chl, the seedlings died (cf. **Figs. 1** and **3**). In contrast, seedlings of mutants *oep16-1;7* and *oep16-1;8* carried on translating photosynthetic proteins at the later stages of light exposure (**Fig. 7B**) and greened normally (cf. **Figs. 1** and **3**). Remarkably, no synthesis of mass stress proteins was detectable in the cotyledons of plants from mutants *oep16-1;5* and *oep16-1;6* (**Fig. 7B**) that would have occurred if cell death triggered in these *oep16-1* mutant types followed the same course as in *flu* plants (Supplementary Fig. S3B).

Mutant *oep16-1;6* phenotypically strongly resembles the *flu* mutant isolated by Meskauskiene et al. (2009). Like *flu*, mutant *oep16-1;6* contains normal levels of PORA protein but over-accumulates free photoexcitable Pchl ide molecules in the dark that cause singlet oxygen production and cell death upon illumination. However, in marked contrast to *flu*, etiolated *oep16-1;6* seedlings do not synthesize stress proteins upon illumination (Supplementary Fig. S3). In order to characterize the differences between *oep16-1;6* and *flu* further, light-adapted, mature plants were used. Plants were grown for 14 d in continuous white light; then the plants were transferred to darkness for 8 h and re-illuminated for variable periods. According to previous work on *flu* (op den Camp, 2004, Wagner et al. 2004, Danon et al. 2005), such treatment was expected to activate the genetic component of singlet oxygen-dependent signaling but without provoking cytotoxic effects. Pulse labeling and polysome profiling experiments revealed that *flu* plants indeed react to singlet oxygen production with the rapid synthesis of stress proteins and the selective depression of synthesis of photosynthetic proteins (**Fig. 8A**, panel a). After 24 h, a drastic decrease in protein synthesis was observed in illuminated *flu* plants (**Fig. 8B**) which

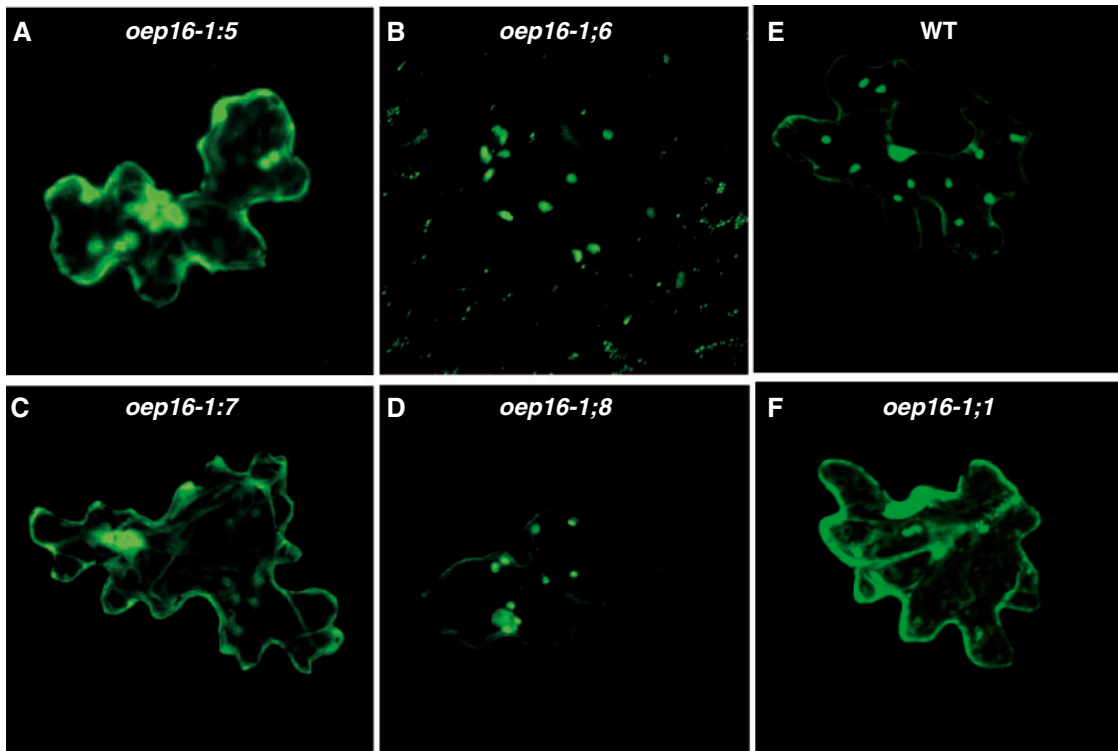


Fig. 6 In vivo import of transA-GFP into plastids of mutants *oep16-1;5* (A), *oep16-1;6* (B), *oep16-1;7* (C) and *oep16-1;8* (D) as well as plastids from the wild-type (WT) (E) and mutant *oep16-1;1* described by Pollmann et al. (2007) (F) after ballistic transformation of leaf pavement cells of *A. thaliana*. GFP fluorescence was collected between 505 and 530 nm, using an excitation wavelength of 488 nm.

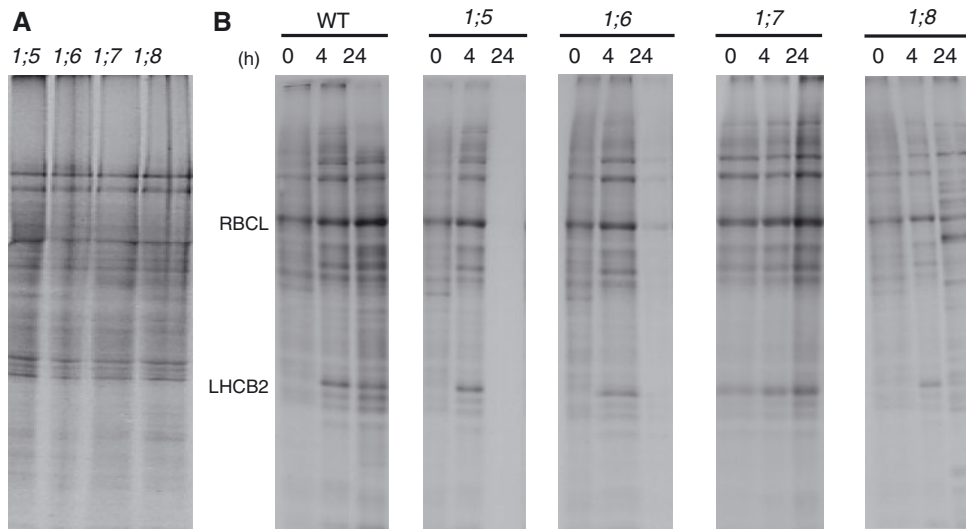


Fig. 7 Protein expression in the different *oep16-1* mutants. (A) Pattern of proteins synthesized in a wheat germ lysate with RNA from mutants *oep16-1;5*, *oep16-1;6*, *oep16-1;7* and *oep16-1;8* after growth in the dark for 5 d and exposure to white light for 2 h. (B) Patterns of ^{35}S -labeled total proteins in wild-type seedlings and seedlings of mutants *oep16-1;5*, *oep16-1;6*, *oep16-1;7* and *oep16-1;8* in the dark (0 h) and after 4 h and 24 h, respectively, of exposure to white light of $125 \mu\text{E m}^{-2} \text{s}^{-1}$. After extraction and SDS-PAGE, proteins were detected by autoradiography. RBCL and LHCB2 mark the large subunit of ribulose-1,5-bisphosphate carboxylase/oxygenase and the major light-harvesting chlorophyll *a/b*-binding protein of PSII.

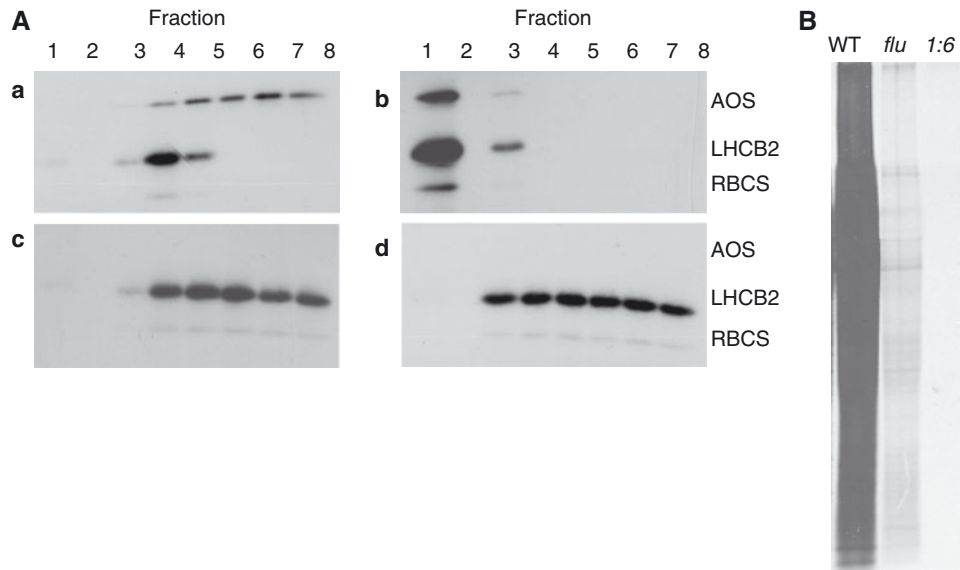


Fig. 8 Protein synthesis in leaf tissues of 14-day-old light-grown wild-type, *flu* and *oep16-1;6* plants after transfer to darkness for 8 h and subsequent illumination. (A) Polysomal synthesis of light-harvesting chlorophyll *a/b*-binding protein of PSII (LHCb2) and the small subunit of ribulose-1,5-bisphosphate carboxylase/oxygenase (RBCS), as well as allene oxide synthase (AOS) in *flu* (a and b), wild-type (c) and *oep16-1;6* (d) plants detected 4 h (a, c and d) and 24 h (b) after the non-permissive dark to light shift. Fraction 1 contained the 40S ribosomal subunit, fraction 2 contained the 60S ribosomal subunit, and fractions 3–8 contained cytoplasmic polysomes of increasing size. Protein from each of the different fractions was separated by SDS–PAGE and subjected to Western blotting using the indicated antisera. (B) Patterns of ^{35}S -labeled total leaf proteins in wild-type, *flu* and *oep16-1;6* plants detected 24 h after the non-permissive dark to light shift.

correlated with a decay of cytoplasmic polysomes (Fig. 8A, panel b). In marked contrast to *flu*, *oep16-1;6* plants reacted to non-permissive dark to light shifts with no early synthesis of stress proteins (Fig. 8A, panel d), although protein synthesis later declined to an even greater extent than in *flu* plants (Fig. 8B). Together, these findings highlighted that only the early reprogramming of translation in response to singlet oxygen is different in *flu* and *oep16-1;6* plants.

Discussion

In the present work, two major questions were addressed. What is the reason for completely different phenotypes described for two *oep16-1* knock-out mutants derived from the T-DNA insertion SALK_024018 (Philippart et al. 2007, Pollmann et al. 2007)? Is the cell death regulation in the *oep16-1* mutant we identified (Pollmann et al. 2007) comparable with the singlet oxygen-dependent pathway reported for the *flu* mutant (Meskauskiene et al. 2001, op den Camp et al. 2004, Wagner et al. 2004, Danon et al. 2005)?

We discovered that the original seed stock provided by the Salk Institute contains several independent knock-out mutants. Four *OEP16-1*-deficient mutants were discovered that all showed a single T-DNA insertion on Southern blots. Obviously, these mutants are different from those described recently by Pudelski et al. (2009) containing additional T-DNA insertions. Presumably because of the prior backcrosses, mutants *oep16-1;5–oep16-1;8* were homozygous for the *oep16-1*

locus and did not contain additional T-DNA fragments on Southern blots. Mutants *oep16-1;5–oep16-1;8* suffered or did not suffer from photooxidative damage under high light conditions and contained or lacked PORA. Mutant *oep16-1;5* had the strongest phenotype. It lacked PORA and rapidly died upon non-permissive dark to light shifts. PORA's function is to bind Pchl_{id}e and to assemble with PORB into larger POR:Pchl_{id}e complexes involved in light harvesting and energy dissipation during greening (Reinbothe et al. 1999, Reinbothe et al. 2003, Buhr et al. 2008), explaining its phenotype. The characteristics of mutant *oep16-1;5* are virtually identical to those of mutant *oep16-1;1* isolated by Pollmann et al. (2007).

Mutant *oep16-1;6* displayed a weaker phenotype. Despite the presence of PORA, almost no Pchl_{id}e-F655 was found. Import and cross-linking studies demonstrated that transA–DHFR entered both Pchl_{id}e-free and Pchl_{id}e-containing mutant plastids. However, the precursor did not seem to interact with the pigment and also it did not establish larger complexes with PORB in etioplasts. Otherwise, Pchl_{id}e-F655 should have accumulated to the same extent as in wild-type plants, which was not the case. In vitro and in planta import assays showed that pPORA is likely to enter the plastids via an import pathway involving TOC75. As shown previously, multiple versions of the TOC machinery exist that differ by an interchange of receptor and regulatory components and exhibit different precursor specificities (Jarvis et al. 1998, Bauer et al. 2000, Ivanova et al. 2004). It is attractive to hypothesize about the presence of an exogenic, presumably point or footprint mutation outside the *AtOEP16-1* gene. It has been reported that

T-DNA insertion lines often contain multiple T-DNA copies of which some or all are lost in subsequent generations, provoking secondary effects (Latham et al. 2006). We hypothesize that the 'hidden' mutation in *oep16-1;6* may affect the composition and/or activity of the plastid envelope protein translocon complexes or the state of cytosolic targeting factors involved in import. Evidence has been obtained for the operation of different cytosolic targeting pathways of nucleus-encoded plastid precursors involving 14-3-3, HSP70 and HSP90 proteins (May and Soll 2000, Qbadou et al. 2006, Schemenewitz et al. 2007) that could be prone to modifications in mutant *oep16-1;6*.

Mutant *oep16-1;7* did not show a cell death phenotype. Even without detectable levels of PORA, etiolated seedlings greened normally. The level of Pchl_a-F631 was drastically reduced in this mutant as compared with wild-type seedlings. It has previously been shown by Lebedev et al. (1995) that greening in the absence of PORA can occur via a pathway involving only PORB. This pathway is likely to operate in line *oep16-1;7*. Mutant *oep16-1;8* is similar to the line isolated by Philippar et al. (2007). It contained normal levels of PORA and wild-type levels of Pchl_a-F655. Upon illumination, etiolated *oep16-1;8* mutant seedlings greened like the wild-type and without any sign of photooxidative damage. It is likely that in this line an additional suppressor mutation is present that affected the cell death phenotype. DNA arrangements provoked by the insertion and loss of multiple T-DNA copies (Latham et al. 2006) may be the reason for the complex genetic background observed in mutant *oep16-1;8*. The identity of these mutations remains to be determined by map-based cloning and whole-genome sequencing approaches.

FLU is an important regulator of Pchl_a accumulation in *A. thaliana* and other angiosperms (Meskauskiene et al. 2001, op den Camp et al. 2004, Wagner et al. 2004, Danon et al. 2005). Its absence causes cell death (Meskauskiene et al. 2001, op den Camp et al. 2004, Wagner et al. 2004, Danon et al. 2005). To what extent *flu* would be involved in controlling cell death in mutants *oep16-1;5* and *oep16-1;6* was as yet undermined, and is explored in the second part of the present study. *flu* plants respond to non-permissive dark to light shifts with growth arrest and/or cell death (Meskauskiene et al. 2001, op den Camp et al. 2004, Wagner et al. 2004, Danon et al. 2005). While etiolated *oep16-1;5* and *oep16-1;6* seedlings share similar cell death symptoms with *flu* seedlings, no growth inhibition was observed for mature green plants. In etiolated plants one might attribute cell death to the cytotoxic effect of singlet oxygen. This explanation, however, does not seem very likely for light-adapted plants. A major clue for understanding the differences in cell death regulation in *oep16-1;6* and *flu* plants was provided by the pulse labeling and polysome profiling studies which revealed a lack of stress protein synthesis both for etiolated and light-adapted *oep16-1;6* plants after non-permissive dark to light shifts. In either case, the normal reprogramming of translation detected for *flu* plants and leading to stress protein synthesis was abrogated. Nevertheless, at later stages of the singlet oxygen-dependent stress response,

protein synthesis declined to similar extents in *flu* and *oep16-1;6* plants. In the *flu* orthologous mutant of barley, *tigrina d12*, the same early as well as later effects on translation have been observed as reported here for *flu* plants (Khandal et al. 2009). Our results show that both effects are separable, implying two different mechanisms of translational control in which singlet oxygen is involved. The *flu* and *oep16-1;6* plants, which are virtually identical with regard to their phenotypic properties (Pchl_a overproduction and presence of PORA), therefore represent tools to explore these mechanisms.

Materials and Methods

Plant growth

Seeds of the *oep16-1* mutant (At2g28900; SALK_024018) and *flu* mutant (At3g14110; SALK_002383) were obtained from the Salk Institute Genomic Analysis Laboratory collection (Alonso et al. 2001) and germinated in the dark on half-strength MS-agar medium containing or lacking 1% (w/v) sucrose. For comparison, the *flu* mutant isolated by Meskauskiene et al. (2001) was used. After variable periods, the seedlings were exposed to high light ($125 \mu\text{E m}^{-2} \text{s}^{-1}$) or low light ($25 \mu\text{E m}^{-2} \text{s}^{-1}$). For dark to light transfer and plastid isolation experiments, seeds were sown on soil and cultivated in continuous white light for appropriate periods.

Mutant identification

Previously described primer combinations (Philippar et al. 2007, Pollmann et al. 2007) were used to identify *oep16-1* knock-out plants by PCR (Innis et al. 1990). High stringency Southern hybridization was performed on DNA filters containing 10 μg of DNA that had been digested with *Clal* or *BsrGI* and probes corresponding to either the ROK2 vector or the left border (LB) and right border (RB) of the T-DNA (Sambrook et al. 1989). LB and RB primer combinations were as follows: NPTII-R2, 5'-CAATATCACGGGTAGCCAAC-3'; NPII-F2, 5'-CG GTTCTTTTGTCAAGACC-3'; LBGT1, 5'-ACTTAATAACACAT TGCGGACG-3'; and LBGT2, 5'-CTTAATCGCCTTGCAGCAC ATC-3'.

Pigment fluorescence analyses

Fluorescence microscopy was performed using excitation filters from 400 to 450 nm and emission filters from 600 to 650 nm. Low temperature fluorescence measurements were performed at 77 K at an excitation wavelength of 440 nm (spectrometer model LS50B, Perkin Elmer Corp.) (Lebedev et al. 1995).

Seedling viability tests

Seedling viability was assessed by tetrazolium staining (Norton 1966). Whereas vital seedlings show a strong red staining, dead seedlings are unable to produce the dye and look whitish. For

statistic assessment, pools of about 250 seeds were analyzed in three independent experiments.

Singlet oxygen measurements

Singlet oxygen generation was measured with the DanePy method (Hideg et al. 1998, Kálai et al. 2002). Fluorescence emission of DanePy was collected between 425 and 625 nm, using an excitation wavelength of 330 nm (Life Sciences spectrometer, model LS50 Perkin Elmer Corp.).

Protein import in vitro and in planta

Construction of chimeric precursors consisting of the N-terminal targeting sequences of pPORA (transA) and pPORB (transB) and GFP or mouse DHFR has been described (Schemenewitz et al. 2007, Reinbothe et al. 2008). To study the import in vivo, leaf pavement cells of *A. thaliana* were transformed by ballistic bombardment according to Finer et al. (1992), using a helium pressure of 6.5 bar, 12 cm target distance, a disperse grid at 7 cm and 1 μ M of gold microcarriers (Bio-Rad). Transformed plantlets were kept under sterile conditions for 24 h in darkness. Confocal laser scanning microscopy was carried out using an LSM 510 Meta microscope (Zeiss) with argon laser excitation at 488 nm. GFP and Chl were detected at emission wavelengths of 505–530 and 650–750 nm, respectively. LSM 510 Meta software release 3.2 (Zeiss) and Adobe Photoshop 7 (Adobe Systems) were used for image acquisition and processing, respectively.

In vitro import reactions were carried out using cDNA-encoded, wheat germ-translated, urea-denatured [35 S]precursors produced by coupled transcription/translation of the respective clones and Percoll/sucrose-purified chloroplasts from *A. thaliana* (Schemenewitz et al. 2007). Chemical cross-linking of DTNB-derivatized [35 S]precursors was carried out as described (Reinbothe et al. 2004b).

Protein analyses

Pulse labeling of protein was performed with [35 S]methionine (37 TBq mmol $^{-1}$, Amersham-Pharmacia) for 2 h prior to seedling harvest. Protein was extracted with 80% (v/v) acetone, and protein pellets obtained after centrifugation were boiled for 5 min in SDS sample buffer [2.9% SDS, 68 mM Tris-HCl, pH 6.8, 10% (v/v) glycerol, 0.1 M β -mercaptoethanol] (Laemmli 1970) (Fig. 7). Alternatively protein was extracted with buffer A [50 mM Tris-HCl, pH 7.8, 25 mM KCl, 10 mM MgCl, 1 mM phenylmethylsulfonyl fluoride, 1 mM NaF, 0.5% (v/v) mercaptoethanol, 1% (v/v) Triton X-100, 250 mM sucrose] (Scharf and Nover 1984) (Supplementary Fig. S3), followed by further homogenization in a Branson Sonifier (model B-12, microtip, 80 W, 1 min) and precipitation with 5% (v/v) trichloroacetic acid (Reinbothe et al. 1990). Protein that had been extracted with acetone and boiled in SDS sample buffer was cleared by centrifugation and only the clear supernatant was used for SDS-PAGE. Protein that had been extracted with buffer A and precipitated with trichloroacetic acid was washed with acetone,

ethanol and ether, dried and resuspended in SDS sample buffer (Laemmli 1970). SDS-PAGE was carried out on 10–20% polyacrylamide gradients (Scharf and Nover 1984). Isolation, fractionation and analysis of polysomes and polysomal messengers were conducted as described (Reinbothe et al. 1993). Immunodetection was carried out using an enhanced chemiluminescence system (Amersham-Pharmacia) and the indicated antisera (Towbin et al. 1979).

Supplementary data

Supplementary data are available at PCP online.

Funding

This study was supported by the French Ministry of Research and Education [Chaire d'Excellence research project grant dedicated to C.R.]; Deutsche Forschungsgemeinschaft (DFG) [Mercator professorship to D.v.W.].

Acknowledgments

We thank K. Apel (Boyce Thompson Institute for Plant Research, Ithaca, USA) for a gift of the *flu* mutant and K. Kálai and E. Hideg (Institute for Plant Biology, Biological Research Centre, Hungarian Academy of Sciences, Szeged, Hungary) for a gift of the DanePy reagent.

References

- Alonso, J.M., Stepanova, A.N., Leisse, T.J., Kim, C.J., Chen, H., Shinn, P. et al. (2003) Genome-wide insertional mutagenesis of *Arabidopsis thaliana*. *Science* 301: 653–657.
- Apel, K. and Hirt, H. (2004) Reactive oxygen species: metabolism, oxidative stress, and signal transduction. *Annu. Rev. Plant Biol.* 55: 373–399.
- Bauer, J., Chen, K., Hiltbrunner, A., Wehrli, E., Eugster, M., Schnell, D. et al. (2000) The major protein import receptor of plastids is essential for chloroplast biogenesis. *Nature* 403: 203–207.
- Buhr, F., el Bakkouri, M., Lebedev, N., Pollmann, S., Reinbothe, S. and Reinbothe, C. (2008) Photoprotective role of NADPH:protochlorophyllide oxidoreductase A. *Proc. Natl Acad. Sci. USA* 105: 12629–12634.
- Crowe, L.M. and Crowe, J.H. (1984) Preservation of membranes in anhydrobiotic organisms: the role of trehalose. *Science* 223: 701–703.
- Danon, A., Miersch, O., Felix, G., op den Camp, R. and Apel, K. (2005) Concurrent activation of cell death-regulating signalling pathways by singlet oxygen in *Arabidopsis thaliana*. *Plant J.* 41: 68–80.
- Drea, S.C., Lao, N.T., Wolfe, K.H. and Kavanagh, T.A. (2006) Gene duplication, exon gain and neofunctionalization of OEP16-related genes in land plants. *Plant J.* 46: 723–735.
- Finer, J.J., Vain, P., Jones, M.W. and McMullen, M.D. (1992) Development of the particle gun for DNA delivery to plant cells. *Plant Cell Rep.* 11: 323–328.

- Hideg, E., Kálai, T., Hideg, K. and Vass, I. (1998) Photoinhibition of photosynthesis in vivo results in singlet oxygen production detection via nitroxide-induced fluorescence quenching in broad bean leaves. *Biochemistry* 37: 11405–11411.
- Huq, E., Al-Sady, B., Hudson, M., Kim, C., Apel, K. and Quail, P.H. (2004) Phytochrome-interacting factor 1 is a critical bHLH regulator of chlorophyll biosynthesis. *Science* 305: 1937–1941.
- Innis, M.A., Gelfand, D.H., Sninsky, J.J. and White, T.J. (1990) PCR Protocols. Academic Press, San Diego.
- Ivanova, Y., Smith, M.D., Chen, K. and Schnell, D.J. (2004) Members of the Toc159 import receptor family represent distinct pathways for protein targeting to plastids. *Mol. Biol. Cell* 15: 3379–3392.
- Jarvis, P., Chen, L.-J., Li, H.-m., Peto, C.A., Fankhauser, C. and Chory, J. (1998) An *Arabidopsis* mutant defective in the plastid general protein import apparatus. *Science* 282: 100–103.
- Kálai, T., Hankovszky, O., Hideg, E., Jeko, J. and Hideg, K. (2002) Synthesis and structure optimization of double (fluorescent and spin) sensor molecules. *ARKIVOC* iii: 112–120.
- Kendrick, M.D. and Chang, C. (2008) Ethylene signaling: new levels of complexity and regulation. *Curr. Opin. Plant Biol.* 11: 479–485.
- Khandal, D., Samol, I., Buhr, F., Pollmann, S., Schmidt, H., Clemens, C. et al. (2009) Singlet oxygen-dependent translational control in the *tigrina-d.12* mutant of barley. *Proc. Natl Acad. Sci. USA* 106: 13112–13117.
- Kim, C., Meskauskiene, R., Apel, K. and Laloi, C. (2008) No single way to understand singlet oxygen signalling in plants. *EMBO Rep.* 9: 435–439.
- Laemmli, U.K. (1970) Cleavage of structural proteins during the assembly of the head of bacteriophage T4. *Nature* 227: 680–685.
- Latham, J., Wilson, A.K. and Steinbrecher, R. (2006) The mutational consequences of plant transformation. *J. Biomed. Biotech.* 2006: 1–7.
- Lebedev, N. and Timko, M.P. (1998) Protochlorophyllide photo-reduction. *Photosynth. Res.* 58: 5–23.
- Lebedev, N., van Cleve, B., Armstrong, G. and Apel, K. (1995) Chlorophyll synthesis in a de-etiolated (*det340*) mutant of *Arabidopsis* without NADPH-protochlorophyllide (PChlide) oxidoreductase (POR) A and photoactive PChlide-F655. *Plant Cell* 7: 2081–2090.
- May, T. and Soll, J. (2000) 14-3-3 proteins form a guidance complex with chloroplast precursor proteins in plants. *Plant Cell* 12: 53–63.
- Meskauskiene, R., Nater, M., Gosling, D., Kessler, F., op den Camp, R. and Apel, K. (2001) FLU: a negative regulator of chlorophyll biosynthesis in *Arabidopsis thaliana*. *Proc. Natl Acad. Sci. USA* 98: 12826–12831.
- Miller, G., Shulaev, V. and Mittler, R. (2008) Reactive oxygen signaling and abiotic stress. *Physiol. Plant.* 133: 481–489.
- Mühlenbock, P., Szechynska-Hebda, M., Plaszczycza, M., Baudo, M., Mullineaux, P.M., Parker, J.E. et al. (2008) Chloroplast signaling and LESION SIMULATING DISEASE1 regulate crosstalk between light acclimation and immunity in *Arabidopsis*. *Plant Cell* 20: 2339–2356.
- Murcha, M.W., Elhafez, D., Lister, R., Tonti-Filippini, J., Baumgartner, M., Philippar, K. et al. (2007) Characterization of the preprotein and amino acid transporter gene family in *Arabidopsis*. *Plant Physiol.* 143: 199–212.
- Nicolai, M., Roncato, M.A., Canoy, A.S., Rouquié, D., Sarda, X., Feysinnet, G. et al. (2006) Large-scale analysis of mRNA translation states during sucrose starvation in *Arabidopsis* cells identifies cell proliferation and chromatin structure as targets of translational control. *Plant Physiol.* 141: 663–673.
- Nortin, J.D. (1966) Testing of plum pollen viability with tetrazolium salts. *Proc. Amer. Soc. Hort. Sci.* 89: 132–134.
- op den Camp, R., Przybyla, D., Ochsenbein, C., Laloi, C., Kim, C., Danon, A. et al. (2004) Rapid induction of distinct stress responses after the release of singlet oxygen in *Arabidopsis*. *Plant Cell* 15: 2320–2332.
- Philippar, K., Geis, T., Ilkavets, I., Oster, U., Schwenkert, S., Meurer, J. et al. (2007) Chloroplast biogenesis: the use of mutants to study the etioplast–chloroplast transition. *Proc. Natl Acad. Sci. USA* 104: 678–683.
- Pohlmeier, K., Soll, J., Steinkamp, T., Hinnah, S. and Wagner, R. (1997) A high-conductance solute channel in the chloroplastic outer envelope from pea. *Proc. Natl Acad. Sci. USA* 94: 9504–9509.
- Pollmann, S., Springer, A., Buhr, F., Lahroussi, A., Samol, I., Bonneville, J.-M. et al. (2007) A plant porphyria related to defects in plastid import of protochlorophyllide oxidoreductase A. *Proc. Natl Acad. Sci. USA* 104: 2019–2023.
- Pudelski, B., Soll, J. and Philippar, K. (2009) A search for factors influencing etioplast–chloroplast transition. *Proc. Natl Acad. Sci. USA* 106: 12201–12206.
- Qbadou, S., Becker, T., Mirus, O., Tews, I., Soll, J. and Schleiff, E. (2006) The molecular chaperone Hsp90 delivers precursor proteins to the chloroplast import receptor Toc64. *EMBO J.* 25: 1836–1847.
- Reinbothe, C., Buhr, F., Pollmann, S. and Reinbothe, S. (2003) In vitro reconstitution of LHPP with protochlorophyllides *a* and *b*. *J. Biol. Chem.* 278: 807–815.
- Reinbothe, C., Lebedev, N. and Reinbothe, S. (1999) A protochlorophyllide light-harvesting complex involved in de-etiolation of higher plants. *Nature* 397: 80–84.
- Reinbothe, C., Phetsarath, P., Pollmann, S., Quigley, F. and Reinbothe, S. (2008) A pentapeptide motif related to a pigment binding site in the major light-harvesting protein of photosystem II, LHClI, governs substrate-dependent plastid import of NADPH:protochlorophyllide oxidoreductase A. *Plant Physiol.* 148: 694–703.
- Reinbothe, C., Pollmann, S. and Reinbothe, S. (2010) Singlet oxygen links photosynthesis to translation and plant growth. *Trends Plant Sci.* 15: 499–506.
- Reinbothe, C., Springer, A., Samol, J. and Reinbothe, S. (2009) Plant oxylipins: role of jasmonic acid during programmed cell death, defense and leaf senescence. *FEBS J.* 276: 4666–4681.
- Reinbothe, S., Krauspe, R. and Parthier, B. (1990) In vitro transport of chloroplast proteins in a homologous *Euglena* system with particular reference to plastid leucyl-tRNA synthetase. *Planta* 181: 176–183.
- Reinbothe, S., Quigley, F., Gray, J., Schemenewitz, A. and Reinbothe, C. (2004a) Identification of plastid envelope proteins required for import of protochlorophyllide oxidoreductase A into the chloroplast of barley. *Proc. Natl Acad. Sci. USA* 101: 2197–2202.
- Reinbothe, S., Quigley, F., Springer, A., Schemenewitz, A. and Reinbothe, C. (2004b) The outer plastid envelope protein Oep16: role as precursor translocase in import of protochlorophyllide oxidoreductase A. *Proc. Natl Acad. Sci. USA* 101: 2203–2208.
- Reinbothe, S., Reinbothe, C. and Parthier, B. (1993) Methyl jasmonate-regulated translation of nuclear-encoded chloroplast proteins in barley (*Hordeum vulgare* L. cv. Salome). *J. Biol. Chem.* 268: 10606–10611.
- Sambrook, J., Fritsch, E. and Maniatis, T. (1989) Molecular Cloning: A Laboratory Manual, 2nd edn. Cold Spring Harbor Laboratory Press, Cold Spring Harbor, NY.

- Samol, I., Rossig, C., Buhr, F., Springer, A., Pollmann, S., Lahroussi, A. *et al.* (2011) The outer chloroplast envelope protein OEP16-1 for plastid import of NADPH:protochlorophyllide oxidoreductase A in *Arabidopsis thaliana*. *Plant Cell Physiol.* 52: 96–111.
- Scharf, K.-D. and Nover, L. (1984) Synthesis, modification and structural binding of heat-shock proteins in tomato cell cultures. *Eur. J. Biochem.* 139: 303–313.
- Schemenewitz, A., Pollmann, S., Reinbothe, C. and Reinbothe, S. (2007) A substrate-independent, 14:3:3 protein-mediated plastid import pathway of NADPH:protochlorophyllide oxidoreductase (POR) A. *Proc. Natl Acad. Sci. USA* 104: 8538–8543.
- Towbin, M., Staehelin, T. and Gordon, J. (1979) Electrophoretic transfer of proteins from polyacrylamide gels to nitrocellulose sheets; procedure and some applications. *Proc. Natl Acad. Sci. USA* 76: 4350–4354.
- Wagner, D., Przybyla, D., op den Camp, R., Kim, C., Landgraf, F., Lee, K.P. *et al.* (2004) The genetic basis of singlet oxygen-induced stress responses of *Arabidopsis thaliana*. *Science* 306: 1183–1185.
- Wasternack, C. (2007) Jasmonates: an update on biosynthesis, signal transduction and action in plant stress response, growth and development. *Ann. Bot.* 100: 681–697.

Fig. S1

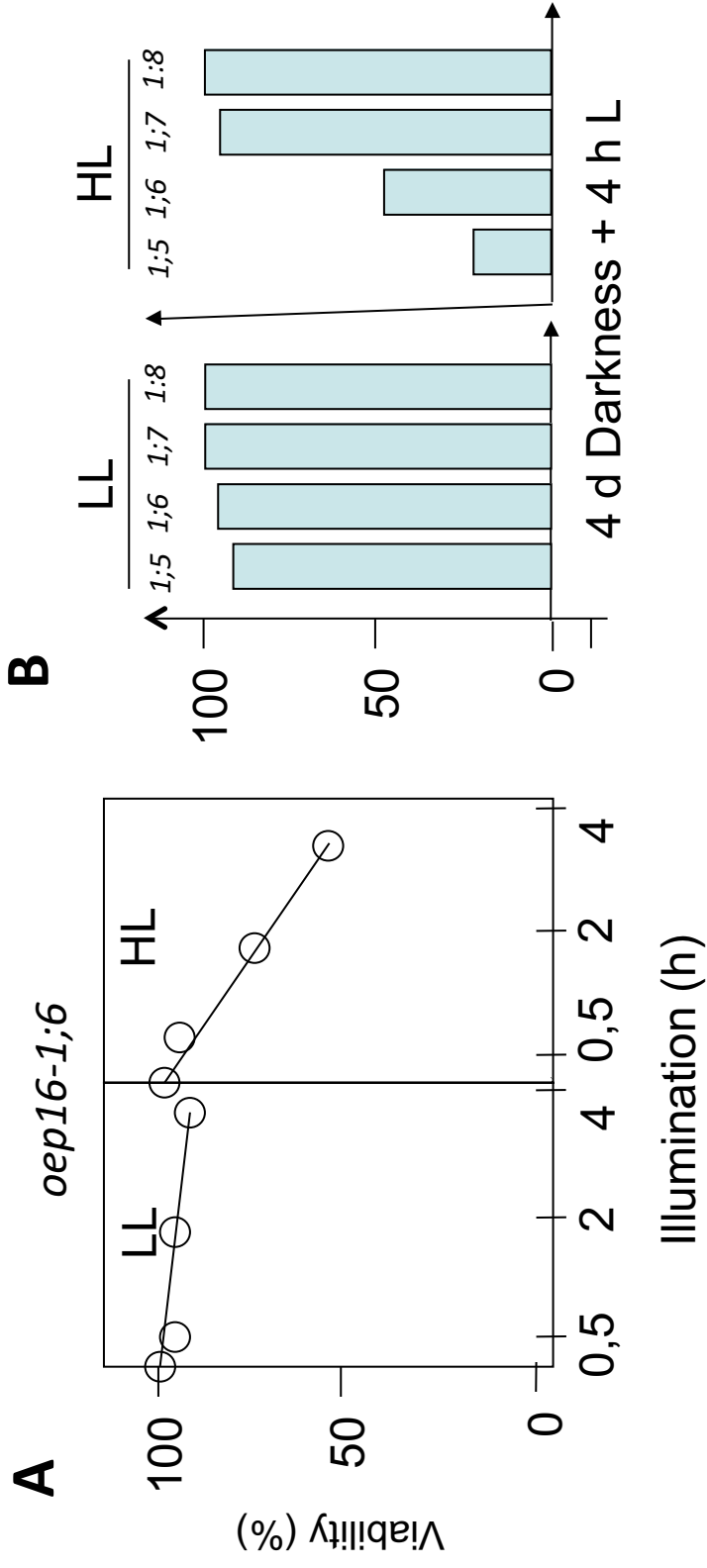


Fig. S1

C

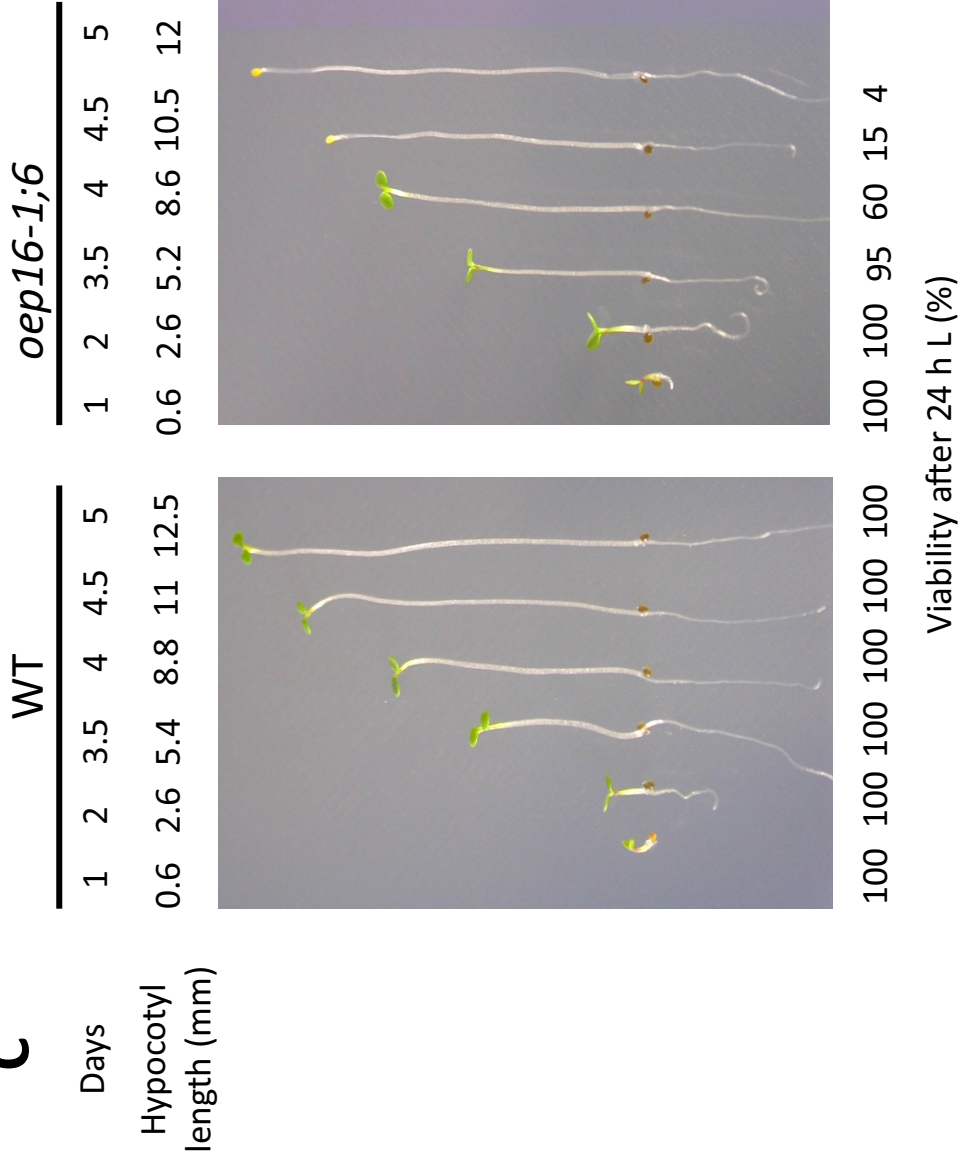


Fig. S2

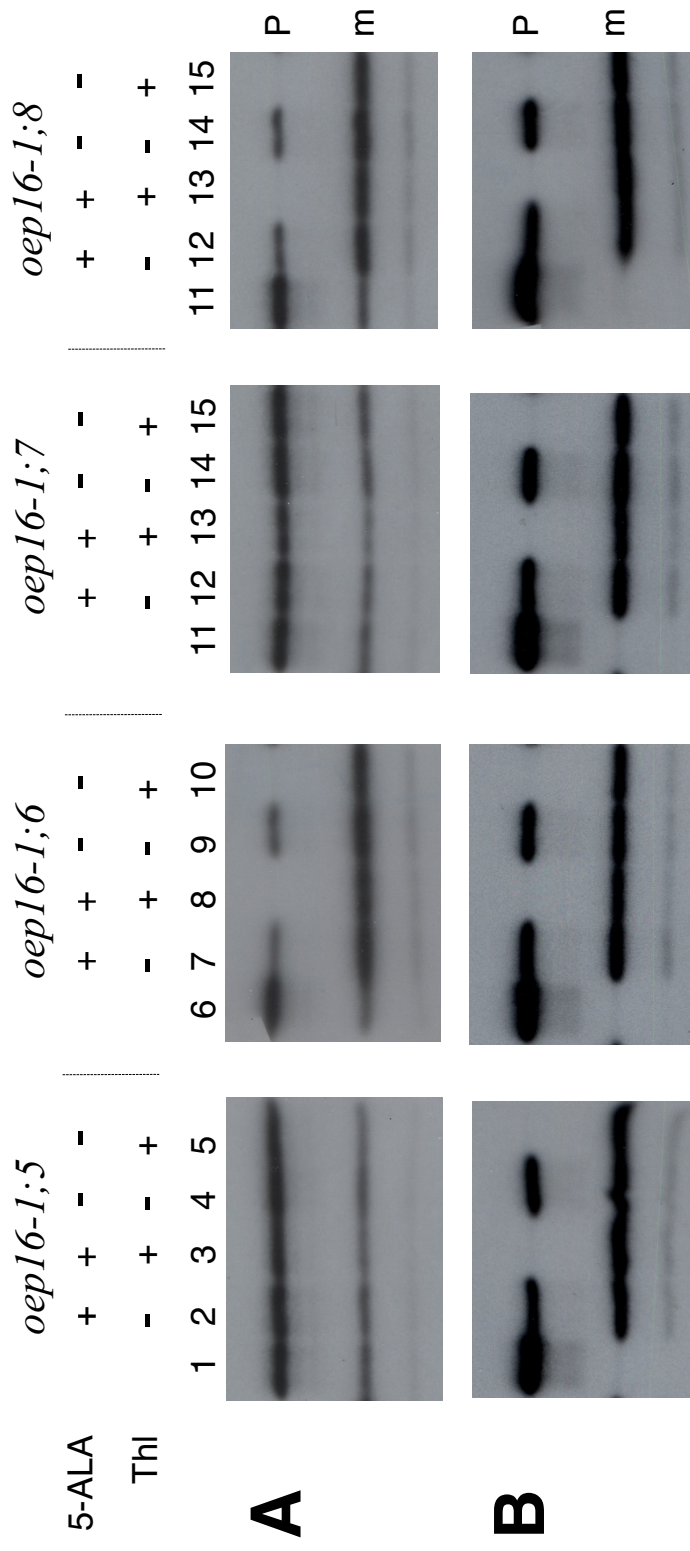


Fig. S3

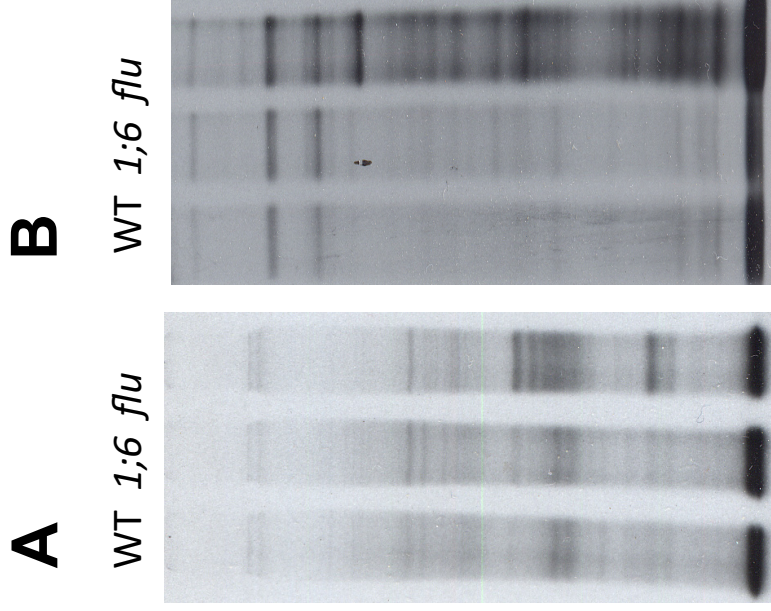
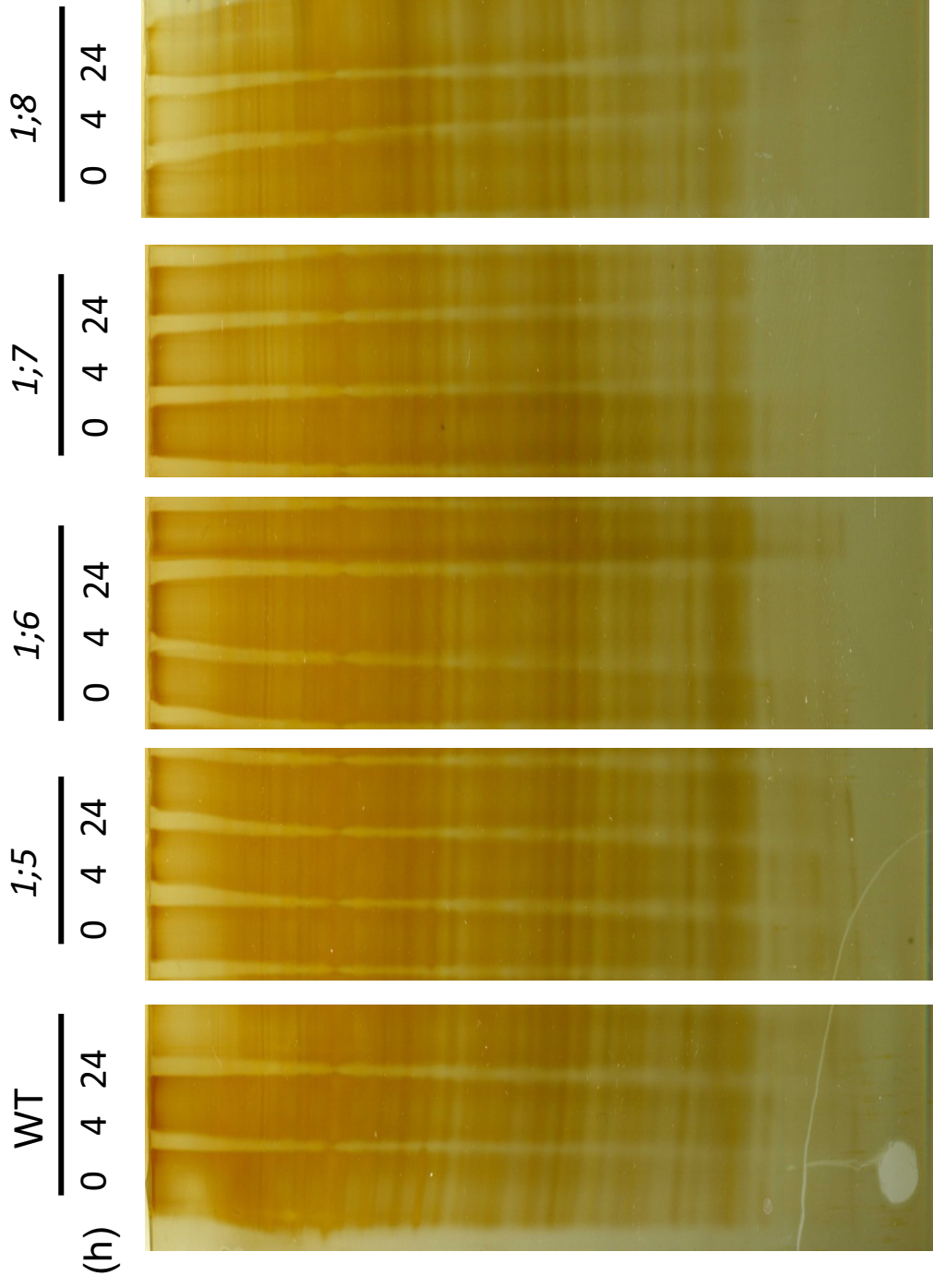


Fig. S4



Supplementary information

Supplementary figures

Fig. S1. Seedling viability as a function of seedling age and light conditions. A, Seedling viability as a function of the light intensity, displayed for mutant *oep16-1;6*, at high light (HL: $125 \mu\text{E m}^{-2} \text{sec}^{-1}$) and low light (LL: $25 \mu\text{E m}^{-2} \text{sec}^{-1}$) conditions. B, Comparison of seedling viability for mutants *oep16-1;5*, *oep16-1;6*, *oep16-1;7* and *oep16-1;8* after a 4 h white light exposure to $125 \mu\text{E m}^{-2} \text{sec}^{-1}$ or $25 \mu\text{E m}^{-2} \text{sec}^{-1}$. C, Seedling viability as a function of seedling age, illustrated for mutant *oep16-1;6*. After different periods of growth in darkness, seedlings were exposed to $125 \mu\text{E m}^{-2} \text{sec}^{-1}$ for 24 h and the percentage of greening seedlings was scored. Note the inverse correlation between hypocotyls length (in mm) and cell viability (% viable seedlings) after the dark-to-light shift.

Fig. S2. *In vitro*-import of ^{35}S -transA-DHFR (A) and ^{35}S -transB-DHFR (B) into chloroplasts isolated from the 4 different *oep16* mutants. Import was studied with Percoll/sucrose-purified chloroplasts that had been fed 5-aminolevulinic acid (5-ALA) to induce intraplastidic Pchl_a synthesis or mock-incubated with phosphate buffer. All import assays were conducted in the dark for 15 min and contained 2.5 mM Mg-ATP and 0.1 mM Mg-GTP. After import, the assays were treated with (+) or without (-) thermolysin (Thl)(1). Protein was precipitated with trichloroacetic acid. After SDS-PAGE, the gel was subjected to autoradiography. P and m define precursor and mature proteins. Note that a fraction of ^{35}S -transA-DHFR is artificially processed at time point zero.

1. Cline, K., Werner-Washburne, M., Andrews, J., and Keegstra, K. (1984) Thermolysin is a suitable protease for probing the surface of intact pea chloroplasts. *Plant Physiol.* 75, 675-678.

Fig.S3. Pattern of proteins translated *in vitro* (A) and *in vivo* (B) in etiolated wild-type (WT), *oep16-1;6* and *flu* seedlings after 2 h of illumination.

Fig.S4. Patterns of silver-stained total proteins in wild-type seedlings and seedlings of mutants *oep16-1;5*, *oep16-1;6*, *oep16-1;7* and *oep16-1;8* in the dark (0 h) and after 4 h and 24 h, respectively, of exposure to white light of $125 \mu\text{E m}^{-2} \text{sec}^{-1}$.

The Outer Chloroplast Envelope Protein OEP16-1 for Plastid Import of NADPH:Protochlorophyllide Oxidoreductase A in *Arabidopsis thaliana*

Iga Samol¹, Claudia Rossig¹, Frank Buhr¹, Armin Springer², Stephan Pollmann³, Abder Lahroussi¹, Diter von Wettstein^{4,5,*}, Christiane Reinbothe¹ and Steffen Reinbothe^{1,4,*}

¹Laboratoire de Génétique Moléculaire des Plantes et Biologie intégrative et systémique (BISy), Université Joseph Fourier, CERMO, BP53, F-38041 Grenoble cedex 9, France

²Lehrstuhl für Pflanzenphysiologie, Universität Bayreuth, Universitätsstraße 30, D-95447 Bayreuth, Germany

³Lehrstuhl für Pflanzenphysiologie, Ruhr-Universität Bochum, Universitätsstraße 150, D-44801 Bochum, Germany

⁴Department of Crop and Soil Sciences & School of Molecular Biosciences, Washington State University, Pullman WA 99164-6420 USA

⁵Research Center for BioSystems, Land Use and Nutrition, Justus Liebig University, Giessen, Germany

*Corresponding author: Diter von Wettstein, E-mail, diter@wsu.edu; Steffen Reinbothe, E-mail, steffen.reinbothe@ujf-grenoble.fr;

Fax, +1-509-335-8674 (DvW); +33-47651-4805 (SR)

(Received June 4, 2010; Accepted November 8, 2010)

The outer plastid envelope protein OEP16-1 was previously identified as an amino acid-selective channel protein and translocation pore for NADPH:protochlorophyllide oxidoreductase A (PORA). Reverse genetic approaches used to dissect these mutually not exclusive functions of OEP16-1 in planta have led to descriptions of different phenotypes resulting from the presence of several mutant lines in the SALK_024018 seed stock. In addition to the T-DNA insertion in the *AtOEP16-1* gene, lines were purified that contain two additional T-DNA insertions and as yet unidentified point mutations. In a first attempt to resolve the genetic basis of four different lines in the SALK_024018 seed stock, we used genetic transformation with the *OEP16-1* cDNA and segregation analyses after crossing out presumed point mutations. We show that *AtOEP16-1* is involved in PORA precursor import and by virtue of this activity confers photoprotection onto etiolated seedlings during greening.

Keywords: Chlorophyll biosynthesis • Photooxidative damage • Porphyrin-regulated plastid protein import • Singlet oxygen.

Abbreviations: DHFR, dihydrofolate reductase; DTNB, 5,5'-dithiobis(2-nitro)benzoic acid; GFP, green fluorescent protein; MS, Murashige and Skoog; Pchl_{id}, protochlorophyllide; pPORA, NADPH:protochlorophyllide oxidoreductase A precursor; TUNEL, deoxynucleotidyl transferase-mediated dUTP nick end labeling; YFP, yellow fluorescent protein.

Introduction

Plastids accomplish key metabolic functions in higher plants. Because of their endosymbiotic origin, plastids are surrounded

by two envelope membranes, called the outer and inner envelope, that are involved in the exchange of metabolites and the uptake of cytosolic precursor proteins (Cavalier-Smith 2006). Plastids need to import the majority of their protein constituents from the cytosol, requiring specialized protein translocon complexes to operate in the outer and inner envelope membranes, termed the TOC and TIC machinery (Bedard and Jarvis 2005, Hofmann and Theg 2005, Kessler and Schnell 2006). Current concepts indicate that multiple versions of the TOC and TIC machinery exist which differ by an interchange of components, allowing the adjustment of precursor import in time and space and according to the developmental and environmental conditions (Jarvis et al. 1998, Bauer et al. 2000, Ivanova et al. 2004, Kubis et al. 2004). Bauer et al. (2000) reported on different TOC receptor proteins designated TOC159, TOC132 and TOC120, sharing conserved acidic domains and transmembrane anchors but differing in the length of their cytosolically exposed pre-sequence-binding domains. A large number of cytosolic precursor proteins contain cleavable N-terminal transit sequences that are involved in the recognition and binding as well as translocation of the precursors across the limiting membranes of chloroplasts (Bedard and Jarvis 2005, Hofmann and Theg 2005, Kessler and Schnell 2006).

Bauer et al. (2000) identified a mutant deficient in TOC159 that is impaired in the import of photosynthetic proteins but not of non-photosynthetic proteins. Smith et al. (2004) observed that transit peptide fusions consisting of the transit peptide of NADPH:protochlorophyllide oxidoreductase A (PORA) and a cytosolic dihydrofolate reductase (DHFR) reporter protein of mouse was not precipitated in pull-down assays using a soluble form of TOC159 whose transmembrane segments had been removed. This finding confirmed studies of competition, antibody blocking and cross-linking which had

Plant Cell Physiol. 52(1): 96–111 (2011) doi:10.1093/pcp/pcq177, available online at www.pcp.oxfordjournals.org

© The Author 2010. Published by Oxford University Press on behalf of Japanese Society of Plant Physiologists.

All rights reserved. For permissions, please email: journals.permissions@oup.com

revealed that the PORA precursor (pPORA) does not interact with TOC75 during import (Reinbothe et al. 2000, Reinbothe et al. 2004a, Reinbothe et al. 2004b). Instead, an ortholog of the outer plastid envelope protein OEP16, originally discovered in pea chloroplasts (Pohlmeyer et al. 1997), was isolated that cross-linked pPORA and respective transA–DHFR fusions in plastids of barley, wheat, pea and *Arabidopsis thaliana* (Reinbothe et al. 2004a, Reinbothe et al. 2004b).

OEP16-1 from barley is closely related to OEP16-1 from pea (PsOEP16) (62% sequence identity) and AtOEP16-1 from *A. thaliana* (52% sequence identity) (Drea et al. 2006). In *A. thaliana* a small gene family encodes three members, designated *AtOEP16-1* (At2g28900), *AtOEP16-2* (At4g16160) and *AtOEP16-4* (At3g62880) (Reinbothe et al. 2004b, Drea et al. 2006, Murcha et al. 2007). A fourth relative exists (*AtOEP16-3*; encoded by At2g42210) that appears not to belong to this group since its encoded product is localized in mitochondria (Murcha et al. 2007).

Two non-exclusive functions have been indicated for the OEP16-1 protein: (i) a voltage-gated, amino acid-selective channel (Pohlmeyer et al. 1997, Philippar et al. 2007) and (ii) a translocation pore for pPORA (Pollmann et al. 2007). Knock-out mutants for *AtOEP16-1* have provided different results (Philippar et al. 2007, Pollmann et al. 2007). We found in an *AtOEP16-1* mutant with absence of OEP16 a lack of import of pPORA, aberrant etioplast ultrastructures and the accumulation of free, photoexcitable protochlorophyllide (Pchl) molecules that triggered cell death upon irradiation of dark-grown seedlings (Pollmann et al. 2007). In contrast, Philippar et al. (2007) observed no import defects of pPORA, normal etioplast ultrastructures and unimpaired greening in the mutant they investigated. Based on these results, we (Samol et al. 2011) and Pudelski et al. (2009) re-screened the original seed stock SALK_024018. Pudelski et al. (2009) showed that two additional T-DNA insertions and at least one point or footprint mutation are present in mutants of the original seed stock SALK_024018 (Alonso et al. 2003) that can affect the establishment of the cell death phenotype. In our recent study (see accompanying paper by Samol et al. 2011), pure lines of four OEP16-deficient mutants with different cell death properties were identified (Samol et al. 2011). All four mutants showed only one T-DNA band on Southern blots (Samol et al. 2011). Two of the mutants overproduced free Pchl in the dark and died after illumination (Samol et al. 2011). The other two mutants avoided excess Pchl accumulation and greened normally (Samol et al. 2011). One of these mutants, *Atoep16-1;6*, imported pPORA by a pathway which did not permit PORA to attain a functional state conferring photoprotection on etiolated seedlings during greening, as concluded from low temperature pigment fluorescence measurements and photo-bleaching/seed viability tests (Samol et al. 2011). Mutant *Atoep16-1;6* was used in the present study to readdress our previous results indicating that OEP16-1 is causally related to the substrate-dependent plastid import of pPORA and efficient seedling de-etiolation. We demonstrate that mutant

Atoep16-1;6 was restored to normal greening by transformation introducing synthesis of OEP16-1 from its cDNA or by cDNA encoding a fusion of OEP16-1 with green fluorescent protein (GFP). GFP::OEP16-1 was localized to chloroplasts, as demonstrated by confocal laser scanning microscopy. In the generated transgenic lines, OEP16-1 operated in the substrate-dependent import of pPORA. As a result, larger PORA:PORB complexes and photoactive Pchl were produced that allowed for efficient seedling de-etiolation. Together, these results demonstrate a functional role for AtOEP16-1 in pPORA import.

Results

Age-dependent expression of the cell death phenotype in mutant *Atoep16-1;6*

Mutant F6-4a that was described by Pudelski et al. (2009) corresponds to mutant *Atoep16-1;6* (Samol et al. 2011). Pudelski et al. (2009) used young, 2.5-day-old seedlings to examine the de-etiolation phenotype, i.e. the lack of greening and cell death. Consistent with the results of Pudelski et al. (2009) and Samol et al. (2011), mutant *Atoep16-1;6* showed strong red Pchl fluorescence in the dark (Fig. 1A). However, we noted that pigment autofluorescence under our experimental conditions appeared only after 3.5–4 d of growth in darkness and was hardly detectable under a fluorescence microscope after 2 d (Fig. 1A). Pchl accumulated in a free, non-POR-bound form and operated as a photosensitizer when the seedlings were irradiated. This is evident from the correlation between Pchl accumulation and cell death during dark growth after 4–5 d and subsequent illumination (Fig. 1C).

Developmental expression of OEP16-1 and PORA

Pudelski et al. (2009) have contested the role of OEP16-1 during greening, using several different arguments. They argued, for example, that there would be no sufficient overlap in the expression of OEP16-1 and PORA during seed germination. To address this point, an antiserum was raised against bacterially expressed and purified OEP16-1 protein (Supplementary Fig. S1a, b) and tested for its reactivity with OEP16-1 and other plant proteins. The results summarized in Supplementary Fig. S1c showed that one protein band was detectable on Western blots of separated plastid proteins. When time course experiments were conducted for 5-day-old, etiolated seedlings that had been illuminated for variable periods, the expression of OEP16-1 remained almost constant and declined only transiently (Fig. 2B). These results were consistent with our previous observation obtained by chemical cross-linking in barley, demonstrating a light-dependent reduction in OEP16-1 expression during the transition of etioplasts to chloroplasts (Reinbothe et al. 2004b). When the Western blots were probed with antiserum against POR, three bands were seen, of which the uppermost representing PORA declined in irradiated seedlings (Fig. 2B). Thus, OEP16 and PORA are

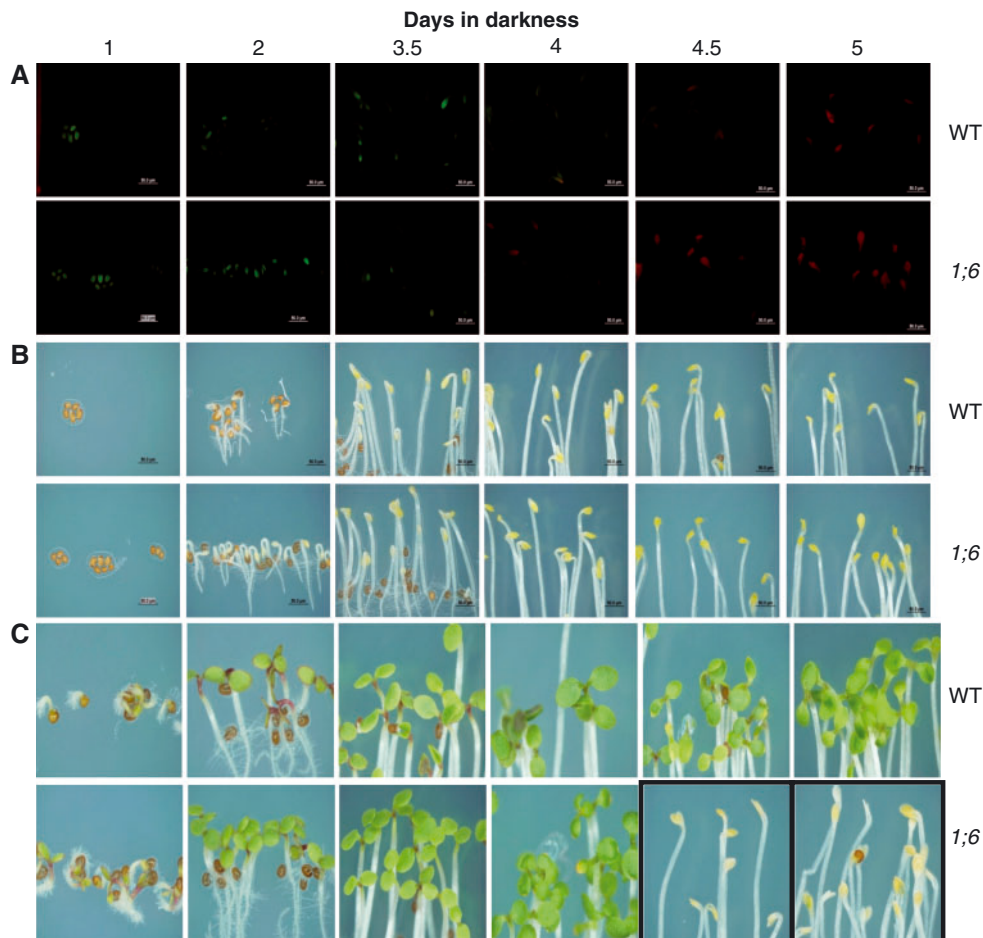


Fig. 1 Photobleaching as a function of Pchlide overaccumulation in mutant *Atoep16-1;6*. *Atoep16-1;6* (1;6) and wild-type (WT) seeds were germinated for different periods in darkness (A and B) and subsequently exposed to strong white light ($210 \mu\text{E m}^{-2} \text{s}^{-1}$) for 24 h (C). (A) Red Pchlide autofluorescence monitored under blue light (400–450 nm). (B) The same as in A, but showing the seedlings under normal daylight. (C) Phenotypes after irradiating etiolated seedlings with white light for 24 h.

expressed simultaneously in etiolated seedlings, in line with the proposed function of OEP16 in pPORA import.

Genetic complementation of mutant *Atoep16-1;6*

Gateway technology was used to assemble the following binary T-DNA overexpression destination vectors (Invitrogen). *OEP16* cDNA provided with the 35S cauliflower mosaic virus promoter ($35S::GFP::OEP16$) was cloned into vector pB7WG2 containing the Bar gene providing resistance to ammonium glufosinate. For placement of the GFP sequence tag between the 35S promoter and the N-terminus of OEP16, the vector pK7WGF2 containing the kanamycin resistance gene was used, while fusion of the yellow fluorescent protein (YFP) sequence tag to the C-terminus of OEP16 was carried out with vector pB7YWG2.

The cloned vector DNAs were transformed into *Agrobacterium tumefaciens*, strain GV3121, via electroporation. The presence of the correct T-DNA was verified by PCR (Innis et al. 1990), before proceeding with the in planta

transformation (Clough and Bent 1998). After transformation, selection of the first, second and third generation of transgenic plants (T_1 , T_2 and T_3) was performed on media with kanamycin (for plants containing $35S::GFP::OEP16$) and with ammonium glufosinate (for plants containing $35S::OEP16$ and $35S::OEP16::YFP$).

Nine transgenic T_3 lines were obtained with vector pB7WG2 containing $35S::OEP16$, and five of these showed rescue from bleaching. Six transgenic lines resulted from transformation with vector pK7WGF2 containing $35S::GFP::OEP16$. One of these provided rescue from bleaching. Four transgenic lines were obtained with plasmid pB7YWG2 containing $35S::OEP16::YFP$, but none provided rescue from bleaching.

A compelling example of a successful complementation is provided by line *Atoep16-1;6:35S::OEP16 E_6* which was composed of 100% homozygous, herbicide-resistant plants (Fig. 3b). After growth in the dark for 5 d and subsequent high light exposure ($210 \mu\text{E m}^{-2} \text{s}^{-1}$) for 24 h, seedlings of *Atoep16-1;6:35S::OEP16 E_6* looked like the wild type and

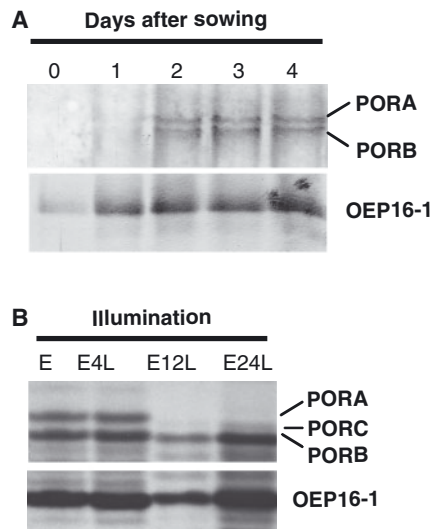


Fig. 2 OEP16-1 and POR expression during post-germination development in the dark (A) and after subsequent irradiation (B). Seeds were sown on agar medium containing 1% sucrose and germinated for variable periods in darkness (A). In a parallel experiment, seedlings were allowed to grow for 4.5 d in the dark (E) before being exposed to strong white light ($210 \mu\text{E m}^{-2} \text{s}^{-1}$) for 4 h (E4L), 12 h (E12L) and 24 h (E24L) (B). After extraction and resolution of total leaf protein on an SDS-containing 10–20% polyacrylamide gel, OEP16-1 and POR expression was assessed by Western blotting using the respective monospecific antisera. The three detected POR protein bands represent PORA, PORB and PORC.

were fully viable (**Fig. 3d**). This result indicated that the introduced *AtOEP16-1* gene had restored normal greening. Indeed, no red fluorescence indicative of the presence of free Pchl_a molecules was seen in etiolated *Atoep16-1;6:35S::OEP16 E_6* seedlings, but was easily detectable in seedlings of the *Atoep16-1;6* mother generation (**Fig. 3c**). Exposure of the etiolated seedlings to white light for 48 h or longer periods did not affect seedling viability (data not shown). Immunoblotting proved the high expression level of *AtOEP16-1* protein (**Fig. 3e**).

Fig. 4 shows results obtained for line *T₃ AtOEP16-1;6:35S::GFP::OEP16 D_8* expressing the GFP::OEP16 fusion protein. Similar to the results for *AtOEP16-1;6:35S::OEP16 E_6*, both the reduction of red Pchl_a fluorescence during plant etiolation (**Fig. 4c**) and normal green appearance without detectable signs of photooxidative damage after illumination (**Fig. 4d**) emphasized that the introduced transgene was active in restoring normal greening. GFP fused to *AtOEP16-1* at its N-terminus thus did not affect the function of *AtOEP16-1* in planta.

In contrast to these results, transformation of mutant *AtOEP16-1;6* with the YFP fusion protein gene did not regenerate plants that were viable during de-etiolation ($n = 4$). In spite of the presence of the *AtOEP16-1* fusion protein in transformed *T₃ AtOEP16-1;6* mutant seedlings (Supplementary Fig. S2e), all analyzed transgenic plants accumulated high levels of red-fluorescing Pchl_a and died after illumination, as did the

untransformed *AtOEP16-1;6* mutant (Supplementary Fig. S2c, d). Together, these findings showed that *AtOEP16-1* with the YFP tag either could not enter the outer envelope of chloroplasts or attained a non-functional conformation with the fusion to the YFP reporter protein.

Confocal laser scanning microscopy was used to study the localization of the GFP–OEP16-1 and OEP16-1–YFP fusion proteins in the regenerated transgenic lines. **Fig. 5** depicts representative images taken for line *T₃ AtOEP16-1;6:35S::GFP::OEP16 D_8*. Clearly, GFP fluorescence in the 35S::GFP::OEP16 transformants co-localized with the red autofluorescence of Chl in chloroplasts of mesophyll cells and guard cells of stomata (**Fig. 5a, b**). This result is in accordance with previous localization data of OEP16-1 (Pohlmeier et al. 1997, Reinbothe et al. 2004a, Reinbothe et al. 2004b). In contrast, no chloroplast import was detectable for transformants expressing OEP16-1–YFP (Supplementary Fig. S2f).

In vitro import of transA–DHFR into plastids of line *AtOEP16-1;6:35S::OEP16 E_6*

Fusion proteins consisting of the first 67 N-terminal amino acids of the pPORA from barley (henceforth referred to as transA) and the DHFR reporter protein of mouse were activated with Ellman's reagent [5,5'-dithiobis(2-nitro)benzoic acid (DTNB)] (Reinbothe et al. 2004b). Then the precursor was imported into etioplasts or chloroplasts that had been isolated from 5-day-old, dark-grown and light-grown *AtOEP16-1;6* mutant, *AtOEP16-1;6:35S::OEP16 E_6* and wild-type seedlings, respectively. Import was assessed under standard conditions in assays containing 2.5 mM Mg-ATP and 0.1 mM Mg-GTP (Reinbothe et al. 2005). **Fig. 6** shows that mutant *AtOEP16-1;6* imported a fraction of DTNB-activated precursor into both their etioplasts and chloroplasts. In either case, a fraction of the precursor (31 kDa) was shifted into a larger, 106 kDa cross-linked product which cross-reacted with TOC75 (75 kDa) in pull-down assays (Supplementary Fig. S3). In plastids from line *AtOEP16-1;6:35S::OEP16 E_6*, however, no 106 kDa cross-linked product appeared and a smaller, 46 kDa product was formed (**Fig. 6**). This cross-linked product consisted of transA–DHFR and OEP16-1, as demonstrated by co-immunoprecipitation experiments (Supplementary Fig. S3). At time zero, some artificial processing occurred. However, the greater proportion of mature protein (DHFR) in etioplasts vs. chloroplasts in line *AtOEP16-1;6:35S::OEP16 E_6* suggests that the introduced OEP16-1 had restored the Pchl_a-dependent import of transA–DHFR. Pchl_a needed for the substrate-dependent import of transA–DHFR is present only in etioplasts, while the pigment level in chloroplasts is too low for the import step in vitro (Reinbothe et al. 1995a, Reinbothe et al. 1995b, Reinbothe et al. 1996). When import assays were carried out for transB–DHFR, consisting of the transit sequence of pPORB and the DHFR, no differences were detectable for plastids isolated from mutant *AtOEP16-1;6* and line *AtOEP16-1;6:35S::OEP16 E_6* (Supplementary Fig. S4).

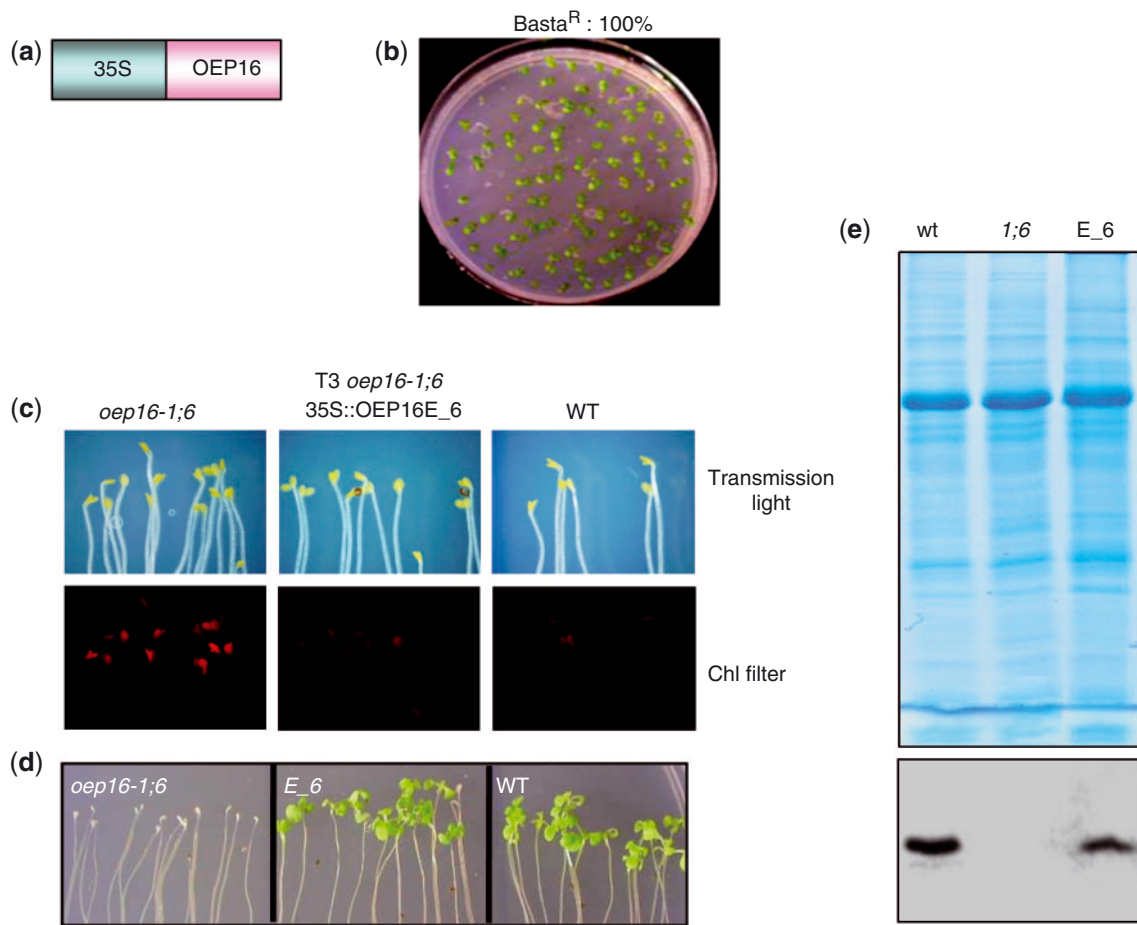


Fig. 3 Genetic complementation of *Atoep16-1;6* by *35S::OEP16*. (a) Structure of the generated *35S::OEP16* construct. (b) Selection of plants corresponding to line T₃ *Atoep16-1;6;35S::OEP16 E_6* on MS medium containing ammonium glufosinate (BASTA, 5 µg ml⁻¹). (c) Phenotypic analysis of T₃ seedlings of *Atoep16-1;6;35S::OEP16 E_6* compared with mutant *Atoep16-1;6* and the wild type after growth in darkness for 5 d without (c) or with (d) a subsequent exposure to strong white light (210 µE m⁻² s⁻¹) for 48 h. Note the strong Pchlde fluorescence in mutant *Atoep16-1;6* and the lack of such fluorescence in line *Atoep16-1;6;35S::OEP16 E_6* and the wild type. (e) Detection of AtOEP16-1 in line T₃ *Atoep16-1;6;35S::OEP16 E_6* but not in untransformed *Atoep16-1;6* seedlings by Western blotting. Total protein was extracted from mature, green plants, separated on a 15% SDS–polyacrylamide gel and probed with an antibody that had been raised against the bacterially expressed and purified AtOEP16-1 protein. The Coomassie stain (upper panel) and Western blot (lower panel) show leaf protein corresponding to 40 µg of bovine serum albumin.

Low temperature fluorescence analysis of pigments in line *Atoep16-1;6;35S::OEP16 E_6*

On the basis of the results presented thus far it seemed likely that re-expressing AtOEP16-1 in mutant *Atoep16-1;6* restored the Pchlde-dependent import of pPORA. As a result, PORA–Pchlde *b*–NADPH complexes would be formed that could further assemble with PORB–Pchlde *a*–NADPH complexes to establish photoactive Pchlde in the prolamellar body of etioplasts (Reinbothe et al. 1999, Reinbothe et al. 2003, Buhr et al. 2008). Pchlde is normally present in two spectral pigment forms in low temperature in planta fluorescence measurements: Pchlde-F631 and Pchlde-F655 (Lebedev et al. 1995, Lebedev and Timko 1998). Pchlde-F655 has been named photoactive Pchlde because it can be converted to chlorophyllide upon a 1 ms flash of white light (Lebedev et al. 1995,

Lebedev and Timko 1998); its establishment is an indicator of the presence of functional PORA:PORB–pigment complexes in the prolamellar body of etioplasts (Lebedev et al. 1995, Lebedev and Timko 1998). These complexes dubbed LHPPs, light-harvesting POR:Pchlde complexes, are involved in light trapping and excess light energy dissipation during greening (Reinbothe et al. 1999, Reinbothe et al. 2003, Buhr et al. 2008). Pchlde-F631, in contrast, is called photoinactive Pchlde because it cannot be converted immediately to chlorophyllide (Lebedev et al. 1995, Lebedev and Timko 1998). Pchlde-F631 is a mixture of POR–pigment–NADPH ternary complexes and free, non-POR bound Pchlde molecules (Reinbothe et al. 1999, Reinbothe et al. 2003, Buhr et al. 2008).

In order to examine the functional state of PORA in planta, low temperature fluorescence spectroscopy was carried out according to standard procedures (Lebedev et al. 1995).

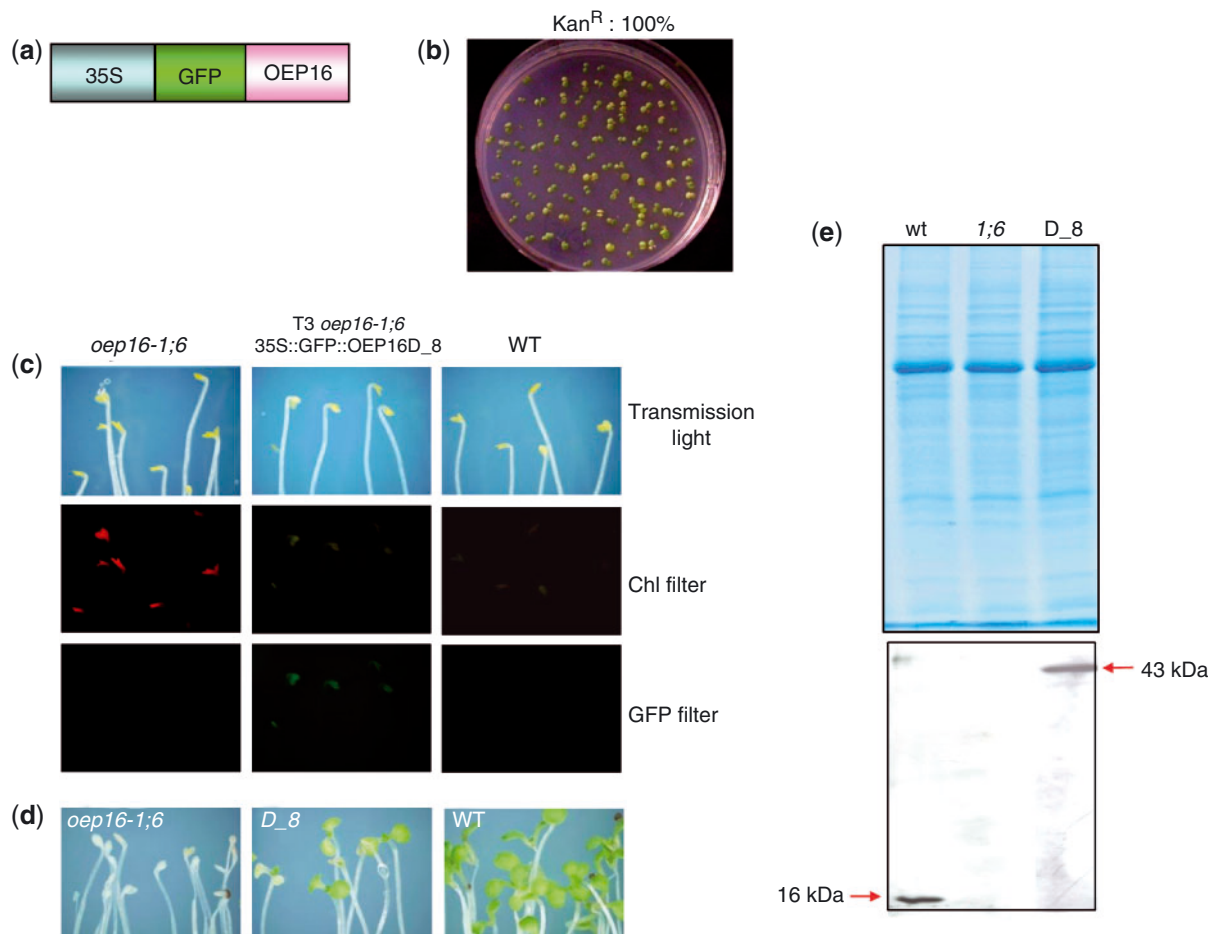


Fig. 4 Genetic complementation of *Atoep16-1;6* by *35S::GFP::OEP16*. As in **Fig. 3**, but depicting the results obtained for line T_3 *Atoep16-1;6:35S::GFP::OEP16 D_8* expressing the GFP::OEP16 fusion protein. (a) Structure of the generated construct. (b) Antibiotic resistance of the produced T_3 line. Note that all of the generated plants are resistant to kanamycin sulfate ($50 \mu\text{g ml}^{-1}$). (c and d) Phenotype of seedlings after growth in darkness (c) and after exposure to strong white light ($210 \mu\text{E m}^{-2} \text{s}^{-1}$) for 48 h (d). (e) Expression of GFP–OEP16-1 in total leaf protein extracts. Note the molecular mass shift of OEP16-1 relative to the wild type for line T_3 *Atoep16-1;6:35S::GFP::OEP16 D_8*. Protein equivalent to $40 \mu\text{g}$ of bovine serum albumin was loaded per lane and the blot was probed with AtOEP16-1 antibody.

Fig. 7A shows that mutant *oep16-1;6* contained large amounts of photoinactive Pchl ide-F631 but little photoactive Pchl ide-F655 . In fact, only a shoulder appeared in the fluorescence emission spectrum at around 650 nm. In line T_3 *Atoep16-1;6:35S::OEP16 E_6* expressing OEP16-1, a substantial fraction of the pre-existing Pchl ide was shifted into the photoactive state, establishing Pchl ide-F655 . When protein extracts were prepared from detergent-solubilized prolamellar bodies of isolated etioplasts and subjected to non-denaturing PAGE, larger PORA:PORB complexes were detectable in line T_3 *Atoep16-1;6:35S::OEP16 E_6*, but not in the *Atoep16-1;6* mutant (**Fig. 7B**). This result indicates that OEP16-1 is involved in pPORA import.

Cell death rescue in *Atoep16-1;6:35S::OEP16 E_6*

Three approaches were used to assess the mechanism of cell death rescue in line *Atoep16-1;6:35S::OEP16 E_6*. First, singlet oxygen measurements were carried using the DanePy

method. The DanePy reagent is a dansyl-based singlet oxygen sensor that undergoes quenching of its fluorescence upon reacting with singlet oxygen (Hideg et al. 1998, Kálai et al. 2002). **Fig. 8A** shows the fluorescence emission spectra of DanePy for mutant *Atoep6-1;6*, line *Atoep16-1;6:35S::OEP16 E_6* and wild-type seedlings. Confirming our previous observations (Samol et al. 2011), DanePy fluorescence quenching and thus singlet oxygen production was readily detectable in seedlings of mutant *Atoep6-1;6* that had been grown in the dark for 5 d and illuminated for 30 min. In contrast, no comparable fluorescence quenching and thus singlet oxygen evolution was detectable for line *Atoep16-1;6:35S::OEP16 E_6* and the wild type (**Fig. 8A**).

Secondly, we carried out terminal deoxynucleotidyl transferase-mediated dUTP nick end labeling (TUNEL) measurements (Gavrieli et al. 1992). This method permits detection of the breakage of nuclear DNA that is a hallmark of cell death and apoptosis in animals and plants. In addition, DNA

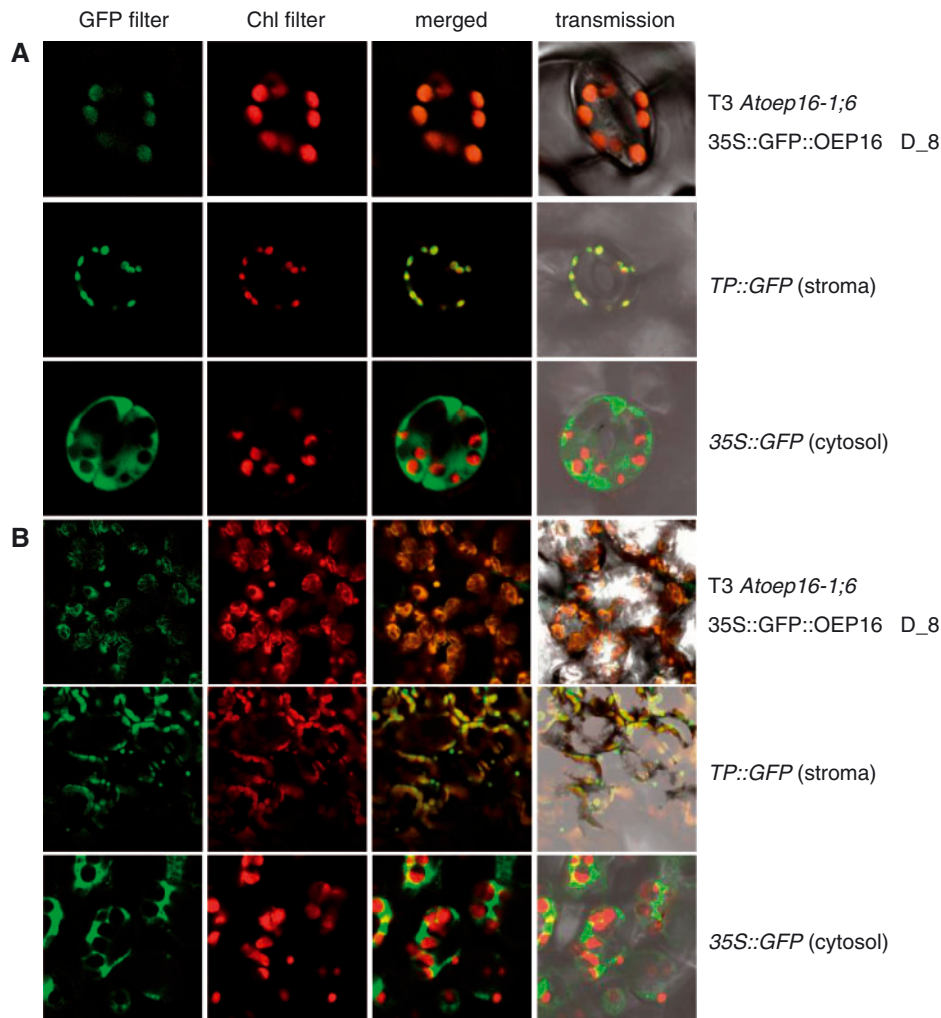


Fig. 5 Cytolocalization of GFP in mutant *Atoep16-1;6* transgenic for *35S::GFP::OEP16*. Plants of line T_3 *Atoep16-1;6:35S::GFP::OEP16* D_8 were grown for 14 d in continuous white light and the localization of the GFP reporter proteins was examined by confocal laser scanning microscopy. (a and b) Co-localization of GFP and Chl fluorescences in guard cells of stomata (a) and in mesophyll cells (b) in plants of line T_3 *Atoep16-1;6:35S::GFP::OEP16* D_8. For imaging acquisition, GFP and Chl were excited at a wavelength of 488 nm, in combination with 493–573 nm (GFP) and 650–800 nm (Chl) emission filters. As a negative control, transgenic plants expressing *35S::GFP* were used which showed cytosolic and nuclear localizations of GFP. As a positive control, transgenic plants expressing a chimeric precursor consisting of the transit peptide of the small subunit of ribulose-1,5-bisphosphate carboxylase/oxygenase and GFP (*TP::GFP*) were used (kindly provided by Dr. Norbert Rolland, CEA, Grenoble, France). In this case, almost all of the detected GFP fluorescence was found in the plastid compartment.

fragmentation was assessed by conventional agarose gel electrophoresis and ethidium bromide staining. **Fig. 8B** showed that while high molecular mass DNA accumulated in seedlings of the wild type and line *Atoep16-1;6:35S::OEP16* E_6, seedlings of mutant *Atoep16-1;6* contained drastically reduced amounts of higher molecular mass DNA and instead contained lower mass DNA species. Similar to line *Atoep16-1;6:35S::OEP16* E_6, the other analyzed transformed lines also contained increased levels of uncleaved DNA (**Fig. 8B**).

Thirdly, we performed pulse labeling studies with [35 S]methionine. Singlet oxygen is a powerful cytotoxin and potent signaling compound that causes changes in gene expression including effects on translation (Miller et al. 2007, Khandal et al. 2009; summarized in Reinbothe et al. 2009). Confirming

previous results (Samol et al. 2011), protein synthesis was hardly detectable in dark-grown *Atoep16-1;6* mutant seedlings after 24 h of illumination (**Fig. 8C**). However, protein synthesis was unchanged in seedlings of line *Atoep16-1;6:35S::OEP16* E_6 and the wild type (**Fig. 8C**). Whereas mutant *Atoep16-1;6* failed to react to singlet oxygen with the synthesis of stress proteins, the previously described *flu* mutant (Meskauskiene et al. 2001) did so and translated key enzymes of jasmonic acid synthesis such as allene oxide synthase (AOS) (Wasternack 2007; summarized in Reinbothe et al. 2009) (**Fig. 8d**). *flu* is impaired in the negative feedback loop inhibiting excess Pchlde accumulation in the dark and suffers from photooxidative damage and eventually dies during greening (Meskauskiene et al. 2001, op den Camp et al. 2004).

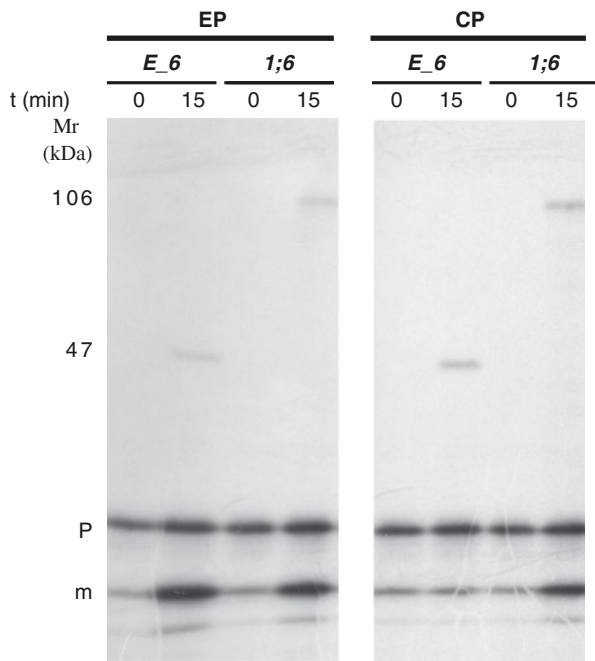


Fig. 6 Cross-linking of DTNB-activated [^{32}S]transA–DHFR in etioplasts (EP) and chloroplasts (CP) isolated from mutant *Atoep16-1;6* (1;6) and line T_3 *Atoep16-1;6:35S::OEP16 E_6* (E_6). The autoradiogram shows precursor (P) and mature (m) proteins as well as cross-linked products of 47 and 106 kDa at time zero (0 min) and after 15 min of import (15 min). The 47 kDa cross-linked product is caused by the formation of a disulfide bond between transA–DHFR and OEP16-1; this product is only detectable in plastids of line *Atoep16-1;6:35S::OEP16 E_6*. The 106 kDa cross-linked product results from the formation of a disulfide bond between transA–DHFR and TOC75; this product is found for plastids from *Atoep16-1;6* mutants.

Backcrosses of mutant *Atoep16-1;6* with the wild type

Mutant F6-4a studied by Pudelski et al. (2009) corresponds to mutant *Atoep16-1;6* (Samol et al. 2011) and contains only one detectable T-DNA insertion (Pudelski et al. 2009, Samol et al. 2011). Pudelski et al. (2009) suggested that mutant F6-4a may contain an additional point or footprint mutation that caused the cell death phenotype. If this point mutation is unlinked to the *Atoep16-1;6* mutation, it should be separable by a backcross with the wild type. In the F_2 of such a backcross, the plants segregated in 40 wild-type seedlings, 89 seedlings with a weak bleaching phenotype and 41 with a strong cell death phenotype. This fits to a monohybrid, semi-dominant expected ratio of 42.5:85.0:42.5 ($\chi^2 = 0.21$; $P = 0.975$) and excluded that the second mutation present in mutant *oep16-1;6* caused the bleaching phenotype. The homozygous F_2 plants with the strong bleaching phenotype lacked PORA (Fig. 9A) and contained exclusively photoinactive Pchlde-F631 (Fig. 9B); they may correspond to mutant *oep16-1;5*. In fact, no seedlings were obtained that were wild type with respect to the *OEP16-1* gene but showed the cell death phenotype. Thus, the cell death phenotype in mutant *oep16-1;5* is causally related

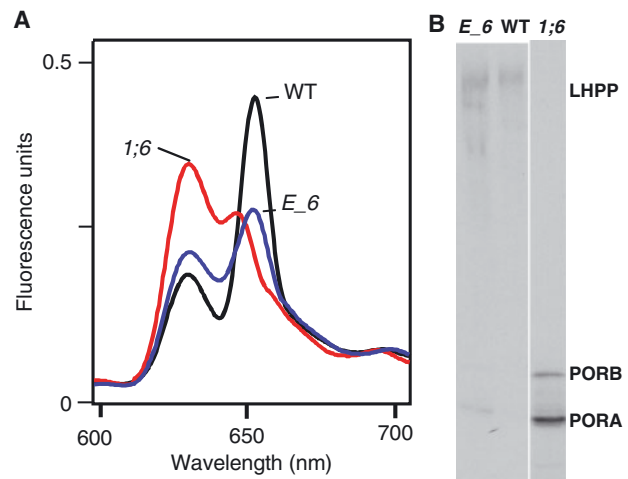


Fig. 7 Presence of PORA:PORB supracomplexes in line T_3 *Atoep16-1;6:35S::OEP16 E_6*. (A) Low temperature fluorescence analysis at 77 K of pigments in 5-day-old, etiolated seedlings of mutant *Atoep16-1;6* (1;6), line *Atoep16-1;6:35S::OEP16 E_6* (E_6) and the wild type (WT). Note the presence of photoactive Pchlde (Pchlde-F655) in line *Atoep16-1;6:35S::OEP16 E_6* and its almost total absence in mutant *Atoep16-1;6*. Spectral intensities refer to an equal cotyledon surface area. (B) Non-denaturing PAGE to detect PORA:PORB supracomplexes in mutant *Atoep16-1;6*, line *Atoep16-1;6:35S::OEP16 E_6* and the wild type.

to the import defect of pPORA, the lack of Pchlde sequestration and the production of singlet oxygen. Interestingly, a similar phenotype was observed for the *porA* knock-out mutant. Furthermore, Lebedev et al. (1995) described that seedlings of the *det340* mutant of *A. thaliana* are extremely susceptible to photooxidative damage and accumulate Chl only at extremely low light intensities. Dark-grown seedlings of the *det340* mutant lack PORA (and photoactive Pchlde) due to the *det* mutation (Lebedev et al. 1995).

To support further the conclusion that OEP16-1 is essential for pPORA import, we generated transgenic plants expressing pPORA–GFP fusion proteins consisting of the full-length PORA precursor (pPORA) of *A. thaliana* (Armstrong et al. 1995) and GFP. In four parallel batches, transgenic plants were generated for the wild type, mutant *Atoep16-1;6*, line *Atoep16-1;6:35S::OEP16 E_6* and the backcross of mutant *Atoep16-1;6*, and assessed for the presence of GFP fluorescence by confocal laser scanning microscopy.

As shown in Fig. 10A, etioplasts of transgenic wild-type plants synthesizing pPORA–GFP readily imported the chimeric precursor protein. Similarly, the pPORA–GFP fusion protein was imported into etioplasts of mutant *Atoep16-1;6*, although the amount of the fluorescent protein per plastid seemed reduced and some discontinuous distribution indicative of aggregation of unimported precursor occurred (Fig. 10B). Line *Atoep16-1;6* transgenic for $35S::OEP16 E_6$ and expressing OEP16-1 imported pPORA–GFP into their plastids, and GFP fluorescence was sharply focused in etioplasts (Fig. 10C).

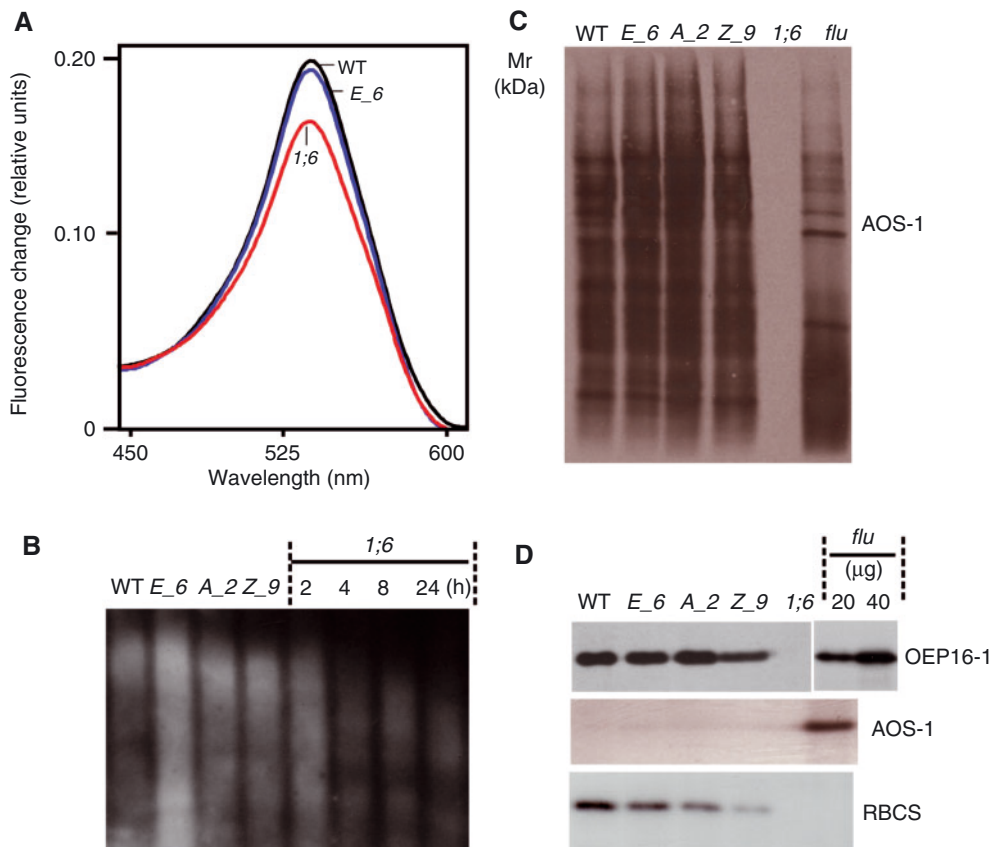


Fig. 8 Cell death rescue in line T_3 *Atoep16-1;6:35S::OEP16 E_6*. (A) Singlet oxygen evolution in 5-day-old, etiolated seedlings of mutant *Atoep16-1;6* (1;6), line *Atoep16-1;6:35S::OEP16 E_6* (*E_6*) and the wild type (WT) after a 30 min white light exposure. The curves show DanePy fluorescence emission spectra collected between 450 and 600 nm at an excitation wavelength of 331 nm. (B) DNA laddering in mutant *Atoep16-1;6*, line *Atoep16-1;6:35S::OEP16 E_6* and the wild type after a 24 h white light exposure. For comparison, DNA laddering was tested for two additional *Atoep16-1;6:35S::OEP16*-expressing lines, designated *A_2* and *Z_9*. The last four lanes show a time course of DNA degradation in mutant *Atoep16-1;6*. (C) Protein synthesis in etiolated seedlings of mutant *Atoep16-1;6*, lines *Atoep16-1;6:35S::OEP16 E_6*, *A_2* and *Z_9*, as well as the wild type after a 24 h white light exposure. Total leaf protein was labeled with [35 S]methionine for 2 h before seedling harvest. After extraction and SDS-PAGE on a 15% polyacrylamide gel, [35 S]-labeled proteins equivalent to 20 μ g of bovine serum albumin were detected by autoradiography. For comparison, protein extracts were prepared from irradiated *flu* seedlings and processed identically. (D) Western blot analysis to detect OEP16-1, allene oxide synthase (AOS) and the small subunit of ribulose-1,5-bisphosphate carboxylase/oxygenase (RBCS) in etiolated seedlings of mutant *Atoep16-1;6*, lines *Atoep16-1;6:35S::OEP16 E_6*, *A_2* and *Z_9*, as well as the wild type and *flu* after a 24 h white light exposure.

In contrast, no GFP fluorescence was detectable in plastids and the precursor was most probably degraded in *Atoep16-1;6* mutant plants backcrossed with the wild type and selected for plants that were homozygous for the *Atoep16-1* mutation. This is illustrated for line *Atoep16-1;6 C_107* (Fig. 10D). That the introduced transgene was expressed in line *Atoep16-1;6 C_107* was proven by Western blotting using etioplast protein extracts from seedlings in which degradation of pPORA-GFP was inhibited by a protease inhibitor cocktail (Supplementary Fig. S5). Together with the in vitro import and cross-linking experiments, these results demonstrated that the 'hidden' mutation present in *Atoep16-1;6* caused the TOC75-dependent import of pPORA-GFP and presumably also of pPORA in planta. In contrast, crossing out this mutation rendered import of pPORA-GFP and pPORA OEP16-1 dependent, and,

therefore, import was undetectable in seedlings of line *Atoep16-1;6 C_107*.

Discussion

OEP16-1 was previously identified as partner of pPORA during its Pchlde-dependent import into barley, wheat, pea and Arabidopsis plastids (Reinbothe et al. 2004a, Reinbothe et al. 2004b, Pollmann et al. 2007). Reverse genetic approaches carried out in two laboratories led to different results (Philippart et al. 2007, Pollmann et al. 2007). Pudelski et al. (2009) recently maintained that OEP16-1 in Arabidopsis is not involved in pPORA import and seedling de-etiolation. Arguments for this conclusion were (i) lack of overlap in the expression of OEP16-1

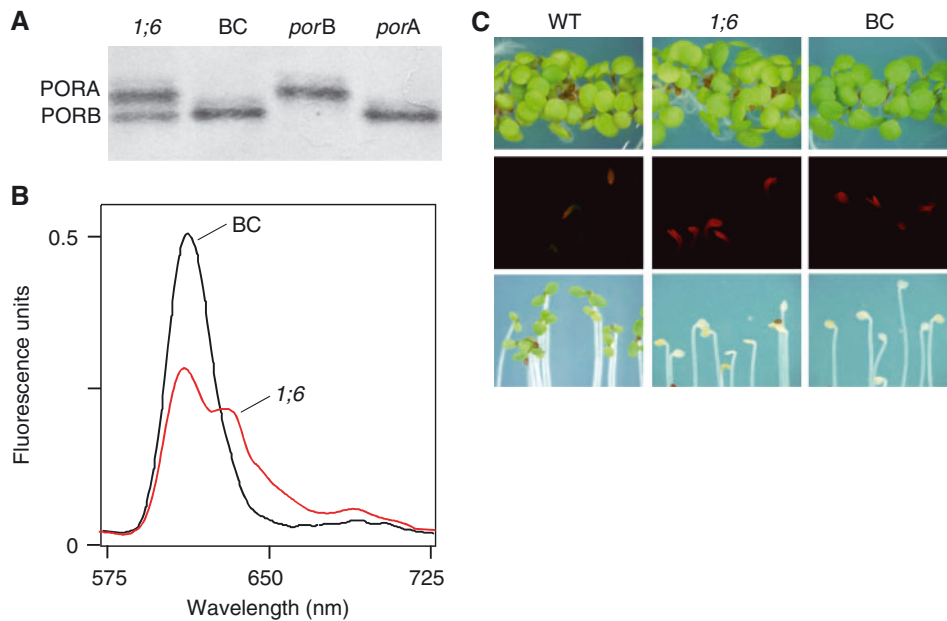


Fig. 9 Phenotypes of homozygous F_2 seedlings from the cross of homozygous mutant *Atoep16-1;6* with the wild type. (A) Western blot of PORA and PORB in mutant *Atoep16-1;6* and homozygous backcross plants (BC). For comparison, protein extracts were prepared from etiolated seedlings of *porA* and *porB* knock-out plants. (B) Low temperature fluorescence spectrum of photoactive Pchlde-F655 and photoinactive Pchlde-F631 in mutant *Atoep16-1;6*, and in homozygous backcross plants containing only photoinactive Pchlde-F631. (C) Phenotype of wild-type, homozygous *Atoep16-1;6* mutant and homozygous backcross seedlings after growth for 5 d in either continuous white light (top) or darkness (middle), and after 24 h of illumination with $210 \mu\text{E m}^{-2} \text{s}^{-1}$ white light following dark growth (bottom).

and PORA during seed germination and seedling growth in the dark; (ii) lack of genetic complementation assays needed to demonstrate a causal relationship between the absence of AtOEP16-1, pPORA import, Pchlde sequestration and cell death progression; and (iii) lack of co-segregation between the *AtOEP16-1* mutation and the cell death phenotype (Pudelski et al. 2009). With the present study, answers are provided to all of these questions.

Overlapping developmental expression patterns of OEP16-1 and PORA

We show that AtOEP16-1 expression is not confined to chloroplasts. With a monospecific antibody raised against the bacterially expressed and purified AtOEP16-1 protein we demonstrate that AtOEP16-1 is also abundant in etiolated plants and that its expression transiently declines in illuminated seedlings. Western blot analyses with POR antibody confirmed high PORA protein levels in the dark and decreasing PORA protein levels in illuminated seedlings. These results are in agreement with previous findings (Armstrong et al. 1995, Reinbothe et al. 2004b) and support the conclusion that there is a significant overlap in the expression of AtOEP16-1 and PORA. Recently, an interesting observation was made for two barley mutants, *albina-e¹⁶* (*alb-e¹⁶*) and *alb-e¹⁷* (Campoli et al. 2009). Both of them are disturbed in porphyrin biosynthesis although at different steps (a block of upstream Mg-protoporphyrin IX biosynthesis in *alb-e¹⁶* and a block before chlorophyllide

biosynthesis in *alb-e¹⁷*). In both mutants, the down-regulation of PORA mRNA was associated with the up-regulation of OEP16 mRNA (Campoli et al. 2009). This observation may suggest a compensatory mechanism to avoid PORA deficiency through higher import rates of the cytosolic precursor protein into the plastids.

Essential role of OEP16-1 as assessed by genetic transformation

Genetic transformation was used to explore whether or not a causal relationship exists between the absence of AtOEP16-1, pPORA import, Pchlde sequestration and cell death progression. Transformation of *oep16-1;6* plants was carried out with OEP16-1, GFP::OEP16-1 and OEP16-1::YFP transgenes driven by the 35S cauliflower mosaic virus promoter, using established procedures. As demonstrated for numerous other transgenes, plant transformation is a hazardous process that produces a vast range of different insert lines. Depending on the site where the foreign DNA has integrated into the genome, a large range of different transgenic lines is normally obtained. These lines differ with respect to the temporal and spatial pattern where the transgene's encoded product is expressed. For example, some of the produced lines may exhibit transgene expression that is too low to allow the detection of the encoded product. In other cases, strong expression of the transgene may occur but the encoded product may aggregate and thus not reach its final destination, therefore not permitting restoration of the

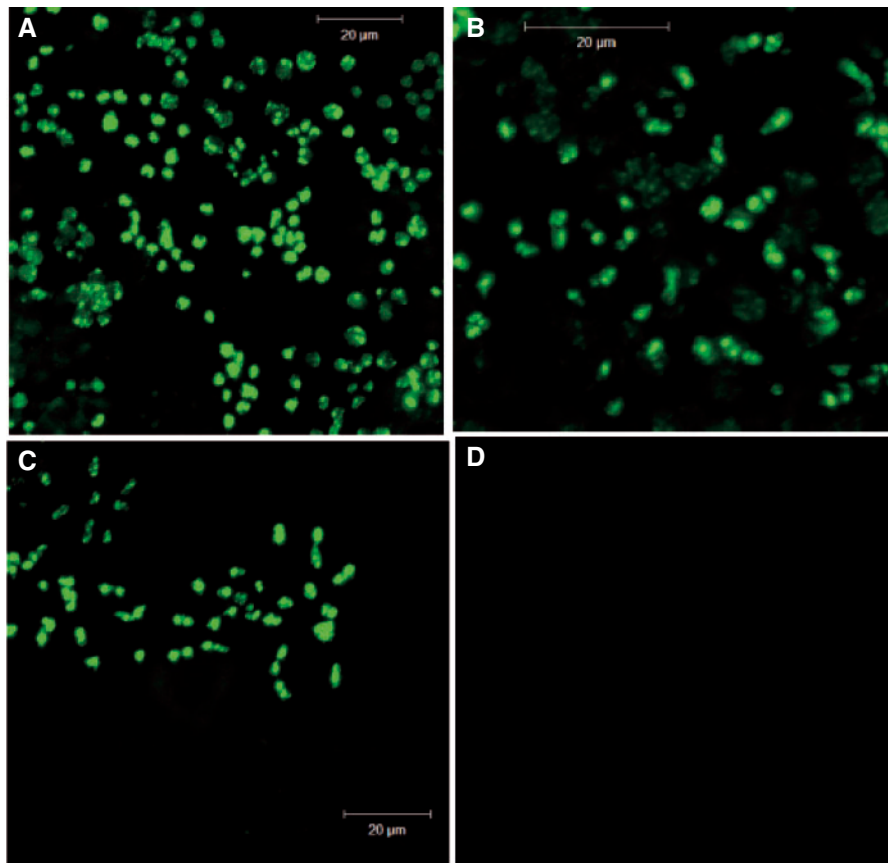


Fig. 10 In planta import of the pPORA–GFP fusion protein into plastids. Transgenic *A. thaliana* plants stably expressing pPORA–GFP under the control of the 35S cauliflower mosaic virus promoter were generated and assessed by confocal laser scanning microscopy for import of the introduced reporter protein. Images show GFP fluorescence in 5-day-old etiolated seedlings of the transgenic wild type (A), mutant *Atoep16-1;6* (B), line *Atoep16-1;6:35S::OEP16 E_6* expressing OEP16-1 (C) and the generated backcross of mutant *Atoep16-1;6*, designated *Atoep16-1;6 C_107* (D).

wild-type phenotype of the transformed mutant. Only in those transgenic lines where an almost wild-type expression level of the product of interest is found will restoration of the wild-type phenotype occur. This would, however, require that the transgene is expressed in the right developmental window and in the correct tissue, two processes that may be prone to variations from line to line. Even though the 35S promoter used in the present study should drive strong constitutive overexpression of the transgene, different lines were obtained, displaying significant variations in the expression level of the OEP16-1, GFP::OEP16-1 and OEP16-1::YFP transgenes. Nine transgenic T₃ lines were obtained containing 35S::OEP16, of which five showed rescue from photobleaching. In contrast, only one of six T₃ lines, 35S::GFP::OEP16, complemented the phenotype. In the case of the T₃ line 35S::OEP16::YFP, none of the produced lines could restore normal greening. Those lines that displayed a cell death rescue showed normal greening and no longer died as a result of Pchlde overaccumulation and excitation, triggering the release of singlet oxygen. No red pigment fluorescence indicative of the presence of free Pchlde molecules was detectable in etiolated (dark-grown) seedlings of the regenerated

transgenic plants. In line with this observation, low temperature pigment measurements identified photoactive Pchlde F-655 that was restored in dark-grown seedlings. Moreover, confocal laser scanning microscopy confirmed that the introduced AtOEP16-1 protein was localized in chloroplasts. Non-denaturing PAGE detected higher molecular mass PORA:PORB complexes in the regenerated transgenic lines. Taken together, these results show that synthesis of AtOEP16-1 protein from the transgene transformed into the mutant restored pPORA import, Pchlde sequestration and greening.

A critical factor that may influence the capability of a transgene to restore the wild-type phenotype of a given mutant (e.g. *oep16-1;6*) is the structure of the encoded protein. To establish its functional state, the protein must fold correctly and attain the natural conformation, thereby interacting with other cellular components, such as, for example, membrane lipids and membrane proteins. In the case of OEP16-1, the protein needs first to be directed to the respective target membrane, i.e. the outer envelope membrane of the chloroplast, before it can form cation-selective pores involved in amino acid and polypeptide transport (Pohlmeyer et al. 1997, Steinkamp

et al. 2000, Linke et al. 2004, Reinbothe et al. 2004b). OEP16-1 is a transmembrane protein which is anchored to the membrane presumably via four α -helices; its exact topology is very controversially discussed (see Pohlmeier et al. 1997, Steinkamp et al. 2000, Linke et al. 2004). OEP16-1 additionally interacts with the other components of the Pchl_{ide}-dependent translocon comprising at least 10 different proteins to be operational in the substrate-dependent import of pPORA (Reinbothe et al. 2004a, Reinbothe et al. 2004b).

Whatever the exact insertion mechanism and topology of OEP16-1 might be, it is obvious that the presence of the reporter that was fused to the OEP16-1 protein affected the functionality of the resulting fusion protein. Any of the intermediate steps in the long and complicated pathway of this transmembrane protein may be impaired in some of the regenerated transgenic lines. For example, the folding of OEP16-1 may not occur correctly in the case of the OEP16-1::YFP fusion protein. On the other hand, the fusion protein may correctly fold but, due to the presence of the bulky reporter, not be able to insert properly into the outer chloroplast envelope membrane. Last, but not least, the OEP16-1::YFP protein may correctly fold and properly bind to the plastids but may not attain a functional, pore-forming and interactive state in the outer envelope membrane. In this case it could not be operational in the Pchl_{ide}-dependent import pathway of pPORA. For all of these reasons, the transgenic approach may have failed in the case of the T₃ 35S::OEP16::YFP lines. In the case of one of the lines studied, T₃ *oep16-1;6:35S::OEP16::YFP G_4*, we noted that YFP fluorescence is detectable but not associated with chloroplasts, explaining why no cell death rescue occurred. In contrast, we found that at least one out of six T₃ lines, *oep16-1;6:35S::GFP::OEP16*, expressed correctly folded and properly targeted as well as functional fusion protein, permitting the Pchl_{ide}-dependent import of pPORA and thereby restoring normal greening. Because five of the nine produced *oep16-1;6:35S::OEP16* lines were capable of restoring normal greening we conclude that OEP16-1 is essential for pPORA import, Pchl_{ide} sequestration and normal greening.

Evidence for the presence of additional mutations in the SALK_024018 seed stock

Because of the existence of four different *Atoep16-1* mutants containing the same, single T-DNA insertion in the OEP16-1 gene, an additional mutation has been postulated to be present in mutant *Atoep16-1;6* (Samol et al. 2011), which corresponds to the mutant F6-4a used by Pudelski et al. (2009). Pudelski et al. (2009) discussed the possible presence of such a mutation in the SALK_024018 seed stock but offered no explanation for its role. Because mutant *Atoep16-1;6* contains a single T-DNA band of the expected size on Southern blots, we suggested that the additional mutation is a point mutation left over after an independent T-DNA insertion event followed by loss of the T-DNA (Samol et al. 2011). Such effects have been reported (Latham et al. 2006). Either cytosolic targeting factors operating

in the post-translational import of pPORA or the plastid envelope protein translocon complexes themselves could be affected in mutant *Atoep16-1;6*, giving rise to TOC75-dependent import. However, the imported and processed enzyme did not assemble into larger complexes with PORB and, thus, no photoactive Pchl_{ide}-F655 was formed.

Previous biochemical approaches have identified cytosolic HSP70 and 14-3-3 proteins as key players for the targeting of pPORA to different import pathways (Schemenwitz et al. 2007). A guidance complex was formed similar to the one reported by May and Soll (2000). Binding of HSP70 and 14-3-3 proteins to the mature region of pPORA provoked a substrate-independent import of pPORA in vitro (Schemenwitz et al. 2007). Also in vivo, such an import route was observed by Kim and Apel (2004) in true leaves. Because no HSP70 and 14-3-3 protein complexes detectably bound to pPORA in protein extracts of etiolated seedlings (Schemenwitz et al. 2007), an explanation was offered as to why the Pchl_{ide} dependency of pPORA import is developmentally regulated and tied to seedling growth in darkness (Kim and Apel 2004).

The existence of a third import pathway of pPORA can be deduced from the results of the present study. We used transA-DHFR to demonstrate substrate-independent import of this model precursor into plastids isolated from mutant *Atoep16-1;6*. Because transA-DHFR does not contain the 14-3-3 recognition motif present in the mature region of the PORA, the import pathway followed in mutant *Atoep16-1;6* must rely on factors other than HSP70 and 14-3-3 proteins forming the guidance complex (May and Soll 2000, Schemenwitz et al. 2008). Qbadou et al. (2006) provided evidence for a HSP90-mediated pathway that could also be involved in directing pPORA to the TOC and TIC import machinery in mutant *Atoep16-1;6*.

For at least two reasons it seems unlikely that the conditional cell death phenotype observed in mutant *Atoep16-1;6* is caused by the additional mutation. First, independent transgenic lines expressing OEP16-1 either alone or as a fusion with GFP were obtained, which showed the same cell death rescue and greened normally. During in planta transformation, the generated vector DNA inserts randomly into the genome. It is unlikely that different transformants integrated the T-DNA at exactly the same site in the genome and that the additional mutation was thereby disrupted. Secondly, our segregation analysis on backcrossed *Atoep16-1;6* mutant plants did not provide seedlings that were both homozygous for the *Atoep16-1* mutation and lacked the cell death phenotype. On the other hand, no seedlings were obtained that were wild type for the *AtOEP16-1* gene but displayed the cell death phenotype. Finally, the transformants obtained for the 35S::OEP16::YFP construct showed that insertion of the foreign DNA on the one hand and expression of the OEP16 protein without its correct localization (integration) in the plastid envelope membrane on the other hand were insufficient to prevent cell death. It is likely that the different position of the reporter in the OEP16-YFP and GFP-OEP16 fusion proteins affected their folding pathways

and topologies, leading to different plastid import properties. On the basis of these and the aforementioned results, we conclude that *AtOEP16-1* is involved in the Pchl_{ide}-dependent import of pPORA into etioplasts. Due to the coupling of pPORA import to Pchl_{ide} synthesis in the plastid envelope, an efficient mechanism is established to sequester the pigment in a protein-bound form and, thereby, avoid photooxidative damage during subsequent greening.

Materials and methods

Plant growth

Mutant *Atoep16-1;6* (At2g28900) has been isolated from SALK_024018 (Alonso et al. 2003) as described (Samol et al. 2011). Seeds of homozygous plants were surface-sterilized and germinated on agar medium containing half-strength Murashige and Skoog (MS) medium in the dark (Samol et al. 2011). For standard cultivation, the medium contained additionally 1% (w/v) sucrose. For photobleaching tests, media lacked sucrose in most cases. After variable periods of cultivation, the seedlings were exposed to white light of the indicated fluence rates of 210 $\mu\text{E m}^{-2} \text{s}^{-1}$. For chloroplast isolation experiments, seeds were sown on soil and cultivated in continuous white light for appropriate periods.

Genetic complementation assay

DNA cloning was performed following Gateway Technology (Invitrogen). cDNA for the *AtOEP16-1* protein of *A. thaliana* was integrated into the binary T-DNA destination vectors pB7WG2, pK7WGF2 and pB7YWG2 to generate the following cDNA constructs: 35S::OEP16, 35S::GFP::OEP16 and 35S::OEP16::YFP. In the case of 35S::OEP16::YFP, the stop codon of the *AtOEP16-1* cDNA was eliminated during PCR cloning using appropriate primers (Innis et al. 1990). These different constructs were then used to transform *Atoep16-1* mutant plants by the floral dip method (Clough and Bent 1998). Plant transformants were identified by PCR (Innis et al. 1990) and Southern blotting (Sambrook et al. 1989), using appropriate primers and probes, respectively.

Pigment fluorescence analyses

Low temperature fluorescence spectroscopy was performed at 77 K at an excitation wavelength of 440 nm and collecting fluorescence emission between 575 and 725 nm (Lebedev et al. 1995) (spectrometer model LS50B, Perkin Elmer Corp.). Fluorescence microscopy was carried out using an excitation filter from 400 to 450 nm and an emission filter from 600 to 650 nm.

Seedling viability tests

Seedling viability was assessed by the previously described greening test (Meskauskiene et al. 2001, Pollmann et al. 2007) and confirmed by tetrazolium staining (Nortin 1966).

While viable seedlings exhibit a strong red staining, dead seedlings are yellow to white. For statistic assessment, pools of about 250 seeds were analyzed in three independent experiments.

Singlet oxygen and TUNEL measurements

Singlet oxygen evolution was measured with the DanePy method (Hideg et al. 1998, Kálai et al. 2002). Fluorescence emission of DanePy, which is quenched by singlet oxygen, was collected between 425 and 625 nm, using an excitation wavelength of 330 nm (Life Sciences spectrometer, model LS50 Perkin Elmer Corp.). DNA laddering during cell death was followed by conventional agarose gel electrophoresis and TUNEL (Gavrieli et al. 1992).

Protein import in vitro and in planta

Construction of chimeric precursors consisting of the N-terminal targeting sequences of pPORA (transA) and pPORB (transB) of barley and DHFR has been described (Reinbothe et al. 1997, Reinbothe et al. 2000). In vitro import reactions were carried out using wheat germ-translated, urea-denatured [³⁵S]precursors produced by coupled transcription/translation of the respective clones and Percoll/sucrose-purified chloroplasts from *A. thaliana* (Schemenwitz et al. 2007). Chemical cross-linking of DTNB-activated [³⁵S]precursors was conducted as described (Reinbothe et al. 2004b).

For studying import in vivo, transgenic lines stably expressing fusion proteins of the pPORA and pPORB of *A. thaliana* (Armstrong et al. 1995) and the jellyfish GFP were produced. Transformed plantlets were grown in the dark or with white light under sterile conditions for appropriate periods and analyzed by confocal laser scanning microscopy (LSM 510 Meta microscope, Zeiss), using argon laser excitation at 488 nm. GFP and Chl were detected at emission wavelengths of 505–530 and 650–750 nm, respectively. LSM 510 Meta software release 3.2 (Zeiss) and Adobe Photoshop 7 (Adobe Systems) were used for image acquisition and processing, respectively.

Purification of bacterially expressed (His)₆-AtOEP16-1 protein and antibody production

The presence of codons for the N-terminal hexa-His tag in pDESTTM17 allowed the affinity purification of recombinant fusion protein using Ni-NTA agarose chromatography. The procedure of batch purification under denaturing conditions was adapted from the protocol of the QIAexpressionist (Qiagen). Bacterial pellets of *Escherichia coli* strain BL21AI grown with L-arabinose (to induce protein expression) for 4 h were lysed in lysis buffer B (8 M urea, 0.1 M NaH₂PO₄, 0.01 M Tris-HCl, pH 8.0) using a French press. Cellular debris was removed by centrifugation at 10,000 × g for 30 min. The cleared lysate was mixed with 1 ml of suspension of 50% (w/v) Ni-NTA in buffer B and incubated on a rotary shaker at 200 r.p.m. overnight at 4°C. After transfer into a Biorad minispin column, the Ni-NTA

resin was washed twice with 4 ml of buffer C (8 M urea, 0.1 M NaH₂PO₄, 0.01 M Tris–HCl, pH 6.3). Recombinant (His)₆-OEP16 protein was eluted with 4 × 0.5 ml of buffer D (8 M urea, 0.1 M NaH₂PO₄, 0.01 M Tris–HCl, pH 5.9), followed by 4 × 0.5 ml of buffer E (8 M urea, 0.1 M NaH₂PO₄, 0.01 M Tris–HCl, pH 4.5). The fractions eluted with buffer D and E were separated by SDS–PAGE. Then, the polyacrylamide gel was stained with Coomassie brilliant blue G250 to identify the recombinant (His)₆-AtOEP16-1 protein. A 2 mg aliquot of each of the recombinant, SDS-denatured and electrophoretically resolved, Coomassie-stained proteins was used for the primary immunization and subsequent boost injections of two independent rabbits. Positive antisera were identified by enzyme-linked immunosorbent assays and conventional Western blotting using SDS–PAGE-resolved recombinant and native protein (Towbin et al. 1979).

Protein analyses

Protein was extracted and precipitated with trichloroacetic acid and analyzed by SDS–PAGE on 10–20% gradients (Laemmli 1970). For resolution of POR–pigment complexes, etioplasts were isolated from 4.5-day-old dark-grown plants and fractionated into prolamellar bodies, envelopes and stroma (Reinbothe et al. 2004a). Prolamellar body membranes were subsequently solubilized with detergent and subjected to electrophoresis on non-denaturing, analytical 7.5% polyacrylamide gels (Buhr et al. 2008). POR–pigment complexes were detected by their Pchl_a autofluorescence under blue light and Western blotting using POR antiserum, respectively (Towbin et al. 1979, Buhr et al. 2008).

Segregation analyses

Reciprocal segregation analyses were carried out according to standard procedures (Weigel and Glazebrook 2002). Anthers were removed from the female parental flowers under a dissecting microscope, while the carpels were left intact. After 48 h, a flower from the male parent was dissected, squeezed, and the anthers were separated from the other flower organs mechanically. F₂ seeds were collected after appropriate periods following fertilization from independent plants.

Supplementary data

Supplementary data are available at PCP online.

Funding

This study was supported by the French Ministry of Research and Education [Chaire d'Excellence research project grant dedicated to C.R.]; Deutsche Forschungsgemeinschaft (DFG) [Mercator professorship to D.v.W.].

Acknowledgments

The technical assistance of Jean-Marc Bonneville and Gabrielle Tichtinsky (Université Joseph Fourier, Grenoble, France) with respect to Gateway cloning of *AtOep16-1* constructs is gratefully acknowledged. We thank K. Apel (Boyce Thompson Institute for Plant Research, Ithaca, USA) for a gift of *flu* mutant seeds and K. Kálai and E. Hideg (Institute for Plant Biology, Biological Research Centre, Hungarian Academy of Sciences, Szeged, Hungary) for a gift of the DanePy reagent.

References

- Alonso, J.M., Stepanova, A.N., Leisse, T.J., Kim, C.J., Chen, H., Shinn, P. et al. (2003) Genome-wide insertional mutagenesis of *Arabidopsis thaliana*. *Science* 301: 653–657.
- Armstrong, G.A., Runge, S., Frick, G., Sperling, U. and Apel, K. (1995) Identification of NADPH:protochlorophyllide oxidoreductases A and B: a branched pathway for light-dependent chlorophyll biosynthesis in *Arabidopsis thaliana*. *Plant Physiol.* 108: 1505–1517.
- Bauer, J., Chen, K., Hiltbrunner, A., Wehrli, E., Eugster, M., Schnell, D. et al. (2000) The major protein import receptor of plastids is essential for chloroplast biogenesis. *Nature* 403: 203–207.
- Bedard, J. and Jarvis, P. (2005) Recognition and envelope translocation of chloroplast preproteins. *J. Exp. Bot.* 56: 287–320.
- Buhr, F., el Bakkouri, M., Lebedev, N., Pollmann, S., Reinbothe, S. and Reinbothe, C. (2008) Photoprotective role of NADPH:protochlorophyllide oxidoreductase A. *Proc. Natl Acad. Sci. USA* 105: 12629–12634.
- Campoli, C., Caffari, S., Svensson, J.T., Bassi, R., Stanca, A.M., Cattivelli, L. et al. (2009) Parallel pigment and transcriptome analysis of four barley *Albina* and *Xantha* mutants reveals the complex network of the chloroplast-dependent metabolism. *Plant Mol. Biol.* 71: 173–191.
- Cavalier-Smith, T. (2006) Cell evolution and earth history: stasis and revolution. *Philos. Trans. R. Soc. B: Bol. Sci.* 361: 969–1006.
- Clough, S. and Bent, A. (1998) Floral dip: a simplified method for *Agrobacterium*-mediated transformation of *Arabidopsis thaliana*. *Plant J.* 16: 735–743.
- Drea, S.C., Lao, N.T., Wolfe, K.H. and Kavanagh, T.A. (2006) Gene duplication, exon gain and neofunctionalization of OEP16-related genes in land plants. *Plant J.* 46: 723–735.
- Gavrieli, Y., Sherman, Y. and Ben-Sasson, S.A. (1992) Identification of programmed cell death in situ via specific labeling of nuclear DNA fragmentation. *J. Cell Biol.* 119: 493–501.
- Hideg, E., Kálai, T., Hideg, K. and Vass, I. (1998) Photoinhibition of photosynthesis in vivo results in singlet oxygen production detection via nitroxide-induced fluorescence quenching in broad bean leaves. *Biochemistry* 37: 11405–11411.
- Hofmann, N.R. and Theg, S.M. (2005) Chloroplast outer membrane protein targeting and insertion. *Trends Plant Sci.* 10: 450–457.
- Innis, M.A., Gelfand, D.H., Sninsky, J.J. and White, T.J. (1990) PCR Protocols. Academic Press, San Diego.
- Ivanova, Y., Smith, M.D., Chen, K. and Schnell, D.J. (2004) Members of the Toc159 import receptor family represent distinct pathways for protein targeting to plastids. *Mol. Biol. Cell* 15: 3379–3392.

- Jarvis, P., Chen, L.-J., Li, H.-m., Peto, C.A., Fankhauser, C. and Chory, J. (1998) An *Arabidopsis* mutant defective in the plastid general protein import apparatus. *Science* 282: 100–103.
- Kálai, T., Hankovszky, O., Hideg, E., Jeko, J. and Hideg, K. (2002) Synthesis and structure optimization of double (fluorescent and spin) sensor molecules. *ARKIVOC* iii: 112–120.
- Kessler, F. and Schnell, D.J. (2006) The function and diversity of plastid protein import pathways: a multilane GTPase highway into plastids. *Traffic* 7: 248–257.
- Khandal, D., Samol, I., Buhr, F., Pollmann, S., Schmidt, H., Clemens, C. *et al.* (2009) Singlet oxygen-dependent translational control in the *tigrina-d.12* mutant of barley. *Proc. Natl Acad. Sci. USA* 106: 13112–13117.
- Kim, C. and Apel, K. (2004) Substrate-dependent and organ-specific chloroplast protein import in planta. *Plant Cell* 16: 88–98.
- Kubis, S., Patel, R., Combe, J., Bédard, J., Kovacheva, S., Lilley, K. *et al.* (2004) Functional specialization amongst the *Arabidopsis* Toc159 family of chloroplast protein import receptors. *Plant Cell* 16: 2059–2077.
- Laemmli, U.K. (1970) Cleavage of structural proteins during the assembly of the head of bacteriophage T4. *Nature* 227: 680–685.
- Latham, J., Wilson, A.K. and Steinbrecher, R. (2006) The mutational consequences of plant transformation. *J. Biomed. Biotech.* 2006: 1–7.
- Lebedev, N. and Timko, M.P. (1998) Protochlorophyllide photoreduction. *Photosynth. Res.* 58: 5–23.
- Lebedev, N., van Cleve, B., Armstrong, G. and Apel, K. (1995) Chlorophyll synthesis in a de-etiolated (*det340*) mutant of *Arabidopsis* without NADPH-protochlorophyllide (PChlide) oxidoreductase (POR) A and photoactive PChlide-F655. *Plant Cell* 7: 2081–2090.
- Linke, D., Frank, J., Pope, M.S., Soll, J., Ilkavets, I., Fromme, P. *et al.* (2004) Folding kinetics and structure of OEP16. *Biochemistry* 43: 1479–1487.
- May, T. and Soll, J. (2000) 14-3-3 proteins form a guidance complex with chloroplast precursor proteins in plants. *Plant Cell* 12: 53–63.
- Meskauskiene, R., Nater, M., Gosling, D., Kessler, F., op den Camp, R. and Apel, K. (2001) FLU: a negative regulator of chlorophyll biosynthesis in *Arabidopsis thaliana*. *Proc. Natl Acad. Sci. USA* 98: 12826–12831.
- Miller, G., Shulaev, V. and Mittler, R. (2008) Reactive oxygen signaling and abiotic stress. *Physiol. Plant.* 133: 481–489.
- Murcha, M.W., Elhafez, D., Lister, R., Tonti-Filippini, J., Baumgartner, M., Philippar, K. *et al.* (2007) Characterization of the preprotein and amino acid transporter gene family in *Arabidopsis*. *Plant Physiol.* 143: 199–212.
- Nortin, J.D. (1966) Testing of plum pollen viability with tetrazolium salts. *Proc. Amer. Soc. Hort. Sci.* 89: 132–134.
- op den Camp, R., Przybyla, D., Ochsenein, C., Laloi, C., Kim, C., Danon, A. *et al.* (2004) Rapid induction of distinct stress responses after the release of singlet oxygen in *Arabidopsis*. *Plant Cell* 15: 2320–2332.
- Philippar, K., Geis, T., Ilkavets, I., Oster, U., Schwenkert, S., Meurer, J. *et al.* (2007) Chloroplast biogenesis: the use of mutants to study the etioplast–chloroplast transition. *Proc. Natl Acad. Sci. USA* 104: 678–683.
- Pohlmeier, K., Soll, J., Steinkamp, T., Hinnah, S. and Wagner, R. (1997) A high-conductance solute channel in the chloroplastic outer envelope from pea. *Proc. Natl Acad. Sci. USA* 94: 9504–9509.
- Pollmann, S., Springer, A., Buhr, F., Lahroussi, A., Samol, I., Bonneville, J.-M. *et al.* (2007) A plant porphyria related to defects in plastid import of protochlorophyllide oxidoreductase A. *Proc. Natl Acad. Sci. USA* 104: 2019–2023.
- Pudelski, B., Soll, J. and Philippar, K. (2009) A search for factors influencing etioplast–chloroplast transition. *Proc. Natl Acad. Sci. USA* 106: 12201–12206.
- Qbadou, S., Becker, T., Mirus, O., Tews, I., Soll, J. and Schleiff, E. (2006) The molecular chaperone Hsp90 delivers precursor proteins to the chloroplast import receptor Toc64. *EMBO J.* 25: 1836–1847.
- Reinbothe, C., Buhr, F., Pollmann, S. and Reinbothe, S. (2003) In vitro reconstitution of LHPP with protochlorophyllides *a* and *b*. *J. Biol. Chem.* 278: 807–815.
- Reinbothe, C., Lebedev, N., Apel, K. and Reinbothe, S. (1997) Regulation of chloroplast protein import through a protochlorophyllide-responsive transit peptide. *Proc. Natl Acad. Sci. USA* 94: 8890–8894.
- Reinbothe, C., Lebedev, N. and Reinbothe, S. (1999) A protochlorophyllide light-harvesting complex involved in de-etiolation of higher plants. *Nature* 397: 80–84.
- Reinbothe, C., Mache, R. and Reinbothe, S. (2000) A second, substrate-dependent site of protein import into chloroplasts. *Proc. Natl Acad. Sci. USA* 97: 9795–9800.
- Reinbothe, C., Pollmann, S. and Reinbothe, S. (2010) Singlet oxygen links photosynthesis to translation and plant growth. *Trends Plant Sci.* 15: 499–506.
- Reinbothe, C., Springer, A., Samol, J. and Reinbothe, S. (2009) Plant oxylipins: role of jasmonic acid during programmed cell death, defense and leaf senescence. *FEBS J.* 276: 4666–4681.
- Reinbothe, S., Pollmann, S., Springer, A., James, R.J., Tichtinsky, G. and Reinbothe, C. (2005) A role of Toc33 in the protochlorophyllide-dependent protein import pathway of NADPH:protochlorophyllide oxidoreductase (POR) A into plastids. *Plant J.* 42: 1–12.
- Reinbothe, S., Quigley, F., Gray, J., Schemenewitz, A. and Reinbothe, C. (2004a) Identification of plastid envelope proteins required for import of protochlorophyllide oxidoreductase A into the chloroplast of barley. *Proc. Natl Acad. Sci. USA* 101: 2197–2202.
- Reinbothe, S., Quigley, F., Springer, A., Schemenewitz, A. and Reinbothe, C. (2004b) The outer plastid envelope protein Oep16: role as precursor translocase in import of protochlorophyllide oxidoreductase A. *Proc. Natl Acad. Sci. USA* 101: 2203–2208.
- Reinbothe, S., Reinbothe, C., Holtorf, H. and Apel, K. (1995b) Two NADPH:protochlorophyllide oxidoreductases in barley: evidence for the selective disappearance of PORA during the light-induced greening of etiolated seedlings. *Plant Cell* 7: 1933–1940.
- Reinbothe, S., Reinbothe, C., Neumann, D. and Apel, K. (1996) A plastid enzyme arrested in the step of precursor translocation *in vivo*. *Proc. Natl Acad. Sci. USA* 93: 12026–12030.
- Reinbothe, S., Runge, S., Reinbothe, C., van Cleve, B. and Apel, K. (1995a) Substrate-dependent transport of the NADPH:protochlorophyllide oxidoreductase into isolated plastids. *Plant Cell* 7: 161–172.
- Sambrook, J., Fritsch, E. and Maniatis, T. (1989) *Molecular Cloning: A Laboratory Manual*, 2nd edn. Cold Spring Harbor Laboratory Press, Cold Spring Harbor, NY.
- Samol, I., Buhr, F., Springer, A., Pollmann, S., Lahroussi, A., Rossig, C. *et al.* (2011) Implication of the *oep16-1* mutation in a *flu-*

- independent, singlet oxygen-regulated cell death pathway in *Arabidopsis thaliana*. *Plant Cell Physiol.* 52: 84–95.
- Schemenewitz, A., Pollmann, S., Reinbothe, C. and Reinbothe, S. (2007) A substrate-independent, 14:3:3 protein-mediated plastid import pathway of NADPH:protochlorophyllide oxidoreductase (POR) A. *Proc. Natl Acad. Sci. USA* 104: 8538–8543.
- Smith, M.D., Rounds, C.M., Wang, F., Chen, K., Afithile, M. and Schnell, D.J. (2004) atToc159 is a selective transit peptide receptor for the import of nucleus-encoded chloroplast proteins. *J. Cell Biol.* 165: 323–334.
- Steinkamp, T., Hill, K., Hinnah, S., Wagner, R., Röhl, T., Pohlmyer, K. *et al.* (2000) Identification of the pore-forming region of the outer chloroplast envelope protein OEP16. *J. Biol. Chem.* 275: 11758–11764.
- Towbin, M., Staehelin, T. and Gordon, J. (1979) Electrophoretic transfer of proteins from polyacrylamide gels to nitrocellulose sheets; procedure and some applications. *Proc. Natl Acad. Sci. USA* 76: 4350–4354.
- Wasternack, C. (2007) Jasmonates: an update on biosynthesis, signal transduction and action in plant stress response, growth and development. *Ann. Bot.* 100: 681–697.
- Weigel, D. and Glazebrook, J. (2002) *Arabidopsis: A Laboratory Manual*. Cold Spring Harbor Laboratory Press, Cold Spring Harbor, NY.

Fig. S1a

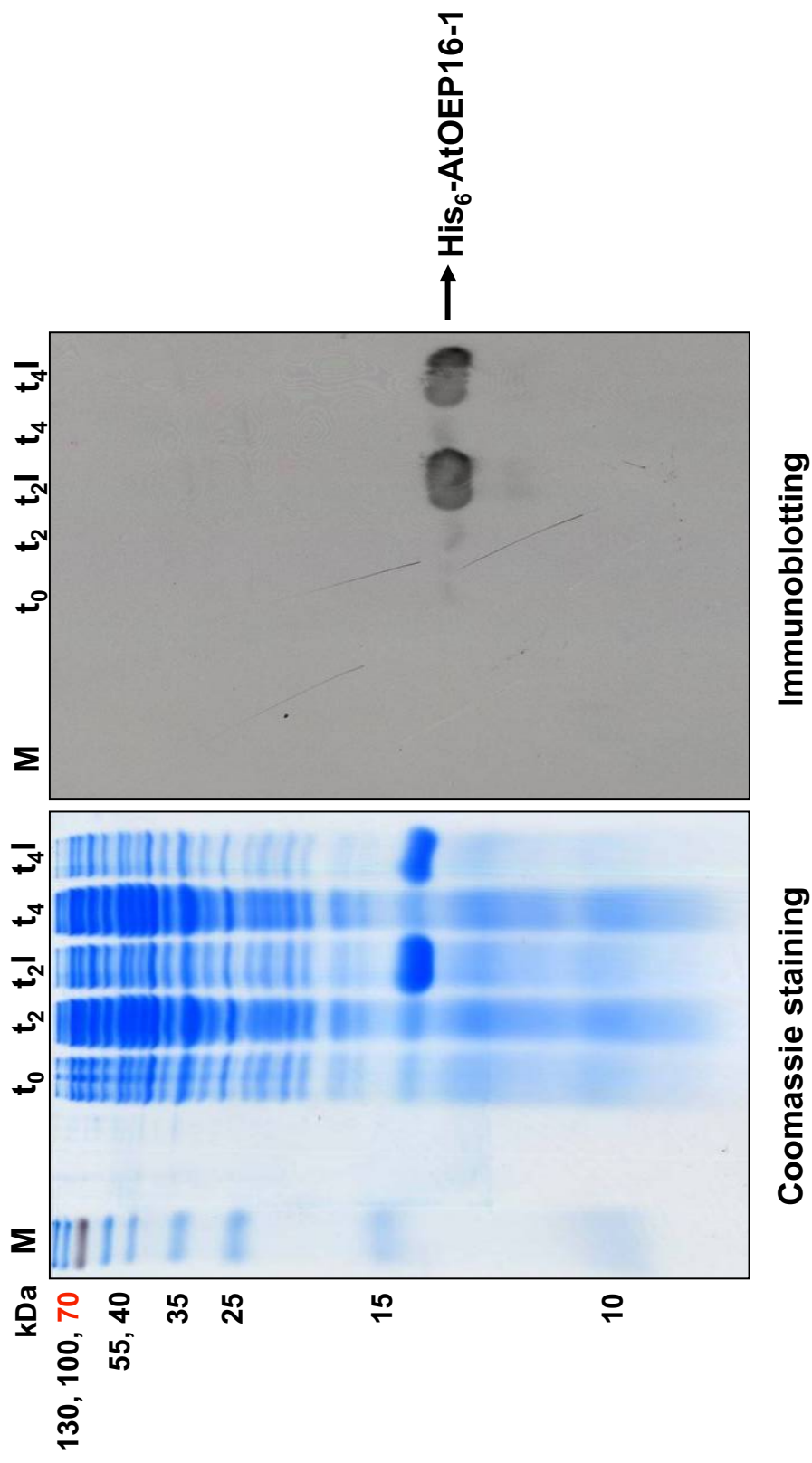


Fig. S1b

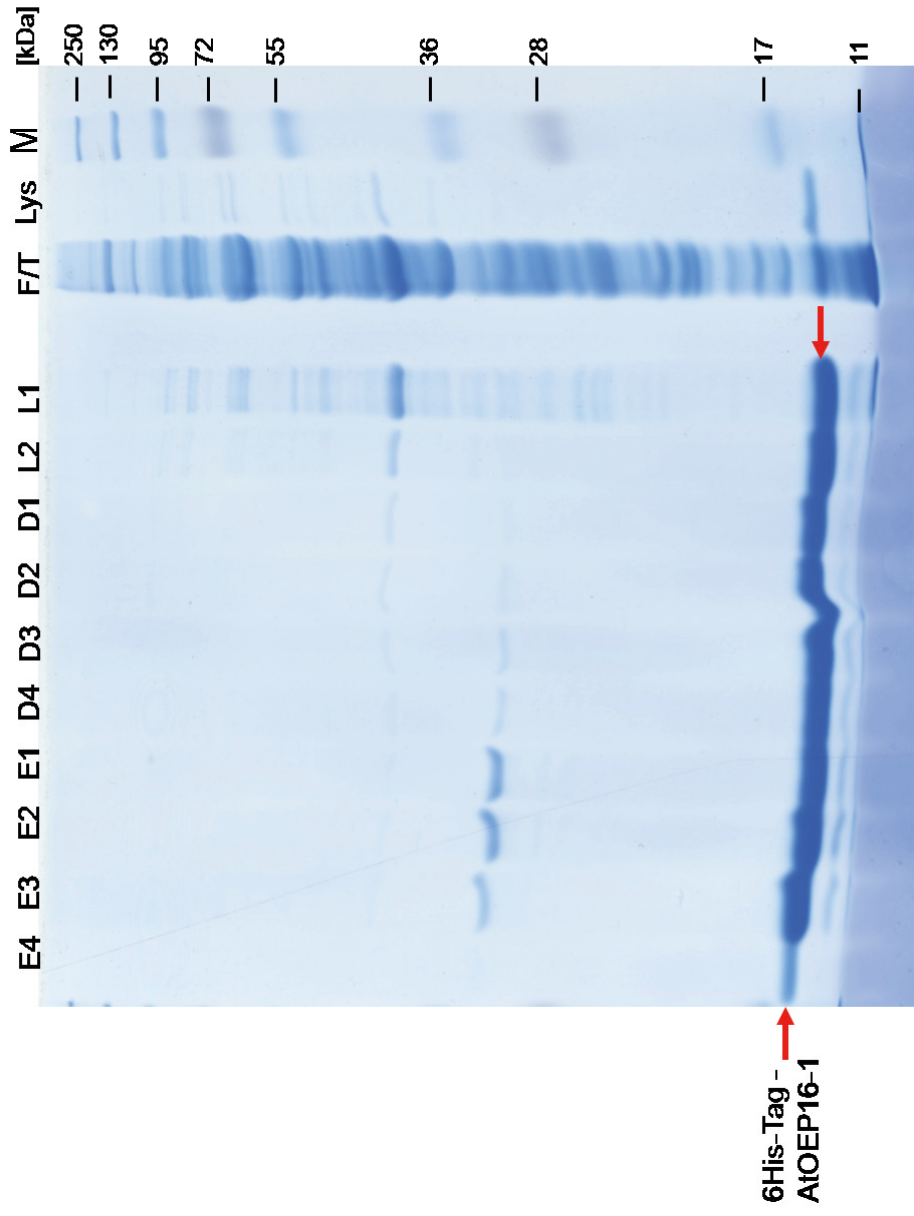


Fig. S1c

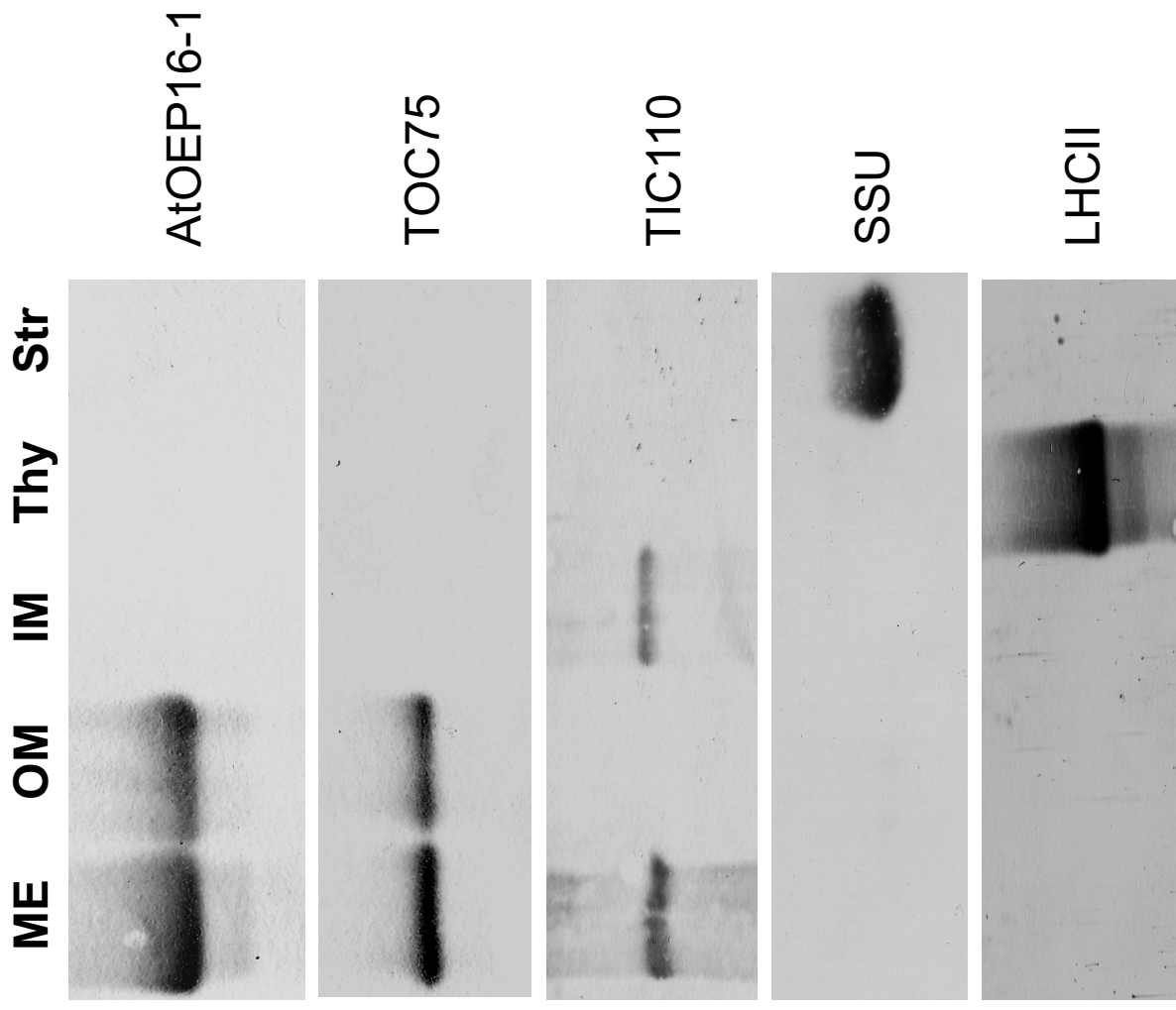
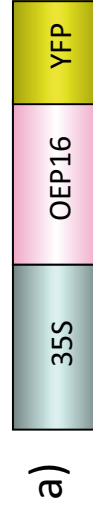


Fig. S2A-E



Basta^R : 100%

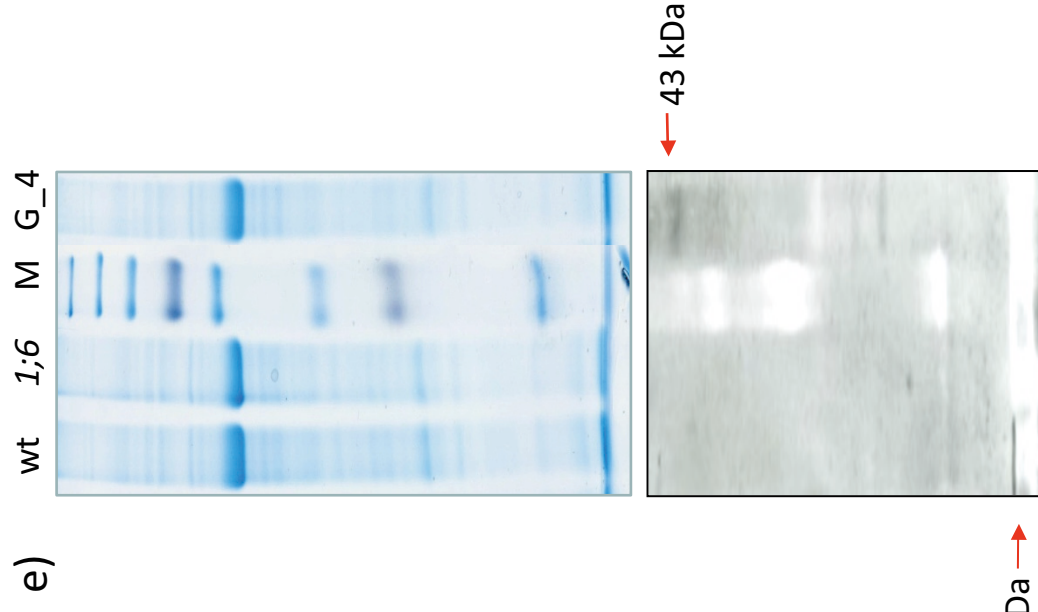
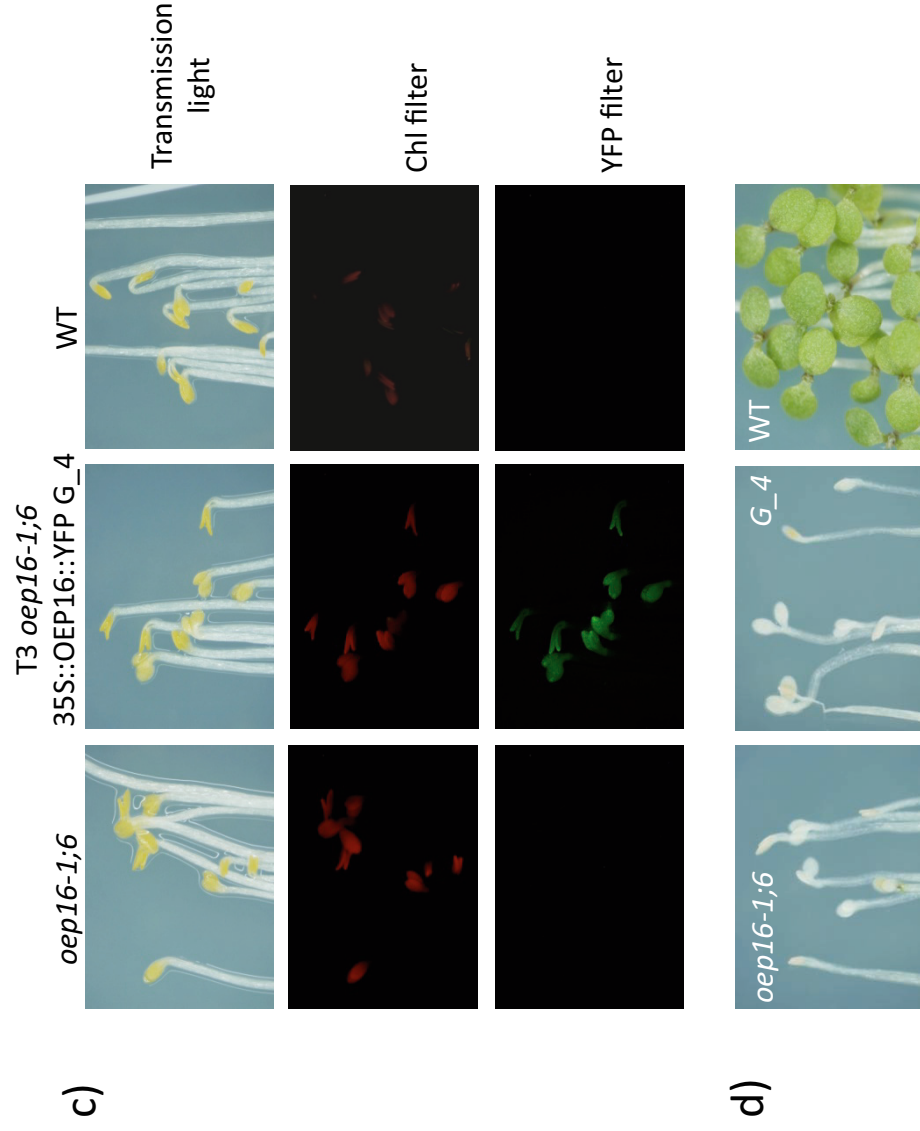
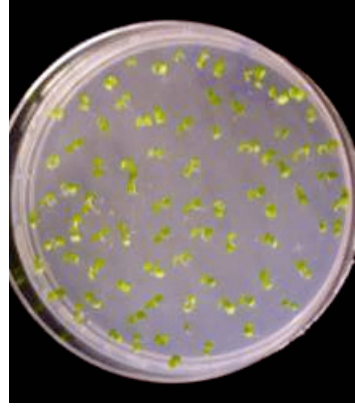


Fig. S2F

f)

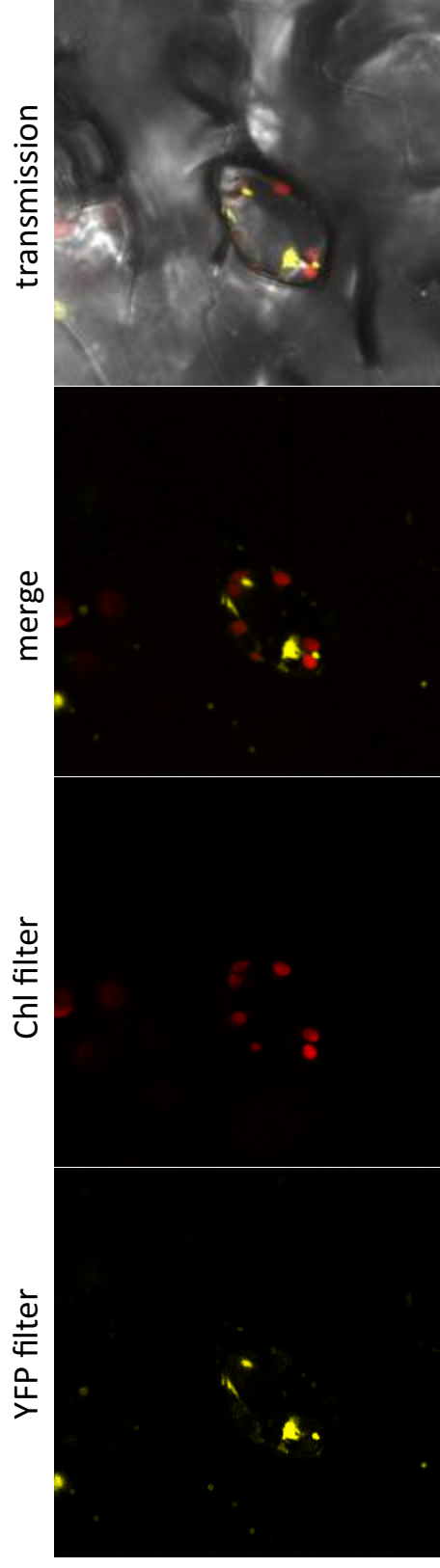


Fig. S3

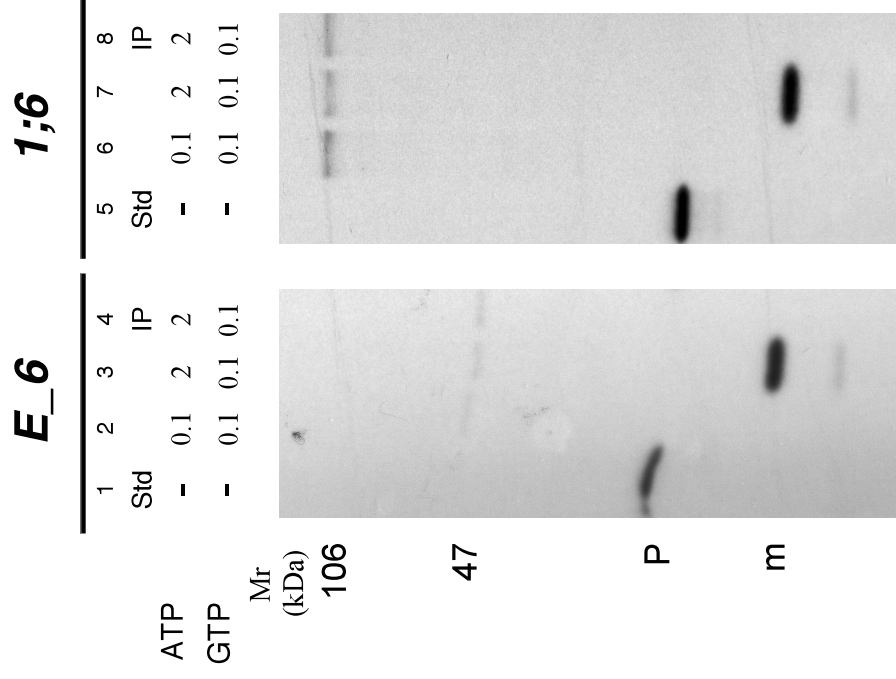


Fig. S4

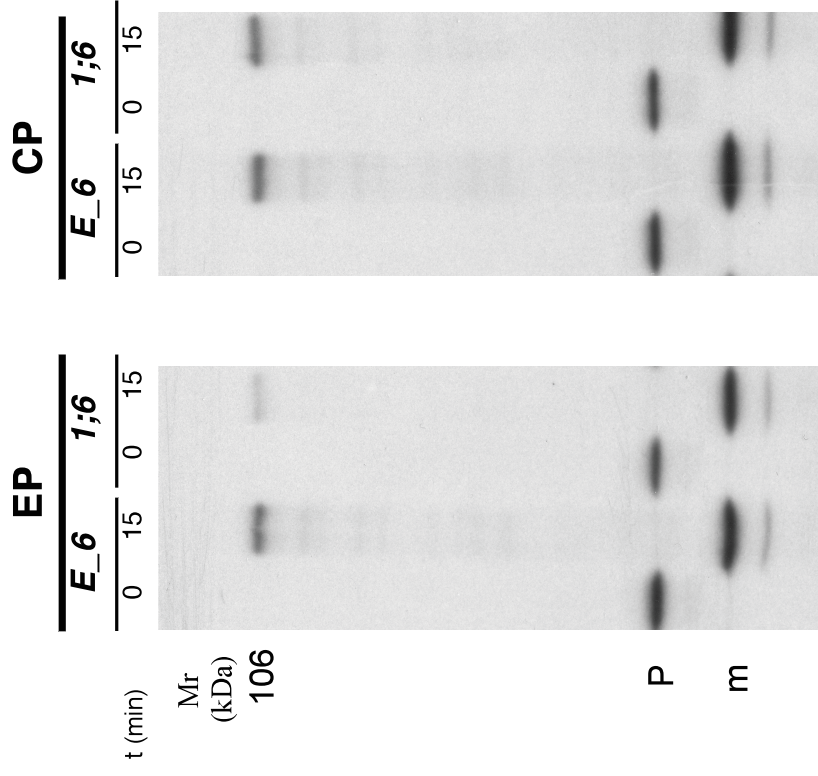
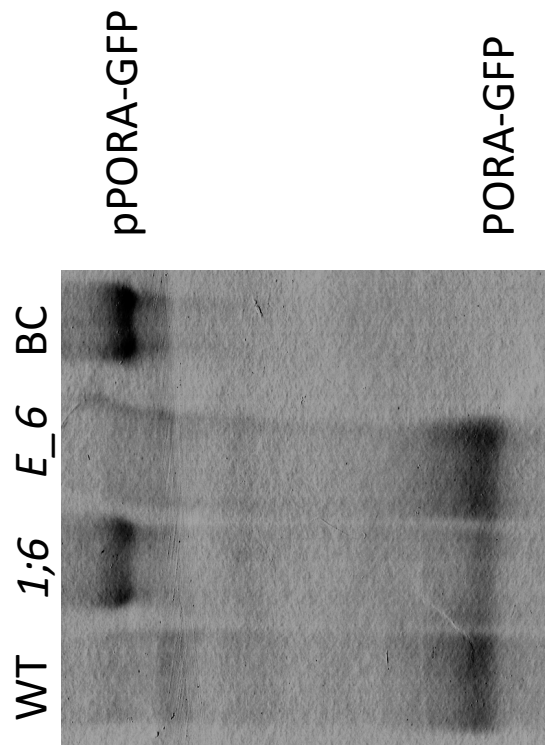


Fig. S5



SI Figures

Fig. S1. Production of AtOEP16-1-(His)₆ antibody.

a) Time course of expression of AtOEP16-1-(His)₆ in *E.coli* strain BL21. All of the following operations were carried out using a Qiagen Ni-NTA agarose chromatography kit. Bacteria were grown in LB medium at 37°C with shaking until the OD₆₀₀ 0.6 was obtained (**t₀**). Then, L-arabinose was added to the culture and expression of AtOEP16-1-(His)₆ followed by Western blotting using a anti-(His)₆ antibody (Qiagen). The image shows the pattern of total bacterial proteins [separated into an insoluble fraction (t₂I, t₄I) and a soluble fraction (t₂, t₄) after harvesting the bacteria after 2 and 4 hours of the induction] and after Western blot analysis using anti-(His)₆ antibody. M refers to protein marker.

b) Purification of AtOEP16-1-(His)₆ by Ni-NTA chromatography. The Coomassie stained gel shows proteins recovered from the lysis extract (L), flow-through (F/L), and L1 and L2 as well as D1-D4 wash fractions that were obtained according to the manufacturer's instructions. E1-E4 represents proteins eluted from the Ni-NTA matrix with buffer E. For antibody production, the pure AtOEP16-1-(His)₆ was injected into rabbits and the collected sera tested.

c) Specificity of the raised OEP16-1 antibody. Plastids were isolated from 5 d-old light-grown seedlings, fractionated into mixed envelopes (ME), outer (OM) and inner envelope (IM)

membranes, thylakoids (Thy) and stroma (Str). Protein was extracted from each of these fractions, resolved by SDS-PAGE and blotted onto a nitrocellulose membrane. The membrane then was probed with antisera against the indicated marker proteins.

Fig. S2. Lack of functional complementation in *Atoep16-1;6* transformed with 35S::OEP16::YFP. As in Fig. 3, but demonstrating that expression of 35S::OEP16::YFP (a and b) does not restore normal greening (c and d). Note that T3 *Atoep16-1;6 35S::OEP16::YFP G_4* seedlings overproduce free Pchl_a molecules in the dark (c) and die when irradiated (d). OEP16-1-YFP expression was verified by Western blotting, using 40 µg of total leaf protein per lane and AtOEP16-1-(His)₆ antibody (e). Lane M shows molecular mass standards. (f) Fluorescence analysis of YFP in line T3 *35S::OEP16::YFP G_4*. Note the lack of co-localization of YFP and Chl fluorescences in plastids. For collecting YFP fluorescence, excitation and emission wavelengths of 514 nm and 520 nm - 550 nm, respectively, were used.

Fig. S3. Identification of the crosslink products formed with DTNB-derivatized ³⁵S-transA-DHFR in chloroplasts isolated from mutant *Atoep16-1;6* and line *Atoep16-1;6 35S::OEP16 E_6*. Import reactions were carried out at the indicated Mg-GTP and Mg-ATP

concentrations for 15 min in the dark. Then, an aliquot of the high Mg-ATP-containing assays (lanes 3 and 7) was subjected to co-immunoprecipitation with either AtOEP16-1-(His)₆ or TOC75 antibody (IP, lanes 4 and 8, respectively). The autoradiogram shows precursor (P) and mature (m) proteins as well as crosslink products of 47 kDa and 106 kDa at time zero (lanes 1 and 5) and after 15 min of import (lanes 2-4 as well as 6-8).

Fig. S4. Crosslinking of DTNB-activated ³⁵S-transB-DHFR in etioplasts and chloroplasts isolated from mutant *Atoep16-1;6* and line *Atoep16-1;6 35S::OEP16 E_6*. The autoradiogram shows the levels of precursor (P) and mature (m) proteins as well as that of a unique 106 kDa crosslink product at time zero (0 min) and after 15 min of import (15 min). The 106 kDa crosslink product represents transB-DHFR bound via a mixed disulfide bond to TOC75, as demonstrated by co-immunoprecipitation experiments using TOC75 antibody (data not shown).

Fig. S5. Expression analysis of pPORA-GFP in 5 d-old etiolated seedlings of the wild-type, mutant *Atoep16-1;6*, line *Atoep16-1;6 35S::OEP16 E_6* expressing OEP16-1, and the generated backcross of mutant *Atoep16-1;6*. Protein was isolated from Percoll/sucrose-purified etioplasts after blocking the degradation of pPORA-GFP with protease inhibitor cocktail (1). Equal amounts, corresponding to 25 µg of bovine serum albumin,

of etioplast protein were separated on a 15% polyacrylamide midigel containing SDS. pPORA-GFP and PORA-GFP were detected by Western blotting using anti-GFP antiserum.

1. Reinbothe, C., Apel, K., Reinbothe, S. (1995) - A light-induced protease from barley plastids degrades NADPH:protochlorophyllide oxidoreductase complexed with chlorophyllide. **Mol. Cell. Biol.** 15: 6206-6212

Résumé

Chez les angiospermes, l'oxygène singulet est la forme majoritaire des espèces réactives de l'oxygène, étant produite lors de la photosynthèse. Son excès provoque le dommage photooxydatif conduisant à la mort cellulaire, observée chez les mutants affectés dans la voie de la biosynthèse de la chlorophylle. Dans ce travail, nous avons utilisé des mutants d'*Arabidopsis thaliana* qui manifestent le phénotype conditionnel de la mort cellulaire, causée par l'absence d'une protéine de l'enveloppe externe des plastides, OEP16-1. Cette protéine est impliquée dans le transport des amines, acides aminés et également dans l'import d'une enzyme clé de la synthèse de la chlorophylle, NADPH: Protochlorophyllide oxydoreductase A (PORA), dans les plastides. Une approche génétique inverse a permis d'isoler et de caractériser quatre mutants indépendants *Atoep16-1*, ayant différentes combinaisons des propriétés de la mort cellulaire et de la présence/absence de la PORA. Deux des mutants accumulent en excès de la protochlorophyllide libre (Pchl) à l'obscurité et meurent après illumination. Dans ce cas, la Pchl agit comme un photosensibilisateur déclenchant la production de l'oxygène singulet. Les deux autres mutants évitent la surproduction de la Pchl et verdissent normalement. En utilisant le mutant de l'orge, *tigrina*^{dl2} comme référence, nous avons montré que la mort cellulaire induite lors du photoblanchiment chez les mutants *Atoep16-1*, intervient dans la voie *flu*-indépendante. L'initiation de la traduction sur des ribosomes 80S, a été identifiée comme étant une cible majeure de l'oxygène singulet, au cours des premières heures du verdissement. Dans un stade plus tardif, l'oxygène singulet a provoqué la dissociation des ribosomes. Nous avons ainsi fourni des preuves que les deux effets sur la traduction sont génétiquement liés et qu'ils peuvent être ensuite étudiés à l'aide des mutants *Atoep16-1* que nous avons isolés et du mutant *flu*, préalablement identifié.

Mots-clés: stress lumineux, l'oxygène singulet, protochlorophyllide, PORA, synthèse des protéines, photoblanchiment, mort cellulaire.

Abstract

In angiosperms, singlet oxygen is a prominent form of reactive oxygen species that is produced during photosynthesis. Its excess causes photooxidative damage leading to cell death, demonstrated in mutants impaired in the chlorophyll biosynthetic pathway. In the present work, we used mutants of *Arabidopsis thaliana* that exhibit a conditional seedling lethal phenotype caused by the absence of the outer plastid envelope protein, OEP16-1. This protein is involved in the transport of amines, amino acids and is also implicated in the import of the key enzyme of chlorophyll synthesis, NADPH: Protochlorophyllide oxydoreductase A (PORA), into the plastids. Using a reverse genetic approach, four independent *Atoep16-1* mutants were isolated and characterized, with different combinations of cell death properties and presence/absence of PORA. Two of the mutants overproduced free protochlorophyllide (Pchl) in the dark and died after illumination. Pchl operated here as a photosensitizer triggering singlet oxygen formation. The other two mutants avoided excess Pchl accumulation and greened normally. Using the mutant of barley, *tigrina*^{dl2} as reference, we show that cell death induced in the photobleaching *Atoep16-1* mutants occurs in a *flu*-independent pathway. Translation initiation at 80S ribosomes was identified to be a major target of singlet oxygen in the early hours of greening. At a delayed stage, singlet oxygen caused ribosome dissociation. We provided evidence that both effects on translation are genetically linked and they can be further studied using the *Atoep16-1* mutant that we isolated and the previously described *flu* mutant.

Keywords: light stress, singlet oxygen, protochlorophyllide, PORA, protein synthesis, photobleaching, cell death.